

553767
028

NASA Contractor Report 4268

**Design of Integrated Pitch Axis
for Autopilot/Autothrottle
and Integrated Lateral Axis
for Autopilot/Yaw Damper for
NASA TSRV Airplane Using
Integral LQG Methodology**

Isaac Kaminer, Russell A. Benson,
Edward E. Coleman, and Yaghoob S. Ebrahimi

CONTRACT NAS1-18027
JANUARY 1990



NASA Contractor Report 4268

Design of Integrated Pitch Axis for Autopilot/Autothrottle and Integrated Lateral Axis for Autopilot/Yaw Damper for NASA TSRV Airplane Using Integral LQG Methodology

Isaac Kaminer, Russell A. Benson,
Edward E. Coleman, and Yaghoob S. Ebrahimi
Boeing Commercial Airplane Company
Seattle, Washington

Prepared for
Langley Research Center
under Contract NAS1-18027



National Aeronautics and
Space Administration
Office of Management
Scientific and Technical
Information Division

1990

TABLE OF CONTENTS

1.0	SUMMARY	1
2.0	INTRODUCTION	2
3.0	SYMBOLS AND ABBREVIATIONS	3
3.1	Symbols	3
3.2	Abbreviations	5
4.0	SETTING UP FLIGHT CONDITIONS AND AERO MODELS	6
4.1	Cruise	9
4.2	Cruise Transition	9
4.3	Landing	10
4.4	Generation of the Open-Loop Airplane Models	10
5.0	CONTROL DESIGN METHODOLOGY	15
5.1	Specify Design Objectives	15
5.2	Formulate Design Requirements	16
5.3	Open Loop Analysis	17
5.3.1	Eigenstructure Decomposition	17
5.3.2	Controllability Analysis	17
5.3.3	Observability Analysis	18
5.3.4	Frequency Response	18
5.3.5	Time Domain Simulation	19
5.4	Controller Structure	19
5.5	Synthesis Model Definition	21
5.5.1	Independent Inputs	21
5.5.2	Regulated Variables	21
5.5.3	Criteria Outputs	21
5.6	Cost Function Weightings, Controller Gains, and Gain Scheduling	22
5.6.1	Cost Function Weightings	22
5.6.2	Controller Gains and Gain Scheduling	23
5.7	Sensor Selections and Output Filtering	24
5.8	Closed Loop Analysis	24
5.8.1	Eigenvalues	25
5.8.2	Broken Loop Frequency Responses	25
5.8.3	Singular Value Analysis	25
5.8.4	Covariance Response	25
5.8.5	Command Frequency Responses	26
5.8.6	Time Domain Simulation	26
5.9	Iteration to Satisfy Design Requirements	26
5.10	Summary of Design Methodology	27
6.0	DESIGN REQUIREMENTS	28
6.1	Longitudinal Axis Design Requirements	28
6.2	Lateral Axis Design Requirements	29
7.0	LONGITUDINAL AXIS DESIGN	32
7.1	Feedforward Modes	32
7.1.1	Altitude Hold Mode	32

TABLE OF CONTENTS (Continued)

7.1.2	Glideslope Capture and Hold	35
7.1.3	Flare Mode.....	37
7.1.4	Go-Around Mode	37
7.1.5	Flight Path Angle Mode	39
7.1.6	Speed Hold Mode.....	39
7.2	Feedback Regulator Design	41
7.2.1	Cruise Regulator Design	41
7.2.1.1	Open Loop Analysis	42
7.2.1.2	Output Criteria Creation	42
7.2.1.3	Gain Scheduling	45
7.2.1.4	Speed on Elevator (SOE) Configuration	47
7.2.2	Landing Regulator Design	47
7.2.2.1	Gain Scheduling	50
7.2.2.2	Airspeed Complementary Filter	50
7.3	Digital Implementation	54
7.4	Results	56
7.4.1	Linear Analysis	56
7.4.2	Nonlinear Testing	59
8.0	LATERAL AXIS DESIGN	61
8.1	Heading Controller Design	61
8.1.1	Regulated Variables	61
8.1.2	Criterion Outputs and Weighting Matrices	63
8.1.3	Gains and Gain Schedules	65
8.1.4	Beta Complementary Filter	65
8.1.5	Closed Loop Heading Controller	67
8.2	Heading Controller Results	67
8.2.1	Eigenvalues	67
8.2.2	Gain and Phase Margins.....	67
8.2.3	Covariance Responses	67
8.2.4	Frequency Responses	70
8.2.5	Time Domain Simulation	70
8.3	Localizer Controller Design	70
8.3.1	Controller Structure and Gains	70
8.3.2	Localizer Capture Logic	70
8.4	Localizer Controller Results	73
8.4.1	Eigenvalues	73
8.4.2	Gain and Phase Margins	73
8.4.3	Covariance Responses	73
8.5	Nonlinear Simulation of Localizer Capture and Track	73
8.6	Summary of Lateral Axis Design	77
9.0	CONCLUSIONS	78
	APPENDIX A: Longitudinal Axis Results	79
	APPENDIX B: Lateral Axis Results	103
	REFERENCES	144

LIST OF FIGURES

Figure

1.	Two-Degrees-of-Freedom Design	1
2.	Stall Speeds	7
3.	Operational Limits and Placards	8
4.	Two-Degrees-of-Freedom Controller Structure	20
5.	Controller Structure	33
6.	Altitude Hold Mode	33
7a.	Glideslope Capture and Hold Mode	35
7b.	Glideslope Geometry	35
7c.	Altitude Integrator Command Computation	36
8.	Flare Mode	38
9.	Go-Around Mode	38
10.	Flight Path Angle Mode	40
11.	Speed Hold (Mach or CAS) Mode	40
12.	Cruise Controller Synthesis Model	43
13.	General Structure of Cruise Feedback Controller	48
14.	Landing Controller - Synthesis Model	49
15.	Landing Controller - Thrust Gains Schedule	52
16.	Landing Controller - Elevator Gains Schedule	52
17.	Complementary Filter	53
18.	Digital Implementation - Delta Coordinates	55
19.	Throttle Limiting - Controller Switching	57
20.	Closed Loop Block Diagram of Integral Model Following Structure	62
21.	Feedforward Controller Showing Regulated Variables and Ideal Models	64
22.	LQG Synthesis Model Showing Criteria Outputs and Weighting Matrices	64
23.	Design Aileron Feedback Gains	66
24.	Feedback Gain Schedules	66
25.	Detailed Closed Loop Block Diagram of Heading Controller	68
26.	Scatter Plot for Heading Controller Using Scheduled Feedback Gains	68
27.	Aileron and Rudder Broken Loop Nyquist Plots for Heading Controller	69
28.	Covariance Responses of Heading Controller to 1 ft/sec Dryden Gust	69
29.	Frequency Responses of Heading Controller from psi Command to psi	71
30.	Time Response of Heading Controller for Heading Command Step	71
31.	Block Diagram of Localizer Capture and Track Controller	72

LIST OF FIGURES (Continued)

Figure

32.	Outline of Localizer Capture Logic	72
33.	Scatter Plot for Localizer Capture and Track Controller	74
34.	Aileron and Rudder Broken Loop Nyquist Plots for Localizer Capture and Track Controller	74
35.	Covariance Responses of Localizer Capture and Track Controller to 1 ft/sec Dryden Gust	75
36.	Flight Path History for Capture from a Parallel Heading with 1500 ft Initial Offset	75
37.	Flight Path History for Capture from a Perpendicular Path with No Initial Offset	76

LIST OF TABLES

Table

1.	Comparison of Controller Design Techniques	2
2.	Light Weight - 80,000 lbs with C. G. Variation of .05 to .3	6
3.	Heavy Weight - 110,000 lbs with C. G. Variation of .05 to .3	6
4a.	Cruise Flight Conditions	11
4b.	Cruise Transition Flight Conditions	12
4c.	Landing Flight Conditions	13
5a.	Transmission Zeroes of Cruise Controller Synthesis Model	46
5b.	Cost Function	46
6a.	Weighting Matrices for Cruise Controller	46
6b.	Feedback Gain Matrix for Cruise Controller	46
7a.	Transmission Zeroes of Landing Controller Synthesis Model	51
7b.	Weighting Matrices for Landing Controller	51
7c.	Feedback Gain Matrix for Landing Controller	51

2.0 INTRODUCTION

A two element controller was designed for each axis to satisfy the two distinct sets of requirements. For the feedback loop, an integral LQG methodology [3] was used in developing the design to comply with feedback requirements. For the feedforward loop, an ideal model was developed using first or second order filters to achieve the necessary frequency separation between feedback and feedforward loops, and provide the desired command limiting as dictated by passenger comfort and airplane dynamics constraints.

With regard to the longitudinal axis, some important differences between the design presented here (i.e., Total Energy Control System - TECS - [4, 5, 6]) and the conventional control systems designs currently used on Boeing commercial airplanes are summarized in Table 1. The design presented herein is identified as BCA RESEARCH in the Table. Item definitions in the Table that are not self-explanatory are defined in the following sections. (NOTE: Table 1 should be referred to when progressing through this document.)

With regard to the lateral axis, the design process presented here represents a departure from most previous techniques in that the roll and yaw axis controllers are designed simultaneously. Most previous techniques have traditionally developed the yaw damper first to control the rudder, and then designed the autopilot to control the ailerons.

Table 1. Comparison of Controller Design Techniques

ITEM	BCA RESEARCH	TECS	CONVENTIONAL
INTEGRATED PITCH / THRUST	YES	YES	NO
MODE SWITCHING	FEEDFORWARD LOOP	FEEDBACK LOOP	FEEDBACK/FEEDFORWARD LOOP
LIMITING	FEEDFORWARD LOOP	FEEDBACK LOOP	FEEDBACK/FEEDFORWARD LOOP
INITIALIZATION	ALL STATES TO 0	CURRENT STATE OF AIRPLANE	CURRENT STATE OF AIRPLANE
DYNAMIC RESPONSE	MODE INDEPENDENT	MODE DEPENDENT	MODE DEPENDENT
INTEGRAL GAINS (outer loop)	HIGH	LOW	LOW
PROPORTIONAL GAINS (inner loop)	LOW	HIGH	HIGH

1.0 SUMMARY

The objective of this task is to design integrated autopilot controllers for both the longitudinal and lateral axes of the NASA TSRV airplane such that the longitudinal axis for autopilot/autothrottle provides independent control of altitude and speed, and the lateral axis for autopilot/yaw damper/sideslip controller provides independent control of heading and sideslip while augmenting dutch roll stability.

The approach used to achieve this objective is the two-degree-of-freedom design philosophy first advocated by I. Horowitz [1]. With this philosophy, one first designs the feedback controller to satisfy stability and performance robustness requirements (i.e., throughout the flight envelope), after which one then designs the feedforward controller to satisfy performance requirements (Milspec [2], or other ideal airplane response specifications). Figure 1 illustrates this concept with the arrows indicating the two degrees of freedom that the designer must follow to obtain a satisfactory design.

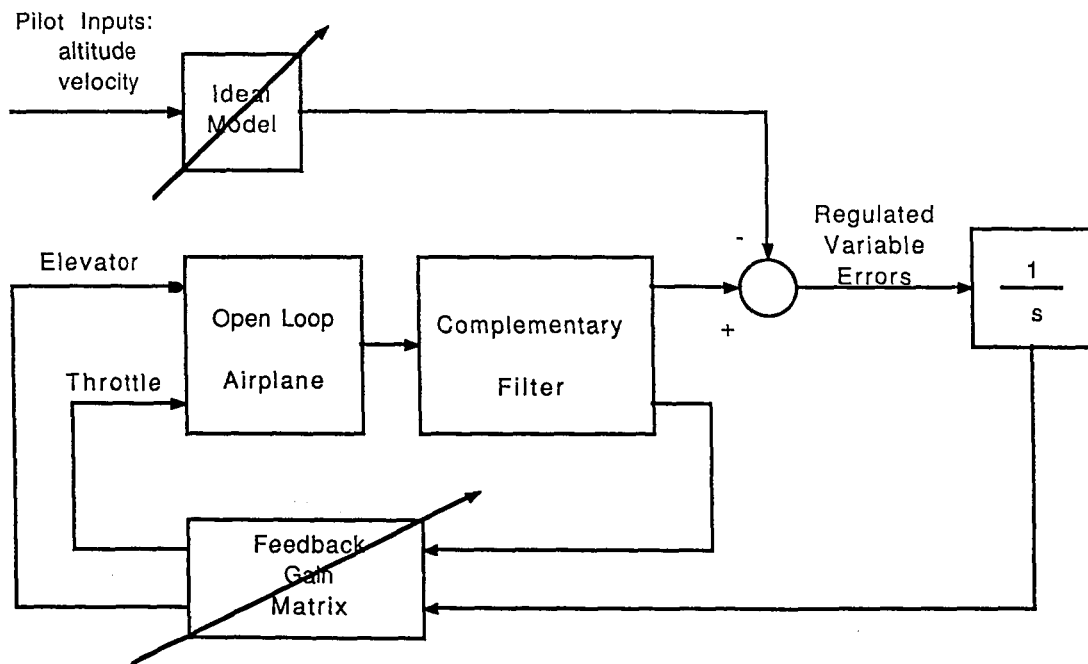


Figure 1. Two - Degree - of - Freedom Design

3.0 SYMBOLS AND ABBREVIATIONS

3.1 SYMBOLS

α	- Angle of attack
ξ	- Damping ratio
δ_e	- Incremental elevator position
δ_{TH}	- Incremental throttle position
θ	- Pitch altitude
τ	- Time constant
γ	- Flight path angle
γ_c	- Flight path angle command
l	- Moment arm
AFTLIM	- Throttle aft limit flag
ALTH	- Altitude hold mode flag
DFM	- Flap position of airplane
g	- Gravity constant
FAFLR	- Flare mode flag
FAFPA	- FPA mode flag
FAGA	- Go-around mode flag
FAGLDA	- Glideslope mode arm flag
FWDLIM	- Throttle forward limit flag
H	- Altitude
\dot{H}	- Altitude rate
H_c	- Altitude command
\dot{H}_c	- Altitude rate command
H_{cg}	- Altitude at center of gravity for airplane
\dot{H}_{cg}	- Altitude rate at center of gravity for airplane
H_e	- Altitude error
HGCG	- Altitude measured at center of gravity for airplane
\dot{H}_{LIM}	- Altitude rate limiter
\ddot{H}_{LIM}	- Altitude acceleration limiter
H _{RAD}	- Radar altitude
I_1	- Integrator #1
I_2	- Integrator #2
I_H	- Altitude integrator
I_v	- Airspeed integrator

KTHR	- Thrust to throttle handle gain ratio
N_{zcg}	- N_z sensed center of gravity for airplane
Q	- Pitch rate
\bar{Q}	- Dynamic pressure
QC	- Dynamic pressure
s	- Laplace transform
SPDH	- Speed hold mode flag
ΔT	- Sampling period
u	- Inertial speed
V	- True airspeed
\dot{V}	- True acceleration
V_c	- Airspeed command
\dot{V}_c	- Acceleration command
VF	- Filtered airspeed
\dot{V}_I	- Inertial acceleration
\dot{V}_{LIM}	- Acceleration command limit
VP	- True airspeed
W	- Weight of airplane
W_n	- Natural frequency

3.2 ABBREVIATIONS

BCA	- Boeing Commercial Airplanes
CAS	- Calibrated airspeed
c.g.	- Center of gravity
EPR	- Engine pressure ratio
4D	- Four-dimensional
FPA	- Flight path angle
GSE	- Glideslope error
IRU	- Inertial reference unit
LQG	- Linear quadratic gaussian
LQR	- Linear quadratic regulator
MCP	- Mode control panel
MPAC	- Control analysis and design package developed at Boeing
rhP	- Right half plane
SOE	- Speed on elevator
TAS	- True airspeed
TSRV	- Transport systems research vehicle
VTAS	- True airspeed

4.0 SETTING UP FLIGHT CONDITIONS AND AERO MODELS

This section contains flight conditions and the procedure by which these conditions were developed for this study. The first step in setting up flight conditions was to create a fairly accurate definition of the flight envelope from the operational manual of the 737-200 airplane. Tables 2 and 3 were generated from the data shown in Figure 2 (stall speeds) and Figure 3 (operational limits and placards).

Table 2. Light Weight - 80,000 lbs. with C. G. Variation of .05 to .3

FLAPS SETTING	V _{stall}	PLACARD SPEED	GEAR
0	128	—	UP
1	106	210	UP
5	100	210	UP
10	96	210	UP
15	94	195	UP
25	91	190	UP
30	89	185	DN
40	87	170	DN

Table 3. Heavy Weight - 110,000 lbs. with C. G. Variation of .05 to .3

FLAPS SETTING	V _{stall}	PLACARD SPEED	GEAR
0	150	—	UP
1	125	210	UP
5	118	210	UP
10	114	210	UP
15	110	195	UP
25	108	190	UP
30	106	185	DN
40	103	170	DN

J18-847

DI 4100 3740 ORIG. 5/71

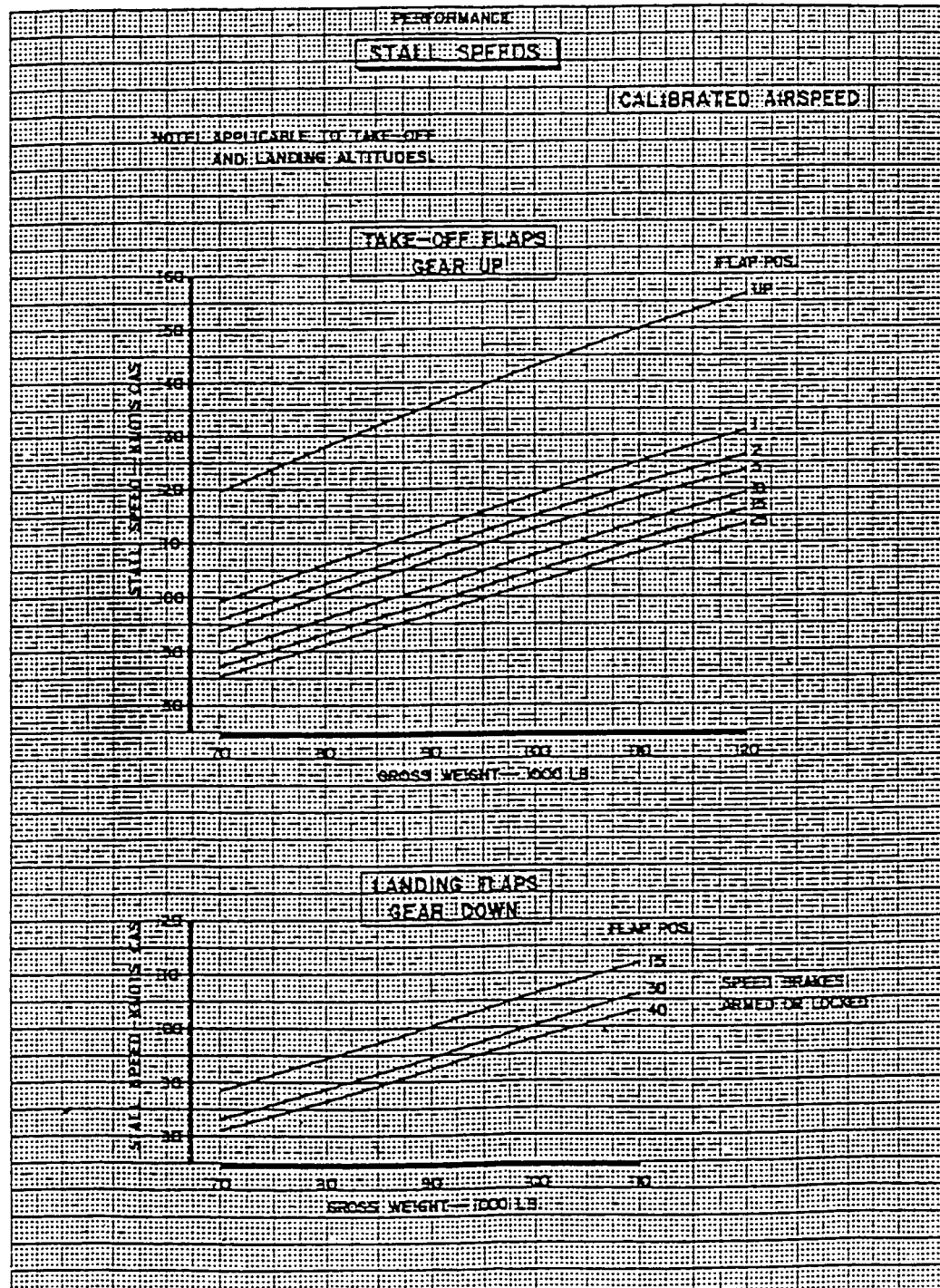


FIGURE 2.0-5

REV SYM

BOEING NO. D6-37208
PAGE 2.0-6



Figure 2. Stall Speeds

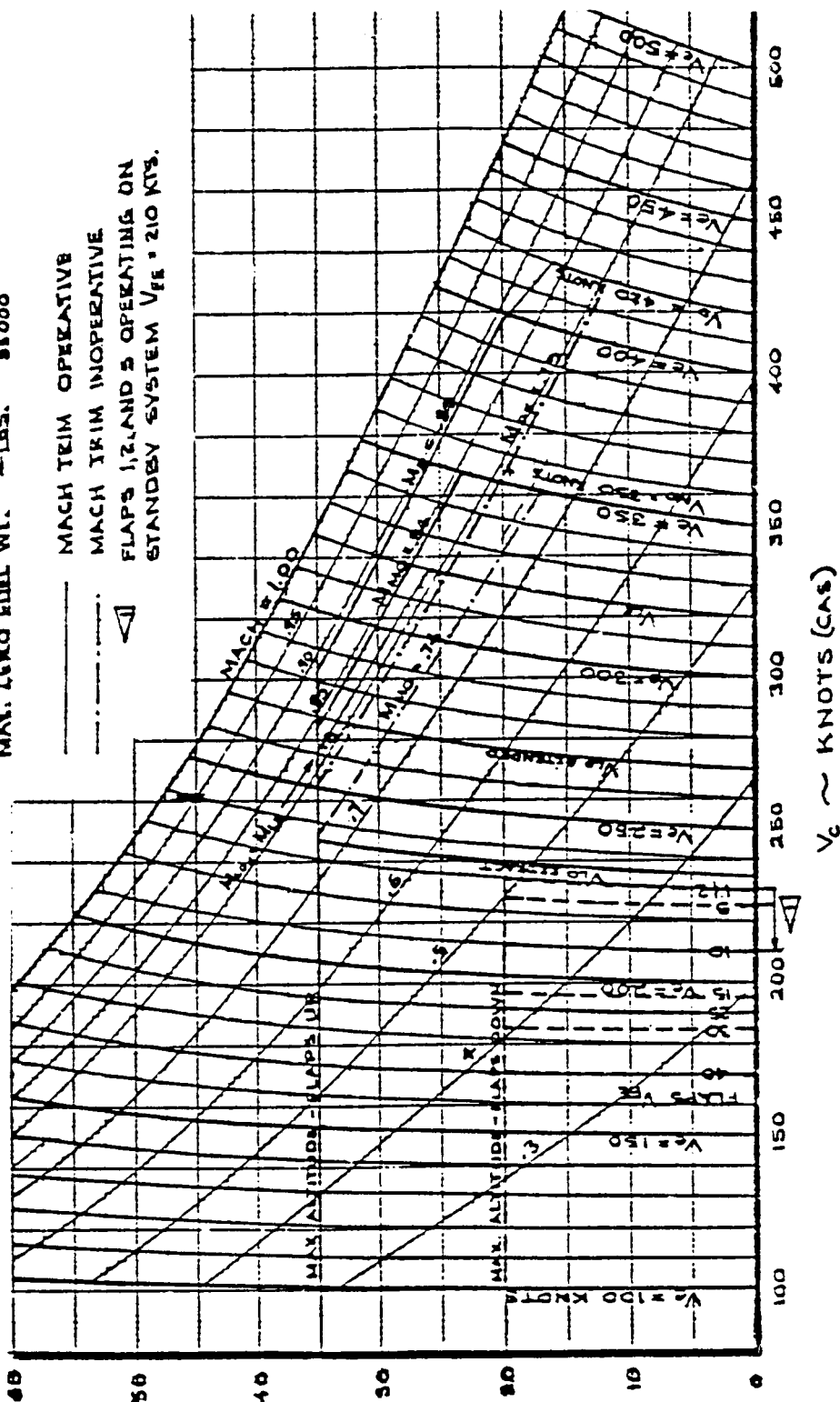


Figure 3. Operational Limits and Placards

FILE		REVISED	DATE	OPERATIONAL LIMITS AND PLACARDS	737-200 ADY
CHECK					06-37208
APP					
APP					
INK				THE BOEING COMPANY	PAGE 2.0-5

Using Tables 2 and 3, the operational envelope was defined by the flight condition files for:

- a. Cruise
- b. Cruise Transition
- c. Landing

4.1 CRUISE

The cruise flight conditions file was constructed using the following data (from Tables 2 and 3:

Flaps	-	0
Altitudes	-	10000 ft, 25000 ft and 35000 ft
Weights	-	maximum take-off weight and minimum in-flight weight plus 10000 lbs
C. G.'s	-	maximum forward and aft C. G.s (i.e., .05 and .3 respectively)
Gear	-	landing gear up
Speeds	-	The low speed limit for 1.3 g maneuver margin to initial buffet, maximum operating speed (M_{mo} or V_{mo}) or highest attainable Mach number, and two intermediate speeds (chosen such that there is equal Mach number spacing between the four Mach numbers).

4.2 CRUISE TRANSITION

The cruise transition flight conditions file was constructed using the following data along with Tables 2 and 3:

Flaps	-	1, 5, 10, 15, 25
Altitude	-	0 ft barometric altitude
Weights	-	maximum landing weight plus 10000 lbs and minimum in-flight weight plus 10000 lbs
C. G.s	-	maximum forward and aft C. G.s (i.e., .05 and .3 respectively)
Gear	-	landing gear up
Speeds	-	1.3 V_s (V_s = stall speed), V_{fp} = Flap Placard Speed, and two intermediate speeds (1.3 V_s and V_{fp} -chosen such that there is approximately equal Q_c spacing between the four speeds).

4.3 LANDING

The landing flight conditions of Glideslope and Flare were constructed using the following data along with Tables 2 and 3:

Flaps	-	30, 40
Altitude	-	0 ft. barometric altitude
Weights	-	maximum landing weight plus 10000 lbs and minimum in-flight weight plus 10000 lbs
C.G.s	-	maximum forward and aft C. G.s
Gear	-	landing gear down
Speeds	-	V_{app} , $V_{app} + 5$ kts, $V_{app} + 20$ kts (V_{app} = approach speed)

The definition and limitation of the parameters for these flight conditions varied slightly due to the trimming of the airplane on the Harris Simulation Computer. Table 4a-c show the detailed definitions of 48 flight conditions for cruise, 80 flight conditions for cruise transition, and 32 flight conditions for landing.

4.4 GENERATION OF THE OPEN-LOOP AIRPLANE MODELS

Each of the flight conditions was read to the Harris Simulator Computer and the program MATGEN (matrix generation) executed to obtain the A and B matrices of the linear airplane models. The A and B matrices were formed by perturbing predefined states and controls when MATGEN was run on the Harris Simulator.

The procedure for MATGEN on the Harris is:

- a. Aircraft is trimmed at specified flight condition.
- b. Perturb state or surface a small amount.
- c. Allow accelerations to settle.
- d. Store resultant changes in the airplane states.
- e. Develop an A matrix for each perturbation (i.e., positive perturbation, negative perturbation, and average of the two).
- f. Develop B matrix similarly to A for each control surface or discrete perturbed.

Table 4a. Cruise Flight Conditions

COND.	MACH	VE ₀	Q _e	VTAS	ALT.	C.G.	WEIGHT	GEAR	FLAPS
COND567890123456789012345678901234567890123456789012345678901234567890									
1	.30999	170.67	100.27	333.98	10000.	5.0000E-02	80000.	0.	0.
2	.41999	231.92	187.76	452.50	10000.	5.0000E-02	80000.	0.	0.
3	.52999	293.75	306.82	571.01	10000.	5.0000E-02	80000.	0.	0.
4	.63999	356.26	461.76	689.52	10000.	5.0000E-02	80000.	0.	0.
5	.30999	170.67	100.27	333.98	10000.	.3	80000.	0.	0.
6	.41999	231.92	187.76	452.50	10000.	.3	80000.	0.	0.
7	.52999	293.75	306.82	571.01	10000.	.3	80000.	0.	0.
8	.63999	356.26	461.76	689.52	10000.	.3	80000.	0.	0.
9	.36999	204.01	144.30	398.63	10000.	5.0000E-02	110000.	0.	0.
10	.45999	254.33	227.20	495.59	10000.	5.0000E-02	110000.	0.	0.
11	.54999	305.06	332.18	592.56	10000.	5.0000E-02	110000.	0.	0.
12	.63999	356.26	461.76	689.52	10000.	5.0000E-02	110000.	0.	0.
13	.36999	204.01	144.30	398.63	10000.	.3	110000.	0.	0.
14	.45999	254.33	227.20	495.59	10000.	.3	110000.	0.	0.
15	.54999	305.06	332.18	592.56	10000.	.3	110000.	0.	0.
16	.63999	356.26	461.76	689.52	10000.	.3	110000.	0.	0.
17	.47999	196.92	134.22	487.66	25000.	5.0000E-02	80000.	0.	0.
18	.53999	222.53	172.45	548.62	25000.	5.0000E-02	80000.	0.	0.
19	.59999	248.48	216.52	609.58	25000.	5.0000E-02	80000.	0.	0.
20	.83999	356.18	461.56	853.41	25000.	5.0000E-02	80000.	0.	0.
21	.47999	196.92	134.22	487.66	25000.	.3	80000.	0.	0.
22	.53999	222.53	172.45	548.62	25000.	.3	80000.	0.	0.
23	.59999	248.48	216.52	609.58	25000.	.3	80000.	0.	0.
24	.83999	356.18	461.56	853.41	25000.	.3	80000.	0.	0.
25	.55999	231.14	186.47	568.94	25000.	5.0000E-02	110000.	0.	0.
26	.65999	274.80	266.88	670.54	25000.	5.0000E-02	110000.	0.	0.
27	.74999	315.01	355.45	761.98	25000.	5.0000E-02	110000.	0.	0.
28	.83999	356.18	461.56	853.41	25000.	5.0000E-02	110000.	0.	0.
29	.55999	231.14	186.47	568.94	25000.	.3	110000.	0.	0.
30	.65999	274.80	266.88	670.54	25000.	.3	110000.	0.	0.
31	.74999	315.01	355.45	761.98	25000.	.3	110000.	0.	0.
32	.83999	356.18	461.56	853.41	25000.	.3	110000.	0.	0.
33	.54999	181.59	113.76	535.08	35000.	5.0000E-02	80000.	0.	0.
34	.64999	216.92	163.63	632.37	35000.	5.0000E-02	80000.	0.	0.
35	.74999	253.36	225.42	729.66	35000.	5.0000E-02	80000.	0.	0.
36	.83999	287.22	292.71	817.22	35000.	5.0000E-02	80000.	0.	0.
37	.54999	181.59	113.76	535.08	35000.	.3	80000.	0.	0.
38	.64999	216.92	163.63	632.37	35000.	.3	80000.	0.	0.
39	.74999	253.36	225.42	729.66	35000.	.3	80000.	0.	0.
40	.83999	287.22	292.71	817.22	35000.	.3	80000.	0.	0.
41	.65999	220.51	169.25	642.10	35000.	5.0000E-02	110000.	0.	0.
42	.71999	242.30	205.53	700.47	35000.	5.0000E-02	110000.	0.	0.
43	.77999	264.53	246.54	758.85	35000.	5.0000E-02	110000.	0.	0.
44	.83999	287.22	292.71	817.22	35000.	5.0000E-02	110000.	0.	0.
45	.65999	220.51	169.25	642.10	35000.	.3	110000.	0.	0.
46	.71999	242.30	205.53	700.47	35000.	.3	110000.	0.	0.
47	.77999	264.53	246.54	758.85	35000.	.3	110000.	0.	0.
48	.83999	287.22	292.71	817.22	35000.	.3	110000.	0.	0.

Table 4b. Cruise Transition Flight Conditions

[illegible]

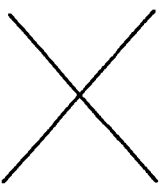
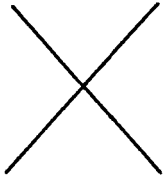
Table 4c. Landing Flight Conditions

COND.	MACH	VE ₀	Q _E	VTAS	ALT.	C.G.	WEIGHT	GEAR	FLAPS
COND567890123456789012345678901234567890123456789012345678901234567890									
1	.17536	116.00	45.908	195.78	100.	5.0000E-02	80000.	30.	1.
2	.21618	143.00	70.044	241.35	100.	5.0000E-02	80000.	30.	1.
3	.24793	164.00	92.467	276.80	100.	5.0000E-02	80000.	30.	1.
4	.27967	185.00	118.15	312.24	100.	5.0000E-02	80000.	30.	1.
5	.17536	116.00	45.908	195.78	100.	.3	80000.	30.	1.
6	.21618	143.00	70.044	241.35	100.	.3	80000.	30.	1.
7	.24793	164.00	92.467	276.80	100.	.3	80000.	30.	1.
8	.27967	185.00	118.15	312.24	100.	.3	80000.	30.	1.
9	.20862	138.00	65.180	232.92	100.	5.0000E-02	110000.	30.	1.
10	.23432	155.00	82.461	261.61	100.	5.0000E-02	110000.	30.	1.
11	.25700	170.00	99.470	286.93	100.	5.0000E-02	110000.	30.	1.
12	.27967	185.00	118.15	312.24	100.	5.0000E-02	110000.	30.	1.
13	.20862	138.00	65.180	232.92	100.	.3	110000.	30.	1.
14	.23432	155.00	82.461	261.61	100.	.3	110000.	30.	1.
15	.25700	170.00	99.470	286.93	100.	.3	110000.	30.	1.
16	.27967	185.00	118.15	312.24	100.	.3	110000.	30.	1.
17	.17083	113.00	43.547	190.72	100.	5.0000E-02	80000.	39.99	1.
18	.20257	134.00	61.418	226.16	100.	5.0000E-02	80000.	39.99	1.
19	.23281	154.00	81.386	259.92	100.	5.0000E-02	80000.	39.99	1.
20	.25700	170.00	99.470	286.93	100.	5.0000E-02	80000.	39.99	1.
21	.17083	113.00	43.547	190.72	100.	.3	80000.	39.99	1.
22	.20257	134.00	61.418	226.16	100.	.3	80000.	39.99	1.
23	.23281	154.00	81.386	259.92	100.	.3	80000.	39.99	1.
24	.25700	170.00	99.470	286.93	100.	.3	80000.	39.99	1.
25	.20257	134.00	61.418	226.16	100.	5.0000E-02	110000.	39.99	1.
26	.22525	149.00	76.122	251.48	100.	5.0000E-02	110000.	39.99	1.
27	.24037	159.00	86.834	268.36	100.	5.0000E-02	110000.	39.99	1.
28	.25700	170.00	99.470	286.93	100.	5.0000E-02	110000.	39.99	1.
29	.20257	134.00	61.418	226.16	100.	.3	110000.	39.99	1.
30	.22525	149.00	76.122	251.48	100.	.3	110000.	39.99	1.
31	.24037	159.00	86.834	268.36	100.	.3	110000.	39.99	1.
32	.25700	170.00	99.470	286.93	100.	.3	110000.	39.99	1.

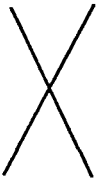
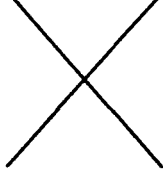
All states are perturbed ± 1 unit, except UA which is perturbed ± 5 ft/sec. All surfaces are perturbed ± 1 unit, except speed brake handle which is moved $\pm .5$ and engine thrust which is changed via throttle handle with movements of ± 100 lb.

The resultant A and B matrices are:

A MATRIX

	U	α	Q	θ	β	P	ϕ	R
$\frac{dU}{dt}$	LONGITUDINAL							
$\frac{d\alpha}{dt}$								
$\frac{dQ}{dt}$								
$\frac{d\theta}{dt}$								
$\frac{d\beta}{dt}$					LATERAL			
$\frac{dP}{dt}$								
$\frac{d\phi}{dt}$								
$\frac{dR}{dt}$								

B MATRIX

	DE	DSPL	DTH	AIL	RUD
$\frac{du}{dt}$	LONGITUDINAL				
$\frac{d\alpha}{dt}$					
$\frac{dQ}{dt}$					
$\frac{d\theta}{dt}$					
$\frac{d\beta}{dt}$				LATERAL	
$\frac{dP}{dt}$					
$\frac{d\phi}{dt}$					
$\frac{dR}{dt}$					

The A and B matrices are then expanded to include additional states and wind disturbances and the output matrices, C and D, are formed.

For the longitudinal axis, the altitude state, H, is added to the A matrix and gust disturbances, U_g and α_g , are added to the B matrix. For the lateral directional axis the yaw and lateral position deviation states, ψ and y , are formed and added to the A matrix, and β_g is added to the B matrix; the outputs $\dot{\beta}$, N_y , \dot{R} and ψ_{GT} are formed and used to derive the C and D matrices. The final ABCD matrices for each axis of each flight condition are then printed. Figures 2 and 3 show a sample case of longitudinal axis ABCD matrices and lateral directional ABCD matrices respectively.

5.0 CONTROL DESIGN METHODOLOGY

This section presents the control system design methodology used for this task. This design methodology has been developed jointly by the Boeing Advanced Systems (BAS) flight controls research and the Boeing Commercial Airplanes (BCA) guidance and control research groups. Sections 7 and 8 document the application of this design approach to the longitudinal and lateral axes of the NASA TRSV airplane respectively. A model emulating the integral linear quadratic gaussian control design technique is used in conjunction with a systematic top down approach. Strong emphasis is placed on understanding the dynamics of the open loop airplane (including coupling, controllability, and observability) and the control task requirements in order to develop specific design requirements that are responsive to the guidance and control problems without overly constraining the problem or violating the controllability limits of the open loop system. The following paragraphs highlight the key ingredients of this Boeing control system design methodology which are presented in the order that these ingredients are used during the design process.

5.1 SPECIFY DESIGN OBJECTIVES

The first step in designing of a control system is to specify the top level design objectives. These start with the vehicle mission goals. For example, the number of passengers, the range of operation, the range of the flight envelope, and the relative importance of speed, fuel economy, ride comfort, and safety.

Although the controls engineer may not have any input in the initial development of the mission goals, it is important that these objectives be understood. All successive requirements, both those imposed upon and those developed by the controls engineer, must be responsive to the top level mission goals. Specifically, the definition of the airplane configuration and the architecture of the control system must be in keeping with the vehicle mission goals. In some instances, it may be the responsibility of the controls engineer to indicate whether the vehicle configuration or the the control system architecture may impede in achieving the top level mission goals that the control system design cannot overcome alone. When this is the case, a thorough understanding of the airplane and its mission goals will allow the engineer to make such a determination.

The goals for the control system are derived directly from the vehicle mission goals. An example of this is automatic landing in which modern commercial aircraft must operate in conditions where normal piloted landings are not possible because the pilot cannot see the ground to judge the approach. In order to continue operation in severely reduced visibility conditions, the plane must be able to land on its own. Therefore the requirements for an automatic landing system follow directly for the mission goal to be able to operate in dense fog.

The pilot/airplane interface must be defined once the top level control system goals have been determined since the mission and control system goals place demands on the airplane control system. The pilot, by the nature of his job, is an integral part of the system that controls the airplane. The control task must be divided between the pilot and the flight control system. The days when there was a sharp delineation between manual flight and autopilot flight on commercial transport aircraft are gone. Today the control systems on modern commercial aircraft have active stability augmentation systems, in the form of yaw dampers, operating during the entire flight (including manually piloted flight). Up front definition of the pilot/airplane interface is essential since the controller design process steps, as described in the following paragraphs, are highly dependent on the pilot/airplane interface definition.

A significant feature of the design methodology is separation of the feedforward and feedback controllers. Integral feedback is used to decouple steady state responses and provide the needed bandwidth and damping. The feedforward controller is used to decouple and shape the transient responses. The design task is split into two subtasks. First, the feedback controller is designed to achieve the desired stability characteristics, and then the feedforward controller is designed. The stability characteristics of the closed loop system are not affected by feedforward controller modifications because of the separation inherent in the controller structure. Within the bandwidth limitations of the feedback controller, the transient response and performance characteristics of the augmented airplane can be modified without affecting the stability and disturbance rejection characteristics.

5.2 FORMULATE DESIGN REQUIREMENTS

Once the design objectives are defined, the next step is formulation of the specific design requirements. The requirements must be responsive to the design objectives, as described in Section 2, without being overly constraining. Each design requirement must be traceable back to the design objective that motivated it.

Separation of the feedforward and feedback controllers allows for a similar separation of the feedforward and feedback design requirements. The feedforward controller must be responsive to the command response characteristics while the feedback controller must meet the disturbance rejection and robustness requirements.

5.3 OPEN LOOP ANALYSIS

A complete understanding of the open loop airplane is necessary prior to designing the controller. Open loop analysis gives insight into the difficulty of achieving the design requirements before launching into the detailed design cycle. Characteristics of the open loop system that will render the design requirements unachievable (e.g., insufficient control authority) can be identified rapidly.

The specific open loop analyses performed are: eigenstructure decomposition, controllability analysis, observability analysis, computation of open loop frequency responses, and open loop time domain simulation. Each of these analysis tools provides a different look at the characteristics of the open loop system. In many cases the information provided by one type of analysis is the same as that provided by another. The objective of open loop analysis is to provide sufficient perspectives of the open loop system to allow the designer on understanding of the system characteristics in order to design a controller. The more that is understood of the system prior to designing, then the more efficiently the designer will be during the design phase. Each of these analysis tools is described in paragraphs 5.3.1 - 5.3.5.

5.3.1 EIGENSTRUCTURE DECOMPOSITION

Eigenstructure decomposition reveals the open loop mode shapes and their frequencies. Many of the design requirements can be translated into constraints on the closed loop eigenstructure. Knowledge of the open loop eigenstructure and the desired closed loop eigenstructure reveals the magnitude of the controller task in terms of how much the eigenstructure must be changed.

5.3.2 CONTROLLABILITY ANALYSIS

Controllability analysis consists of computing and analyzing the controllability matrix. The controllability matrix, as used here, is the B matrix of the modalized open loop model:

$$\text{Controllability matrix} = T^{-1} B$$

where

T = modal transformation matrix

B = input-to-state rate matrix

This analysis reveals the effect of each of the open loop system inputs on the each of its modes. Modes whose eigenstructure cannot be modified, because none of the inputs affects them, can be identified. Control inputs with identical effect on the eigenstructure, and thus only a single degree of input freedom among them, can be identified.

5.3.3 OBSERVABILITY ANALYSIS

Observability analysis is the output dual of controllability analysis. The observability matrix is the C matrix of the modalized open loop model:

$$\text{Observability matrix} = C T$$

where

C = state-to-output matrix

T = modal transformation matrix

The observability matrix indicates which modes are measurable via which outputs. In order for an open loop mode to be successfully modified via feedback control, it must be both observable and controllable.

5.3.4 FREQUENCY RESPONSE

Two types of open loop frequency responses are computed: control effector responses and disturbance input responses. The control effector responses show the effect of the control inputs on the airplane states and outputs. These analyses reveal the ability of each control input to control the various airplane states and outputs at different frequencies. The phase relationships reveal the need for lead or lag compensation when using classical design techniques.

The disturbance response characteristics revealed by the second set of open loop frequency responses illustrate the need for active disturbance rejection. Often closed loop disturbance

response requirements can be met without active compensation if the open loop responses are sufficiently small. Active control will be required for all outputs whose open loop responses to disturbances fail to meet the closed loop requirements.

5.3.5 TIME DOMAIN SIMULATION

Open loop time domain simulation is used to understand the characteristic responses of the open loop system to control and disturbance inputs. Although the information revealed via simulation is the same as that given for frequency response analysis, some designers are more familiar with the time domain.

5.4 CONTROLLER STRUCTURE

The control structure used for this design task (see Figure 4) is a two-degree-of-freedom approach which maintains separation between the feedforward and feedback controllers. The function of the feedback controller is to provide the necessary stability augmentation, sufficient command response bandwidth to satisfy the performance requirements, and robustness to parameter uncertainties. Whereas the function of the feedforward controller is to shape the pilot inputs such that the closed-loop performance requirements are met.

The feedback controller has a full state integral structure. A regulated variable is chosen for each independent control input (see paragraph 5.5.2). The feedback controller places an integrator on each of the regulated variables that is not itself the output of an integrator within the open loop system. The feedback gain matrix contains gains from each of the open loop model states and the regulated variable integrators to each of the independent control inputs. Feedback signal estimation is included for those signals not directly available over the required frequency range using sensor outputs.

The feedforward controller consists of an ideal model defining the desired regulated variable response to each pilot input command. Command limiting, envelope protection, and transient smoothing are all part of the feedforward controller. In some cases the feedforward controller will send cross feeds to two different regulated variables to decouple the closed-loop responses. An example of this would be to feed the heading command to sideslip and improve turn coordination during turn initiation. Separation of the feedforward and feedback controllers

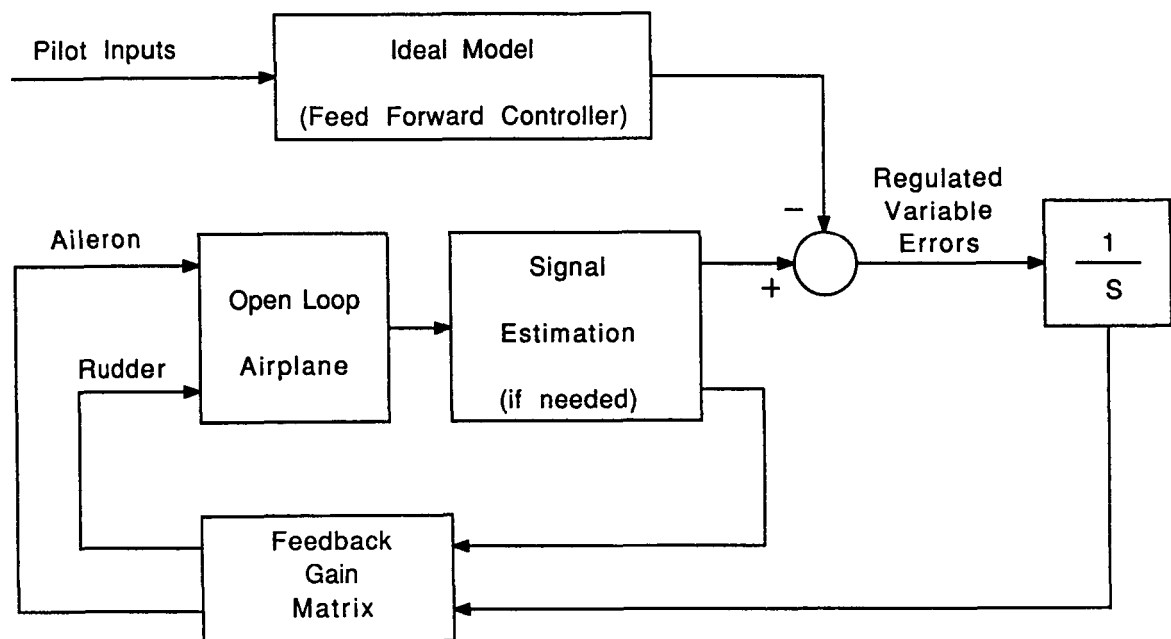


Figure 4. Two - Degrees - of - Freedom Controller Structure

High gain at low frequency will result in large penalties for steady state errors. The Riccati solution will provide good steady state tracking. Low gain at high frequency will result in small penalties for high frequency errors. The Riccati solution will ignore high frequency errors, thus avoiding excessive bandwidths that would lead to input actuator limiting.

Since the synthesis model is square (i.e., the number of inputs equals the number of outputs), its transmission zeros can be computed. With LQG design, the transmission zeros of the synthesis model designate the asymptotic locations for the closed loop poles. Furthermore, zeros created when forming criteria outputs become transmission zeros of the synthesis model. This feature is used during criteria output formation to establish targets for closed loop poles whose open loop characteristics are not satisfactory. An example is the pair of complex zeros added to the sideslip criterion output to attract the dutch roll mode.

The primary concerns during formation of the criteria outputs are the input/output frequency response shape (gain and phase) and the placement of transmission zeros. Selection of the weighting values (see paragraph 5.6) is used to scale the magnitudes of the synthesis model input/output frequency responses.

5.6 COST FUNCTION WEIGHTINGS, CONTROLLER GAINS, AND GAIN SCHEDULING

Once the synthesis model is formed, the next task is to determine the feedback gains by choosing the cost function weightings, solving the Riccati equation to specify the gains, and using gain scheduling to define the controller for a range of flight conditions. The emphasis with this design methodology is directed at making the tasks described herein as simple as possible. The bulk of the design effort is spent designing the criteria outputs. Once the synthesis model is complete, computation of the feedback gains is automated by the Riccati equation.

5.6.1 COST FUNCTION WEIGHTINGS

For LQG design the synthesis model is used by the Riccati equation in conjunction with diagonal input and output weighting matrices to minimize the following quadratic cost function:

$$J = 1/2 \quad (Q^T y Q + R^T u R) \, d$$

isolates the stability and performance characteristics of the closed loop system. Modifications made to the feedforward controller will not affect system stability.

5.5 SYNTHESIS MODEL DEFINITION

The synthesis model is used as an input to the Riccati equation which solves for the full state feedback gains. The synthesis model is built using the open loop model as its core. Criteria outputs are formed for output weighting with the Riccati equation.

5.5.1 INDEPENDENT INPUTS

The first step in forming the synthesis model is identification of the independent control inputs to be driven by the controller. It is important to verify via controllability analysis that the selected inputs are independent. For the longitudinal and lateral examples presented in Sections 7 and 8, two independent control inputs are used in each case: elevator and throttle are used for the longitudinal design, whereas ailerons and rudder are used for the lateral design.

5.5.2 REGULATED VARIABLES

Once the independent inputs are chosen, the next task is selection of regulated variables. A regulated variable is one that is to be controlled in steady state. One regulated variable is chosen for each independent input. Regulated variables must be available as sensor outputs (or estimates) for feedback. Of particular importance is the low frequency integrity of regulated variable signals since they will be integrated to provide steady state tracking. In the longitudinal case, the regulated variables are altitude and speed. Heading and sideslip are used for the lateral axis synthesis model.

5.5.3 CRITERIA OUTPUTS

The final step in building the synthesis model is formation of the criteria outputs. One criteria output is formed for each regulated variable. An integrator is added to each regulated variable output that is not itself the output of an integrator in the open loop system. Criteria outputs are then formed by adding together the regulated variable, its integrator, and any other open loop system outputs. Scaling between the signals that compose each criteria output are chosen with the objective of constructing the criteria outputs such that the frequency responses from the inputs to the criteria outputs exhibit high gain at low frequency and roll off at high frequency.

where

y = vector of criteria outputs

u = vector of control inputs

Q = diagonal criteria output weighting matrix

R = diagonal control input weighting matrix

The diagonal Q matrix weights the criteria outputs which are composed of linear combinations of the synthesis model states. The same cost function could be realized by applying the appropriate full Q' matrix to the synthesis model state vector. The design process used here simplifies the weighting matrix selection task, without loss of generality, by first forming criteria outputs and then using a diagonal Q rather than the full Q' along with the state vector.

Cost function weightings are used to place the bandwidth of the closed-loop system. Increasing the weighting on an input will lower the bandwidth, while increasing an output weighting will increase the bandwidth. The degree to which changing the relative weighting magnitude between inputs (or outputs) changes the closed-loop system will depend on the coupling within the synthesis model. Relative weighting magnitude will determine the level of cross coupling of the closed loop response. For example, the amount of sideslip response to a heading command.

Initial values for the weighting matrices are chosen by looking at the open loop frequency responses of the synthesis model. The closed loop bandwidths will be approximately the same as the bandwidths of these open loop responses. Iteration is used, looking at the closed-loop system characteristics, to arrive at the final set of weightings.

5.6.2 CONTROLLER GAINS AND GAIN SCHEDULING

Once the weighting matrices are selected the feedback gains are computed using the Riccati equation. The gain matrix that results is specific to the flight condition of the open loop model used to form the synthesis model. The next task is to define the feedback controller gains to meet the design requirements throughout the flight envelope.

The longitudinal and lateral controller design examples found in Sections 7 and 8 respectively illustrate two different approaches to gain scheduling. The technique used for the longitudinal axis takes the Riccati solution for one middle-of-the-envelope flight condition and schedules it

based on flight condition parameters known to influence the airplane dynamics and control effectiveness (e.g., such as dynamic pressure and speed) in deriving a definition for gains that meets the requirements throughout the envelope.

The gain scheduling technique used for the lateral controller example first solves the Riccati equation in determining the optimal gains at each flight condition. Whenever possible, the same set of criteria outputs and weighting matrices is used for all flight conditions. A check is made to make sure that the Riccati solution at each condition provides a closed-loop system that meets the design requirements. Gain schedules are then developed by plotting each gain against a number of flight condition parameters by choosing the plot showing the greatest level of correlation and curve fitting the data.

5.7 SENSOR SELECTION AND OUTPUT FILTERING

The gain matrices produced in paragraph 5.6 include feedback gains from all of the synthesis model states to each of the control inputs. The next task is for sensor selection and output filtering to provide the necessary feedback signals. State signals that are available directly from sensors are fed directly to the gain matrix.

Some states will be measurable over different frequency ranges using different sensors. For those states, complementary filters can be used to combine low frequency data from one source with high frequency data to another source. An example of this is altitude feedback where barometric altitude is used for low frequencies complemented by vertical acceleration data to provide high frequency information.

Other states may not be directly measurable and require estimation. Although the design examples presented here do not include any such states, either full order Kalman estimation or reduced order estimation could be used if the need arose.

5.8 CLOSED LOOP ANALYSIS

The chief objective of closed loop analysis is to verify that the design requirements have been met. In the event that the requirements are not met, closed-loop analysis should identify the problem areas to focus the design effort. Although different types of closed-loop analysis will

be used depending on the types of requirements in place, the analysis techniques described in paragraphs 5.8.1 - 5.8.6 will be sufficient to verify compliance with most design requirements.

5.8.1 EIGENVALUES

Computation of the closed-loop eigenvalues verifies compliance with mode frequency and damping ratio requirements.

5.8.2 BROKEN LOOP FREQUENCY RESPONSES

Gain and phase margins are determined via broken loop frequency analysis. The closed-loop system is broken, one loop at a time, at the input to each actuator and at each sensor output. Compliance with gain and phase margin requirements is verified by computing the margins for the resulting broken loop system.

5.8.3 SINGULAR VALUE ANALYSIS

In many cases the traditional robustness measures, gain and phase margins are not adequate because they are usually used on one loop at a time, thus overlooking the problem of simultaneous variations in different loops or, more generally, different system parameters. In their place, singular value analysis has been developed. Although singular value analysis is not used in the example designs presented in Sections 7 and 8, since it is not required by the design requirements (see Section 5), a brief description is included here for completeness.

Singular value analysis is a multiple input/multiple output extension of classical single loop gain and phase margin analysis. Singular value analysis identifies the tendency of the system toward singularity (instability) for variations in more than one loop at a time rather than the one loop at a time structure for phase and gain analysis. An extension of singular value analysis, (i.e., structured singular value analysis) allows the designer to analyze the system for robustness to variations of specified structures.

5.8.4 COVARIANCE RESPONSE

Covariance response analysis predicts the RMS response of closed-loop system states and outputs to wind disturbance inputs. Wind turbulence is modelled as filtered white noise. The two most widely used turbulence models are Von Karman and Dryden filters. Each defines the

frequency content and magnitude of each component of six degree-of-freedom (three translational and three rotational velocities) air turbulence as a function of altitude, speed, and turbulence severity.

After appending the appropriate wind model to the closed-loop airplane model, the covariance of the complete system to white noise is computed. The resulting response level data for airplane states, outputs, and control surface inputs are checked against the design requirements to verify that ride quality is within the required bounds and to control input activity levels.

5.8.5 COMMAND FREQUENCY RESPONSE

Closed loop frequency response analysis from pilot inputs to airplane states and control surfaces is used to check for compliance with performance requirements. Command response bandwidths must be at least as high as required without excessive control input activity (which might drive actuators into saturation) or high vehicle accelerations (exceeding structural or passenger comfort levels).

5.8.6 TIME DOMAIN SIMULATION

The final type of closed-loop analysis is time domain simulation. Often control system performance requirements are defined in terms of time histories. These requirements are verified via time domain simulation. In addition, all of the other analysis techniques are restricted to linear (or linearized) systems. Time domain analysis allows for inclusion of complex nonlinearities that cannot be properly treated using other analysis methods.

5.9 ITERATION TO SATISFY DESIGN REQUIREMENTS

An important feature of this, and any, design process is the iteration to satisfy all of the design requirements. The nature of control system design is making the trade-offs between control activity, performance level, and robustness to uncertainties and unmodelled dynamics. No single pass design methodology would be able to sufficiently explore and optimize this trade-off.

5.10 SUMMARY OF DESIGN METHODOLOGY

The strength of this controller design methodology is that it provides the power of LQG design in a way that is understandable from a classical frequency domain point of view. The intuition and experience of classical design is merged with the ability of LQG design to efficiently handle multiple input / multiple output design problems. Standard analysis tools have been employed to provide insight via open loop analysis. Historically proven frequency domain compensation techniques are used to form the criteria outputs completing the synthesis model. Once the synthesis model is complete, the Riccati equation is used to simultaneously solve for the complete set of feedback gains. After closing the loop, traditional analysis tools are used once again to verify compliance with design requirements. In addition, singular value and structured singular value analysis may be used to analyze multiple loop robustness.

6.0 DESIGN REQUIREMENTS

The design requirements to be met by the controller consist of two sets: 1) the feedforward requirements based on ideal model specifications, passenger comfort and airplane dynamics constraints, and 2) the feedback requirements based on stability and performance robustness specification. These two distinct sets of requirements dictate the feedforward/feedback structure of the resulting controller.

The design requirements for the longitudinal and lateral axes are presented separately in paragraphs 6.1 and 6.2, respectively.

6.1 LONGITUDINAL AXIS DESIGN REQUIREMENTS

A. Feedforward Loop

1. Duplicate modes available in TECS
 - a. speed hold (Mach, CAS)
 - b. altitude hold
 - c. glideslope capture and hold
 - d. flare
 - e. go-around
 - f. flight path angle (FPA)
2. Provide necessary command limiting to ensure
 - a. passenger comfort
 - b. proper energy distribution when throttles are at the limit

B. Feedback Loop

1. Robust Stability
 - a. Gain margin of at least ± 6 dB, and phase margin of at least ± 45 deg in all control and sensor loops.
 - b. Sufficient rolloff in elevator loop at higher frequencies to avoid exciting unmodelled dynamics.
 - c. Minimum phugoid damping ratio .55, minimum short period damping ratio .4.

2. Robust Performance

- a. Command loop bandwidth:
 - 0.6 - 1.2 rad/sec in cruise for both altitude and speed command loops
 - 1 - 1.2 rad/sec in landing for altitude command loop
 - .4 - .6 rad/sec in landing for speed command loop
- b. Control loop bandwidth:
minimum required to achieve command loop bandwidth requirements.
- c. Gust response:
same or better than TECS.

It should be noted here, that in defining the requirements, TECS was used as a baseline, and the term "robust" should be interpreted to mean "throughout the flight envelope".

6.2 LATERAL AXIS DESIGN REQUIREMENTS

A. Performance Requirements

1. Zero Steady State Error
 - a. Heading error when in heading mode.
 - b. Localizer cross track error when following ILS localizer beam.
 - c. Steady crosswind should not cause steady state errors in either mode.
2. Zero Time Domain Overshoot
 - a. Heading overshoot when in heading mode.
 - b. Localizer beam overshoot when following ILS localizer beam
(assuming capture is initialized with sufficient space to turn onto the beam without crossing the center line).
 - c. Steady crosswind should not cause overshoot in either mode.
3. Response Limitations
 - a. Bank angle not to exceed 30 degrees during maneuvers.
 - b. Lateral acceleration (nominally zero) not to exceed 0.05 g for maneuvers in still air.
4. Bandwidth Requirements
 - a. Maximize response bandwidths within limitations on overshoot, surface activity, eigenvalues, and disturbance responses.

B. Control Activity Requirements

1. Aileron Activity
 - a. Position not to exceed ± 15 deg
 - b. Rate not to exceed ± 30 deg/sec
2. Rudder Activity
 - a. Position not to exceed ± 15 deg
 - b. Rate not to exceed ± 30 deg/sec

C. Gust Response Requirements

Gust response upper bounds given here are RMS values in response to a lateral Dryden gust with 1 ft/sec RMS intensity. Units are feet and degrees where appropriate.

1. Heading and Sideslip Angular Responses
 - a. Psi not more than 0.2 deg RMS
 - b. Beta not more than 0.2 deg RMS
2. Heading and Sideslip Angular Rate Responses
 - a. Psi not more than 0.2 deg/sec RMS
 - b. Beta not more than 0.2 deg/sec RMS
3. Aileron and Rudder Angular Position Responses
 - a. Aileron not more than 1.0 deg RMS
 - b. Rudder not more than 1.0 deg RMS
4. Aileron and Rudder Angular Rate Responses
 - a. Aileron not more than 2.0 deg/sec RMS
 - b. Rudder not more than 2.0 deg/sec RMS
5. Localizer Cross Track Response
 - a. Position not more than 5 ft
 - b. Rate not more than 5 ft/sec

D. Robustness Requirements

1. Eigenvalues

- a. All eigenvalues, 0.4 damping or better
- b. Dominant eigenvalues, (lowest frequency), 0.6 damping or better

2. Stability Margins

- a. Aileron input: simultaneous ± 6 dB and ± 45 deg
- b. Rudder input: simultaneous ± 6 dB and ± 45 deg
- c. All sensor inputs: simultaneous ± 6 dB and ± 45 deg.

7.0 LONGITUDINAL AXIS DESIGN

The longitudinal controller structure reflects the design requirements discussed in paragraph 6.1 and consists of the feedforward and feedback loops.

The feedforward controller receives pilot commands through the Mode Control Panel (MCP) and generates altitude, altitude rate, speed and speed rate commands, which the feedback regulator loop must track. The decision to have both position and rate commands was made in order to follow TECS structure as close as possible, and also to be compatible with 4D mode (time and space) if one is added in the future.

The feedback regulator receives both feedforward commands and airplane sensor signals from which it generates elevator and throttle commands. Figure 5 shows the general structure of the control system as well as all the major interfaces. The pilot, via MCP, selects the mode he wants the airplane to fly by entering the desired altitude and speed targets. At any given time, only two modes can be engaged: one speed mode and one altitude mode (i.e., each mode generates either speed or altitude commands). Hence, the feedback regulator has a common interface with all feedforward modes.

7.1 FEEDFORWARD MODES

Each feedforward mode shown in Figure 5 will be described in detail in the following paragraphs.

7.1.1 ALTITUDE HOLD MODE

The altitude hold mode is a direct engage mode, (i.e., when pilot engages this mode any other mode that controls altitude is automatically disengaged) consisting of a second order filter which limits the first and second derivatives of altitude command (i.e., altitude rate and acceleration). The bandwidth of the filter is selected to assure proper altitude command response. The filter receives an altitude target from MCP and generates altitude and altitude rate commands for the feedback regulator as shown in Figure 6. The transfer functions from altitude target to filter outputs are:

$$F(\dot{H}_C, H_{MCP}) = \frac{s W_n^2}{s^2 + 2\xi W_n s + W_n^2} \quad (1)$$

and

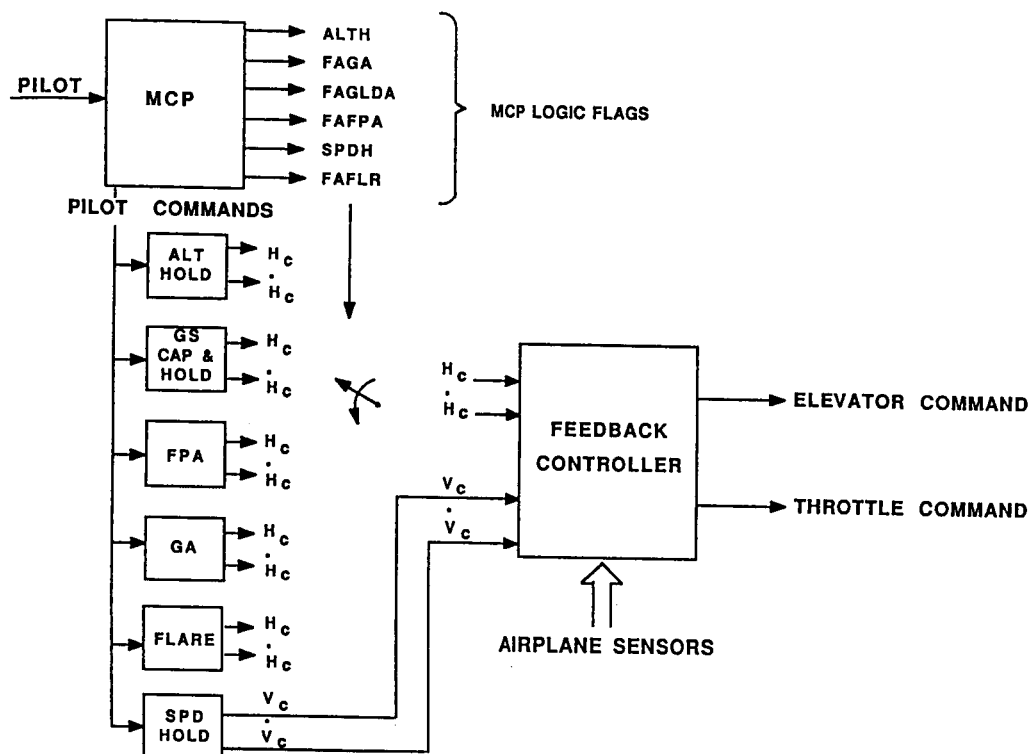
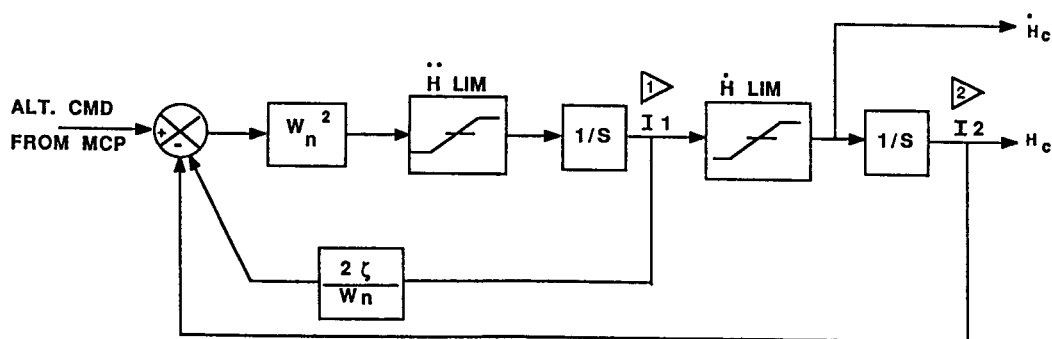


Figure 5. Controller Structure



$$\dot{H} \text{ LIM} = \pm (|\dot{H}_{DOT}| + 10)$$

$$W_n = .15$$

$$\ddot{H} \text{ LIM} = 0.05g = 1.6 \text{ fps}^2$$

$$\zeta = 1$$

$$\text{1} \quad \text{IF (NOT. ALTH) } I1 = \dot{H} \text{ LIM TECS}$$

$$\text{2} \quad \text{IF (NOT. ALTH) } I2 = H$$

Figure 6. Altitude Hold Mode

$$\frac{H_c}{H_{MCP}} = \frac{W_n^2}{s^2 + 2\xi W_n s + W_n^2} \quad (2)$$

where

$$\xi = 1$$

$$W_n = .15$$

The altitude rate limit (\dot{H}_{LIM}) taken from TECS is rather loose, $\dot{H}_{LIM} = \pm (|\dot{H}_{LIM}| + 10)$, hence the \dot{H} signal will rarely be on the limit. (\ddot{H}_{LIM}) is much stricter: $\ddot{H}_{LIM} = \pm .05 g$ and is introduced to ensure passenger comfort. The value of this limit was selected so as to never command a total of more than .1g during simultaneous altitude and speed command changes, since speed command second derivative is also limited to .05g.

When the airplane is not in the altitude hold mode, the \dot{H} integrator (I1) should be initialized to current altitude rate, and the H integrator (I2) to current altitude.

It should be noted that the natural frequency of the filter was selected to be slightly higher than the required altitude command bandwidth of .06 to .12 rad/sec ($W_n = .15$). W_n was adjusted to ensure an overshoot free linear response of the total control system to pilot commands. Since in nonlinear situations the filter will be on the \ddot{H} limit most of the time, the value of W_n is not of great importance.

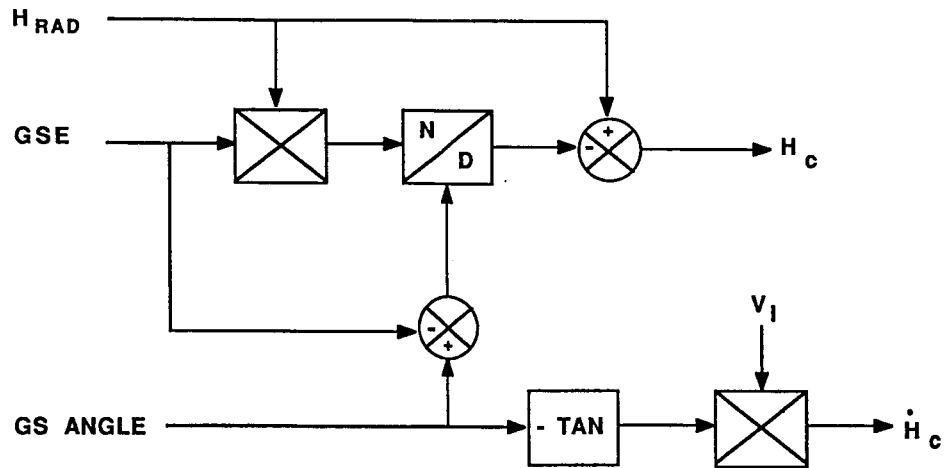
7.1.2 GLIDESLOPE CAPTURE AND HOLD

The glideslope mode shown in Figure 7a is a direct arm/automatic engage mode (i.e., when the pilot receives a valid glideslope signal he arms the glideslope mode). Glideslope capture is automatically engaged and disengages any previous mode when a certain criteria is satisfied.

To understand how the glideslope mode works, one must have a clear picture of glideslope geometry (i.e., the position of the airplane with respect to glideslope beam and the variable definitions associated with it). The glideslope geometry is shown in Figure 7b.

The valid glideslope signal received by the onboard receiver is the glideslope error (GSE) or the angular deviation of the airplane's flight path from glideslope beam centerline. Based on

DIRECT ARM / AUTOMATIC ENGAGE MODE



GLIDESLOPE CAPTURE CRITERIA:

$$\text{IF } ((H_E/15 + (\dot{H}_c - \dot{H})) H_E/15 \text{ .LT. } 0) \text{ FAGLD} = 1$$

GLIDESLOPE HOLD CRITERIA:

$$\text{IF } (|H_E| \text{ .LT. } 10 \text{ .AND. } |\dot{H}_c - \dot{H}| \text{ .LT. } 3) \text{ FAGLDH} = 1$$

Figure 7a. Glideslope Capture and Hold Mode

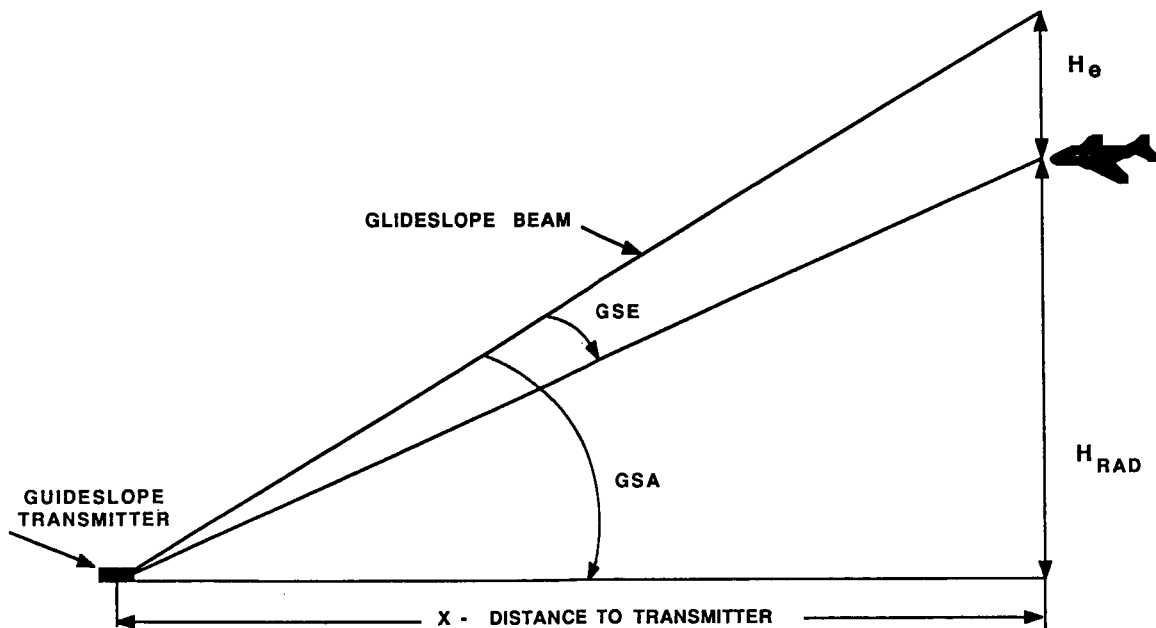


Figure 7b. Glideslope Geometry

glideslope geometry, the GSE angle is converted into altitude error (H_e) and the valid altitude command is then computed:

$$H_c = H_{RAD} + H_e \quad (3)$$

The H command is computed to avoid switching inside the feedback loop, (since GSE is an error signal) and maintaining the uniformity of the feedback/feedforward interface. Its computation is based on the assumption that the glideslope angle is known and usually equal to 3 degrees.

Computation of H_e and \dot{H} are presented in Appendix A.

The glideslope capture criterion is based on the feedback regulator structure, namely, the altitude integrator computation, shown in Figure 7c.

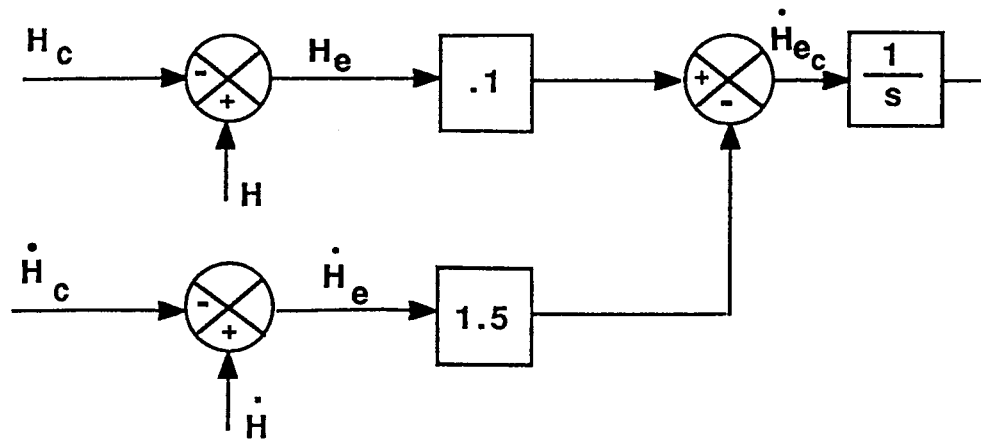


Figure 7c. Altitude Integrator Command Computation

The airplane is on the overshoot-free glideslope capture envelope when $\dot{H}_{e_c} = 0$, or

$$.1 H_e + 1.5 \dot{H}_e = 0$$

or

$$1/15 H_e + \dot{H}_e = 0$$

(4)

When (4) is zero, the expression $H_e/15 \cdot (H_e/15 + \dot{H}_e)$ changes sign. This criterion is used to set glideslope engage flag (FAGLD).

The feedback regulator has two separate sets of gains: one for cruise and one for landing. The switch between the two occurs when the airplane is on the glideslope beam. The successful capture of the beam is determined by the following criterion: $|H_e| < 10$ ft and $|\dot{H}_e| < 3$ ft/sec. When this criterion is satisfied, the glideslope hold flag (FAGLDH) is set, and the landing gains replace the cruise ones.

7.1.3 FLARE MODE

The flare mode is an automatic engage mode and is engaged at 45 feet above the runway. The mode generates an inertial altitude path to land the airplane 1200 feet from the flare engagement point as shown in Figure 8.

An extensive study of autoland flare control has been done by A. Lambregts et al for the NASA TSRV airplane [7]. The study concluded that inertial path tracking is a better way to accomplish low touchdown dispersion. This recommendation has been followed in this design.

An inertial path must satisfy four boundary constraints: at flare engagement, the altitude command must equal 45 feet and the altitude rate command must equal the current descent rate of the airplane, and at touchdown, the altitude command must be zero and altitude rate command must equal -2.5 fps. The algebraic function selected to satisfy these constraints was a hyperbola, as depicted in Figure 8. The computation of the polynomial coefficients A, B, C and D can be found in Appendix A.

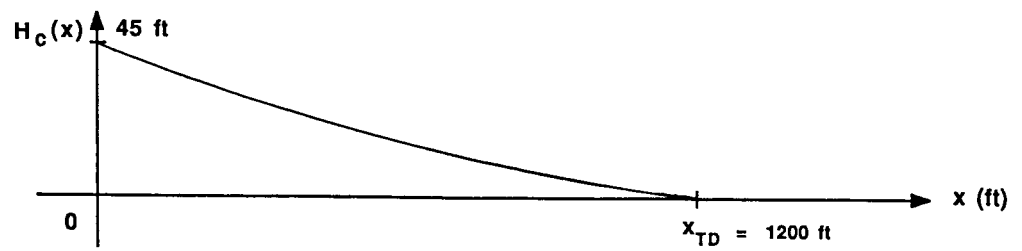
7.1.4 GO-AROUND MODE

The go-around mode is a direct engage mode, used in case of an aborted landing. The airplane is commanded to climb out at 10 deg FPA. As shown in Figure 9, FPA command (γ_c) is converted into \dot{H}_C as follows:

$$\dot{H}_C = \gamma_c \cdot V_I / 57.3 \quad (5)$$

$$H_C = \frac{1}{s} \dot{H}_C \quad (6)$$

The integrator in (6) should be initialized to current altitude when not in go-around mode.



$$H_c(x) = Ax^3 + Bx^2 + Cx + D$$

$$H_c(x) = 3A \frac{V_I}{x_{TD}} x^2 + 2B \frac{V_I}{x_{TD}} x + C \frac{V_I}{x_{TD}}$$

BOUNDARY CONDITIONS:

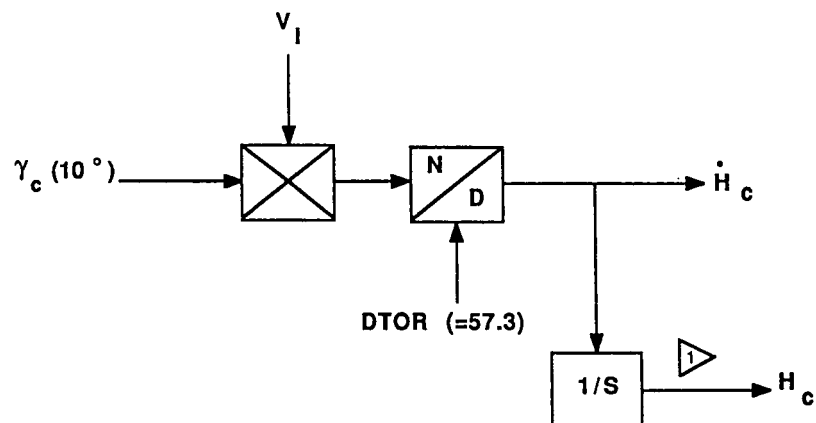
$$H_c(0) = 45 \text{ ft.}$$

$$\dot{H}_c(0) = \dot{H} \text{ of airplane}$$

$$H_c(x_{TD}) = 0$$

$$\dot{H}_c(x_{TD}) = -2.5 \text{ fps}$$

Figure 8. Flare Mode



1 IF (.NOT. FAGA) $H_c = H$

Figure 9. Go - Around Mode

7.1.5 FLIGHT PATH ANGLE MODE

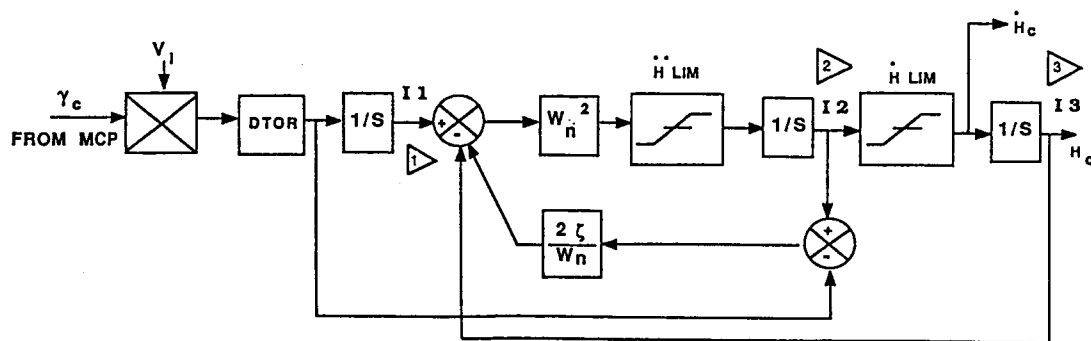
The Flight Path Angle (FPA) mode is a direct engage mode. The pilot enters the desired FPA he wants the airplane to follow through the MCP. Commanded FPA is then converted to \dot{H}_C and H_C as described in the previous sections, and then processed through a second order filter as shown in Figure 10. This filter is similar to the one used for the altitude mode, except \dot{H}_C (computed from γ_C) comes through a feedforward path to improve filter command tracking. The FPA mode was designed to duplicate TECS capability, but its intended function can be successfully accomplished by using altitude hold mode.

7.1.6 SPEED HOLD MODE

The Speed Hold mode is a direct engage mode. The Pilot enters the desired speed target, MACH or CAS, into the MCP. The command is then converted into TAS command (see Appendix A) as shown in Figure 11. The TAS speed target is then passed through a second order filter to generate speed and acceleration commands, as required by feedback regulator interface. The filter dynamics are identical to the altitude hold filter dynamics. Thus, when in the linear region, both filters provide coordinated commands to feedback regulator.

The speed command filter has \dot{V} and \ddot{V} limiters (Figure 11). The \ddot{V} limiter is computed to provide vertical acceleration limiting of $.05 g \left(\frac{52}{VTAS} \right)$ to ensure passenger comfort. The \dot{V} limiter is used to limit forward acceleration to $.1g$ (3.2 fps) when the throttles are in the linear region. When the throttle is on either limit, the feedback regulator is in the speed-on-elevator (SOE) configuration, and \dot{V} limit is computed to ensure proper energy distribution between potential and kinetic energies of the airplane. When throttles are at the forward limit, the upper value of \dot{V}_{LIM} is computed to ensure that a minimum rate of climb (10 fps) is maintained. When throttle is at the aft limit, the lower value of \dot{V}_{LIM} is computed to allow the airplane to level off, but not climb in descent. The formulas for both limiters are explained in Appendix A.

When not in the speed hold mode, both integrators (I1 and I2) should be initialized to current true acceleration and VTAS, respectively.



$$\dot{H} \text{ LIM} = \pm (|\dot{H}| + 10)$$

$$\ddot{H} \text{ LIM} = 0.05g = 1.6 \text{ fps}^2$$

$$\text{1 IF (.NOT. FAFPA) } I1 = H$$

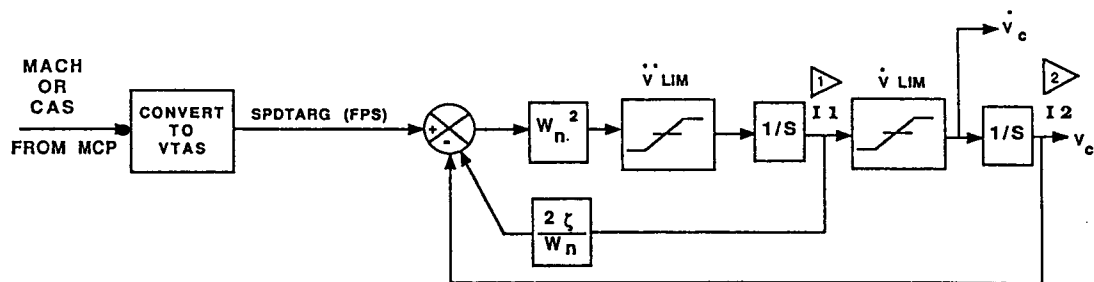
$$\text{2 IF (.NOT. FAFPA) } I2 = \dot{H}$$

$$\text{3 IF (.NOT. FAFPA) } I3 = H$$

$$W_n = .15$$

$$\zeta = 1$$

Figure 10. Flight Path Angle Mode



$$\text{1 IF (.NOT. SPDH) } I1 = \text{VDOT}$$

$$\text{2 IF (.NOT. SPDH) } I2 = \text{VTAS}$$

$$\zeta = 1$$

$$W_n = .15$$

$$\ddot{V} \text{ LIM} = \pm 52/\text{VTAS} \text{ (.05g)}$$

$$\dot{V} \text{ LIM: } \text{VDMAX} = 3.2 \text{ fps}^2$$

$$\text{VDMIN} = 3.2 \text{ fps}^2$$

$$\text{IF (FWD LIM) } \text{VDMAX} = \left(\frac{\dot{H}}{\text{VTAS}} - 10 \right) \cdot g$$

$$\text{IF (AFT LIM) } \text{VDMIN} = \frac{\dot{H}}{\text{VTAS}} \cdot g$$

Figure 11. Speed Hold (Mach or CAS) Mode

7.2 FEEDBACK REGULATOR DESIGN

Reference [3] describes in detail the methodology used to design the feedback regulator. Here, this methodology is applied to design a controller to satisfy the feedback requirements.

It is clear that there are two distinct sets of requirements for the cruise and landing portions of flight envelope (i.e., a more sluggish airplane is desired in cruise, whereas in landing a tight tracking of glideslope beam and flare path is required). Hence, the decision was made to design two sets of feedback gains: one for cruise and one for landing. The structure consists of an integral regulator plus a complimentary filter for true airspeed (VTAS) and acceleration. The altitude (H) and altitude rate (\dot{H}) signals are already synthesized by the onboard IRU.

The integral regulator portion of the design will be presented first, assuming V and \dot{V} are available, followed by a description of the complementary filter.

The standard transport airplane longitudinal dynamics model consists of four states: u, α , Q, θ and two control effectors, δ_e and δ_{TH} . To complete the model two more states were added: H and EPR (an output of first order engine model as shown in Figure 12). Since α is a very noisy signal, it was replaced by \dot{H} state, using a similarity transformation: $\alpha = \theta - \frac{VTAS}{57.3} \dot{H}$. All flight conditions used for linear controller design and analysis are listed in Appendix B.

The following paragraphs describe the design of the cruise and landing regulators.

7.2.1 CRUISE REGULATOR DESIGN

For cruise design, a heavy weight cruise condition (#159) was selected. It is listed in Appendix A. The design then proceeded in the following steps:

1. Open loop analysis
2. Output criteria creation
3. Diagonal weightings, Q and R, selection
4. Closed loop analysis

Each step, or the combination of several of them, were iterated many times before a satisfactory solution was achieved. Results of each step are now briefly described.

7.2.1.1 Open Loop Analysis

The results of open loop analysis can be found in Appendix A. There were no surprises. Both the elevator and throttles have sufficient gains at d.c. to provide steady state control of either altitude or speed, as is clear from SISO frequency responses. The elevator is the best effector to control both the phugoid and short period modes. The throttles best control the energy mode. There is right half plane transmission zero at 7 rad/sec, which is outside of the frequency range of interest, and hence is of no concern. There are no observability problems, since all the states are available.

7.2.1.2 Output Criteria Creation

The complete synthesis model (airplane plus output criteria) is shown in Figure 12. Two criteria outputs were created, H_CRIT and V_CRIT (see Figure 12) because there are two control effectors (elevator and throttles). Furthermore, since the synthesis model is square, the transmission zeros of the total system are the ones of the airplane plus the ones created by criteria outputs.

H_CRIT output is a frequency weighted combination of altitude (H), altitude rate (\dot{H}) and vertical acceleration (\ddot{H}) and has the following expression:

$$H_CRIT = \frac{K_I}{s} [.1 (-H_C + H) - \dot{H}_C + \dot{H}] + K_{P1} (-\dot{H}_C + \dot{H}) - K_{P2} H + \ddot{H} \quad (7)$$

Since

$$\begin{aligned} \dot{H} &= sH \\ \ddot{H} &= s^2 H \end{aligned}$$

then

$$H_CRIT = - \frac{K_1 s^2 + K_I s + .1 K_I}{s} H_C + \frac{s^3 + K_1 s^2 + K_2 s + K_3}{s} H \quad (8)$$

where

$$K_1 = K_{P1} = 3.2$$

$$K_2 = K_I - K_{P2} = 5$$

$$K_{P2} = 5$$

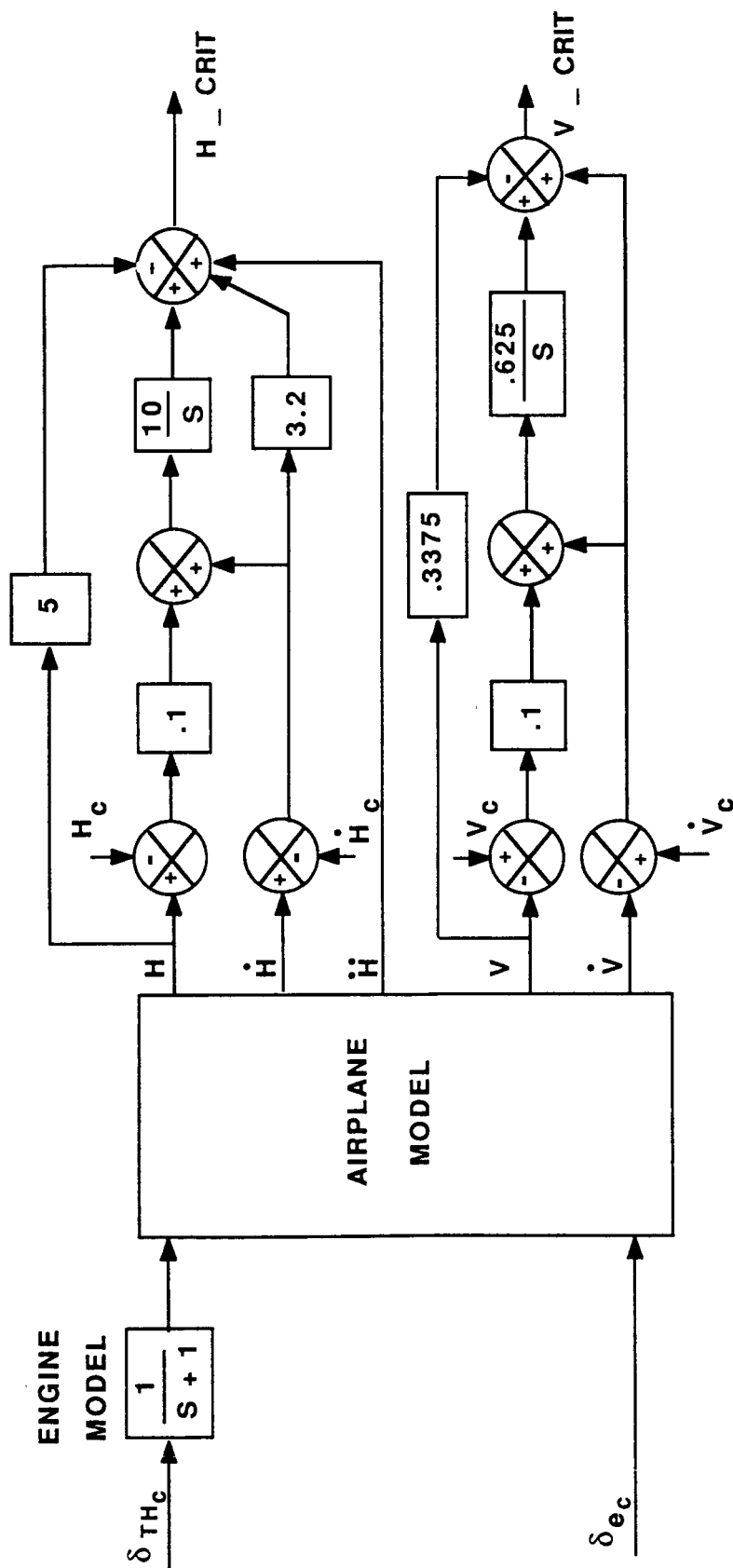


Figure 12. Cruise Controller Synthesis Model

$$K_3 = .1 K_I = 1$$

Therefore, H_CRIT adds three transmission zeros to the synthesis model, which are the roots of the polynomial $s^3 + 3.2s^2 + 5s + 1 = (s + .232)(s^2 + 2.97s + 4.31)$.

The real transmission zero will attract the altitude mode, and the complex pair of transmission zeros will attract the short period of the aircraft.

The V_CRIT output is a combination of airspeed (V) and acceleration (\dot{V}). The expression for V_CRIT is:

$$\begin{aligned} V_CRIT &= \frac{K_I}{s} [(.1(V_C - V) + \dot{V}_C - \dot{V})] - K_P V + \dot{V}_C - \dot{V} \quad \text{or} \\ &= \frac{s^2 + K_I s + .1 K_I}{s} V_C - \frac{s^2 + (K_P + .1 K_I)s + .1 K_I}{s} \cdot V \end{aligned} \quad (9)$$

where

$$\dot{V} = sV$$

$$K_P = .3375$$

$$K_I = .625$$

V_CRIT adds a pair of complex zeros to the synthesis model to attract the phugoid mode of the airplane. The zeros are the roots of the polynomial $s^2 + .4s + .0625$. All the zeros of the synthesis model are listed in Table 5. Once the criteria variables have been selected, diagonal elements of the Q & R matrices in the cost function J must be determined, based on desired crossovers in broken loop responses, [3]. J assumes the following form:

$$J = \int_0^{\infty} \begin{bmatrix} H_CRIT & V_CRIT & \delta_{e_c} & \delta_{TH_c} \end{bmatrix} \begin{bmatrix} Q & 0 \\ 0 & R \end{bmatrix} \begin{bmatrix} H_CRIT \\ V_CRIT \\ \delta_{e_c} \\ \delta_{TH_c} \end{bmatrix} \quad (10)$$

The values of Q & R matrices and resulting feedback regulator solution are shown in Table 6.

7.2.1.3 Gain Scheduling

Once the nominal cruise regulator had been designed, it was tested for all cruise and glideslope capture conditions (#1 - 79, 113-160). The results showed that gain-scheduling is necessary to achieve uniform response throughout the flight envelope.

The following schedules were used:

$$\delta_{e_c} = \frac{300}{Q} \cdot \text{nominal } \delta_{e_c}$$

$$\delta_{TH_c} = \frac{250 \cdot W}{110,000 KTHR} \cdot \text{nominal } \delta_{TH_c}$$

$$K\dot{H} = 1.5 \cdot \text{nominal } K\dot{H}$$

where

Q - dynamic pressure

W - airplane's weight

$KTHR$ - thrust to throttle handle gain ratio

$K\dot{H}$ - altitude rate feedback gain on the \dot{H} input to the controller

Table 5a. Transmission Zeroes of Cruise Controller Synthesis Model

REAL	IMAG	DAMPING	FREQ
6.964	0	1	6.964
-.2319	0	1	2.319
-.2	-.15	.8	.25
-.2	.15	.8	.25
- 1.484	-1.452	.7147	2.076
- 1.484	1.452	.7147	2.076
- 6.888	0	1	6.888

Table 5b. Cost Function

$$J = \int_0^{\infty} [H_CRIT \ V_CRIT \ \delta_{e_c} \ \delta_{TH_c}] \begin{bmatrix} Q & 0 \\ 0 & R \end{bmatrix} \begin{bmatrix} H_CRIT \\ V_CRIT \\ \delta_{e_c} \\ \delta_{TH_c} \end{bmatrix} dt$$

Table 6a. Weighting Matrices for Cruise Controller

$$Q = \begin{bmatrix} H_CRIT & V_CRIT \\ 20 & 0 \\ 0 & 1.6E-4 \end{bmatrix}$$

$$R = \begin{bmatrix} \delta_{e_c} & \delta_{TH_c} \\ 30 & 0 \\ 0 & 0.6 \end{bmatrix}$$

Table 6b. Feedback Gain Matrix for Cruise Controller

$$\begin{bmatrix} \delta_{e_c} \\ \delta_{TH_c} \end{bmatrix} = \begin{bmatrix} V & HDOT & Q & THETA & H & EPR & I_V & I_H \\ .1787 & 6.01E-02 & .6223 & .5769 & 1.53E-03 & -.4178 & .2871 & 1.9E-2 \\ -.7494 & -.5444 & .1574 & -2.865 & -.1143 & -6.067 & 2.981 & -9.2E-2 \end{bmatrix}$$

7.2.1.4 Speed on Elevator (SOE) Configuration

An important issue concerning the feedback regulator design is the throttle limiting cases. When the throttles are either at the forward or aft limit, the elevator will control airspeed, and, as described earlier, speed command processor will properly distribute aircraft's total energy. Therefore, when the throttles reach the limit, the altitude integrator and altitude gains in the elevator command computation are set to zero (Table 6). This design results in poor phugoid damping for the new closed loop system. To improve the damping, both speed integrator gains are increased 2 times, and the total elevator command gain by 2.5 times.

Figure 13 shows the general structure of the cruise controller. It is similar to TECS structure [4], except the cross-couplings are at the outputs of the integrators, rather than at the inputs as in TECS.

7.2.2 LANDING REGULATOR DESIGN

The landing regulator was designed to satisfy glideslope hold and flare requirements and hence, it has much faster command responses accompanied by much higher feedback gains than does the cruise controller.

The nominal design of the landing controller was done for flight condition #102. This is a landing condition with flaps set at 30 degrees and landing gear down.

The open loop analysis (Appendix A) shows a right half plane transmission zero at 3 rad/sec, inside the frequency bandwidth trying to be controlled. This zero is one of the pair of so-called "percussion zeros", usually nearly symmetric about imaginary axis. The non-minimum phase zero is due to the fact that airplane's center of percussion is forward of the c.g. If the N_z and H sensors are moved forward of the center of percussion, then the zeros will become minimum phase. This is done mathematically using the formulae:

$$\begin{aligned}N_z &= N_{zcg} + L/G \dot{Q} \\ \dot{H} &= \dot{H}_{cg} + L \cdot \dot{Q} \\ H &= H_{cg} + L \cdot \theta\end{aligned}\tag{11}$$

where L is the distance forward of the center of gravity.

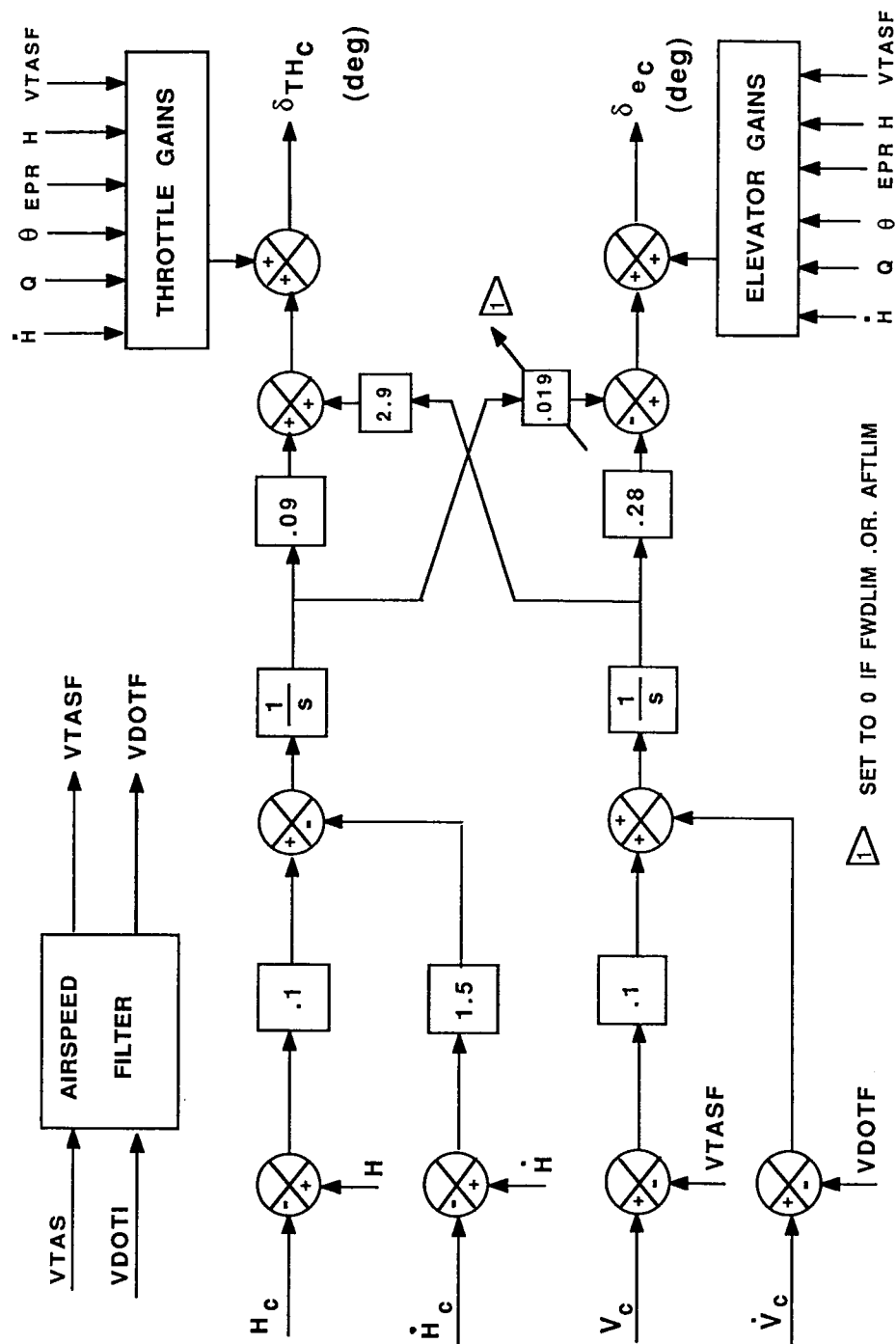


Figure 13. General Structure of Cruise Feedback Controller

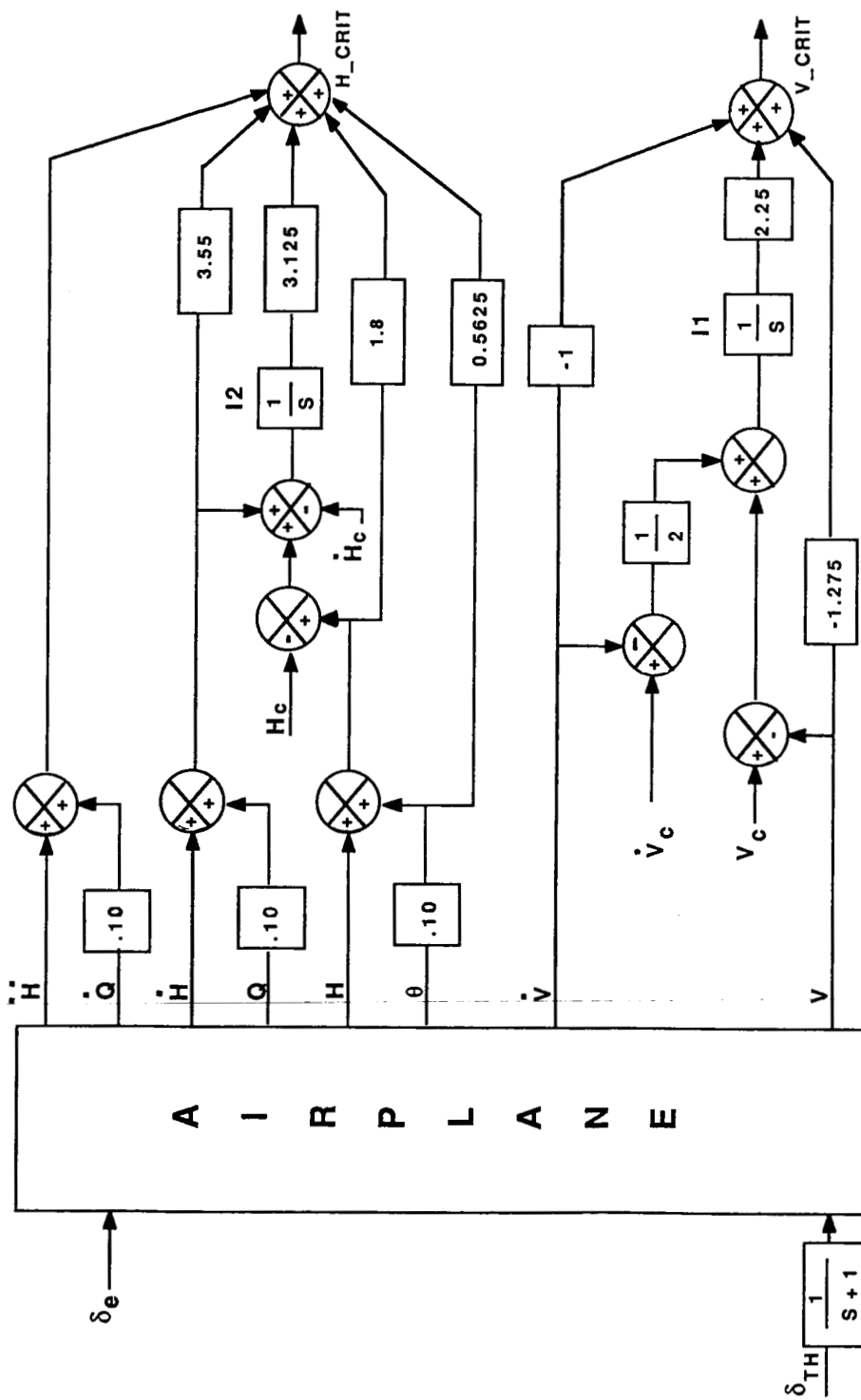


Figure 14. Landing Controller - Synthesis Model

Figure 14 contains the synthesis model for the landing controller with redefined H , \dot{H} , and \ddot{H} as in (11) (i.e., the H and N_z sensors have been moved 6 feet forward of the airplane's c.g.).

The transmission zeros created by criteria outputs, the Q and R weighting matrices and the regulator feedback solution for landing controller can be found in Table 7. The mathematically redefined percussion zeros of the airplane are now at 13.09 rad/sec and -14.61 rad/sec, outside of the control bandwidth.

7.2.2.1 Gain Scheduling

Once the nominal design for the landing controller had been completed, it was tested on the remainder of landing conditions (# 1-112). The results were found to be inadequate; therefore, the following gain scheduling scheme was developed. For each landing condition, a regulator solution was obtained for the cost function used to design the nominal controller. Thus, a total of 16 feedback gains had been derived for each of the 112 conditions. Each of the gains was then plotted versus a flight condition parameter (e.g., such as H , α , \bar{Q} , K_{THR} , etc.).

Figures 15 and 16 present an example of such plots. In Figure 15, K_H (altitude to throttle command gain) is plotted versus \bar{Q} (dynamic pressure). For each flap setting there is a clear hyperbolic dependence of K_H on \bar{Q} . Figure 16 shows a plot of K_U (airspeed to elevator command gain) versus \bar{Q} . A hyperbolic relationship between K_U and \bar{Q} is obvious and is independent of flap setting. The expression of the form:

$$K = \frac{A + BX}{1 + CX} \quad (12)$$

was used to find a curve fit for each gain. In (12), A , B , and C are either constants or functions of flaps and X is an independent variable (e.g., \bar{Q} , α , H , etc.). Appendix A contains complete information for each gain.

7.2.2.2 Airspeed Complementary Filter

The airspeed filter (Figure 14) uses airdata and inertial signals to generate accurate airspeed and acceleration signals over a large frequency range. As shown in Figure 14, the filter's time constant τ is scheduled as a function of altitude since tight tracking of airspeed is not required at higher altitudes.

Table 7a. Transmission Zeroes of Landing Controller Synthesis Model

REAL	IMAG	DAMPING	FREQ
13.09	0.0000	-1.000	13.09
-0.8900	0.9818	0.6716	1.325
-0.8900	-0.9818	0.6716	1.325
-1.200	0.9000	0.8000	1.500
-1.200	-0.9000	0.8000	1.500
-1.777	0.0000	1.000	1.777
-14.61	0.0000	1.000	14.61

Table 7b. Weighting Matrices for Landing Controller

$$Q = \begin{matrix} & \begin{matrix} H_CRIT & V_CRIT \end{matrix} \\ \begin{matrix} 1.5 & 0 \\ 0 & .3 \end{matrix} \end{matrix} \quad R = \begin{matrix} & \begin{matrix} \delta_{e_c} & \delta_{TH_c} \end{matrix} \\ \begin{matrix} 10 & 0 \\ 0 & 10 \end{matrix} \end{matrix}$$

Table 7c. Feedback Gain Matrix for Landing Controller

$$\begin{bmatrix} \delta_{e_c} \\ \delta_{TH_c} \end{bmatrix} = \begin{matrix} & \begin{matrix} V & HDOT & Q & THETA & H & EPR & I_V & I_H \end{matrix} \\ \begin{bmatrix} 0.6035 & 2.733 & 3.491 & 7.425 & 2.173 & 8.624 & 0.04 & 1.2 \\ -1.9 & -0.3028 & -0.2504 & -0.5707 & -0.4037 & -17.85 & 0.3876 & -0.1263 \end{bmatrix} \end{matrix}$$

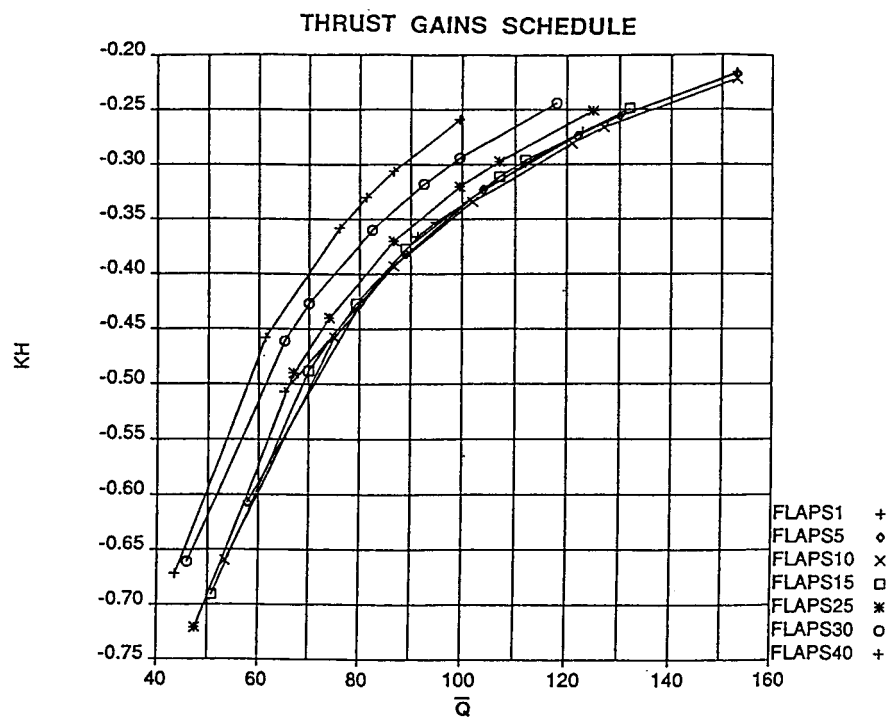


Figure 15. Landing Controller - Thrust Gains Schedule

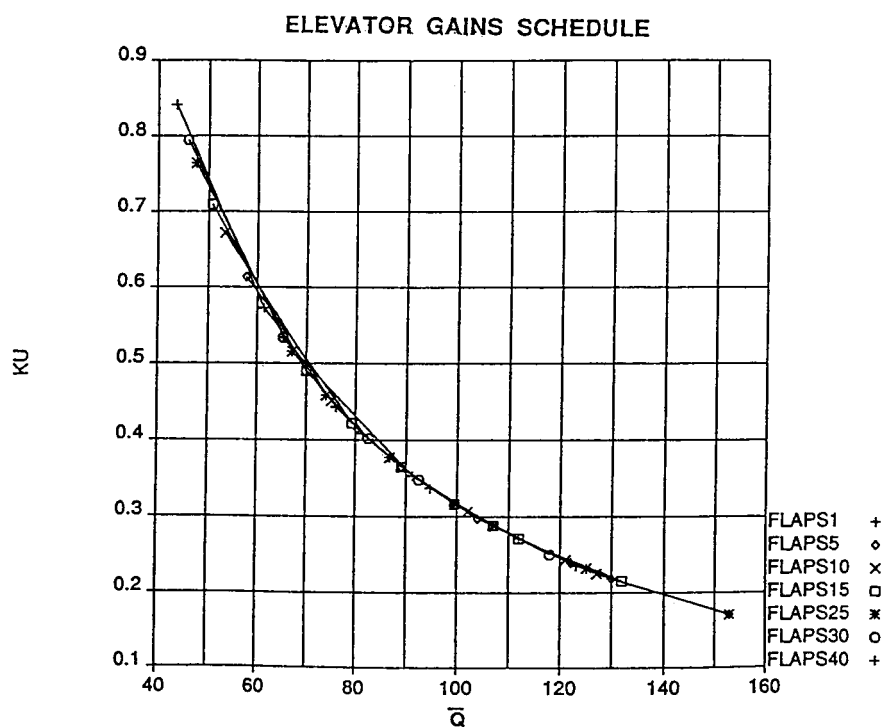


Figure 16. Landing Controller - Elevator Gains Schedule

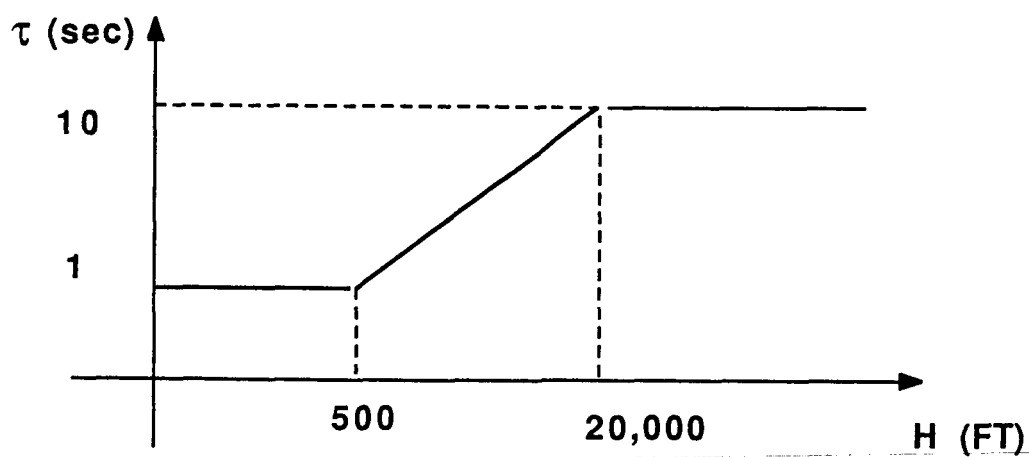
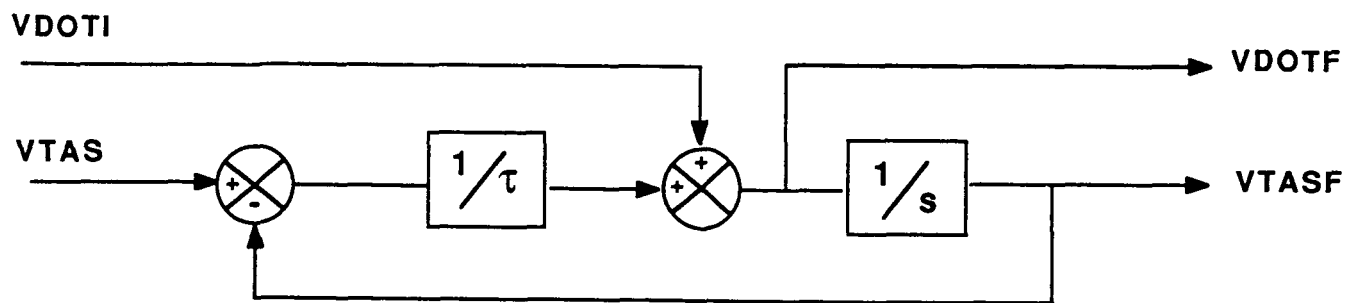


Figure 17. Complementary Filter

7.3 DIGITAL IMPLEMENTATION

The feedback controller (with the regulator solution and complementary filter solutions combined) has 3 states (complementary filter state, altitude and speed integrator states), 7 sensor, 4 command inputs and 2 outputs (elevator and throttle commands) and the following general form:

$$\dot{x} = Ax + By$$

$$u = Cx + Dy \quad (13)$$

where

$$A = \begin{bmatrix} \frac{-1}{\tau} & 0 & 0 \\ \left(\frac{1}{\tau} - .1\right) & 0 & 0 \\ 0 & 0 & 0 \end{bmatrix} \quad (13a)$$

$$B = \begin{bmatrix} 0 & 0 & 0 & 0 & \frac{1}{\tau} & 1 & 0 & 0 & 0 & 0 \\ 0 & 0 & 0 & 0 & \frac{-1}{\tau} & -1 & .1 & 0 & 1 & 0 \\ 1.5 & 0 & 0 & 0 & .1 & 0 & 0 & -.1 & 0 & -1.5 \end{bmatrix} \quad (13b)$$

$$C = \begin{bmatrix} K_{V_{\delta_e}} & K_{I_{V_{\delta_e}}} & K_{I_{H_{\delta_e}}} \\ K_{V_{\delta_{TH}}} & K_{I_{V_{\delta_{TH}}}} & K_{I_{H_{\delta_{TH}}}} \end{bmatrix} \quad (13c)$$

$$D = \begin{bmatrix} K_{H_{\delta_e}} & K_{Q_{\delta_e}} & K_{Q_{\delta_e}} & K_{EPR_{\delta_e}} & K_{H_{\delta_e}} & K_{V_{\delta_e}} & 0 & 0 & 0 & 0 & 0 \\ K_{H_{\delta_{TH}}} & K_{Q_{\delta_{TH}}} & K_{\theta_{\delta_{TH}}} & K_{EPR_{\delta_{TH}}} & K_{H_{\delta_{TH}}} & K_{V_{\delta_{TH}}} & 0 & 0 & 0 & 0 & 0 \end{bmatrix} \quad (13d)$$

$$x = (VF, IV, IH)^T$$

$$u = (\dot{H}, Q, \theta, EPR, H, VTAS, \dot{V}_L, V_C, H_C, \dot{V}_C, \dot{H}_C)^T$$

$$y = (\delta_{e_c}, \delta_{TH_c})^T$$

where the K's in the C and D matrices are distinct for cruise and landing solutions.

The feedback controller was discretized using the following formula:

$$x_{k+1} = e^{A\Delta T} x_k + \left(\int_0^{\Delta T} e^{A\sigma} d\sigma \right) B u_k = A_d x_k + B_d u_k$$

$$y_{k+1} = C x_k + D u_k \quad (14)$$

where

ΔT = sampling period

x_k = discretized controller state vector

Since τ is a function of altitude in 13a and 13b, closed form expressions had to be obtained for A_d and B_d in

(14). The results are presented in Appendix A.

The discretized feedback controller was implemented digitally using delta-coordinates concept (Figure 18). The 's' and '1/s' meaning differentiation and integration, respectively, are an abuse of notation in this case. Rather than computing actual derivatives of the command and sensor signals, the difference between present and previous values of each signal is found. At the output, the integrator is initialized to current elevator and throttle positions, and the controller outputs are then added to the previous values of the integrator.

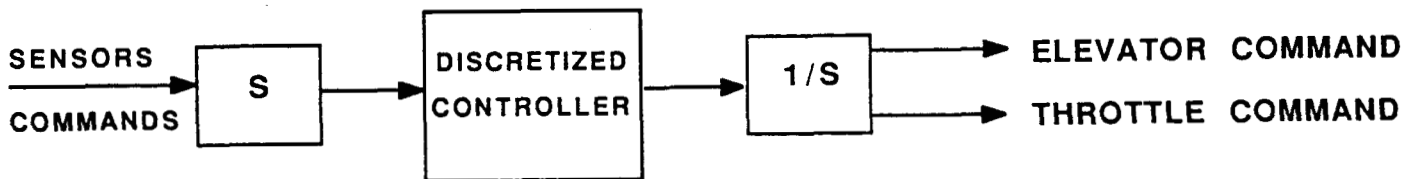


Figure 18. Digital Implementation - Delta Coordinates

The delta concept offers significant advantages over the full signal implementation:

- a. During controller switching (e.g., between cruise and landing controllers) all states of the new controller should be initialized to 0.

- b. Full scale implementation may lead to incorrectly computed gains, which are scheduled as a function of quickly changing flight parameters (e.g., α). This problem is avoided with delta concept [8].
- c. The issues that arise during throttle limiting can be easily dealt with as described in the following.

Figure 19 shows in greater detail the delta implementation of the feedback controller. When FAGLDH flag is set, the switch between cruise and landing controllers takes place. At this point, all landing controller states are initialized to 0. Both controllers generate an incremental throttle command, δ_{TH_c} . When the throttle lever reaches the forward limit (FWDLIM) and δ_{TH_c} is positive, it should also be set 0. If the throttle lever is at the aft limit (AFTLIM) and δ_{TH_c} is negative, it should be set 0. By setting δ_{TH_c} to 0, throttle integrator saturation is avoided. Also, the sign of δ_{TH_c} determines when to take the throttle off the limit. The advantages of this strategy are described in paragraph 7.4.2.

Some of the feedforward loop modes have second order filters, which were also discretized using expression 14. It should be noted that the feedforward loop modes were not implemented using a delta coordinates concept. The A_d , B_d matrices for the discretized feedforward loop are given in Appendix 7.

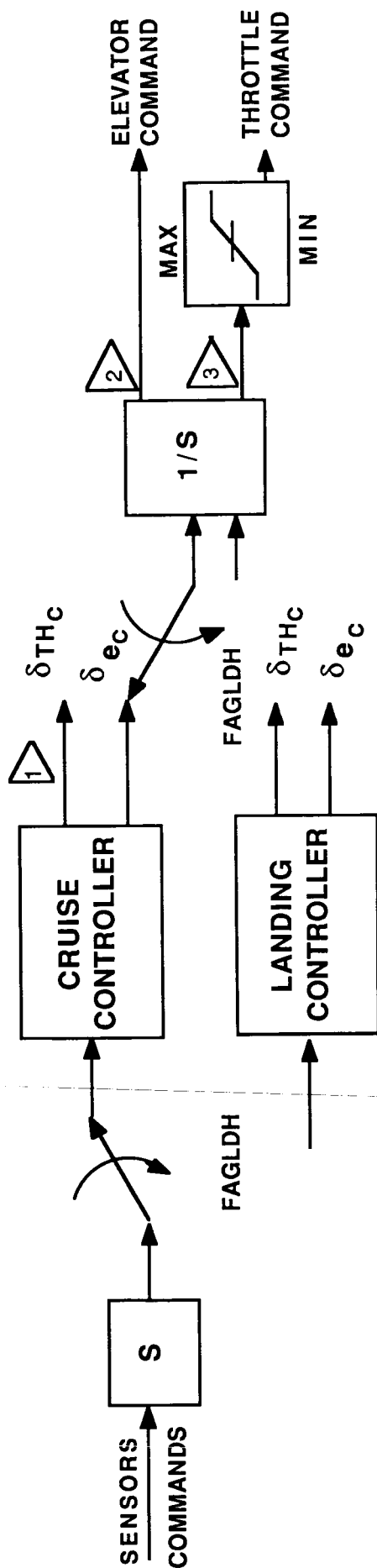
7.4 RESULTS

The complete analysis and testing of the total design consisted of two parts: 1) linear analysis of the feedback controller, and 2) nonlinear testing of several feedforward modes, (i.e., feedforward and feedback loops combined).

7.4.1 LINEAR ANALYSIS

Linear analysis of the feedback regulator included the following items:

- a. Open loop eigenvalues
- b. Closed loop eigenvalues



1 IF (AFTLIM .AND. $\delta_{TH_C} \text{LT. } 0$) $\delta_{TH_C} = 0$

IF (FWDLIM .AND. $\delta_{TH_C} \text{GT. } 0$) $\delta_{TH_C} = 0$

2 IC TO CURRENT ELEVATOR POSITION

3 IC TO CURRENT THROTTLE POSITION

Figure 19. Throttle Limiting - Controller Switching

Appendix A contains the results of the linear analysis of the cruise controller over a substantial portion of the flight envelope.

Plots 1 - 4 show open and closed loop eigenvalues for 48 (#113 - 160) flight conditions. It is clear that significant improvement in eigenvalue damping has been achieved with feedback. Both phugoid and short period modes damping ratios satisfy the closed loop damping requirements.

Plot 5 shows gain margins plotted versus flight condition for conditions # 113-160 for all control and sensor loops. Plot 6 shows phase margins for the same conditions. It is clear from both plots that gain and phase margin requirements have been satisfied.

Plots 7 and 8 show crossover frequencies for elevator and throttle control loops. The maximum elevator loop crossover frequency is at 4.1 rad/sec, which is well below 15 rad/sec (the bandwidth of the elevator actuator). The throttle loop crossover frequency remains constant throughout the flight envelope at around .35 rad/sec, which is, again, well below 1 rad/sec (commonly accepted to be the engine bandwidth).

Plots 9 - 12 show closed loop frequency responses of the airplane's altitude and speed to altitude and speed commands for conditions #113 - 128. There is little variation in responses as flight conditions change. In fact, this sample of 16 conditions is representative of the rest of the flight envelope. The H/H_C (Plot 9) response has a bandwidth of .08 rad/sec, V/V_C (Plot 12) has a bandwidth of .1 rad/sec. Both are within the command response bandwidth requirements for the cruise controller. Plots 10 and 11 show the crosscoupling effects of altitude and speed commands. H_C has little effect on speed response (Plot 10). V_C effects the airplane's altitude significantly in the frequency range between .01 and .5 rad/sec. This result is to be expected because of the low bandwidth feedback controller in cruise. This kind of altitude response is also wanted by the pilots, who would rather have the airplane drop 100 feet, than see throttles move 1 degree.

Plots 13 - 19 show closed loop aircraft covariance responses to 1 fps longitudinal and vertical Dryden turbulence. Plots 13, 14 and 15 show airspeed, altitude and N_z responses plotted versus flight condition. All show very small variations around the mean. Plots 16 and 17 show elevator and throttle covariance responses and plots 18 and 19 show elevator and throttle rate responses to Dryden turbulence plotted versus flight condition. It is clear from the plots, that there is little control effector activity in turbulence during cruise.

7.4.2 NONLINEAR TESTING

The term 'nonlinear' is an exaggeration, since only the nonlinear controller was implemented, the airplane model remained linear. The nonlinear controller implementation included discretized linear controller with all the limiting and switching which takes place in the feedforward loop. This implementation was done to illustrate the nonlinear capabilities of the controller. The results of the 'nonlinear' simulation are presented in Appendix A.

Plots 20 - 24 present the results of a simulated glideslope capture and hold. Plot 20 shows the altitude and glideslope profiles. The discontinuity in glideslope profile indicates the time when glideslope capture mode is engaged. Proper switching time results in overshoot free capture of glideslope beam. Once the beam is captured, a switch occurs from cruise to landing controllers. Plots 21 - 24 show the rest of the airplane's variables to better demonstrate the airplane's performance during capture.

Plots 25 - 29 demonstrate the airplane's performance in speed hold and altitude hold modes. The airplane is trimmed at 35,000 feet when the pilot dials in a simultaneous altitude change command of 3,000 feet and speed increase command of 30 fps, conventionally known as flight level change maneuver.

Plot 25 shows the altitude profile and points out throttle limiting times. The simplicity of the logic associated with throttle limiting is obvious.

Plot 26 presents the same profile, except the logic events are shown that would normally take place in the conventional control system, consisting of separate autopilot and autothrottle boxes. Once a sufficiently large altitude change is requested, the autothrottle switches into MAX EPR mode to control the engines to maximum EPR for given flight condition. The maximum EPR command is retrieved from the data base. The autopilot switches to speed on elevator (SOE) mode. While the aircraft is climbing, the autopilot computes the top of climb (T/C) point where it will switch to a path capture mode, which uses a nonlinear capture controller. At this time, the autothrottle will switch back to speed on throttle mode. Once the desired altitude target is captured, the autopilot will switch to a path hold mode, a linear altitude hold control law. The operation of the conventional control system is presented here to demonstrate the advantages of the integrated design.

Plot 27 shows airspeed, altitude rate and throttle position profiles for the flight level change maneuver. These signals are plotted together to better illustrate the limiting that takes place in the speed command processor when throttles reach the forward limit. Throttle limiting occurs after 10 sec into the maneuver. As shown, airspeed response levels off at 25 fps above trim value and altitude rate levels off at 10 fps, while throttles are at the limit. This behavior is a result of \dot{V} limiter in the speed command processor (i.e., when throttles are at the limit the speed command processor limits the speed command to maintain a minimum rate of climb of 10 fps). This is the reason why airspeed levels off at 25 fps, rather than reaching the target of 30 fps right away. When the throttles go off the limit, the airplane starts to pitch over and the remainder of the speed target and altitude target are captured. In addition, the ripple created when the throttles initially go off the limit in throttles position profile is due to the fact that the excess energy released by the airplane pitching over is used to capture the remainder of the airspeed target.

Plot 28 shows the change in N_z level of the aircraft during the flight level change maneuver. It doesn't exceed .05 g, which was achieved by the \ddot{H} limiter in the altitude command processor.

Plot 29 shows the elevator position profile for the same maneuver.

8.0 LATERAL AXIS DESIGN

This section presents an airplane autopilot design process, illustrated by an example design for a transport airplane, using an integral LQG design technique. Fourteen linear models trimmed at different flight conditions were used during design and analysis phases (see Section 4 for open loop airplane description).

The objective was to design a single autopilot control system to provide both lateral axis stability augmentation and aircraft directional control across the flight envelope. The autopilot provides heading and ground track heading hold for cruise, and localizer beam capture and hold for landing approach.

The approach was to use ailerons and rudder to independently control heading and sideslip. The feedback controller was designed to provide stability augmentation and sufficient command response bandwidth to meet the performance requirements. A separate feedforward controller was designed to filter pilot inputs to achieve desired transient responses. An additional outer loop controller generates heading commands for localizer capture and hold.

8.1 HEADING CONTROLLER DESIGN

The heading controller was designed using an integral LQG model following technique. (Figure 20 is a block diagram of the controller structure.) The feedforward and feedback controllers were designed separately. Feedforward design was driven by performance requirements while feedback design was dominated by stability and robustness issues. The following paragraphs outline the design process referring to the specific example for illustration.

8.1.1 REGULATED VARIABLES

For each independent control input a regulated output is chosen. For this example the independent inputs were aileron and rudder while the regulated variables were heading and sideslip. Likewise, for each regulated output a pilot input is designated and an ideal model defining the desired response of the regulated variable to pilot inputs is selected.

For this design the input for heading command was a compass direction entered via the autopilot control panel. Sideslip command was given by the rudder pedals (even though it is rare that a sideslip command would be input during autopilot flight). The ideal model for heading response

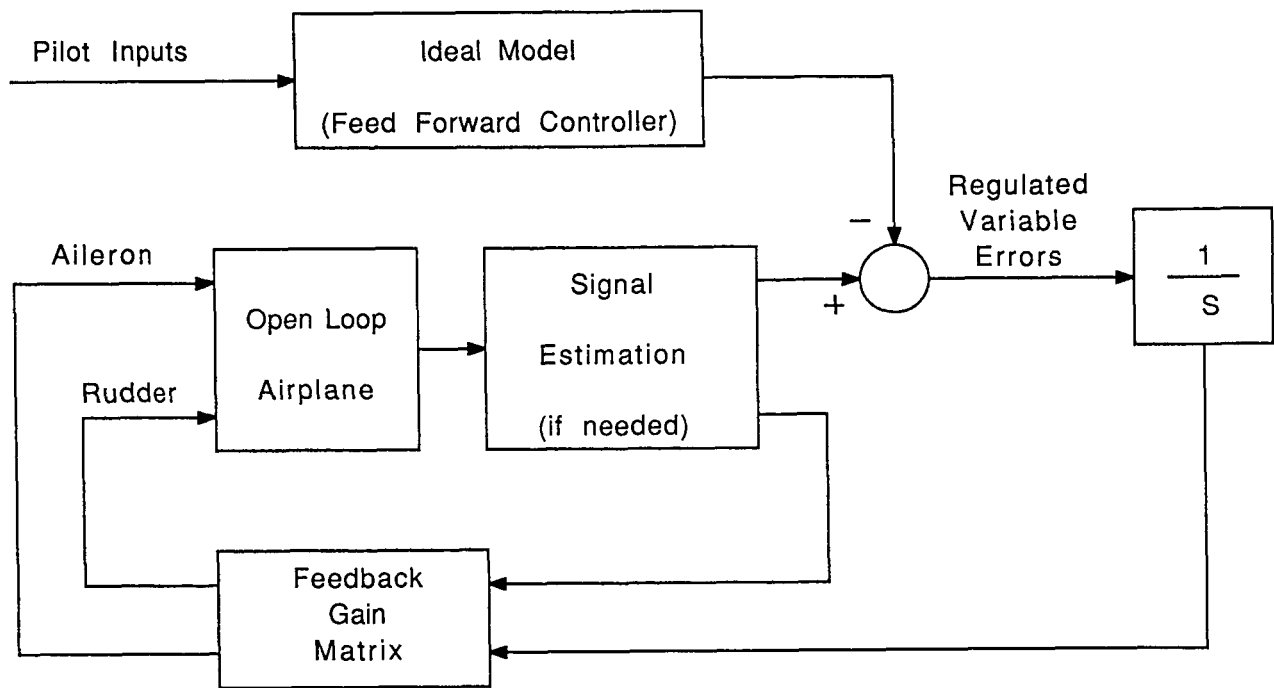


Figure 20. Closed Loop Block Diagram of Integral Model Following Structure

8.1.3 GAINS AND GAIN SCHEDULES

The steps given in paragraph 8.1.2 are part of an iterative process that involves solving the Riccati equation for the feedback gain matrix followed by closed loop analysis to check for compliance with the design requirements. The objective is to find a single set of criterion outputs and weighting matrix values that yield adequate closed loop characteristics throughout the flight envelope.

Failing this, the flight envelope may have to be partitioned into sub-regions and a separate design completed for each. The example presented here yielded a single set that proved satisfactory throughout the envelope.

Having defined the criterion outputs and weighting matrix values, the next step was computation of the feedback gains at each of the fourteen flight conditions presented with this problem. The results (see Figure 23) show that some of the gains remained relatively constant for the various flight conditions while others exhibited large variations. Since the airplane flies through a continuum of conditions, a method of defining the gains to be used at any flight condition is necessary.

The task of generating continuous functions defining the gains is called gain scheduling. Gain schedules define the gain values as a function of measurable flight condition parameters (e.g., dynamic pressure, speed, altitude, flap angle setting, etc.). Each gain is scheduled separately by plotting the design values against the various flight condition parameters. The flight condition parameter exhibiting the greatest correlation is used for scheduling a particular gain. The schedule function is derived by curve fitting the plot of design values versus flight condition parameter. For the heading controller design example, some of the gains were set to constant values while others were scheduled against calibrated airspeed, mach number, or flap setting (see Figure 24). Note that Figures 23 and 24 the integral Beta to aileron gain has been zeroed. This was done to avoid instability in the event of a loss of rudder. Zeroing this gain had little effect on closed loop performance and robustness.

Results are shown here for fourteen flight conditions. Plots 30A and 30B found in Appendix B along with the accompanying gain schedules and controller block diagram define the controller for the complete design suite of 160 flight conditions.

8.1.4 BETA COMPLEMENTARY FILTER

The final step in the design process is estimation of any feedback states that are not directly measurable with the required fidelity. If needed, a full state Kalman estimator can be designed.

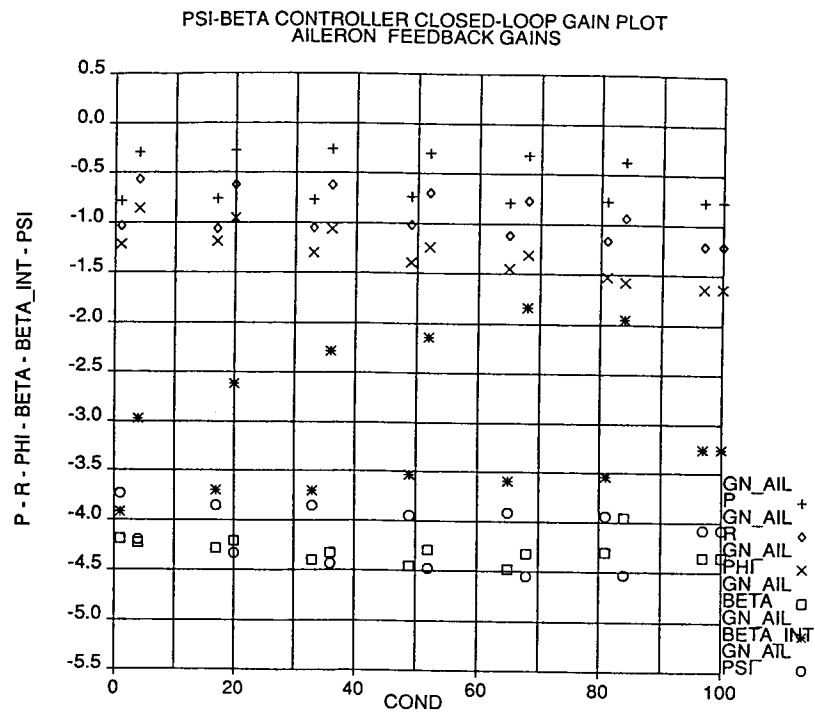


Figure 23. Design Aileron Feedback Gains

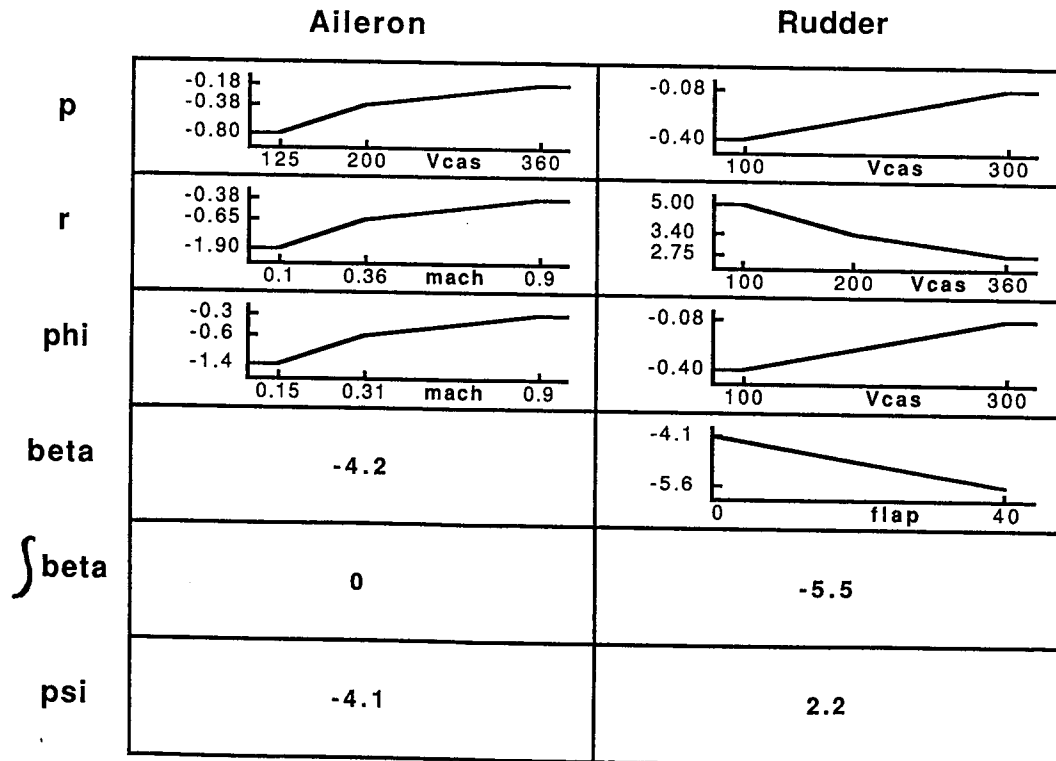


Figure 24. Feedback Gain Schedules

was a 0.4 rad/sec lag including a rate limiter to limit bank angle to 30 degrees. The sideslip ideal model was a 0.5 rad/sec lag. Error signals used for feedback control are defined by taking the difference between the output of each ideal model and its corresponding regulated variable. (Figure 21 is a block diagram of the feedforward controller.)

8.1.2 CRITERION OUTPUTS AND WEIGHTING MATRICES

The next step is to form criterion outputs for use during LQG synthesis. One criterion output is defined for each regulated variable.

The first step in forming the criterion outputs is to provide high gain at low frequency between the control inputs and the criterion outputs. The result is large penalties on steady state errors leading to good steady state tracking. Often, as was the case between aileron and heading, the plant itself provides sufficient low frequency gain. In other instances, as with sideslip, an integrator is introduced to provide infinite gain at steady state.

The second step in forming the criterion outputs is to examine the transmission zeros of the synthesis model. Because the synthesis model is square (same number of control inputs as criterion outputs) its transmission zeros can be computed. An important feature of this design technique is the asymptotic tendency of the closed loop eigenvalues to migrate toward the transmission zeros. The plant itself will have transmission zeros over which the designer has no control (other than choosing different inputs and outputs). In addition to the natural zeros, the designer can modify the synthesis model by adding other output signals to the criteria outputs to create additional zeros. In the example presented here, a real zero was added to the heading criteria ($s = -3$) to attract the heading state. A complex pair of zeros ($\omega_n = 2$, $\zeta = .8$) was added to the sideslip output to attract the dutch roll mode.

Once the criterion outputs are defined, the final step is selection of the diagonal Q and R weighting matrices for LQG synthesis of the feedback gain matrix. Q and R have the same dimensions since there are the same number of control inputs and criterion outputs. In this example both were [2x2]. As with any LQG technique, the weightings are chosen to make the trade off between control and output activity. To aid in choosing the weightings the frequency responses from control inputs to criterion outputs are computed. The bandwidth of the closed loop system will be approximately that of the open loop synthesis model. Figure 22 contains a block diagram of the synthesis model and the design weightings used for this example.

Select Regulated Variables:

- o Heading angle (Psi)
- o Sideslip angle (Beta)

Define Ideal Models:

- o Heading command processor: first order lag at 0.4 rad/sec
 - Heading command processor output is rate limited to limit bank angle at 30 degrees
- o Sideslip command processor: first order lag at 0.5 rad/sec

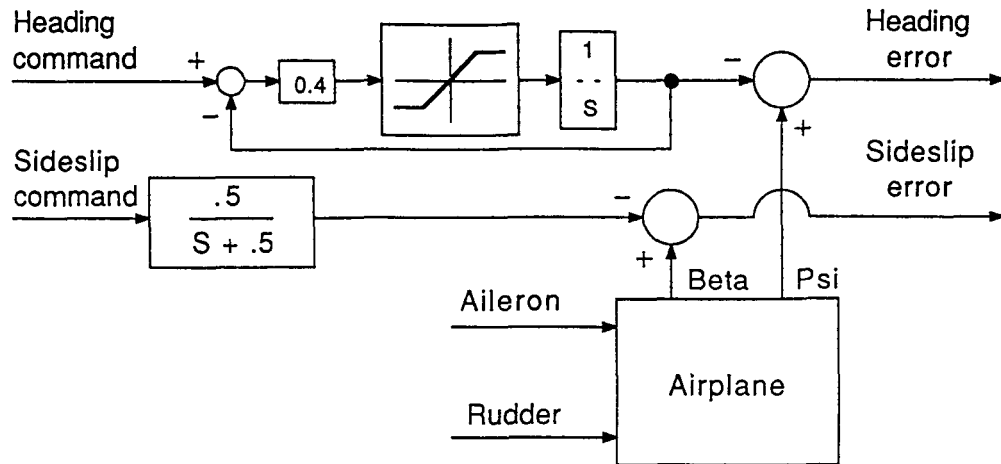
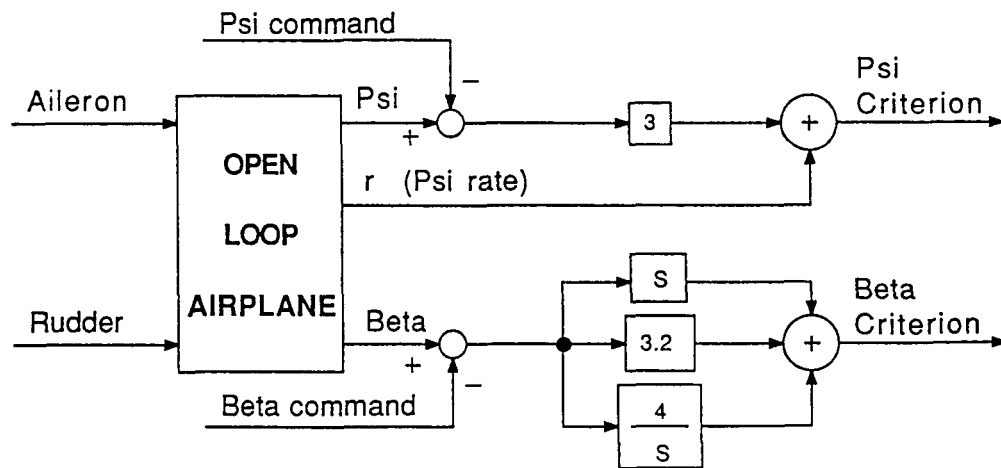


Figure 21. Feedforward Controller Showing Regulated Variables and Ideal Models



Synthesis Transmission Zeros:

- o Psi Criterion: 1 real zero: $s = -3$
- o Beta Criterion: 2 complex zeros:
 $W_n = 2$ $Zeta = .8$

LQG Weighting Matrices:

$$Q = \begin{bmatrix} 2.5 & \\ & 2.5 \end{bmatrix} \quad R = \begin{bmatrix} 1 & \\ & 1 \end{bmatrix}$$

Figure 22. LQG Synthesis Model Showing Criteria Outputs and Weighting Matrices

For this example, only the sideslip state was deemed insufficient for direct feedback. The approach taken was to use a complementary filter to estimate Beta. It was assumed that an air data sensor would give low frequency Beta while high frequency information could be derived from inertial data. A simple first order complementary filter at 0.1 rad/sec was proposed. Since the complementary filter does not affect the system stability it did not figure in the following analysis. A complete analysis of the performance of the Beta filter would require analysis of the sensor characteristics which is beyond this example.

8.1.5 CLOSED LOOP HEADING CONTROLLER

Figure 25 is a block diagram of the closed loop system for the heading control including the sideslip complementary filter.

8.2 HEADING CONTROLLER RESULTS

The following paragraphs present closed loop heading controller analysis results. The feedback controller gains were defined per the gain schedules presented in paragraph 8.1.4 using the structure given in Figure 25. Expanded analysis giving results for all 160 design flight conditions is presented in Plots 31 through 45 found in Appendix B.

8.2.1 EIGENVALUES

Figure 26 is a scatter plot of the eigenvalues of the closed loop heading controller. The dutch roll damping ratio, with a couple of minor exceptions, is above 0.6 for each of the fourteen design flight conditions.

8.2.2 GAIN AND PHASE MARGINS

Figure 27 shows the phase and gain margin characteristics for the rudder and aileron loops. Cross plots of the broken loop frequency response real and imaginary components show that no loops violate the region designating ± 4 dB and ± 40 degrees. Similar results were achieved for the sensor loops.

8.2.3 COVARIANCE RESPONSES

Figure 28 shows the position covariance responses of aileron, rudder, heading, and sideslip to a unit magnitude lateral dryden gust. These data are plotted versus flight condition number. These responses, as well as the rate responses, meet the requirements.

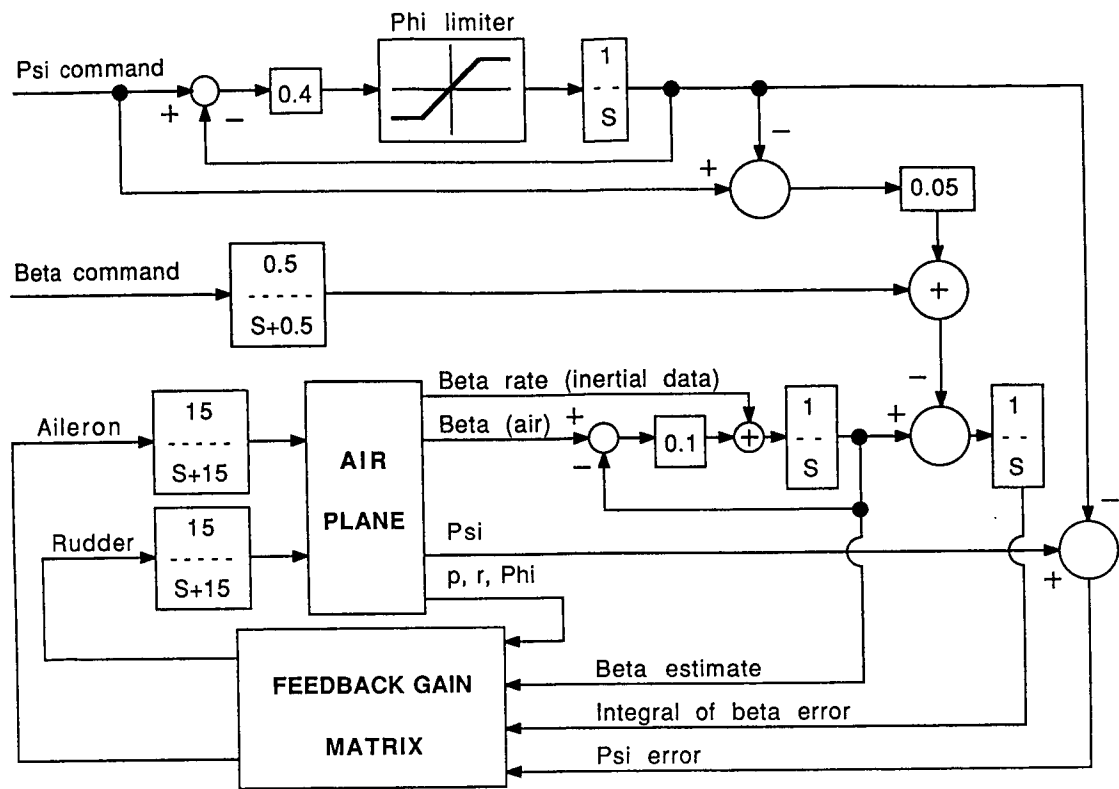


Figure 25. Detailed Closed Loop Block Diagram of Heading Controller

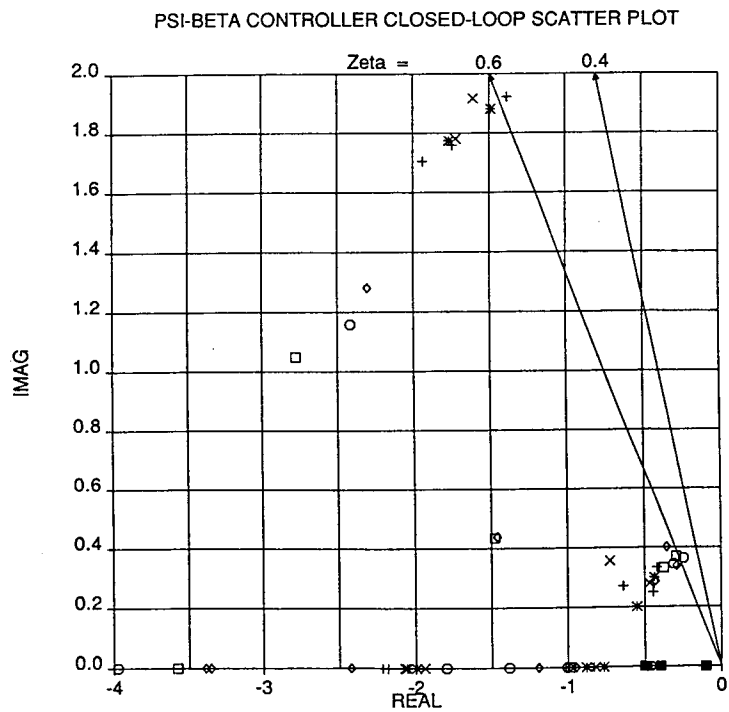


Figure 26. Scatter Plot for Heading Controller Using Scheduled Feedback Gains

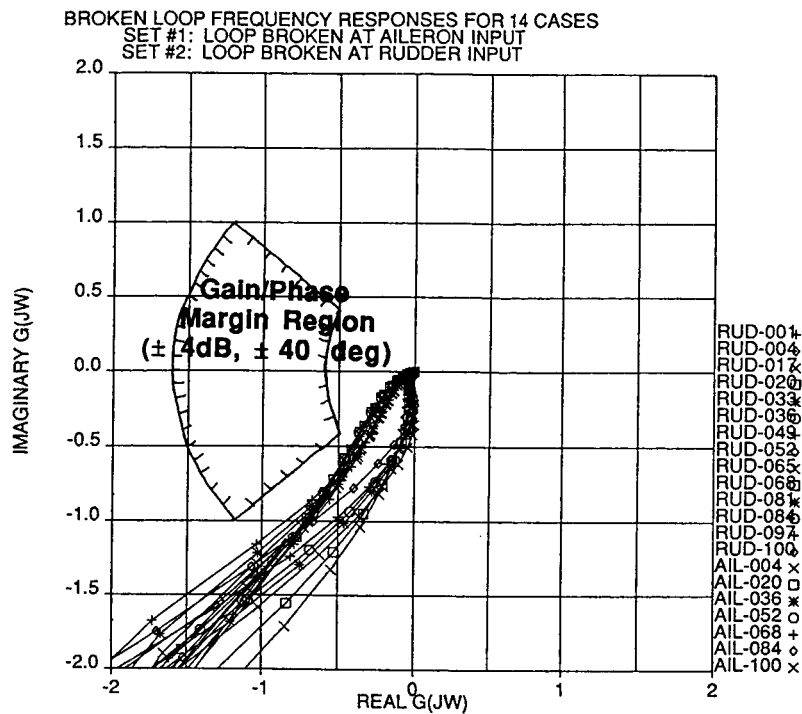


Figure 27. Aileron and Rudder Broken Loop Nyquist Plots for Heading Controller

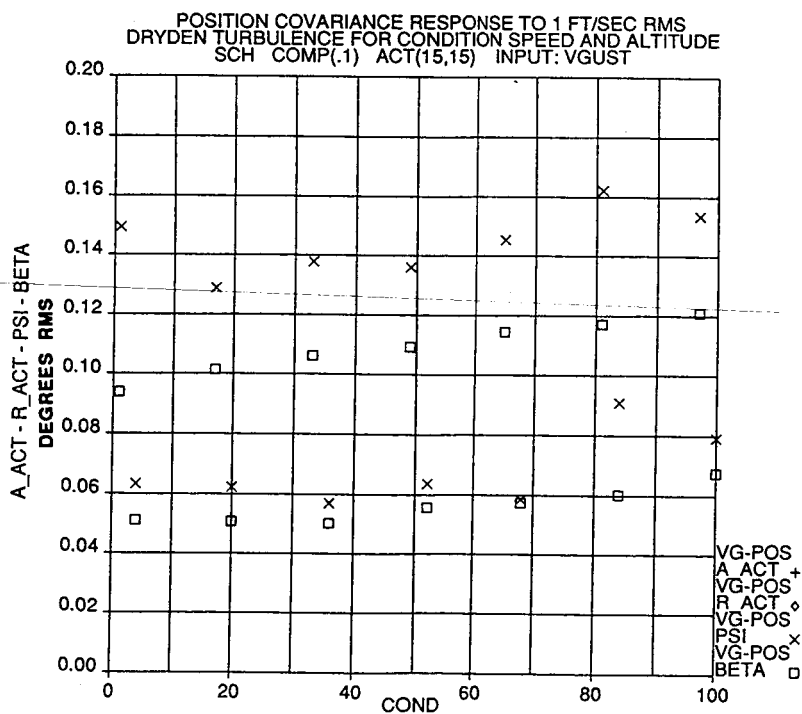


Figure 28. Covariance Responses of Heading Controller to 1 Ft / Sec Dryden Gust

8.2.4 FREQUENCY RESPONSES

Figure 29 shows the heading command to heading frequency responses for each of the fourteen flight conditions. Since the response is, by design, dominated by the ideal model, there is very little variation in response from condition to condition.

8.2.5 TIME DOMAIN SIMULATION

Figure 30 shows time history plots of aileron, rudder, heading, and sideslip in response to a step in heading command for condition 1. Plots 46-57 found in Appendix B present nonlinear simulation results for a 90 degree heading command change. Plots 46-51 show results for a low speed flight condition while Plots 52-57 show the same data for a high speed flight condition.

8.3 LOCALIZER CONTROLLER DESIGN

The localizer controller was designed using the heading controller developed in paragraph 8.1 as an inner loop. A classical root locus technique was used. The cross track error is sensed and fed back to command a change in heading. The inner loop heading controller then commands the airplane to fly to a new heading.

8.3.1 CONTROLLER STRUCTURE AND GAINS

The structure of the localizer controller is proportional plus integral cross track error fed back to form the heading command. Classical root locus was used to determine the localizer controller gains. (Figure 31 shows the block diagram of the localizer controller including the gain values.) The feedback gain is scaled by the inverse of airspeed to avoid aggressive control leading to overshoots during capture at high speed.

8.3.2 LOCALIZER CAPTURE LOGIC

When an autopilot approach for landing is made the airplane flies along under heading control until the localizer beam signal is received. Once the localizer signal is available, the plane must maneuver to capture the beam and follow it into the runway. The logic employed to transition from heading control to localizer track is described in the following.

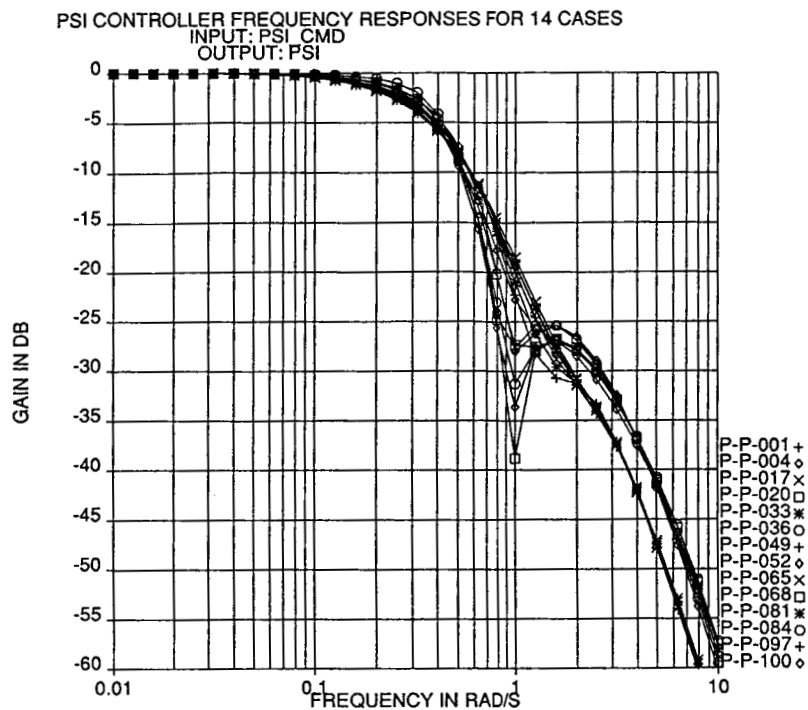


Figure 29. Frequency Responses of Heading Controller from psi Command to psi

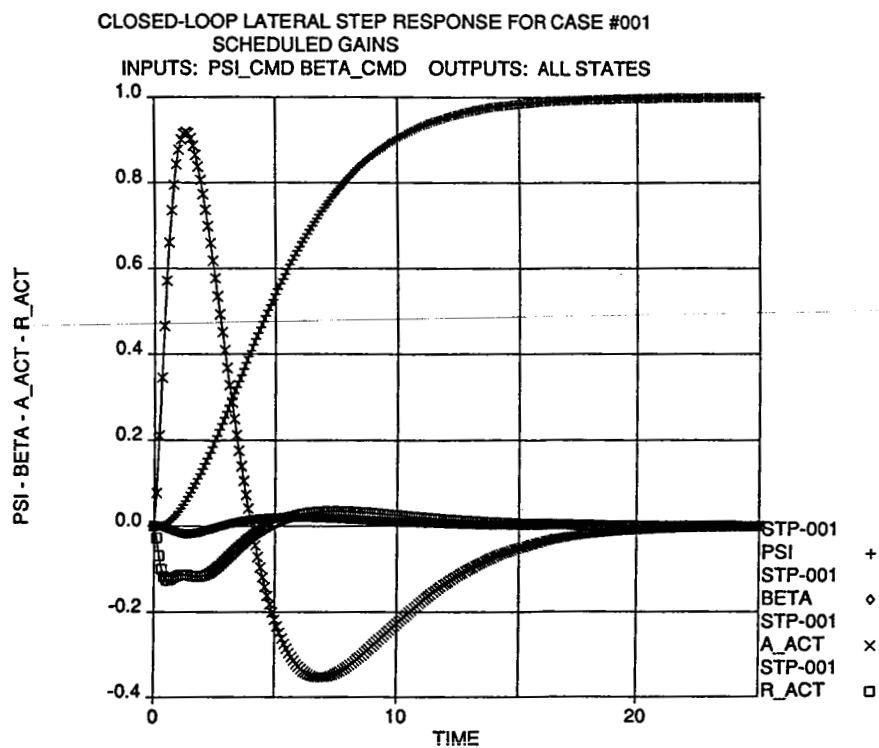


Figure 30. Time Response of Heading Controller for Heading Command Step

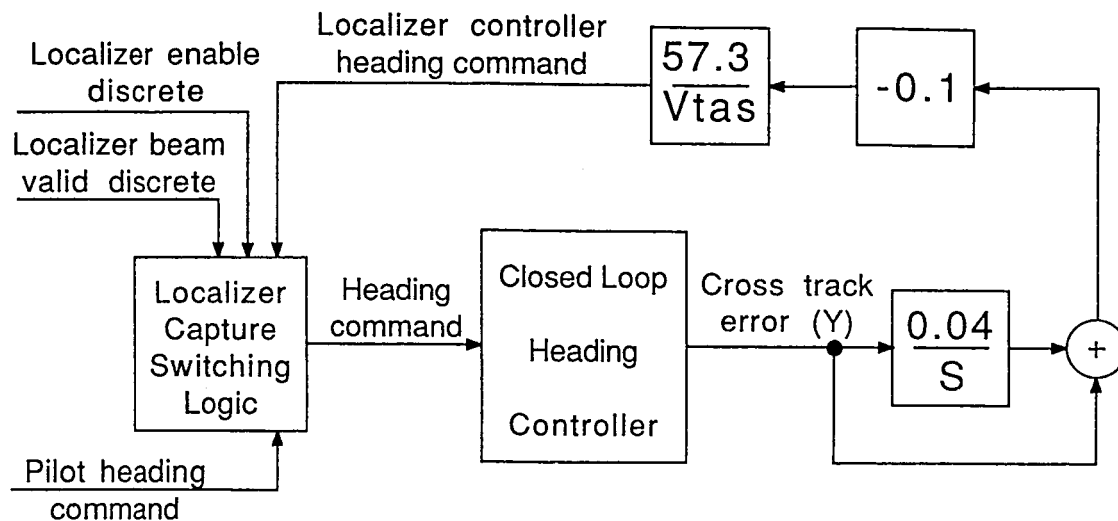


Figure 31. Block Diagram of Localizer Capture and Track Controller

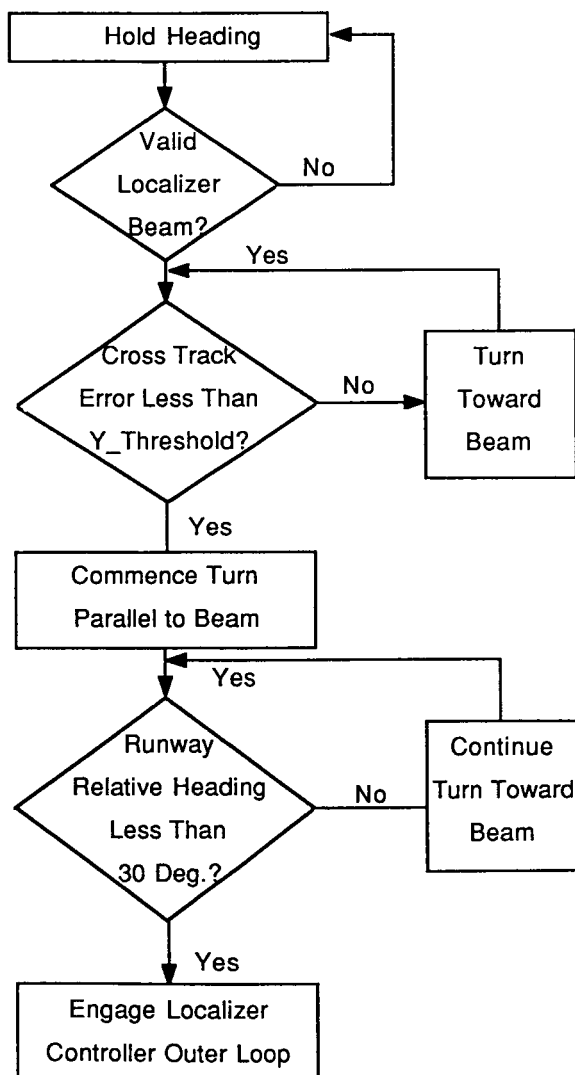


Figure 32. Outline of Localizer Capture Logic

Figure 32 outlines the localizer capture logic. The critical portion of the logic is testing to see if cross track error is less than a threshold defined by the velocity and maximum desired bank angle for autopilot turns. If the airplane is outside the threshold it turns toward the localizer beam until it is flying perpendicular to the beam with maximum closing speed. Once the airplane closes within the threshold it is commanded to turn parallel to the beam. When the difference between the airplane heading and the runway heading falls below 30 degrees, the localizer controller is engaged for final capture and track.

8.4 LOCALIZER CONTROLLER RESULTS

The following paragraphs present results from analysis of the closed loop localizer controller as defined by the block diagram in Figure 31.

8.4.1 EIGENVALUES

Figure 33 is a scatter plot of the eigenvalues of the closed loop localizer controller for each of the fourteen design flight conditions. Damping of 0.6 was achieved for all conditions.

8.4.2 GAIN AND PHASE MARGINS

Figure 34 shows the phase and gain margin characteristics for the rudder and aileron loops. Cross plots of the broken loop frequency response real and imaginary components show that no loops violate the region designating ± 4 dB and ± 40 degrees. Similar results were achieved for the sensor loops.

8.4.3 COVARIANCE RESPONSES

Figure 35 shows the position covariance responses of aileron, rudder, heading, and sideslip to a unit magnitude lateral dryden gust. These data are plotted versus flight condition number. These responses, as well as the rate responses, meet the requirements.

8.5 NONLINEAR SIMULATION OF LOCALIZER CAPTURE AND TRACK

The time history plots in Figures 36 and 37 illustrate two localizer capture scenarios. Figure 36 shows the ground track path followed for capture from an initial condition flying parallel to the localizer beam with a displacement of 15000 feet, while Figure 37 shows the ground track path followed for capture from an initial condition flying 90 degrees to the beam with initial displacement of zero. These two test cases illustrate the function of transition from heading control to localizer capture and track.

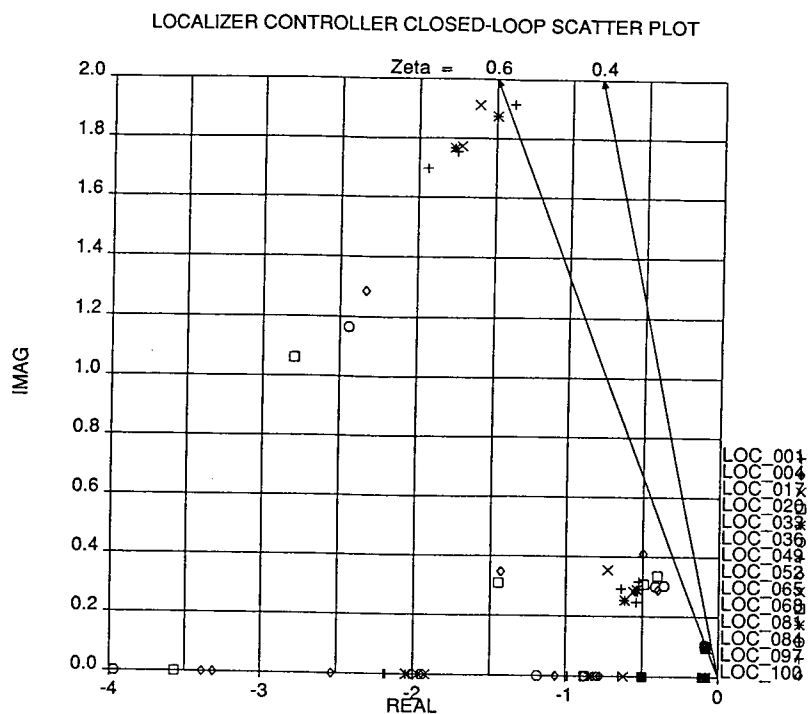


Figure 33. Scatter Plot for Localizer Capture and Track Controller

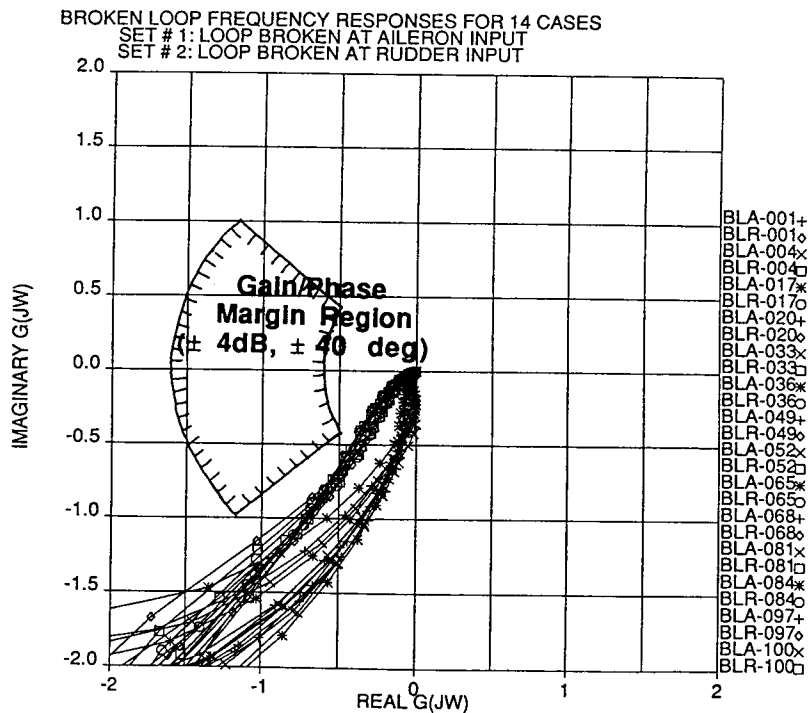


Figure 34. Aileron and Rudder Broken Loop Nyquist Plots for Localizer Capture and Track Controller

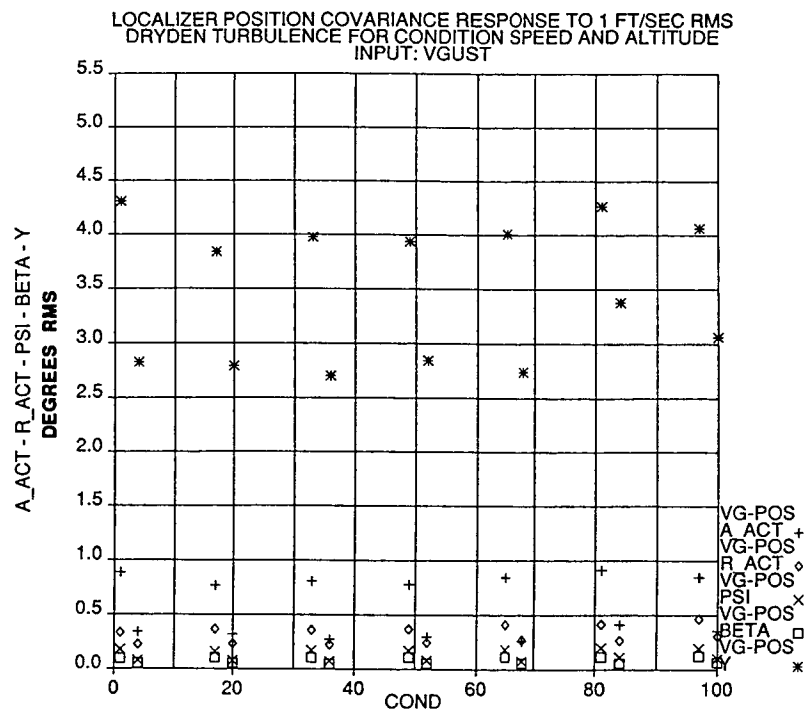


Figure 35. Covariance Responses of Localizer Capture and Track Controller to 1 Ft / Sec Dryden Gust

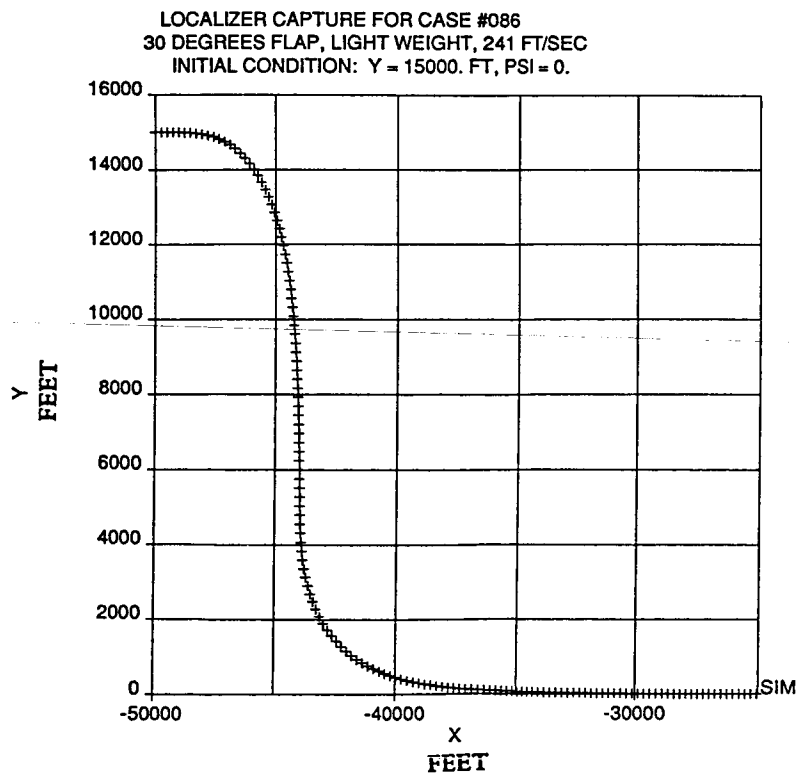


Figure 36. Flight Path History for Capture from a Parallel Heading with 1500 Ft Initial Offset

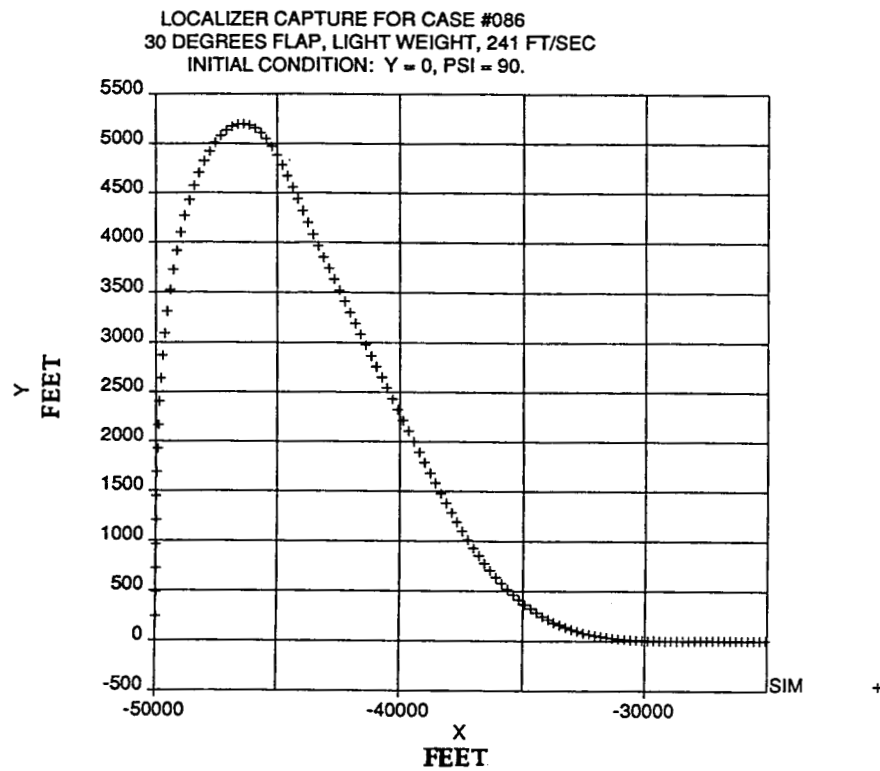


Figure 37. Flight Path History for Capture from a Perpendicular Path with No Initial Offset

Additional non-linear simulation results for the localizer capture and track controller are presented in Plots 58-81 found in Appendix B. These 24 plots are divided into four groups (58-63, 70-75, and 76-81) corresponding to a low and high speed captures from a heading 45 degrees relative to the runway and low and high speed captures from a heading 90 degrees relative to the runway respectively. Each plot gives three traces: 1) still air, 2) a 20 ft/sec crosswind flowing toward the runway centerline, and 3) a 20 ft/sec crosswind blowing away from the runway centerline. A listing of the FORTRAN program used to generate these plots is found at the end of Appendix B.

8.6 SUMMARY OF LATERAL AXIS DESIGN

The integral LQG design process presented in this section is an efficient technique for the design of multiple input / multiple output control systems. Unlike classical root locus methods, requirements of more than one loop can be handled at a time. In addition, the systematic approach to selecting regulated variables and forming criteria outputs affords more insight than LQG techniques using state weighting only. The use of transmission zeros, both inherent in the plant and created by the designer, is crucial since they dictate the asymptotic nature of the closed loop eigenvalues.

Although classical root locus techniques treating one loop at a time have been adequate in the past for the design of transport airplane control systems, the need is arising for multiple loop design methods. For example, in search of greater efficiency, airplane structural stiffness has been reduced leading to lower frequency flexible modes. The result is a challenging controls problem since control inputs now risk exciting structural modes. The technique presented here allows engineers with experience applying classical design methods to quickly learn a multiple loop design approach since the single loop compensation ideas they are familiar with are the same tools used to develop criterion outputs, the central feature of this method.

9.0 CONCLUSIONS

An integrated autopilot/autothrottle control system has been developed. A two-degree-of-freedom approach was used to achieve a satisfactory design that offers the designer the fundamental advantages of:

- a. Simple mode switching logic
- b. Limiting done in feedforward loop, hence, no stability effects
- c. Uniform closed loop response throughout the flight envelope.

Within the two-degree-of-freedom framework, the feedback regulator was designed using an integral LQR design technique, which offers a systematic approach to satisfy desired feedback performance requirements and guarantees stability margins in both control and sensor loops.

The resulting feedback controller was discretized and implemented using a delta coordinate concept, which allows for transient free controller switching by initializing all controller states to zero and provides a simple solution for dealing with throttle limiting cases.

In conclusion, it was shown, that a systematic top-down approach to complex control design problems combined with proper application of modern control synthesis techniques yields a satisfactory solution in a reasonably short time period.

APPENDIX A

GLIDESLOPE MODEL COMPUTATIONS

The computations shown here are based on [5].

From Figure 5.5:

$$x = H_{RAD} \cot (GSA - GSE)$$

$$H_C = x \tan GSA$$

$$\therefore H_e = H_C - H_{RAD}$$

$$= x \tan GSA - H_{RAD}$$

$$= H_{RAD} \left(\frac{\tan GSA}{\tan (GSA - GSE)} - 1 \right)$$

and, using small angle approximations:

$$H_e = H_{RAD} \frac{GSE}{GSA - GSE}$$

To compute \dot{H}_C consider:

$$\dot{H}_C = \frac{d}{dt} H_C = \frac{d H_C}{dx} \cdot \frac{dx}{dt}$$

but

$$\frac{d H_C}{dx} = \tan GSA \cong \frac{GSA}{57.3}$$

and

$$\frac{dx}{dt} = V_I$$

$$\therefore \dot{H}_C = V_I \frac{GSA}{57.3}$$

FLARE PATH COMPUTATIONS

Altitude command:

$$H_C(x) = A x^3 + B x^2 + C x + D$$

Altitude rate command:

$$\dot{H}_C(x) = 3A \frac{V_I}{x_{TD}} x^2 + 2B \frac{V_I}{x_{TD}} + C \frac{V_I}{x_{TD}}$$

x_{TD} = distance to touchdown from flare initiation = 1200 ft

V_I = inertial speed of the aircraft

Find A, B, C, D from boundary conditions:

$$x = 0$$

$$x = 1200$$

$$H_C = 45 \text{ ft}$$

$$H_C = 0$$

$$\dot{H}_C = \dot{H}$$

$$\dot{H}_C = -2.5 \text{ fps}$$

$$D = 45 \text{ ft}$$

$$C = \frac{\dot{H}/x=0 \cdot x_{TD}}{V_I}$$

$$B = 2C - 3D - 45 \frac{x_{TD}}{V_I}$$

$$A = \frac{\dot{H} x_{TD}}{3V_I} - \frac{2B}{3} - \frac{C}{3}$$

SPEED HOLD COMPUTATIONS

1. Speed conversion

MACH \rightarrow VTAS:

By definition

$$V_{TAS} = MACH \cdot c \quad (1)$$

where

c is a speed of sound

VCAS \rightarrow VTAS [5]:

$$V_{TAS} = VCAS \frac{1}{1 - 10^{-5} H} \quad (2)$$

2. Limiter computations:

\ddot{V} limiter: Consider \dot{E}_s (energy rate per pound of weight) equation:

$$\dot{E}_s = \dot{H} + V \cdot \frac{\dot{V}}{g} \quad (3)$$

$$\frac{\dot{E}_s}{V} = \frac{\dot{H}}{V} + \frac{\dot{V}}{g} = \frac{T-D}{W} \quad (4)$$

When thrust is constant:

$$\frac{\ddot{E}_s}{V} \cong \frac{\ddot{H}_s}{V} + \frac{\ddot{V}}{g} = 0 \quad (5)$$

$$\therefore \ddot{V} \cong -g \frac{\ddot{H}}{V}$$

$$\ddot{H} \text{ limit is } 0.05 g = 1.6 \text{ fps}^2$$

Hence,

$$\ddot{V}_{LIM} = \frac{32.2 \cdot 1.6}{V} = \frac{52}{V} \quad (6)$$

\dot{V} limiter: When throttles are at the limit, airplane's energy rate is constant, (4) , assuming drag doesn't change. Therefore, any speed change must be accomplished at the expense of climb rate.

Let H_{min} be the minimum climb rate desired. Then

$$\frac{\Delta \dot{E}_s}{V} = \frac{\dot{H}_{min} - \dot{H}}{V} + \frac{\dot{V}_{LIM}}{g} = 0 \quad (7)$$

$$\therefore \dot{V}_{LIM} = g \left(\frac{\dot{H} - \dot{H}_{min}}{VTAS} \right) \quad (8)$$

In climb $\dot{H}_{min} = 10 \text{ fps}$

In descent $\dot{H}_{min} = 0 \text{ fps}$

\therefore In climb (max thrust):

$$\dot{V}_{max} = g \left(\frac{\dot{H} - 10}{VTAS} \right) \quad (9)$$

In descent (min thrust)

$$\dot{V}_{min} = g \frac{\dot{H}}{V} \quad (10)$$

NOMINAL FLIGHT CONDITION FOR CRUISE CONTROLLER DESIGN

```

A MATRIX (5X5)      .STATE SPACE MODEL OF THE AIRPLANE
-0.422307E-01      -0.391491E+00      -0.775813E+00      -0.560582E+00      0.000000E+00
-0.279749E-02      -0.542493E+00      0.999048E+00      0.247901E-05      0.000000E+00
0.686186E-01      -0.207439E+01      -0.907272E+00      0.170303E-03      0.000000E+00
0.000000E+00      0.000000E+00      0.100000E+01      0.000000E+00      0.000000E+00
-0.196946E-06      -0.132435E+02      0.000000E+00      0.132435E+02      0.000000E+00
B MATRIX (5X5)
-0.661506E-01      -0.507741E-02      0.292118E-01      0.422307E-01      0.391491E+00
-0.321807E-01      0.942430E-02      -0.131920E-03      0.279749E-02      0.542493E+00
-0.297967E+01      0.291736E-01      0.218543E-01      -0.686186E-01      0.207439E+01
0.000000E+00      0.000000E+00      0.000000E+00      0.000000E+00      0.000000E+00
0.000000E+00      0.000000E+00      0.000000E+00      0.196946E-06      0.132435E+02
C MATRIX (8X5)
-0.422307E-01      -0.391491E+00      -0.775813E+00      -0.560582E+00      0.000000E+00
0.100000E+01      0.000000E+00      0.000000E+00      0.000000E+00      0.000000E+00
-0.196946E-06      -0.132435E+02      0.000000E+00      0.132435E+02      0.000000E+00
0.000000E+00      0.000000E+00      0.000000E+00      0.000000E+00      0.100000E+01
0.000000E+00      0.000000E+00      0.000000E+00      0.000000E+00      0.000000E+00
0.000000E+00      0.000000E+00      0.100000E+01      0.000000E+00      0.000000E+00
0.000000E+00      0.000000E+00      0.000000E+00      0.100000E+01      0.000000E+00
-0.122523E-02      -0.223450E+00      -0.179852E-02      -0.101611E-02      0.000000E+00
D MATRIX (8X5)
-0.661506E-01      -0.507741E-02      0.292118E-01      0.422307E-01      0.391491E+00
0.000000E+00      0.000000E+00      0.000000E+00      -0.100000E+01      0.000000E+00
0.000000E+00      0.000000E+00      0.000000E+00      0.196946E-06      0.132435E+02
0.000000E+00      0.000000E+00      0.000000E+00      0.000000E+00      0.000000E+00
0.000000E+00      0.000000E+00      0.185995E-01      0.000000E+00      0.000000E+00
0.000000E+00      0.000000E+00      0.000000E+00      0.000000E+00      0.000000E+00
0.000000E+00      0.000000E+00      0.000000E+00      0.000000E+00      0.000000E+00
-0.133329E-01      0.386026E-02      -0.116222E-05      0.122523E-02      0.223450E+00
STATES (5)
'U' 'ALPHA' 'Q' 'THETA' 'H'
INPUTS (5)
'DE' 'DSPL' 'DTH' 'UG' 'ALFG'
OUTPUTS (8)
'UD' 'UO' 'HDO' 'HO' 'EPRO' 'QO' 'THO' 'NZ'
END
CONDITION#      159
MACH      0.7799900
FLAPS      0.0000000
H      35000.00
GAMMA      -1.1285000E-05
VTAS      758.8500
VCAS      264.5300
CG      0.3000000
WEIGHT      110000.0
ALFA      3.349600
Q      246.5400
GEAR      0.0000000
THRUST/THROTTLE 134.9190

```

NOMINAL FLIGHT CONDITION FOR LANDING CONTROLLER DESIGN

```

A MATRIX (5X5)      .STATE SPACE MODEL OF THE AIRPLANE
-0.460346E-01      0.383599E+00      -0.374943E-01      -0.561453E+00      0.000000E+00
-0.736570E-01      -0.755050E+00      0.100284E+01      -0.722729E-04      0.000000E+00
-0.100121E-02      -0.339359E+00      -0.739641E+00      -0.301061E-03      0.000000E+00
0.000000E+00      0.000000E+00      0.100000E+01      0.000000E+00      0.000000E+00
-0.367103E-07      -0.394695E+01      0.000000E+00      0.394695E+01      0.000000E+00
B MATRIX (5X5)
0.194268E-02      -0.971315E-02      0.224840E+00      0.460346E-01      -0.383599E+00
-0.519616E-01      0.343995E-01      -0.554790E-03      0.736570E-01      0.755050E+00
-0.104851E+01      0.344566E-01      0.128302E+00      0.100121E-02      0.339359E+00
0.000000E+00      0.000000E+00      0.000000E+00      0.000000E+00      0.000000E+00
0.000000E+00      0.000000E+00      0.000000E+00      0.367103E-07      0.394695E+01
C MATRIX (7X5)
-0.460346E-01      0.383599E+00      -0.374943E-01      -0.561453E+00      0.000000E+00
0.100000E+01      0.000000E+00      0.000000E+00      0.000000E+00      0.000000E+00
-0.367103E-07      -0.394695E+01      0.000000E+00      0.394695E+01      0.000000E+00
0.000000E+00      0.000000E+00      0.000000E+00      0.000000E+00      0.100000E+01
0.000000E+00      0.000000E+00      0.000000E+00      0.000000E+00      0.000000E+00
0.000000E+00      0.000000E+00      0.100000E+01      0.000000E+00      0.000000E+00
0.000000E+00      0.000000E+00      0.000000E+00      0.100000E+01      0.000000E+00
D MATRIX (7X5)
0.194268E-02      -0.971315E-02      0.224840E+00      0.460346E-01      -0.383599E+00
0.000000E+00      0.000000E+00      0.000000E+00      -0.100000E+01      0.000000E+00
0.000000E+00      0.000000E+00      0.000000E+00      0.367103E-07      0.394695E+01
0.000000E+00      0.000000E+00      0.000000E+00      0.000000E+00      0.000000E+00
0.000000E+00      0.000000E+00      0.000000E+00      0.000000E+00      0.000000E+00
0.000000E+00      0.000000E+00      0.226125E-01      0.000000E+00      0.000000E+00
0.000000E+00      0.000000E+00      0.000000E+00      0.000000E+00      0.000000E+00
0.000000E+00      0.000000E+00      0.000000E+00      0.000000E+00      0.000000E+00
STATES (5)
'U' 'ALPHA' 'Q' 'THETA' 'H'
INPUTS (5)
'DE' 'DSPL' 'DTH' 'UG' 'ALFG'
OUTPUTS (7)
'UD' 'UO' 'HDO' 'HO' 'EPRO' 'QO' 'THO'
END
CONDITION#      102
MACH      0.2025700
FLAPS      39.99900
H      100.0000
GAMMA      -2.1035000E-06
VTAS      226.1600
VCAS      134.0000
CG      0.3000000
WEIGHT      80000.00
ALFA      0.5426800
Q      61.41800
GEAR      1.000000
THRUST/THROTTLE 559.0780

```

ELEVATOR GAINS FOR LANDING CONTROLLER

$$K_{I_V} = \frac{A + B (Q_c - Q_{c_o})}{1 + C (Q_c - Q_{c_o})}$$

$$K_{I_H} = 1.2$$

$$K_u = \frac{(0.841 - 0.0023(Q_c - 43.5))}{1 + 0.00223 (Q_c - 43.5)}$$

$$K_H = \frac{D + E (\alpha - \alpha_o)}{1 + F (\alpha - \alpha_o)}$$

$$K_Q = \frac{3.44 + 0.0229(Q_c - 43.5)}{1 + 0.0183(Q_c - 43.5)}$$

$$K_\theta = 7.1$$

$$K_{EPR} = \frac{G + H (Q_c - Q_{c_o})}{1 + I (Q_c - Q_{c_o})}$$

$$K_H = \frac{H + K (\alpha - \alpha_o)}{1 + L (\alpha - \alpha_o)}$$

Q_{c_o} = NOMINAL DYNAMIC PRESSURE

WHERE A, B, C, D, E, F, G, H, I, J, K, L a function of flap position

THROTTLE GAINS FOR LANDING CONTROLLER

$$K_{I_V} = \frac{A + B(Q_c - Q_{c_o})}{1 + C(Q_c - Q_{c_o})}$$

$$K_{I_H} = \frac{D + E(Q_c - Q_{c_o})}{1 + F(Q_c - Q_{c_o})}$$

$$K_u = \frac{-2.153 + 0.0078(Q_c - 43.5)}{1.0 - 0.0033(Q_c - 43.5)}$$

$$K_H = \frac{G + H(Q_c - Q_{c_o})}{1 + I(Q_c - Q_{c_o})}$$

$$K_Q = \frac{J + K(Q_c - Q_{c_o})}{1 + L(Q_c - Q_{c_o})}$$

$$K_\theta = \frac{0.422 - 0.238(\alpha + 2.81)}{1.0 + 0.007(\alpha + 2.81)}$$

$$K_{EPR} = \frac{-18.3 + 0.22(\text{THTRM} - 13.87)}{1.0 - 0.0046(\text{THTRM} - 13.87)}$$

$$K_H = \frac{M + N(Q_c - Q_{c_o})}{1 + P(Q_c - Q_{c_o})}$$

WHERE A, B, C, D, E, F, G, H, I, J, K, L, M, N, P are a function of flap position

DISCRETIZED CONTROLLER COMPUTATIONS

1. Feedback controller:

$$A_d = \begin{bmatrix} e^{-\Delta \frac{T}{\tau}} & 0 & 0 \\ (1 - .1\tau)\left(1 - e^{-\Delta \frac{T}{\tau}}\right) & 1 & 0 \\ 0 & 0 & 1 \end{bmatrix}$$

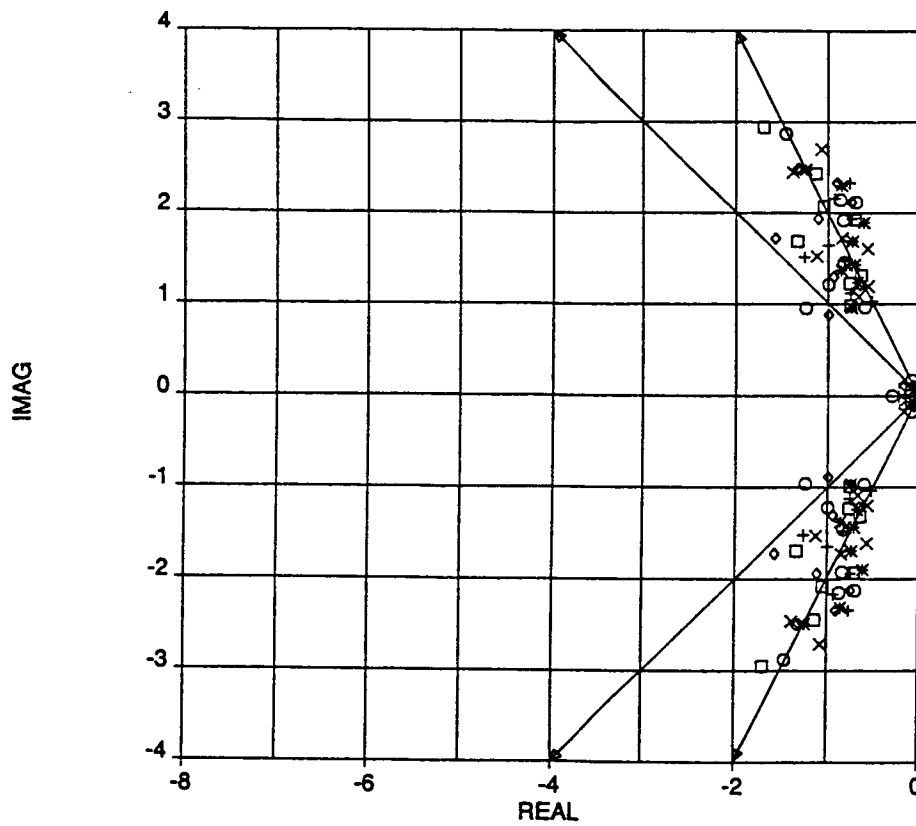
$$B_d = \begin{bmatrix} \left(1 - e^{-\Delta \frac{T}{\tau}}\right) & 0 & 0 \\ (1 - .1\tau)\left(\Delta T - \tau\left(1 - e^{-\Delta \frac{T}{\tau}}\right)\right) & \Delta T & 0 \\ 0 & 0 & 1 \end{bmatrix}$$

2. Feedforward controller:

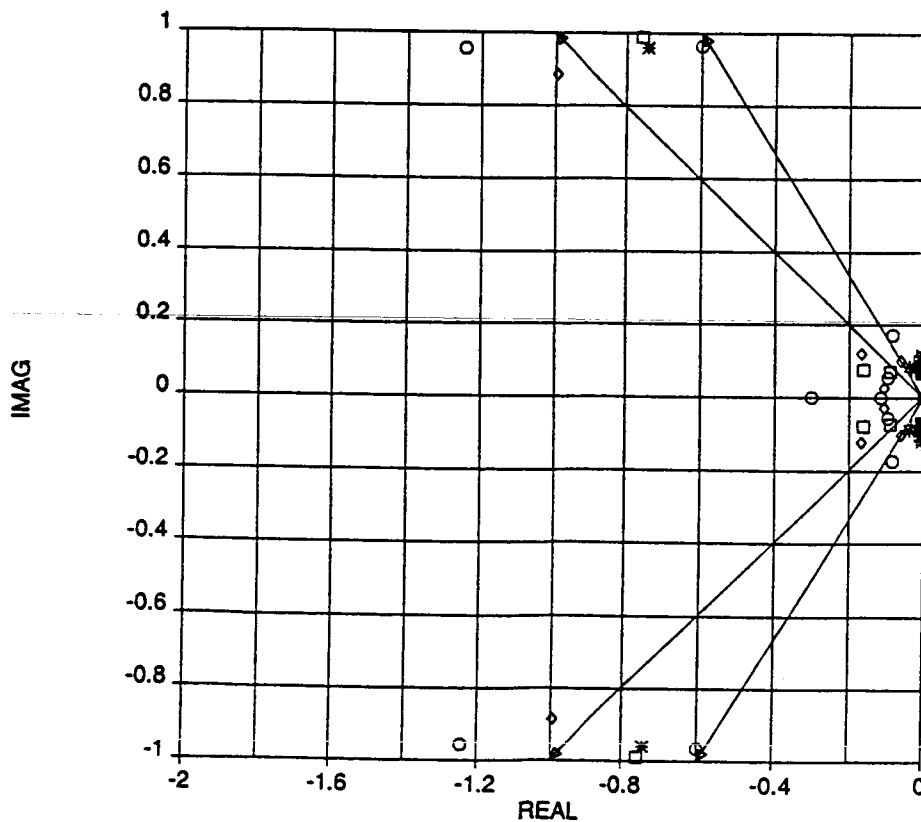
$$A_d = \begin{bmatrix} .9851 & -1.117E-3 \\ 4.96E-2 & 1 \end{bmatrix}$$

$$B_d = \begin{bmatrix} 1.117E-3 \\ 2.8E-5 \end{bmatrix}$$

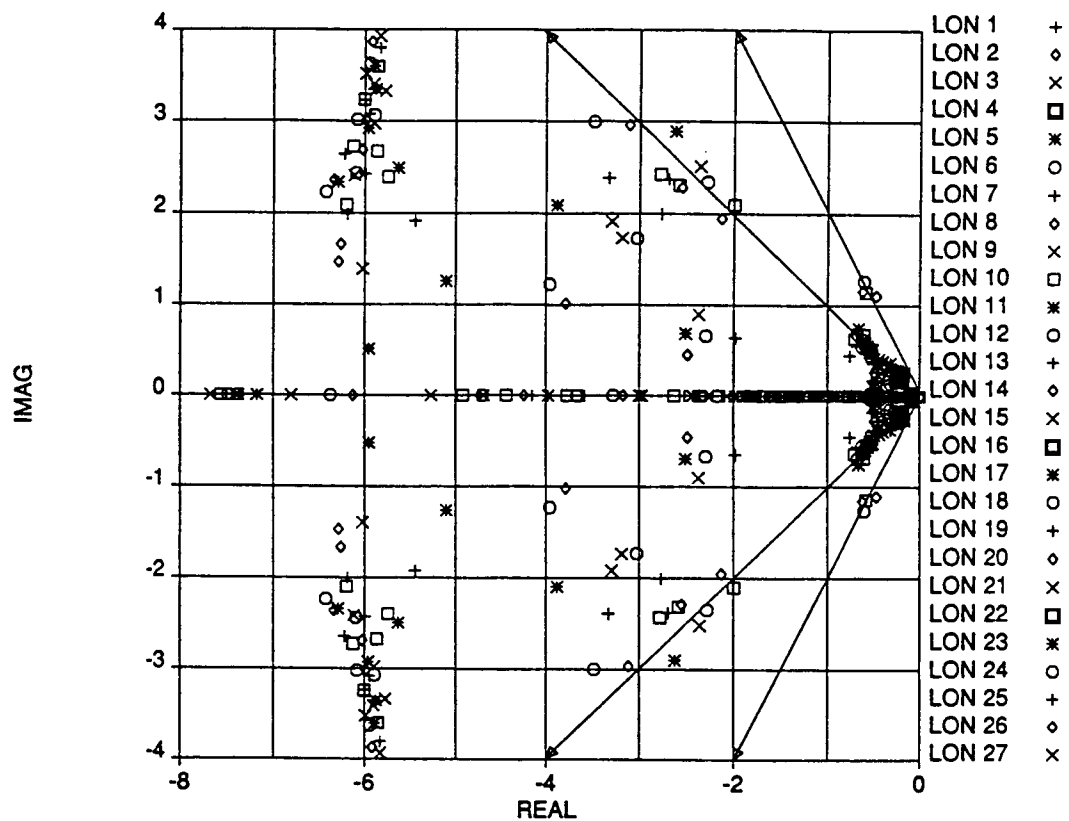
LINEAR ANALYSIS RESULTS



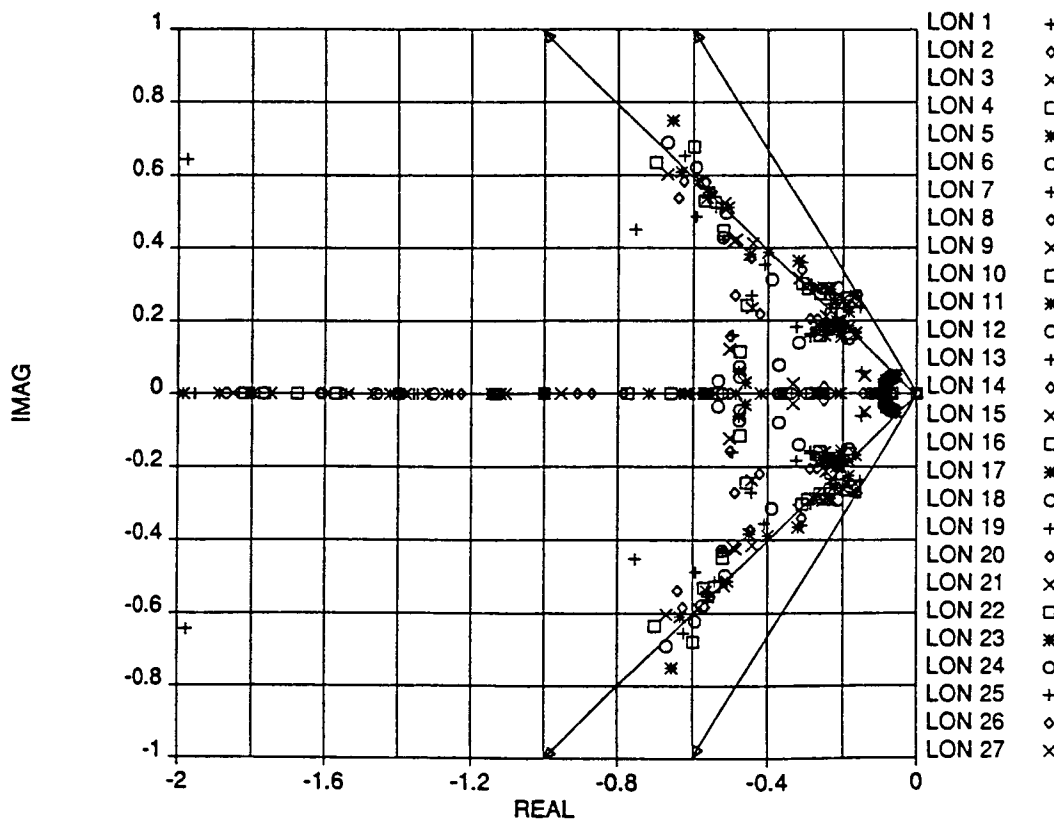
Plot 1. Open Loop Short Period Poles Scatter Plot for Conditions 113 - 160



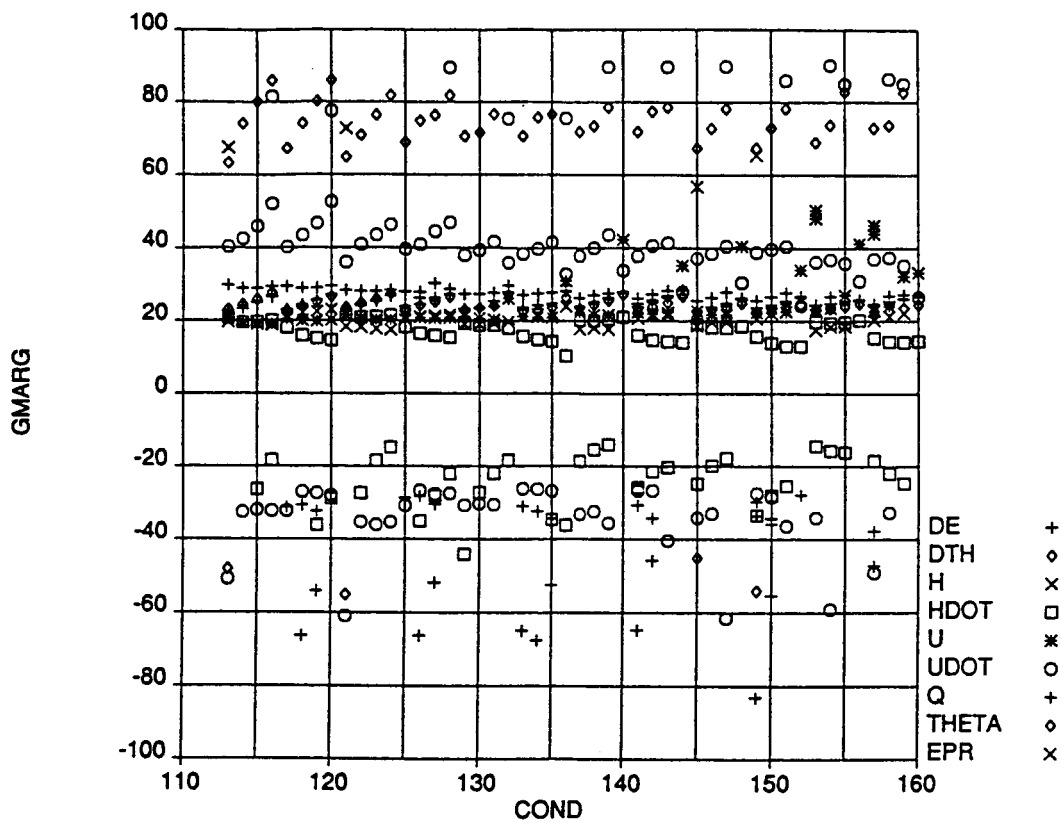
Plot 2. Open Loop Short Phugoid Poles Scatter Plot for Conditions 113 - 160



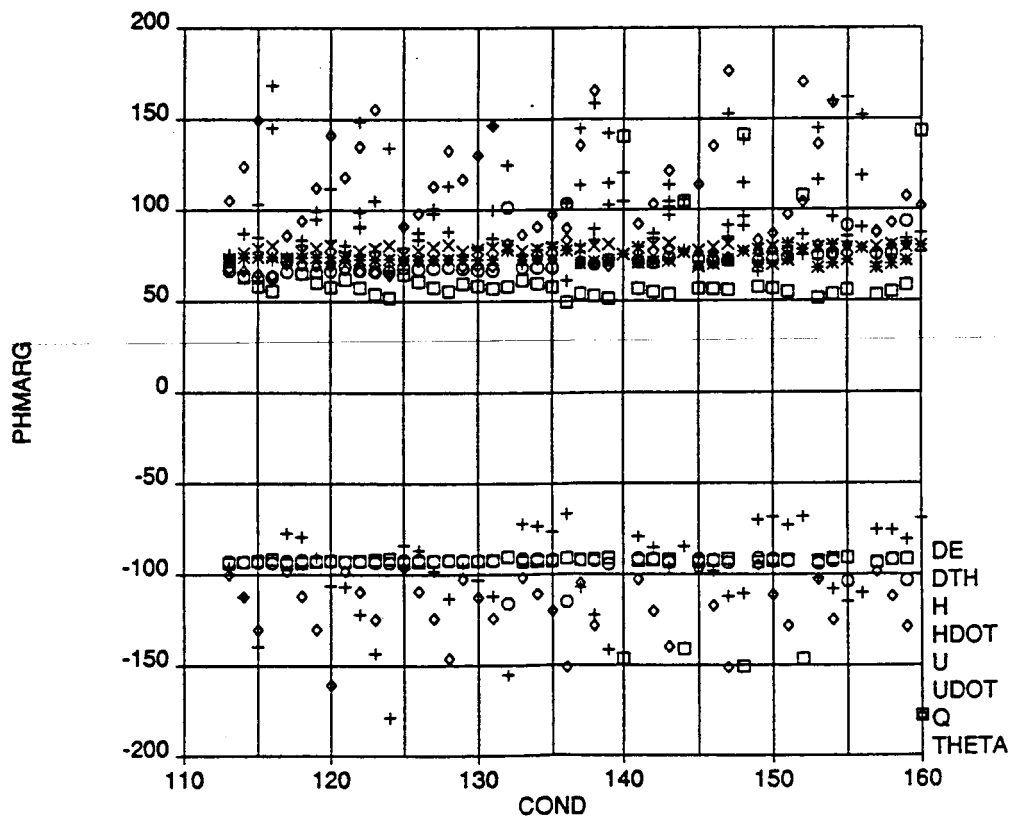
Plot 3. Cruise Controller Closed Loop Short Period Eigenvalues Scatter Plot



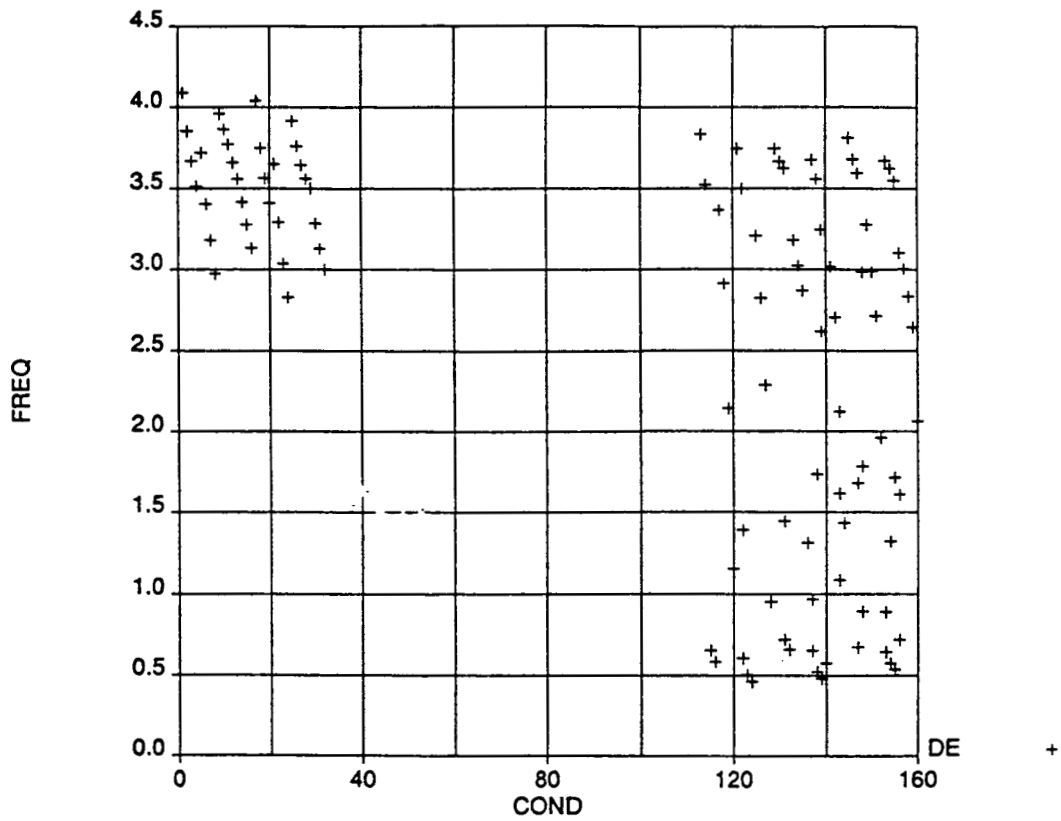
Plot 4. Cruise Controller Closed Loop Phugoid Eigenvalues Scatter Plot



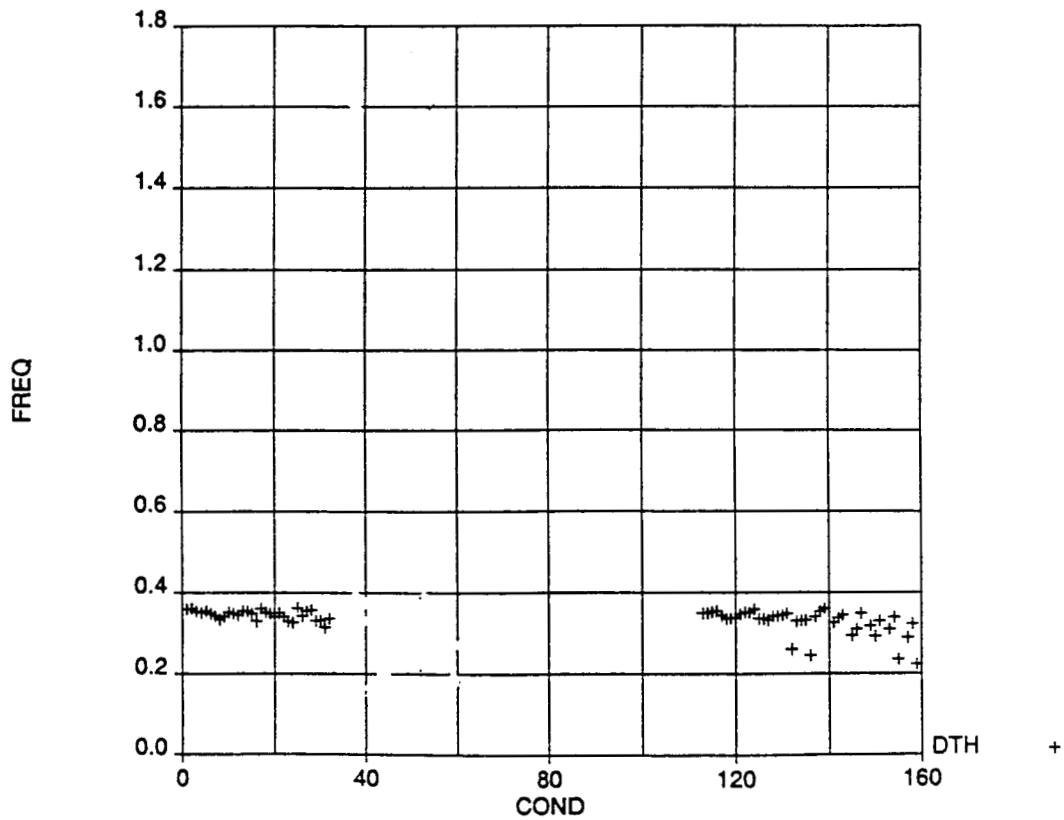
Plot 5. Cruise Controller Broken Loop Analysis Plot of Gain Margins vs Flight Condition for All Control and Sensor Loops



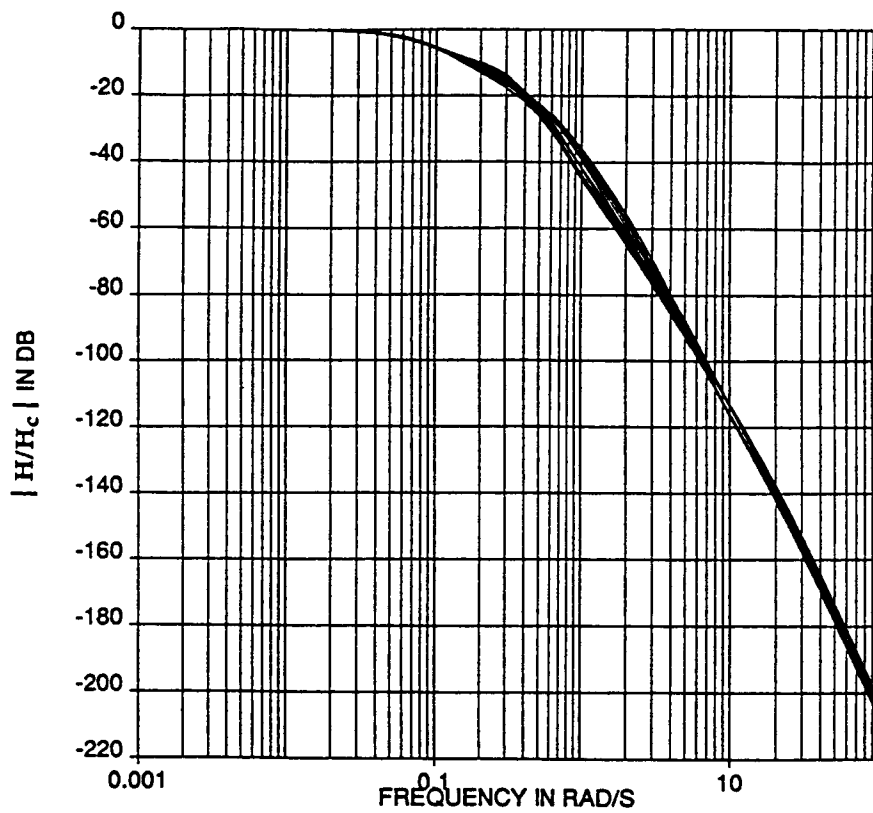
Plot 6. Cruise Controller Broken Loop Analysis Plot of Phase Margins vs Flight Condition for All Control and Sensor Loops



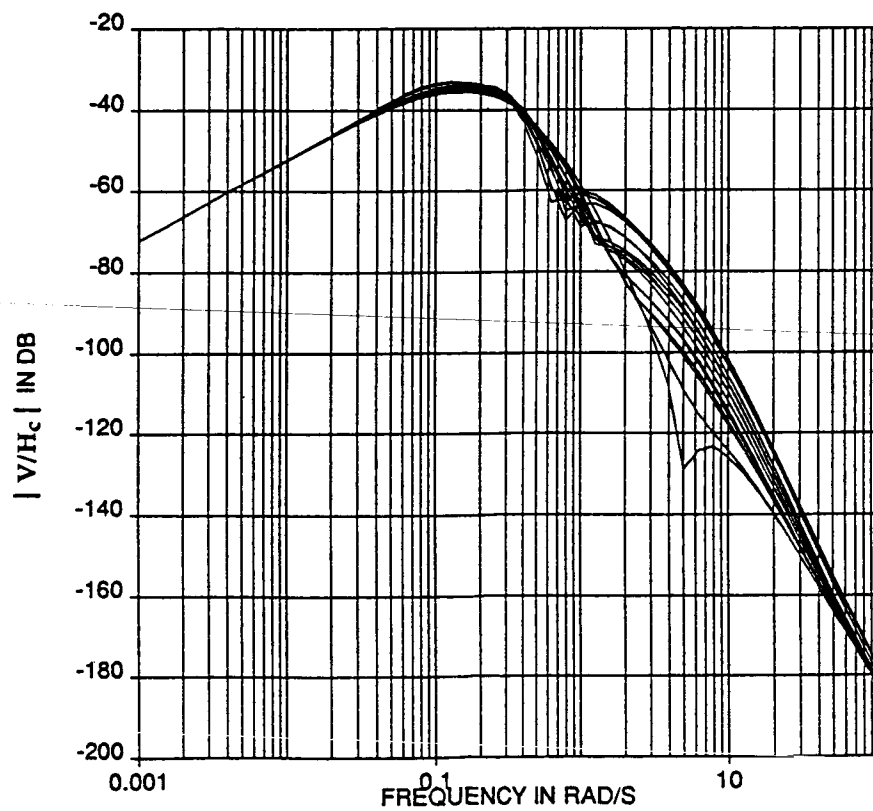
Plot 7. Cruise Controller Broken Loop Analysis Plot of Crossover Frequency vs Flight Condition for Elevator Loop



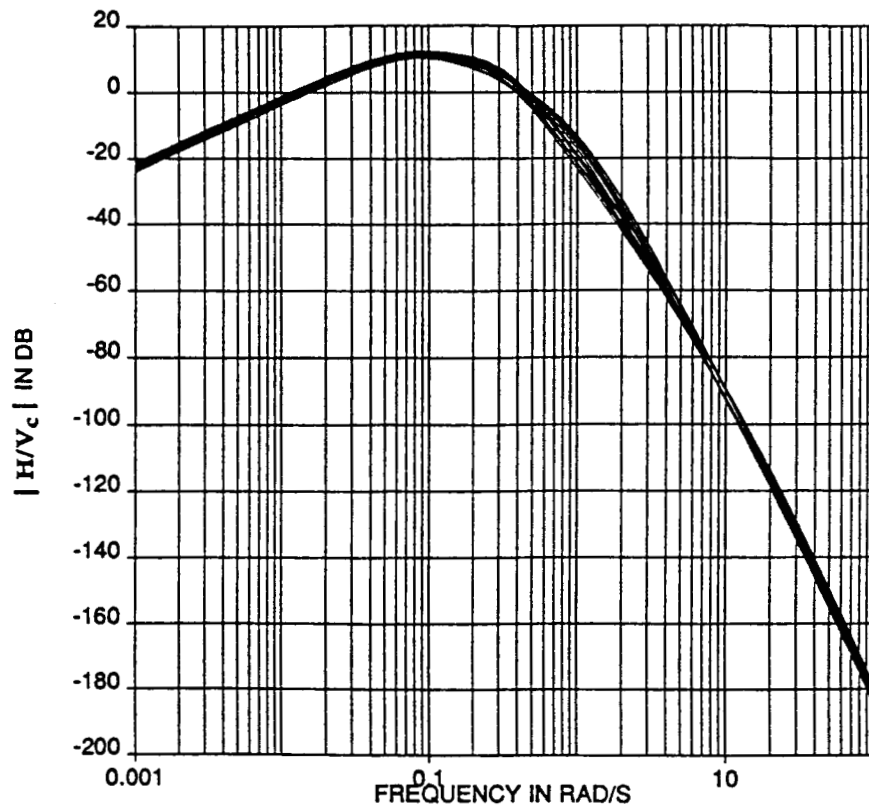
Plot 8. Cruise Controller Broken Loop Analysis Plot of Crossover Frequency vs Flight Condition for Throttle Loop



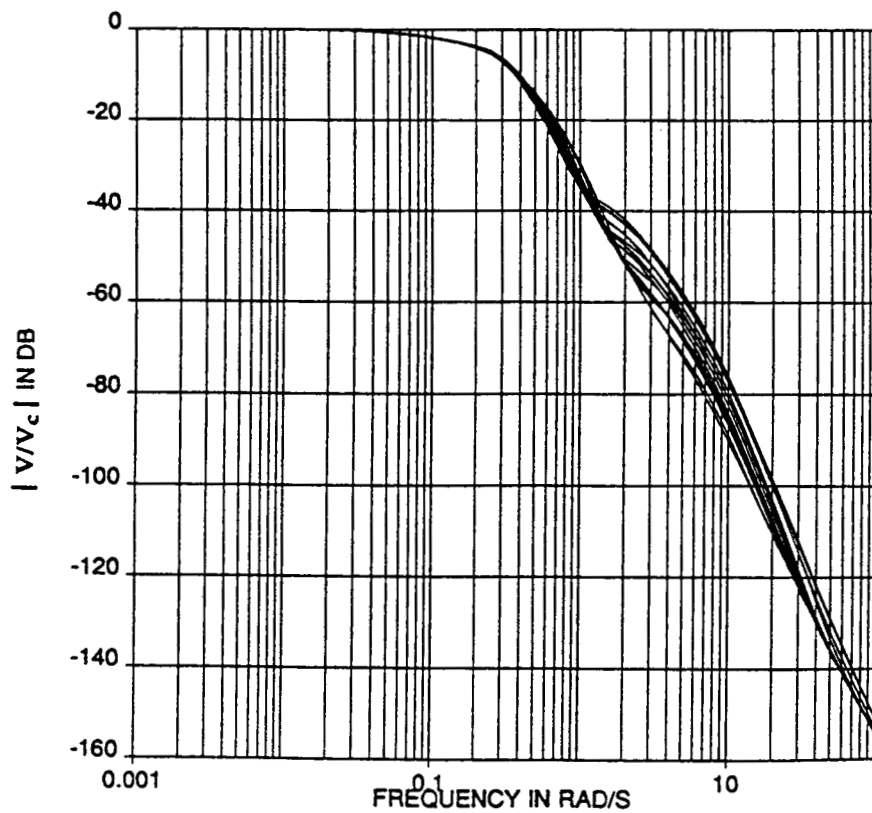
Plot 9. Cruise Control Law Closed Loop Frequency Response Analysis for Conditions 113 - 128



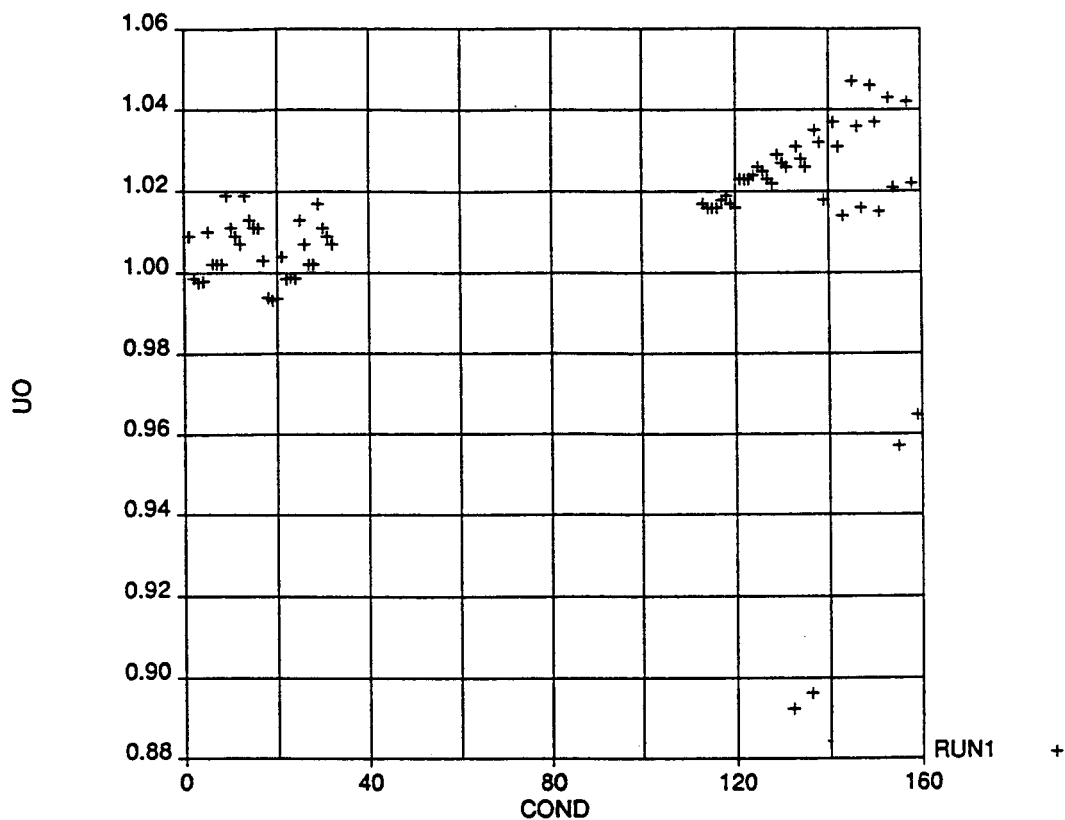
Plot 10. Cruise Control Law Closed Loop Frequency Response Analysis for Conditions 113 - 128



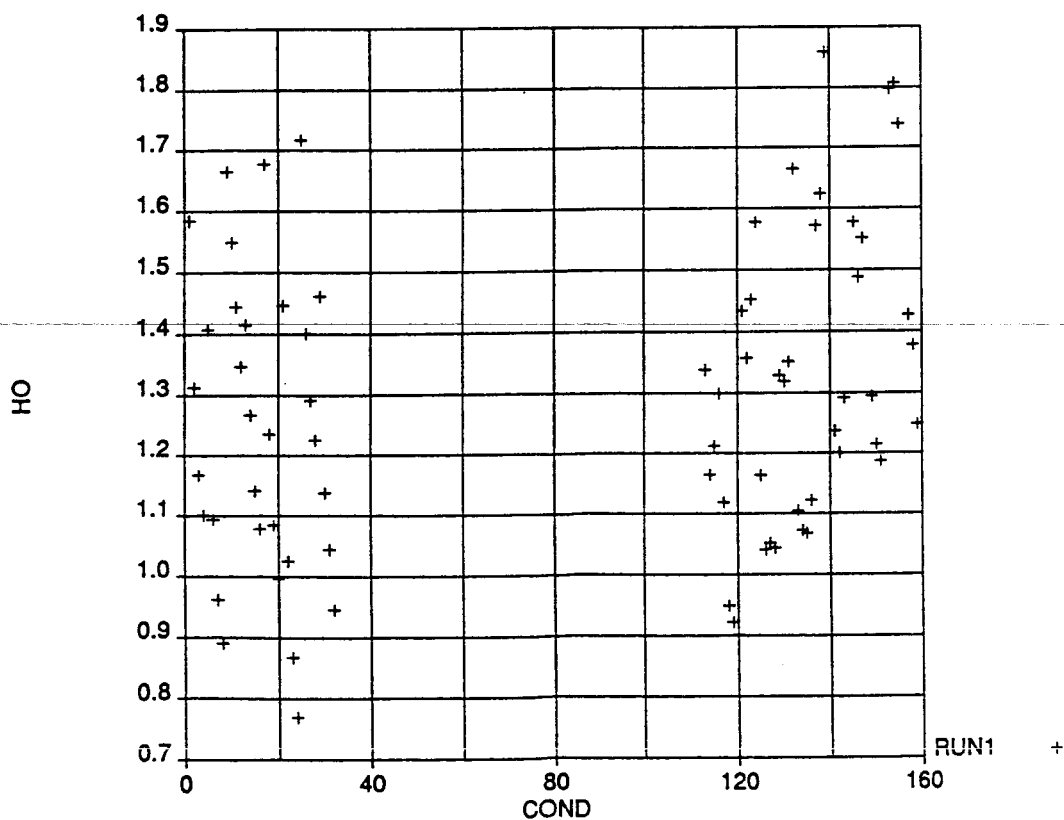
Plot 11. Cruise Control Law Closed Loop Frequency Response Analysis for Conditions 113 - 128



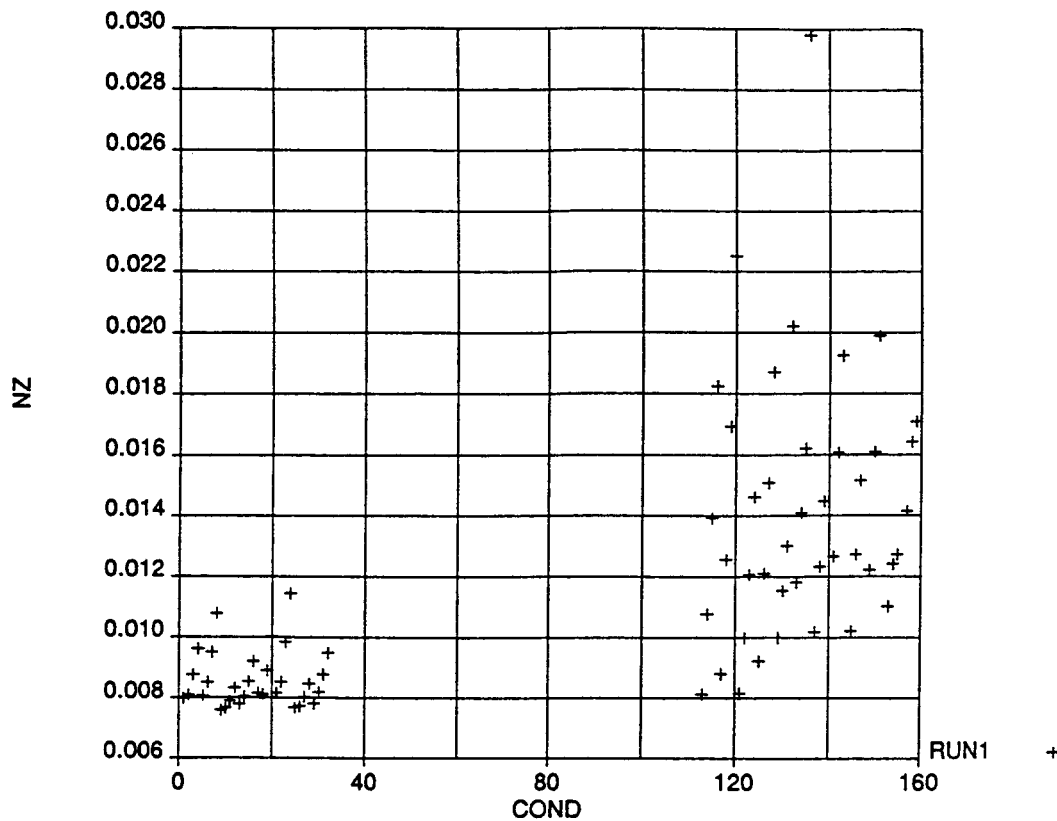
Plot 12. Cruise Control Law Closed Loop Frequency Response Analysis for Conditions 113 - 128



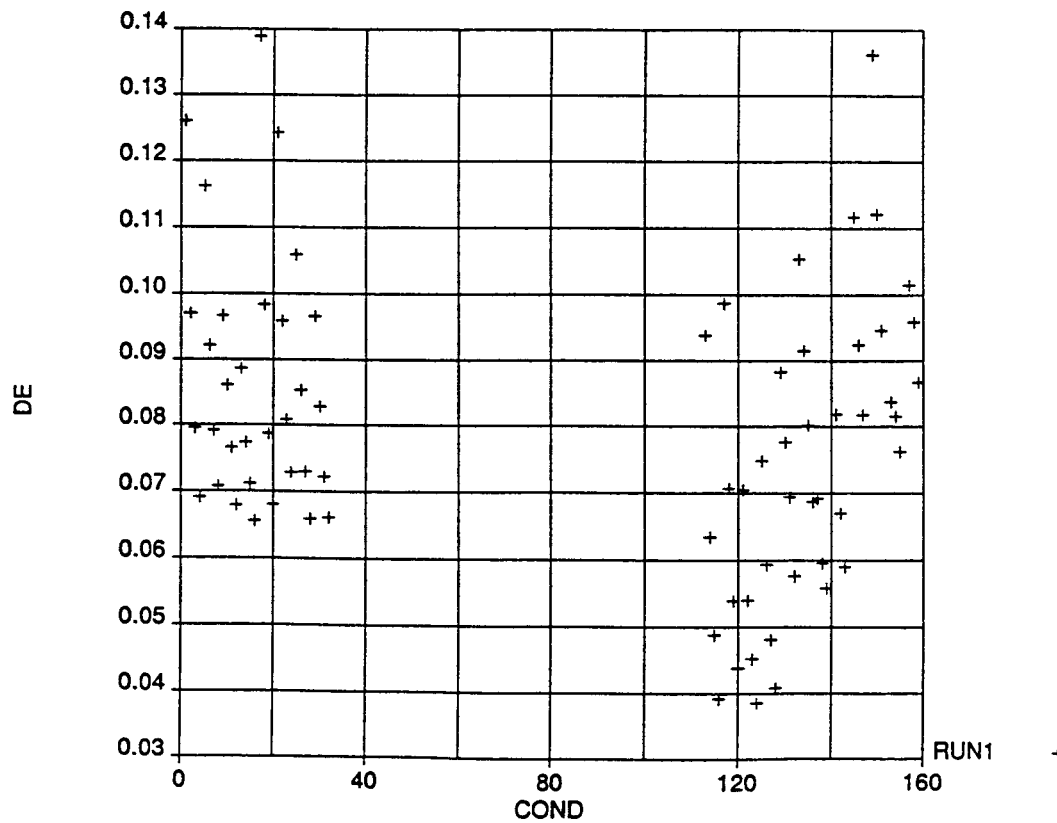
Plot 13. Cruise Control Law Turbulence Response Analysis Covariance Response to Dryden Turbulence vs Flight Condition (Airspeed in FPS)



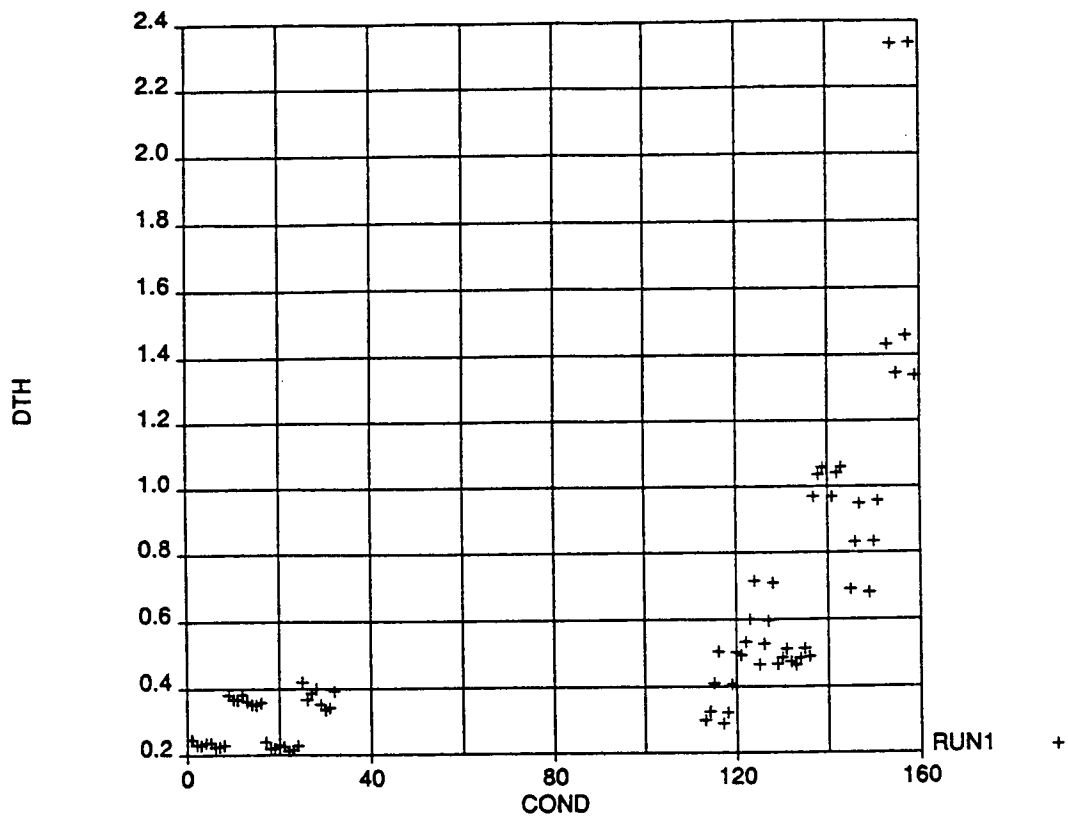
Plot 14. Cruise Control Law Turbulence Response Analysis Covariance Response to Dryden Turbulence vs Flight Condition (Altitude in Ft)



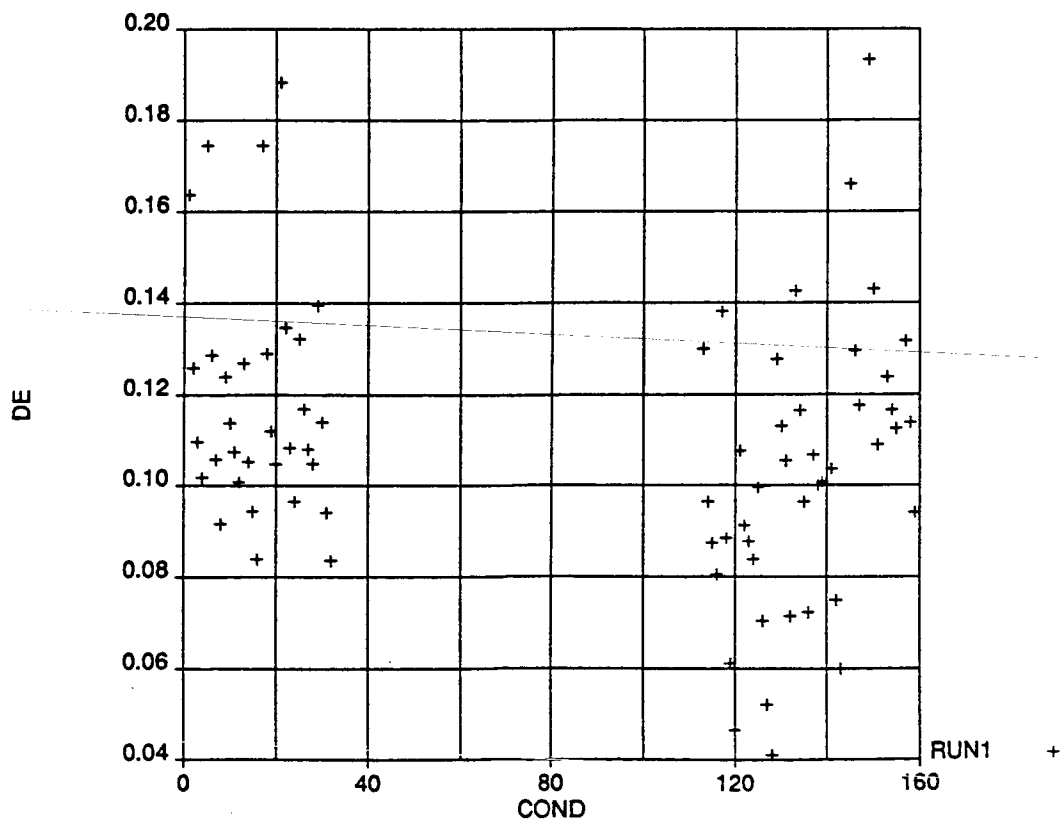
Plot 15. Cruise Control Law Turbulence Response Analysis Covariance Response to Dryden Turbulence vs Flight Condition (NZ in G's)



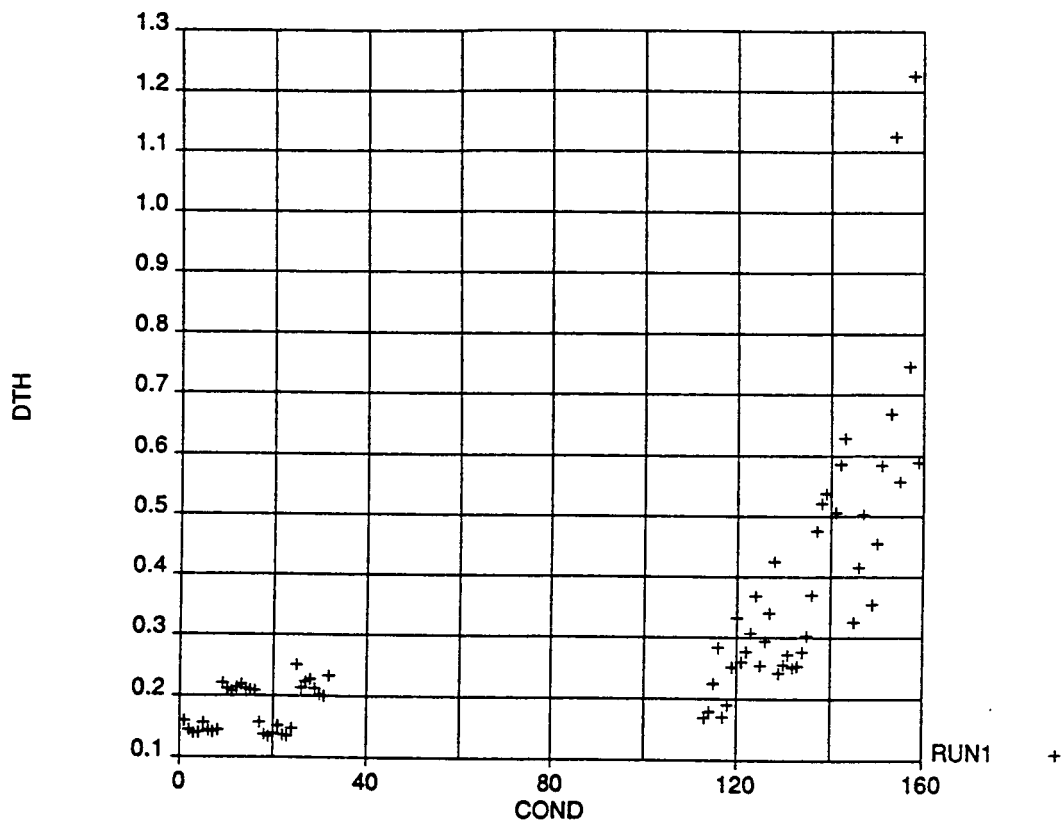
Plot 16. Cruise Control Law Turbulence Response Analysis Covariance Response to Dryden Turbulence vs Flight Condition (Elevator in Deg)



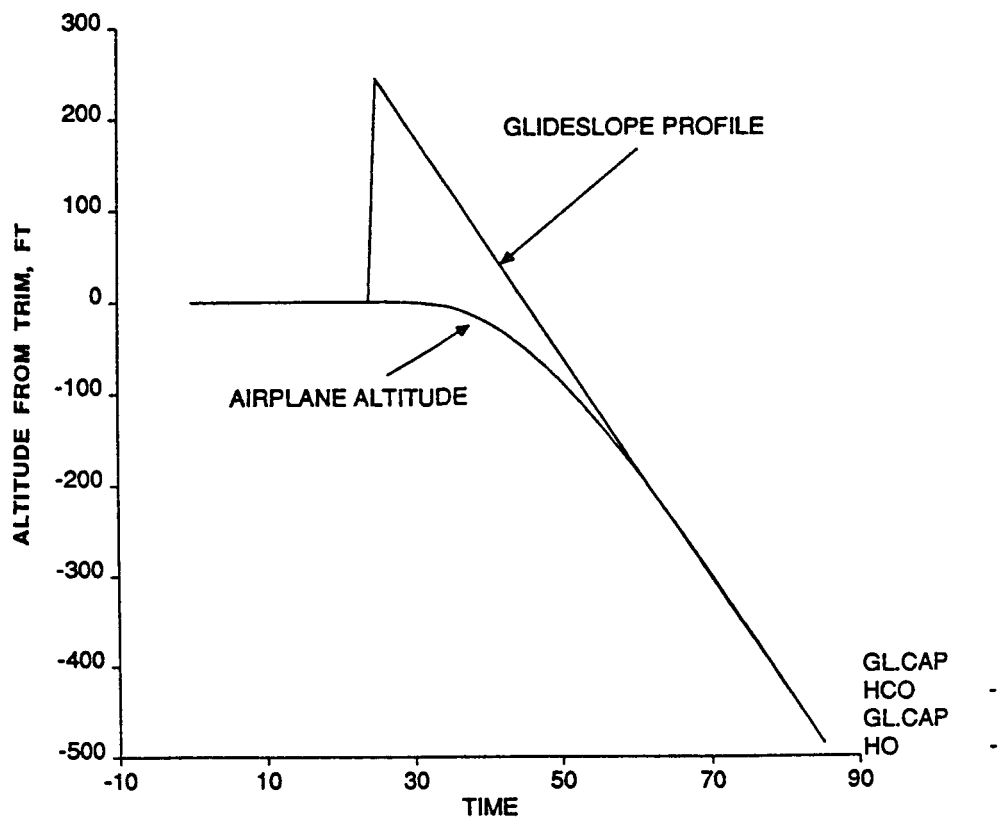
Plot 17. Cruise Control Law Turbulence Response Analysis Covariance Response to Dryden Turbulence vs Flight Condition (Throttle in Deg)



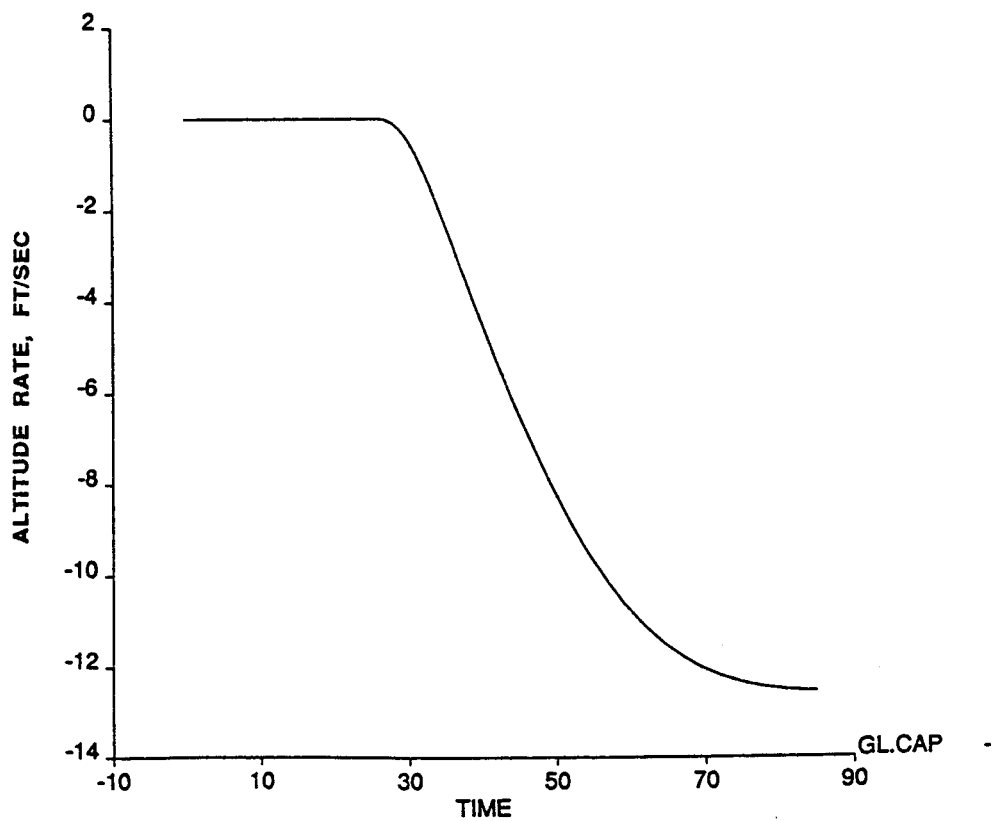
Plot 18. Cruise Control Law Turbulence Response Analysis Covariance Response to Dryden Turbulence vs Flight Condition (Elevator Rate in Deg / Sec)



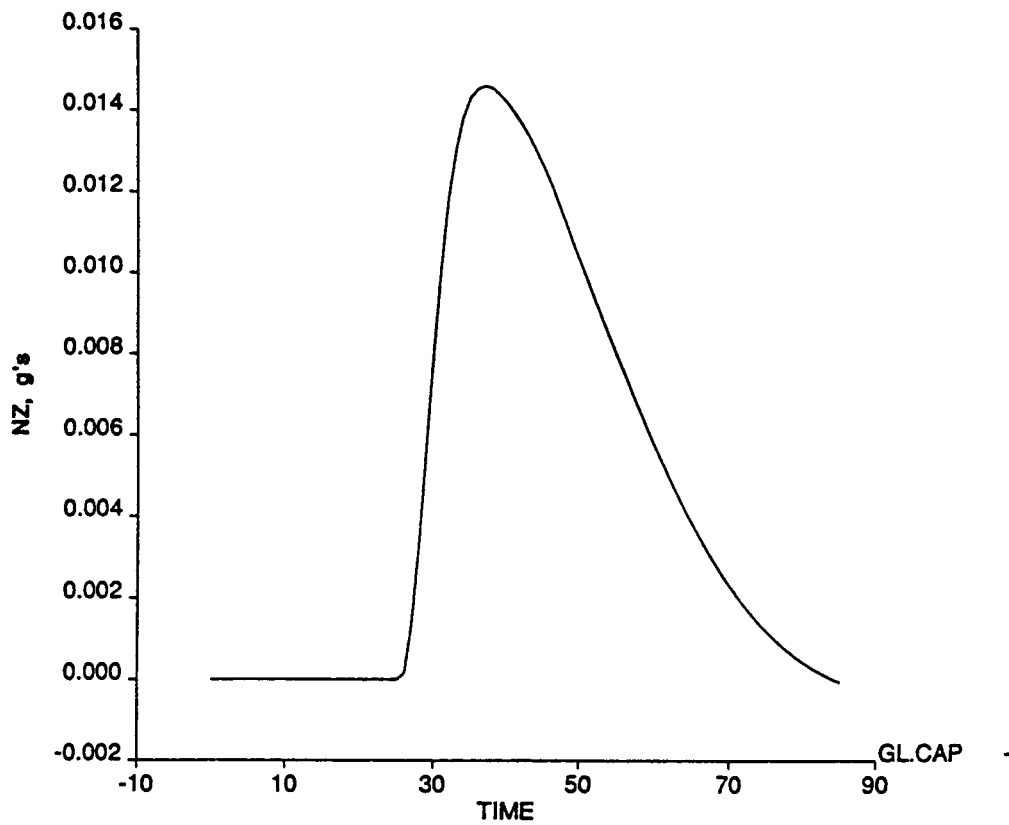
NONLINEAR TESTING RESULTS



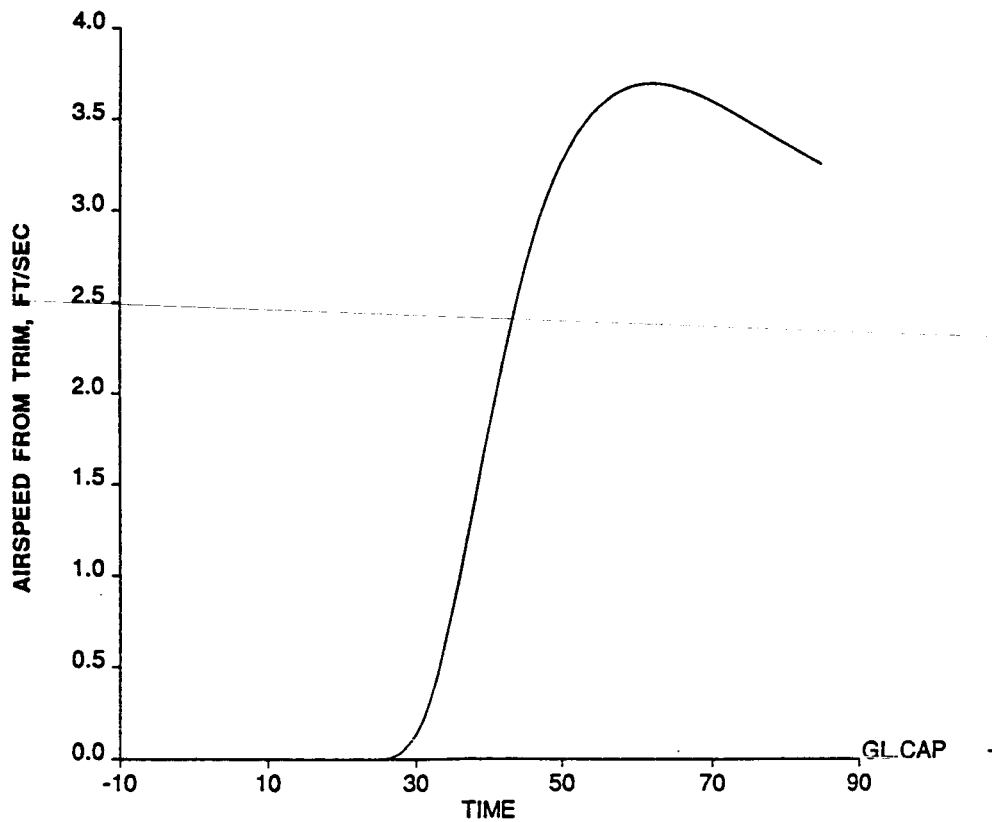
Plot 20. Nonlinear Analysis: Glideslope Capture Airplane is Trimmed at 2000 Ft, Flaps 25



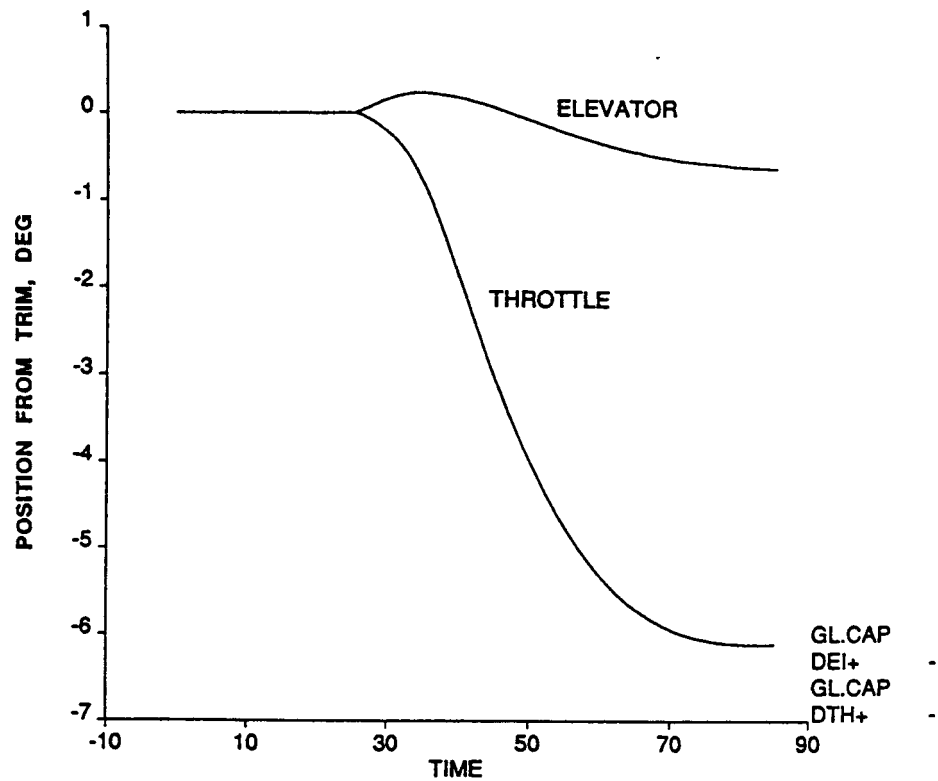
Plot 21. Nonlinear Analysis: Glideslope Capture Airplane is Trimmed at 2000 Ft, Flaps 25



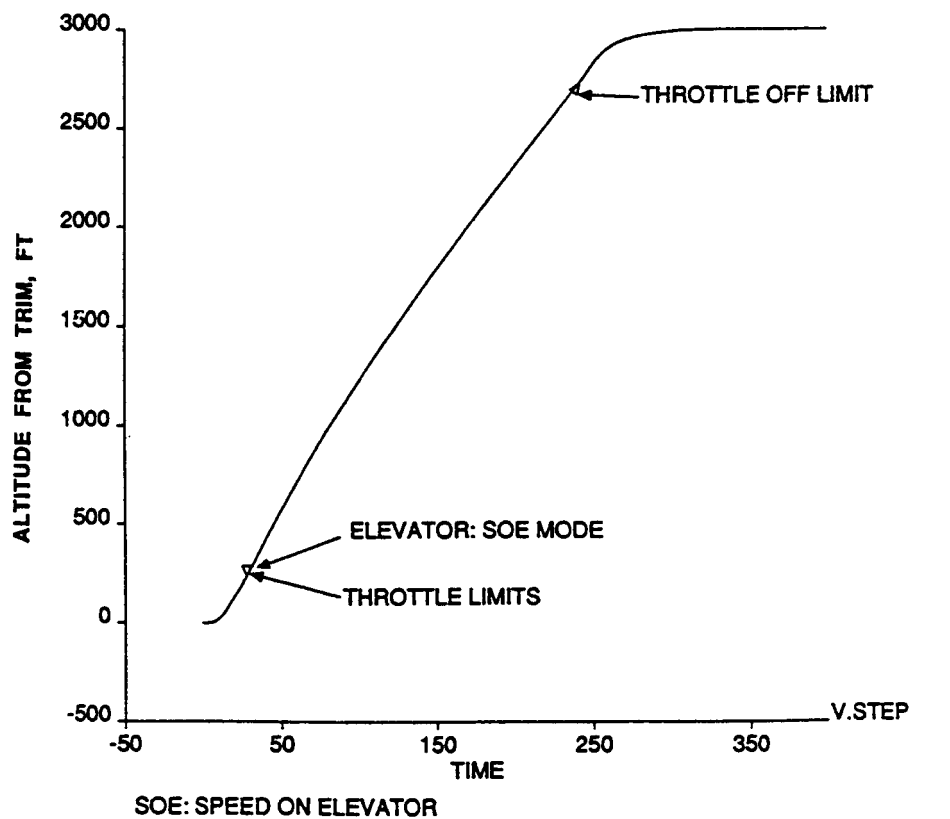
Plot 22. Nonlinear Analysis: Glideslope Capture Airplane is Trimmed at 2000 Ft, Flaps 25



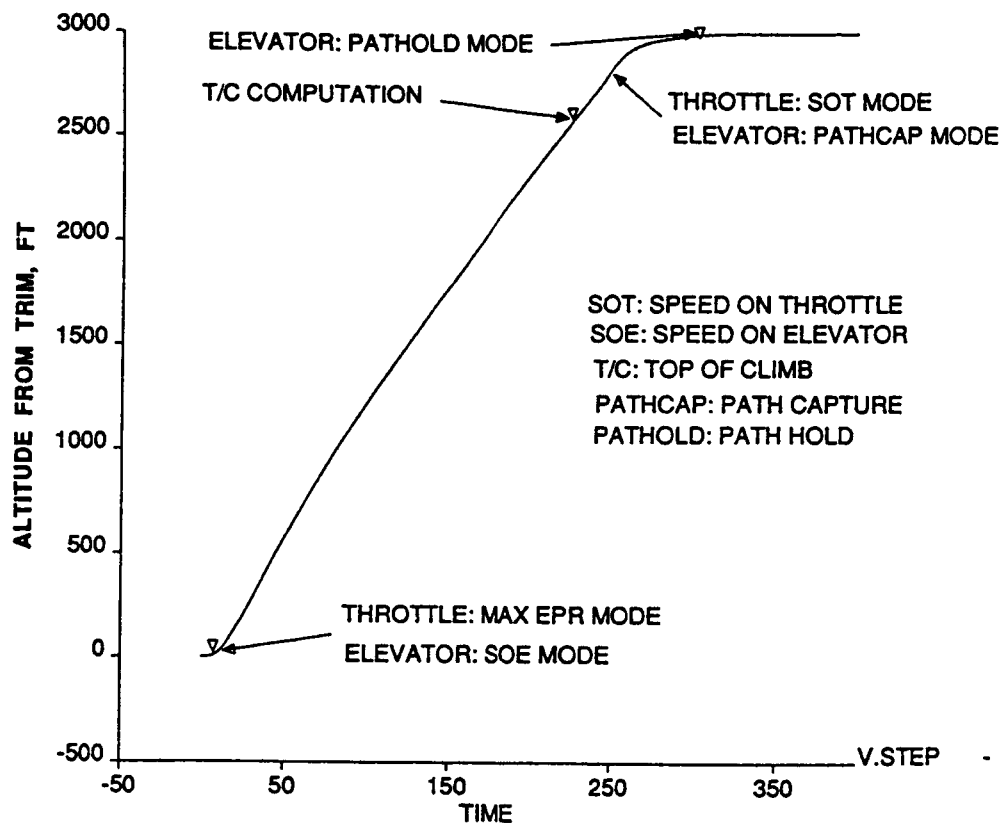
Plot 23. Nonlinear Analysis: Glideslope Capture Airplane is Trimmed at 2000 Ft, Flaps 25



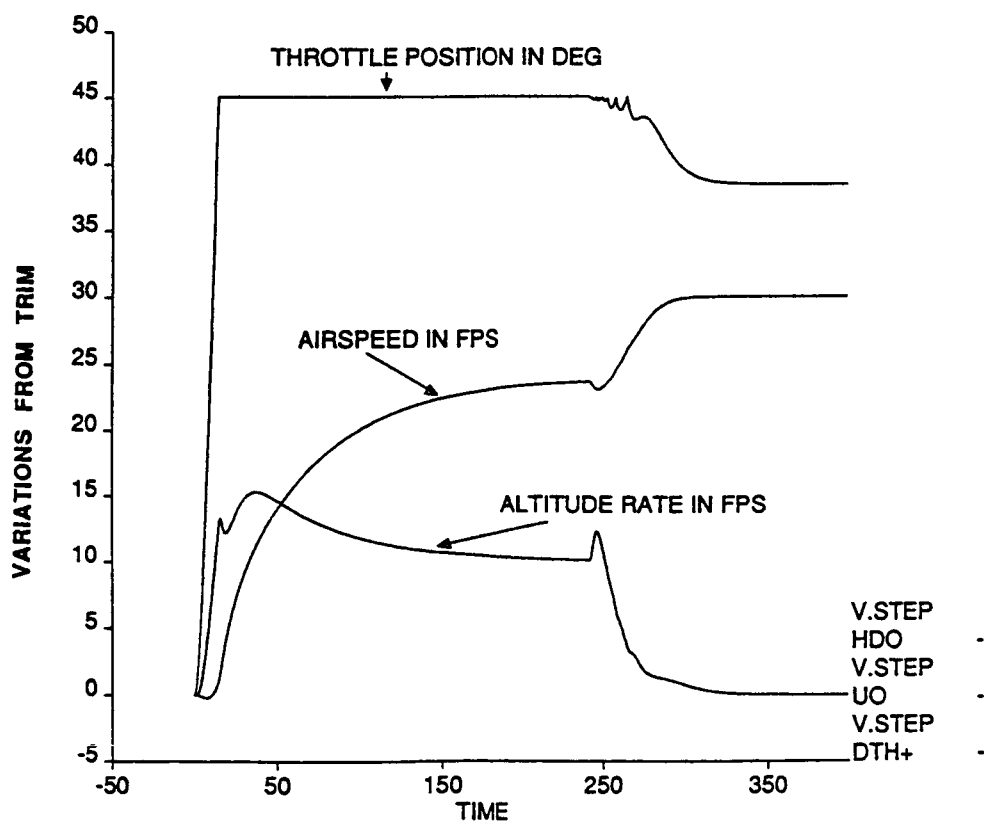
Plot 24. Nonlinear Analysis: Glideslope Capture Airplane is Trimmed at 2000 Ft, Flaps 25



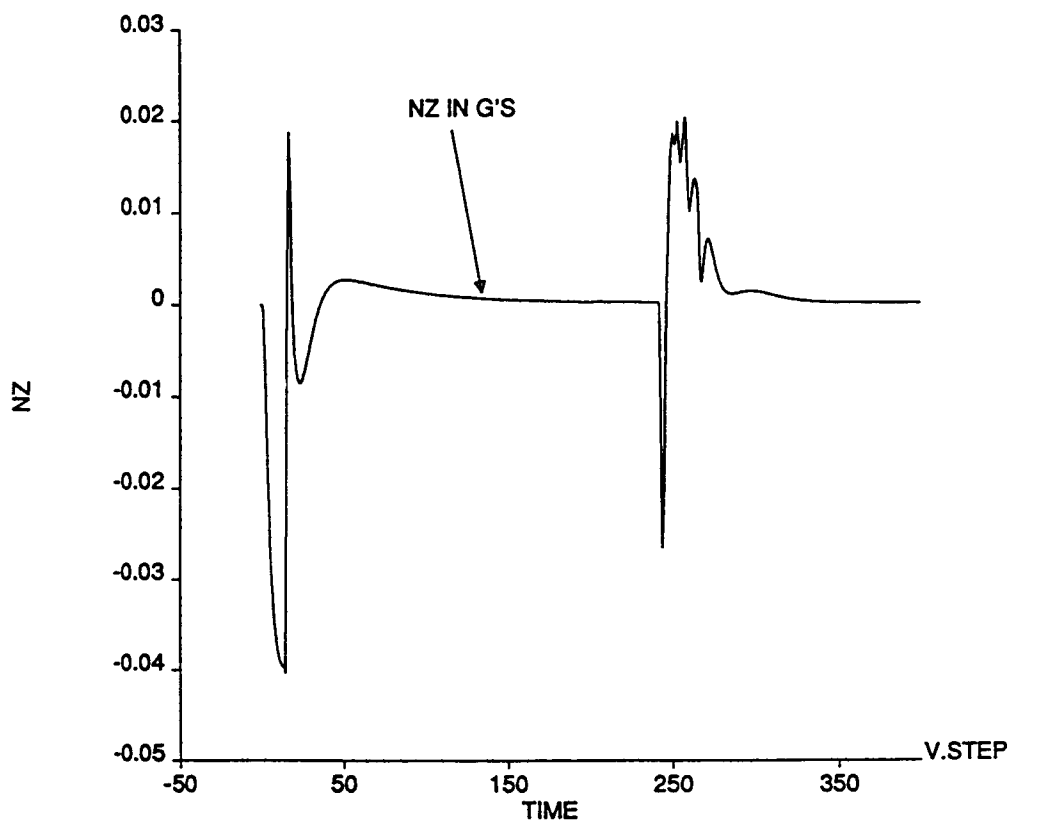
Plot 25. Nonlinear Analysis: Cruise Controller Response to Simultaneous Altitude and Speed Commands with Throttle Limiting (Nominal Plant is Trimmed at 35,000 Ft)



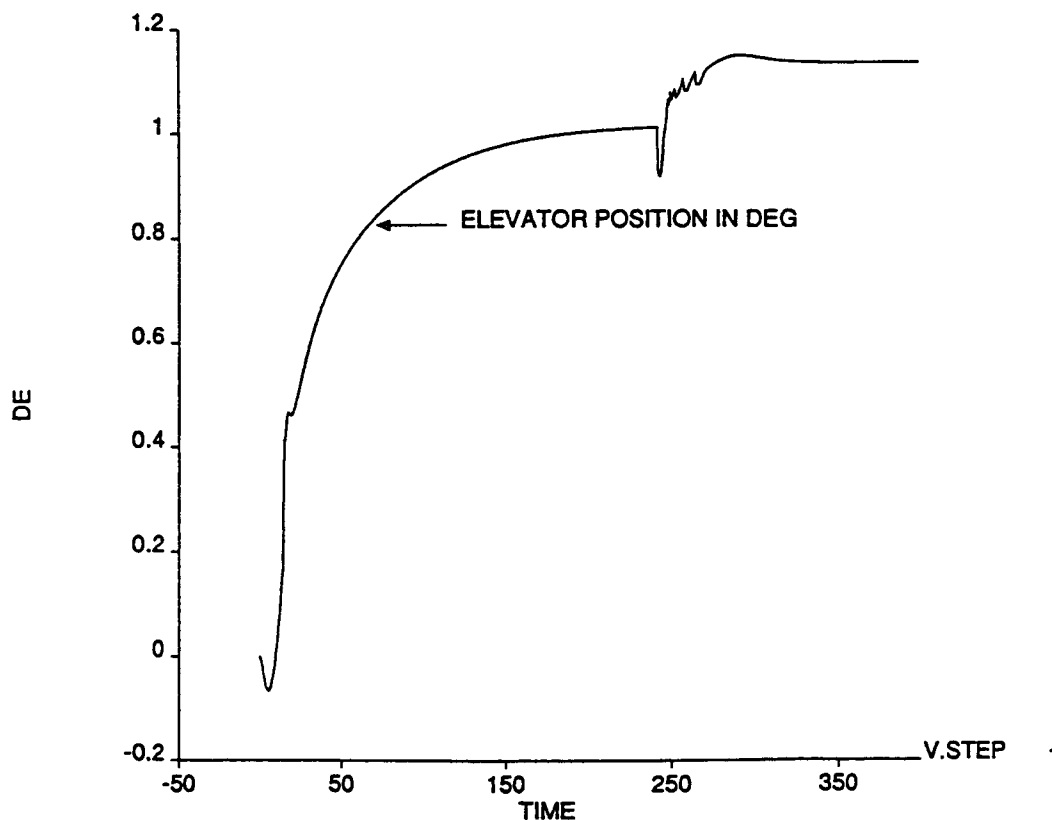
Plot 26. Typical Submode Logic Events for Flight Level Change Mode of Conventional Autopilot / Autothrottle



Plot 27. Nonlinear Analysis: Cruise Controller Response to Simultaneous Altitude and Speed Commands with Throttle Limiting (Nominal Plant is Trimmed at 35,000 Ft)



Plot 28. Nonlinear Analysis: Cruise Controller Response to Simultaneous Altitude and Speed Commands with Throttle Limiting (Nominal Plant is Trimmed at 35,000 Ft)

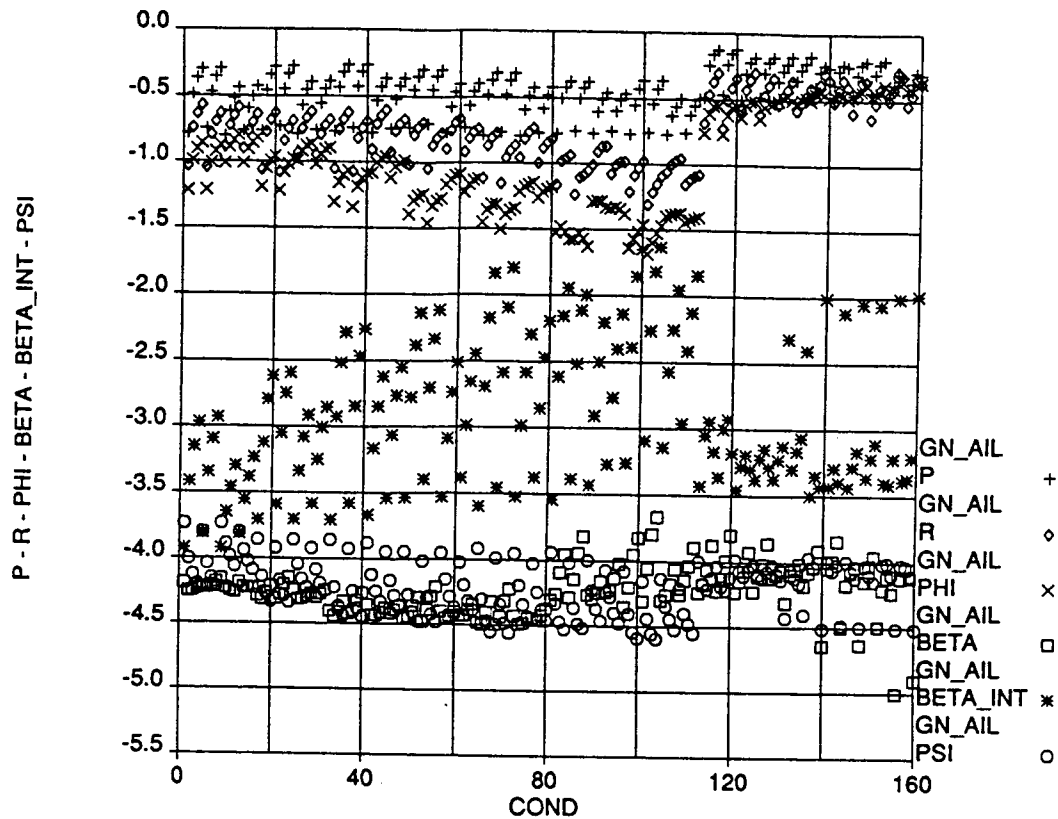


Plot 29. Nonlinear Analysis: Cruise Controller Response to Simultaneous Altitude and Speed Commands with Throttle Limiting (Nominal Plant is Trimmed at 35,000 Ft)

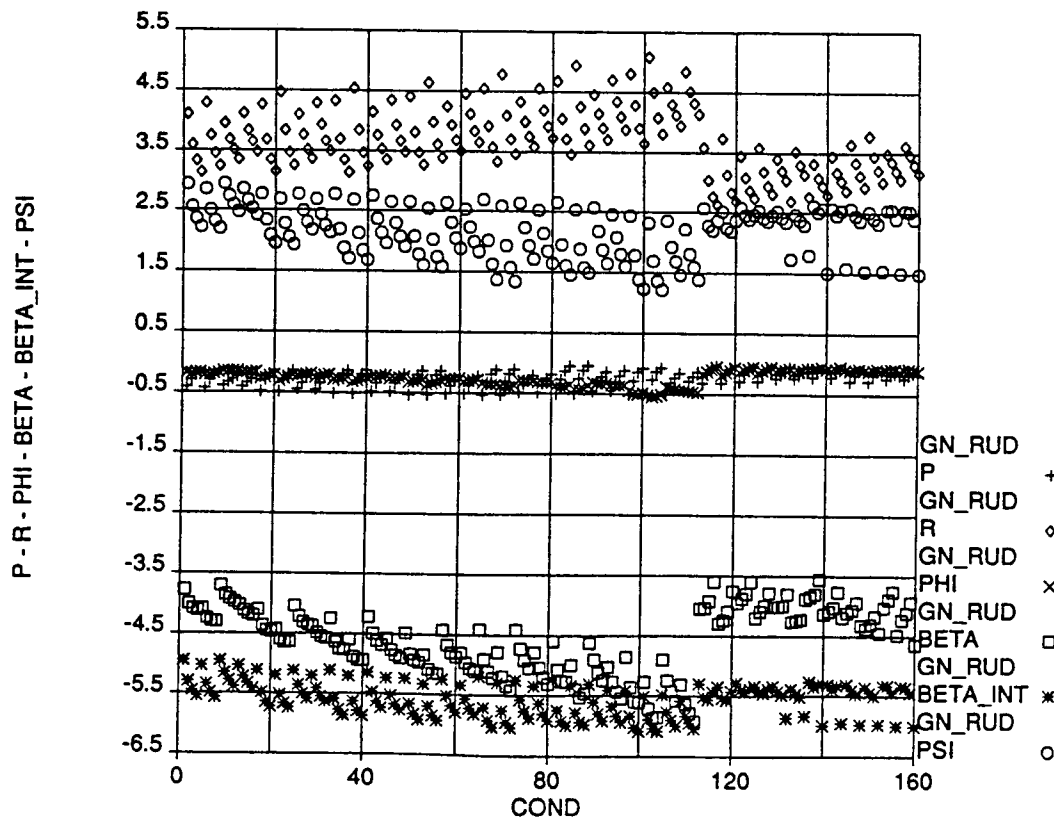
APPENDIX B

LATERAL AXIS RESULTS:

AILERON AND RUDDER GAIN SCHEDULES FOR CRUISE CONTROLLER



Plot 30A. Design Aileron Feedback Gains for Each Flight Condition



Plot 30B. Design Rudder Feedback Gains for Each Flight Condition

Aileron Gain Schedules For Cruise Controller

$$K_{P_a} \begin{cases} - .80 & V_{CAS} < 125 \\ - .80 + .42 \left(\frac{V_{CAS} - 125}{75} \right) & 125 < V_{CAS} < 200 \\ - .38 + .20 \left(\frac{V_{CAS} - 200}{160} \right) & 200 < V_{CAS} < 360 \\ - .18 & 360 < V_{CAS} \end{cases}$$

$$K_{r_a} \begin{cases} - 1.90 & MACH < 0.1 \\ - 1.90 + 1.25 \left(\frac{MACH - .1}{.26} \right) & 0.1 < MACH < 0.36 \\ - .65 + .27 \left(\frac{MACH - .36}{.54} \right) & 0.36 < MACH < 0.90 \\ - .18 & 0.90 < MACH \end{cases}$$

$$K_{\phi_a} \begin{cases} - 1.4 & MACH < 0.15 \\ - 1.40 + .80 \left(\frac{MACH - .15}{.16} \right) & 0.15 < MACH < 0.31 \\ - .60 + .30 \left(\frac{MACH - .31}{.59} \right) & 0.31 < MACH < 0.90 \\ - .30 & 0.90 < MACH \end{cases}$$

$$K_{\beta_a} = -4.2$$

$$K_{I_{\beta_a}} = 0$$

$$K_{\psi_a} = -4.1$$

Rudder Gain Schedules For Cruise Controller

$$K_{P_r} \begin{cases} -0.40 & V_{CAS} < 100 \\ -0.40 + .32 \left(\frac{V_{CAS} - 100}{200} \right) & 100 < V_{CAS} < 300 \\ -0.08 & 300 < V_{CAS} \end{cases}$$

$$K_{r_r} \begin{cases} 5.00 & V_{CAS} < 100 \\ 5.00 + 1.60 \left(\frac{V_{CAS} - 100}{100} \right) & 100 < V_{CAS} < 200 \\ 3.40 - .65 \left(\frac{V_{CAS} - 200}{160} \right) & 200 < V_{CAS} < 360 \\ 2.75 & 360 < V_{CAS} \end{cases}$$

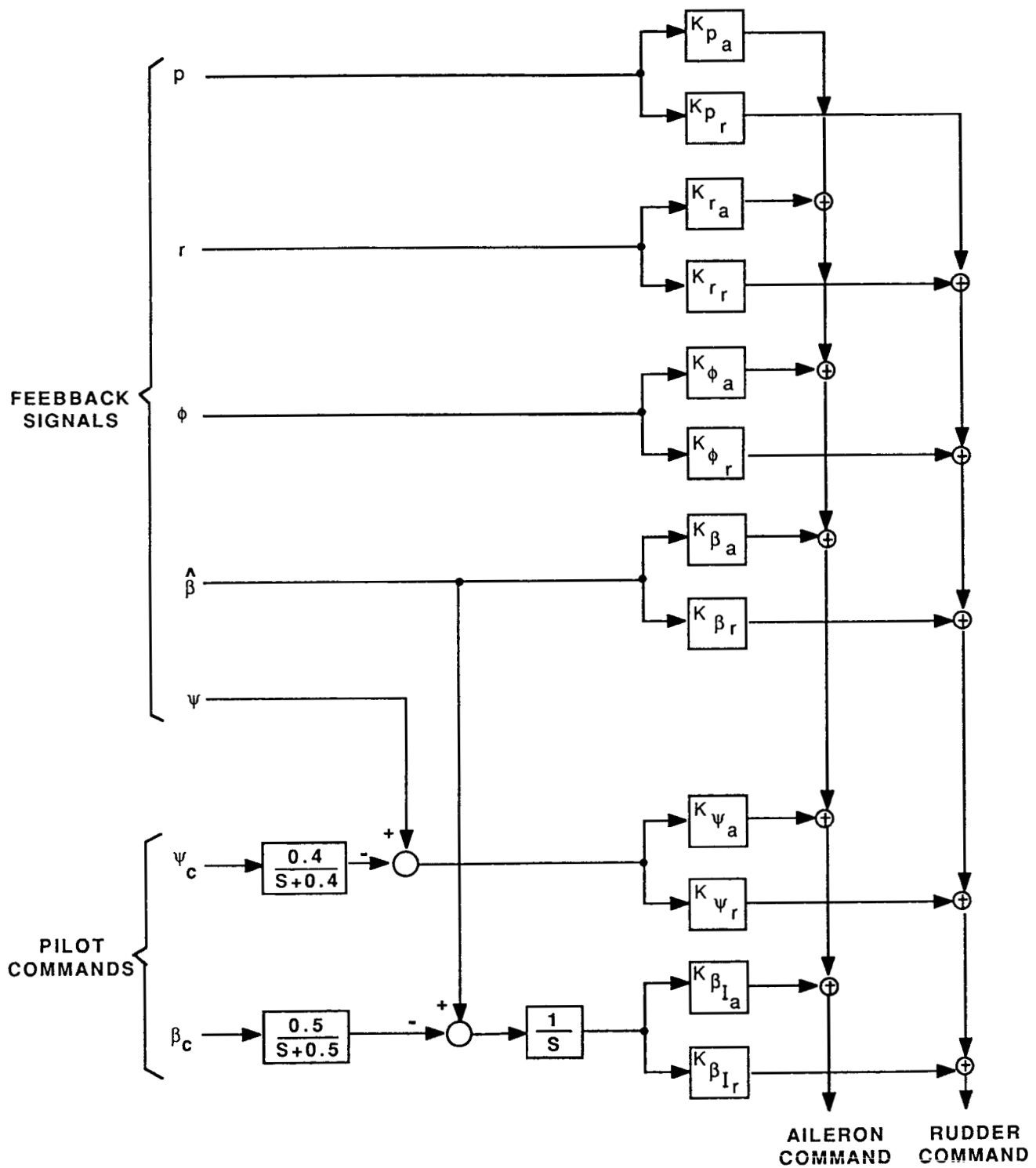
$$K_{\phi_r} \begin{cases} -0.40 & V_{CAS} \\ -0.40 + .32 \left(\frac{V_{CAS} - 100}{200} \right) & 100 < V_{CAS} < 300 \\ -0.08 & 300 < V_{CAS} \end{cases}$$

$$K_{\beta_r} = 4.1 - 1.5 \left(\frac{FLAP}{40} \right) \quad 0 \leq FLAP \leq 40$$

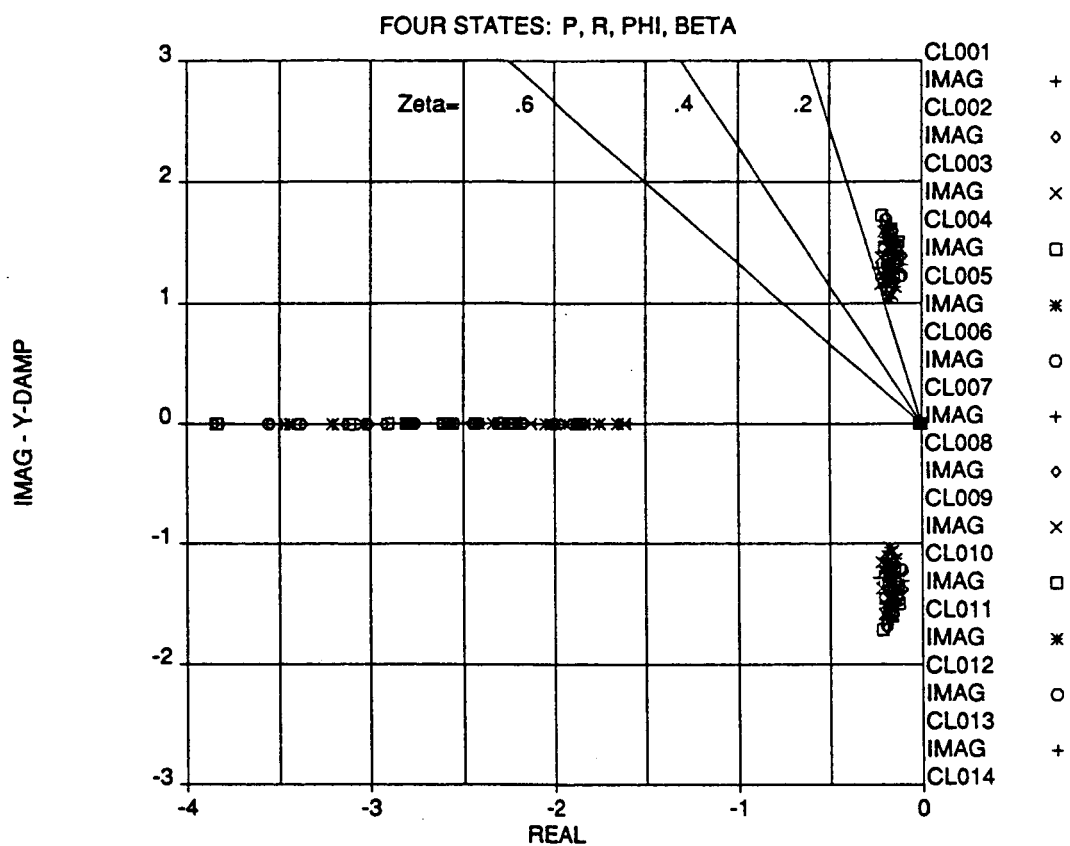
$$K_{I_{\beta_r}} = -5.5$$

$$K_{\psi_r} = 2.2 \quad V_{CAS}$$

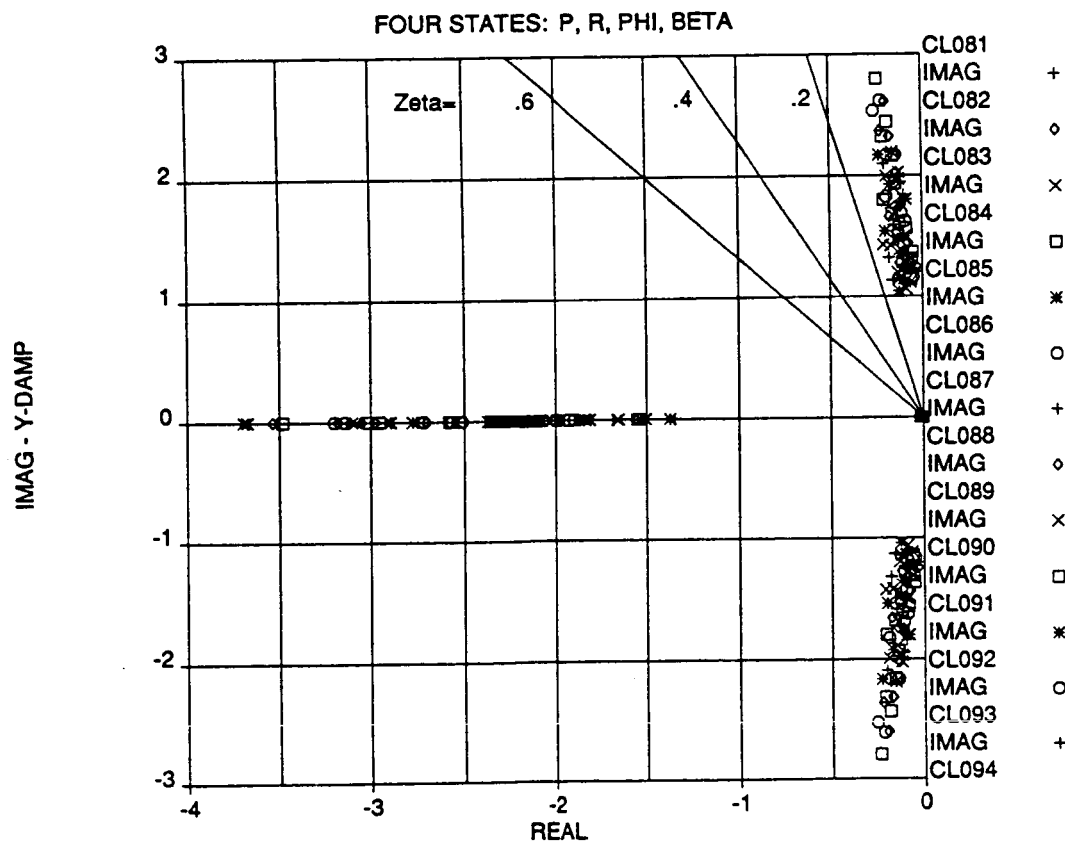
Cruise Controller Structure



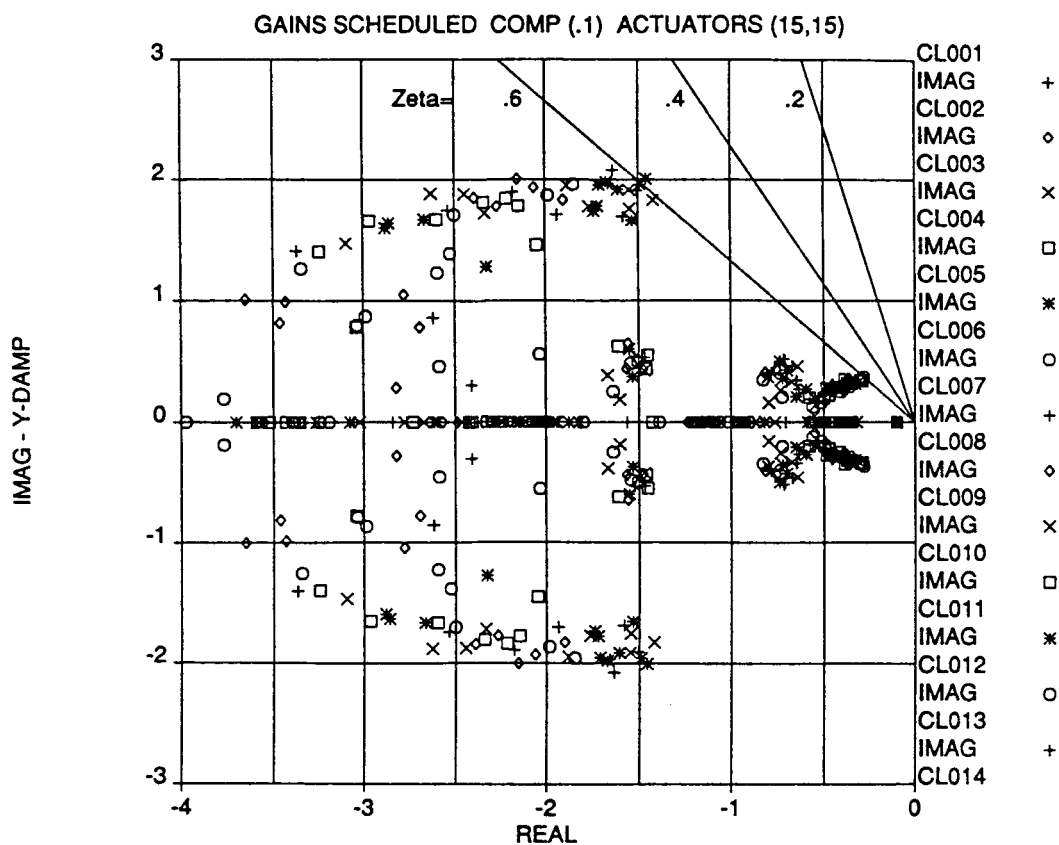
LINEAR ANALYSIS RESULTS



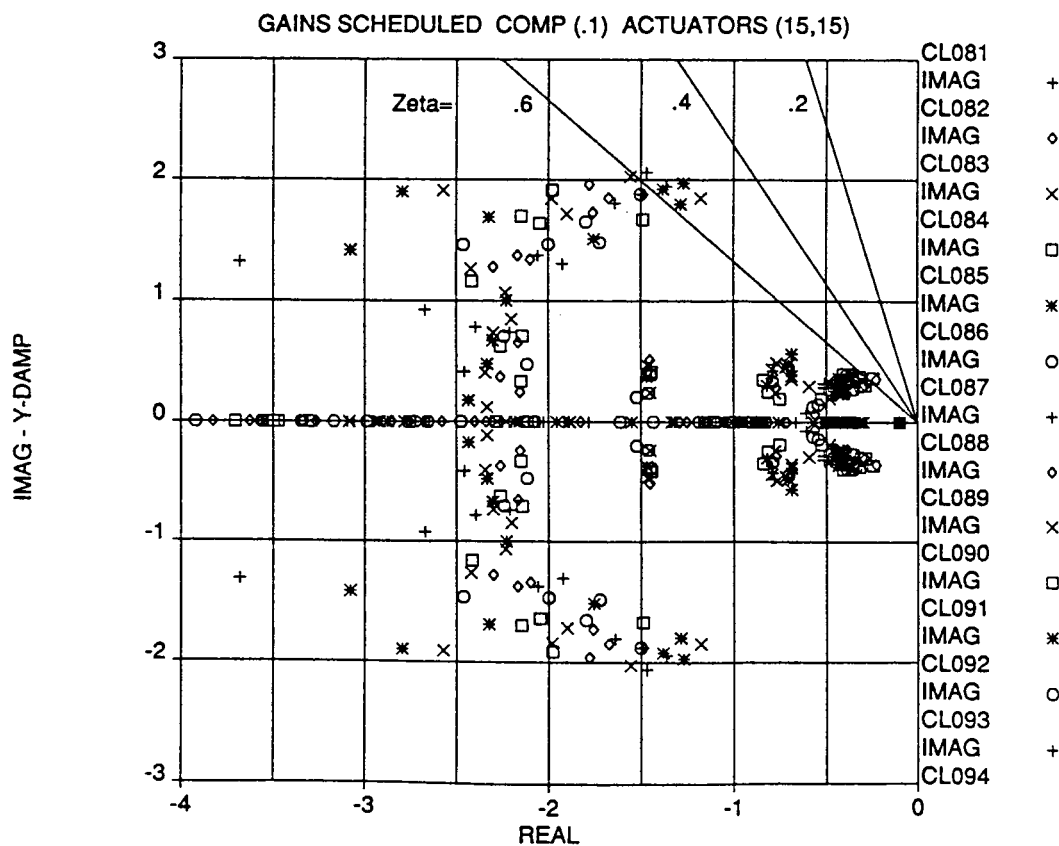
Plot 31. Open Loop Poles for Flight Conditions 1 - 80



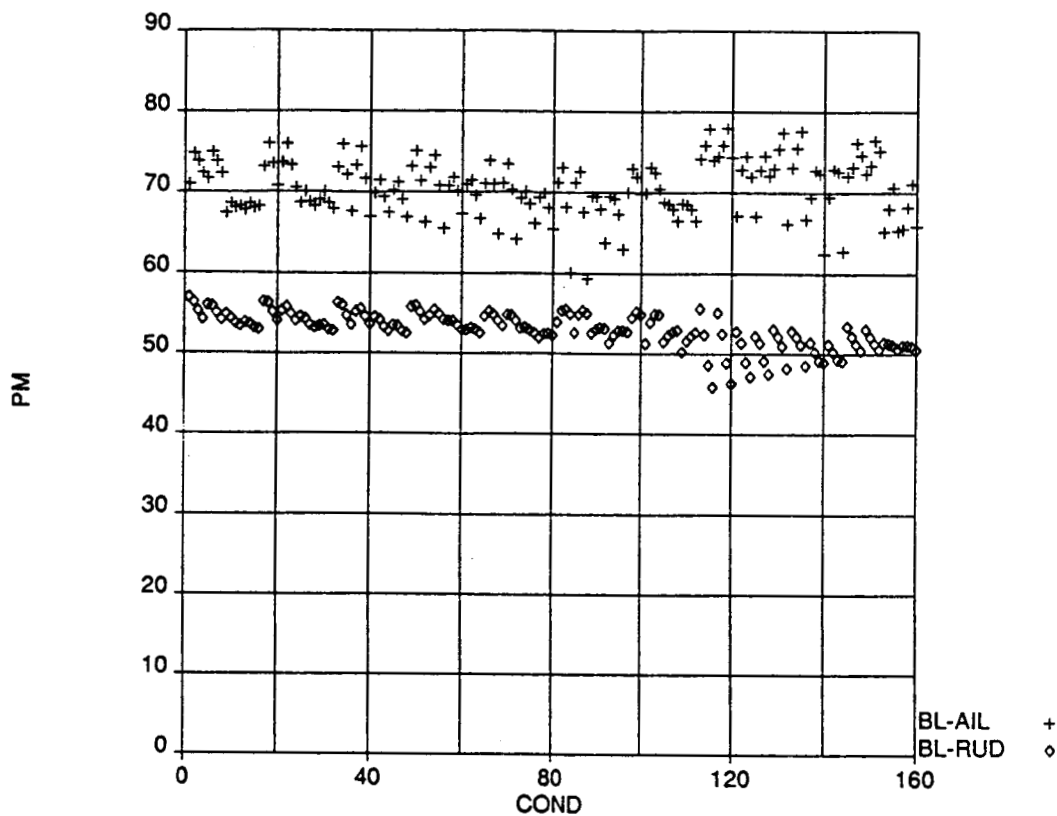
Plot 32. Open Loop Poles for Flight Conditions 81 - 160



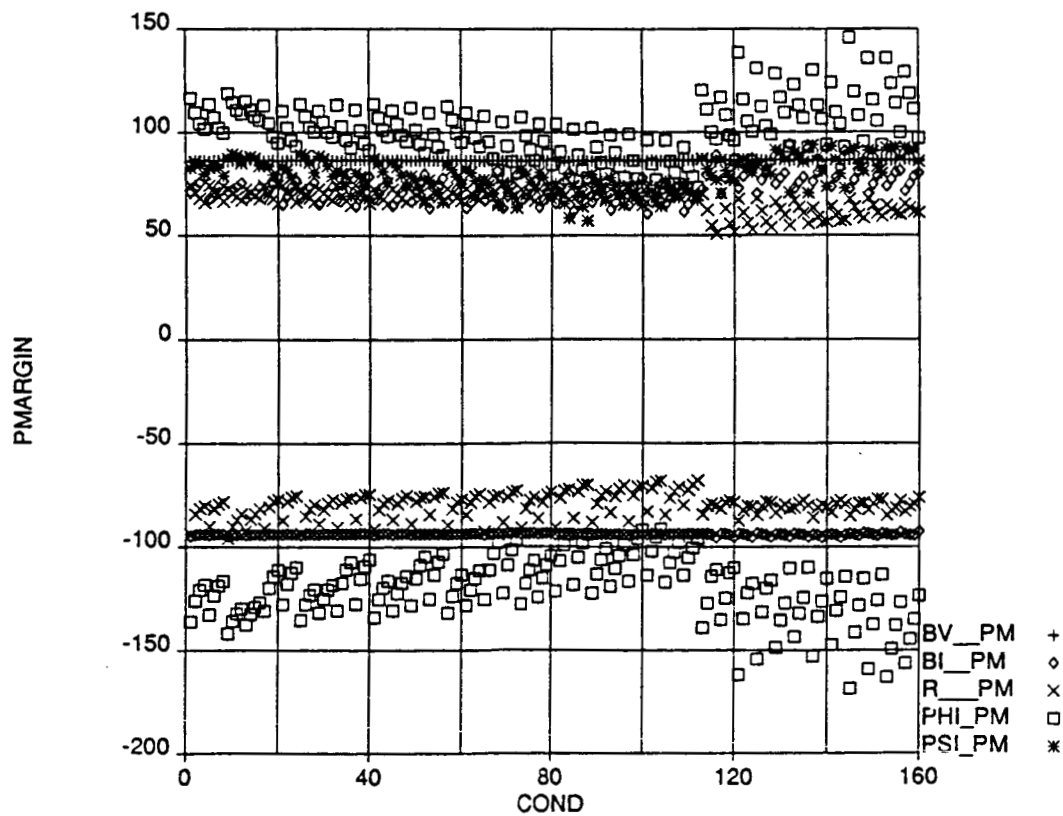
Plot 33. Closed Loop Poles for Flight Conditions 1 - 80



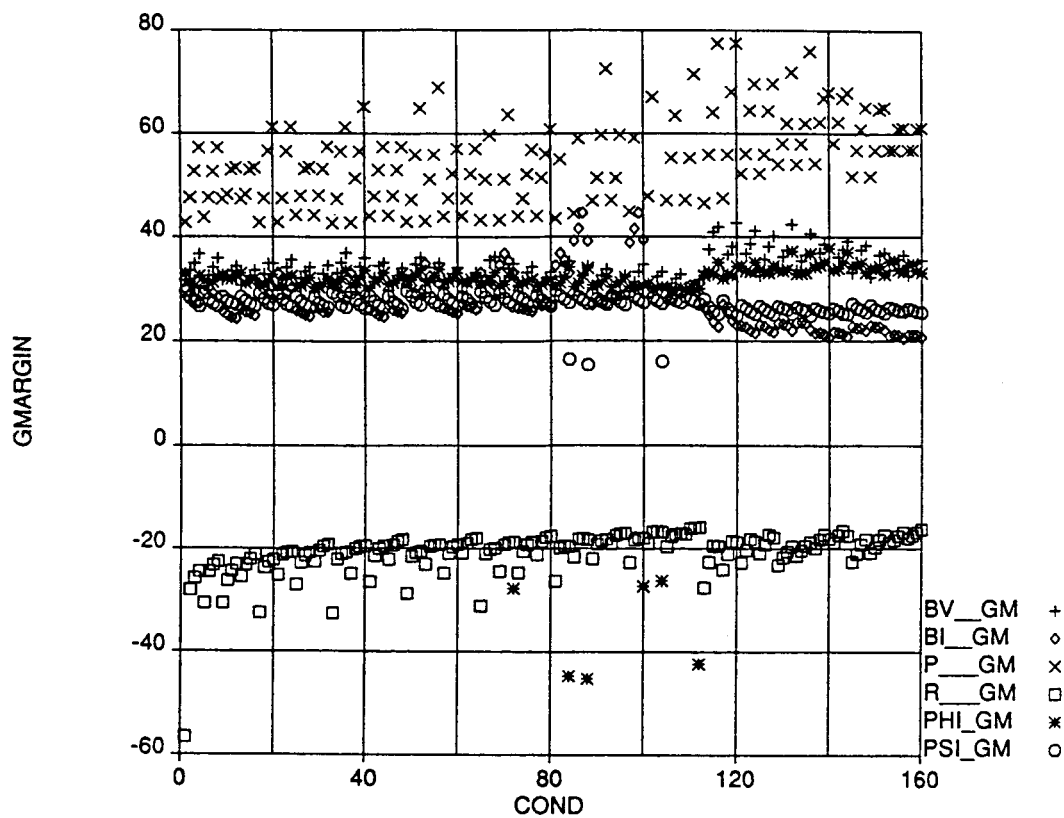
Plot 34. Closed Loop Poles for Flight Conditions 81 - 160



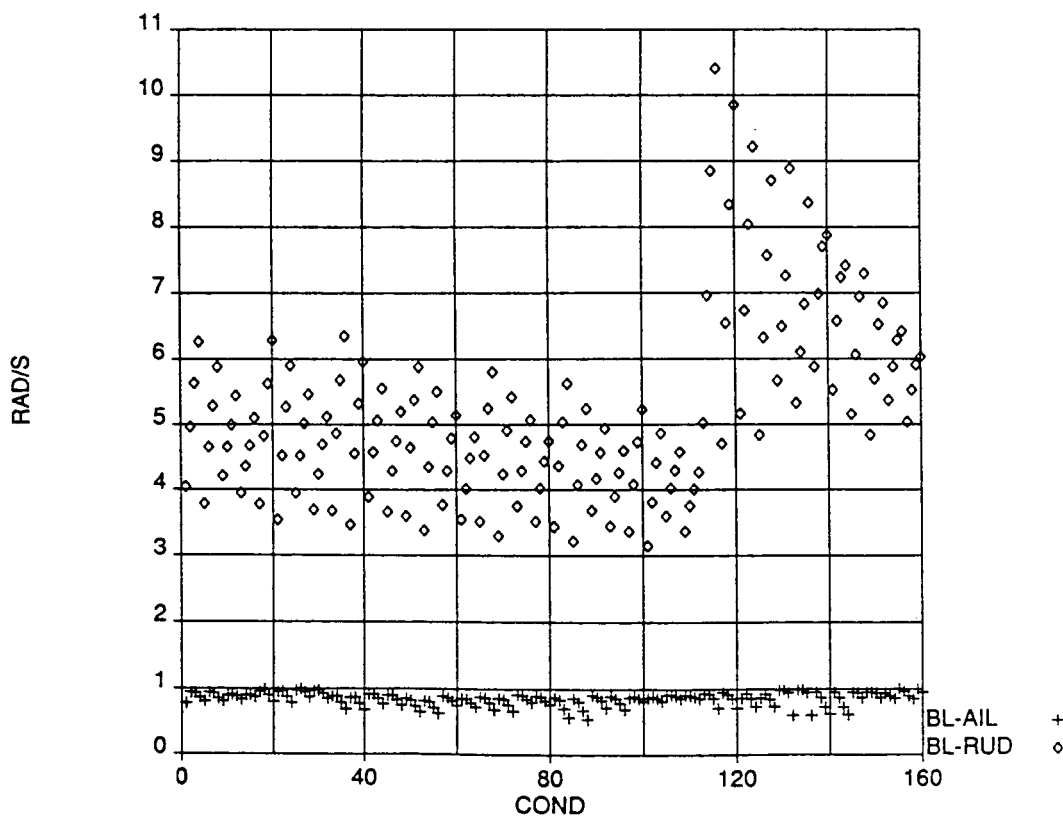
Plot 35. Broken Loop Phase Margins for Aileron and Rudder Loops at All Flight Conditions



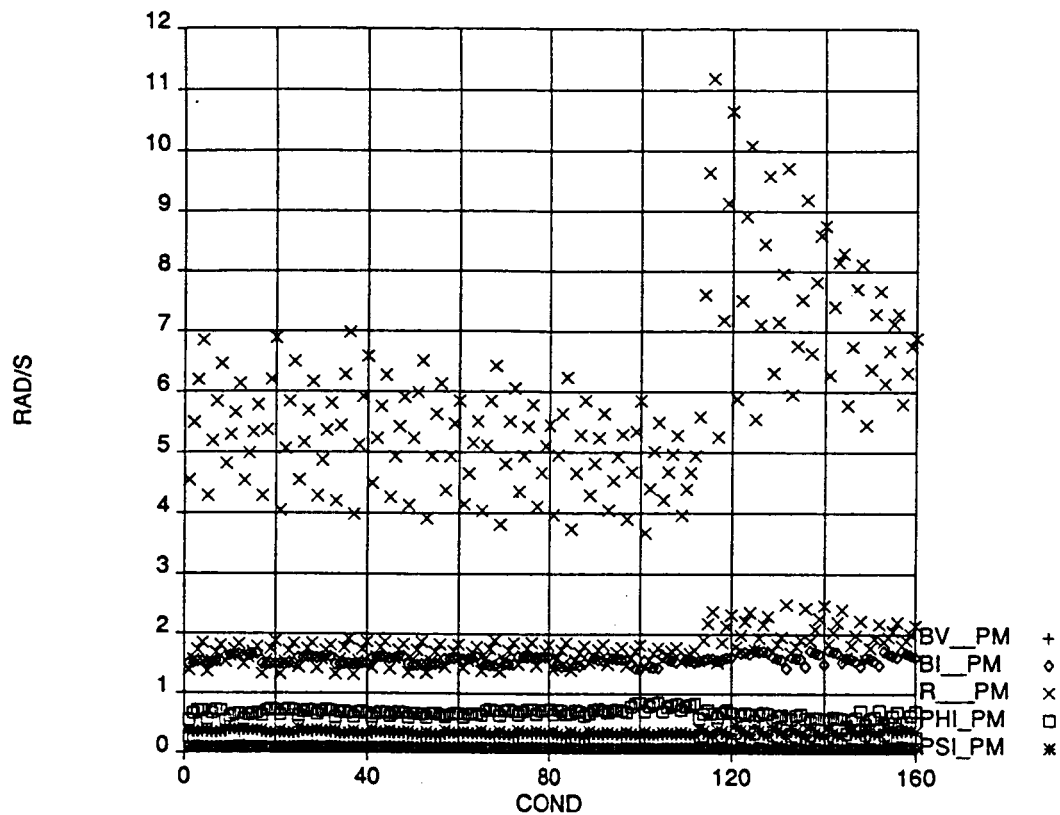
Plot 36. Broken Loop Phase Margins for All Sensor Loops at All Flight Conditions



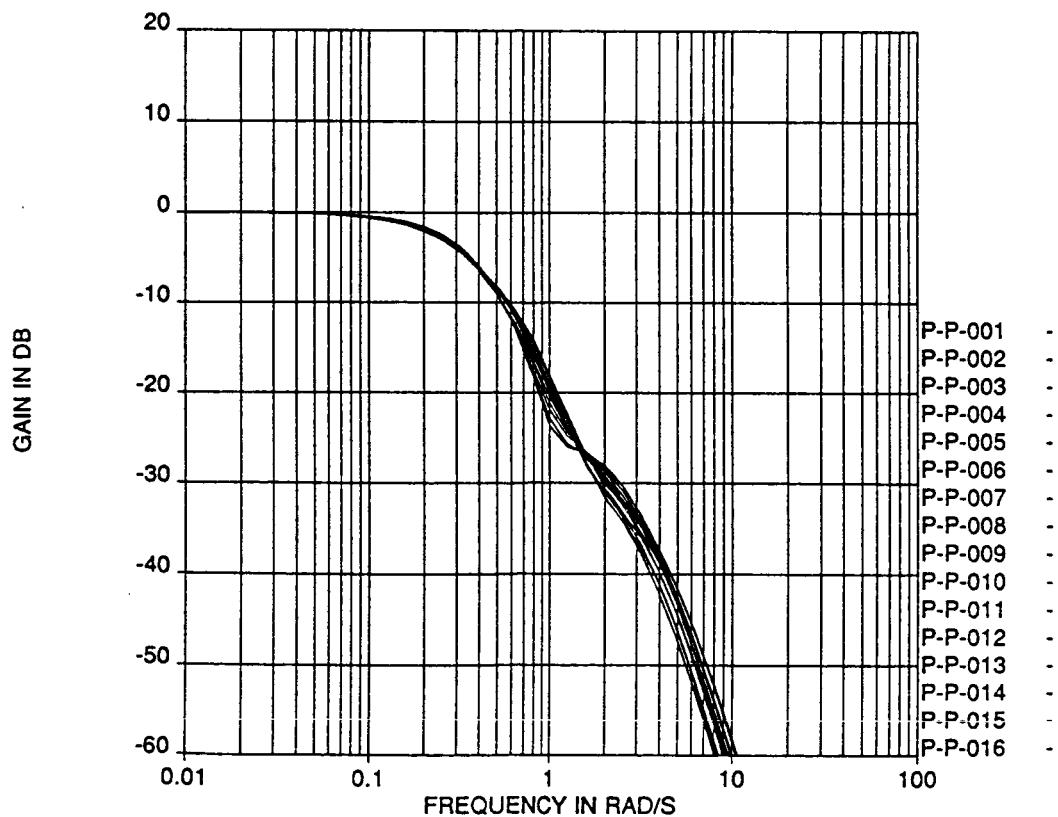
Plot 37. Broken Loop Gain Margins for All Sensor Loops at All Flight Conditions



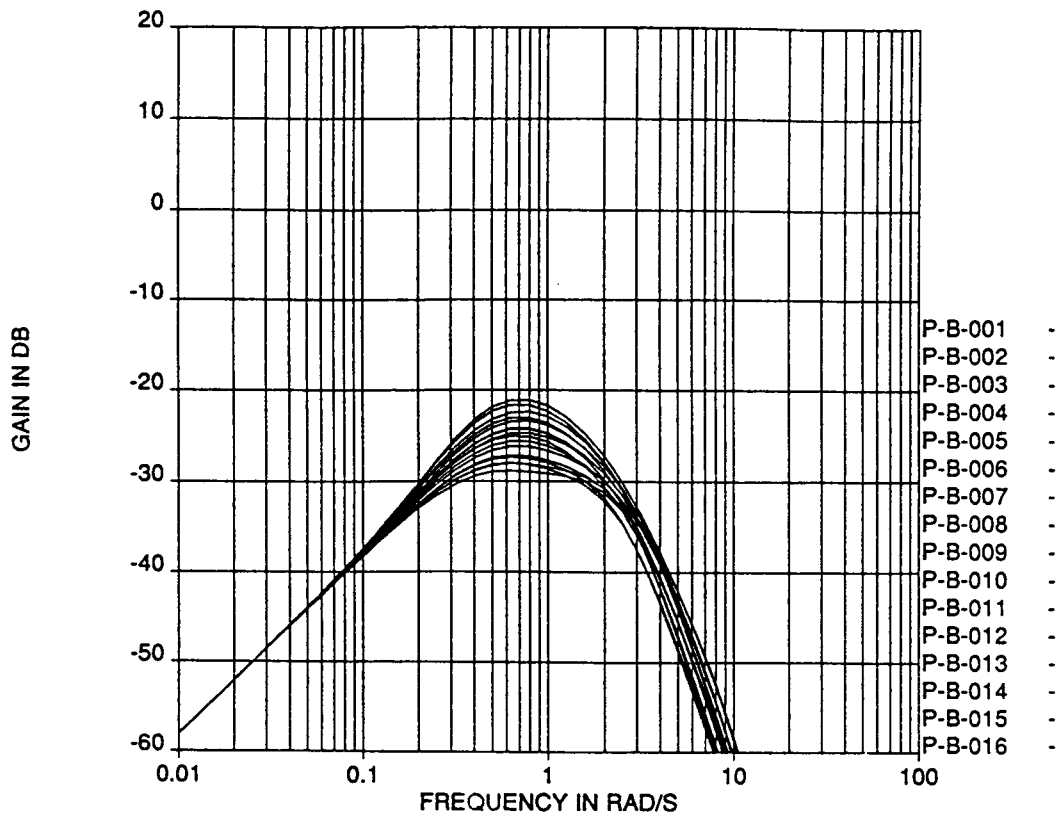
Plot 38. Aileron and Rudder Broken Loop Bandwidths at All Flight Conditions



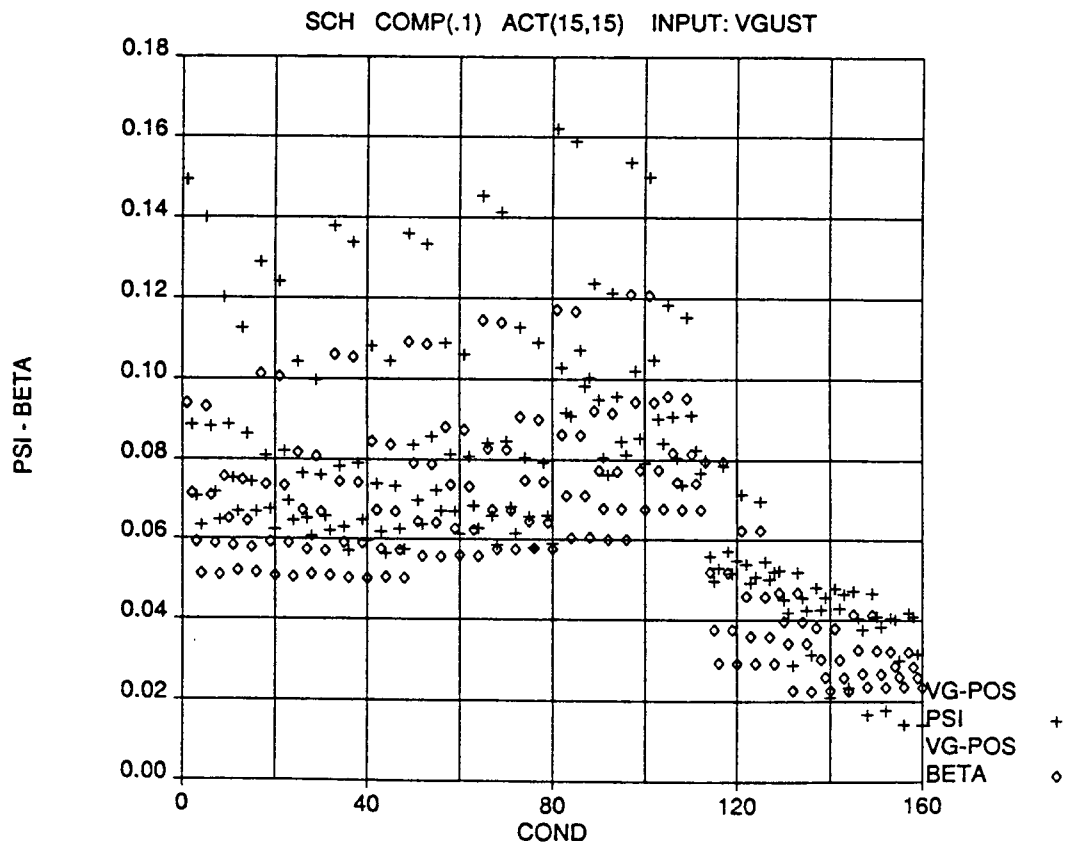
Plot 39. Sensor Broken Loop Bandwidths at All Flight Conditions



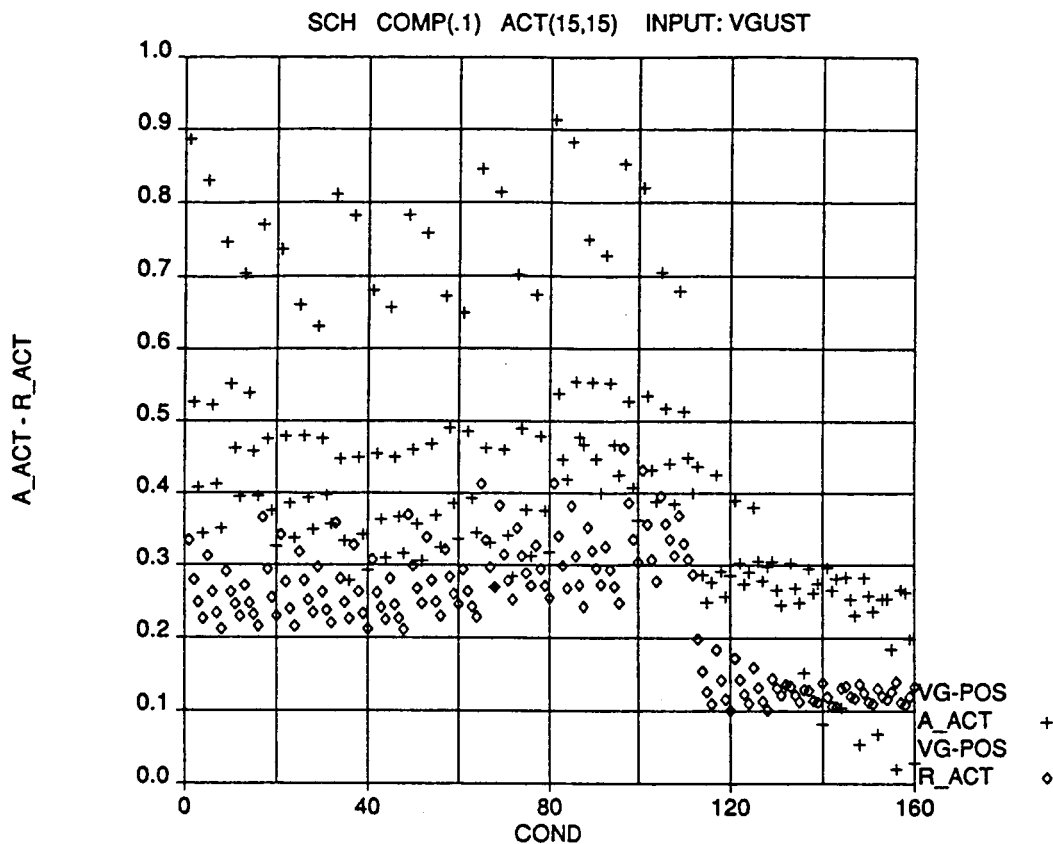
Plot 40. Closed Loop Command Frequency Response From ψ_{CMD} To ψ
(Typical of all conditions)



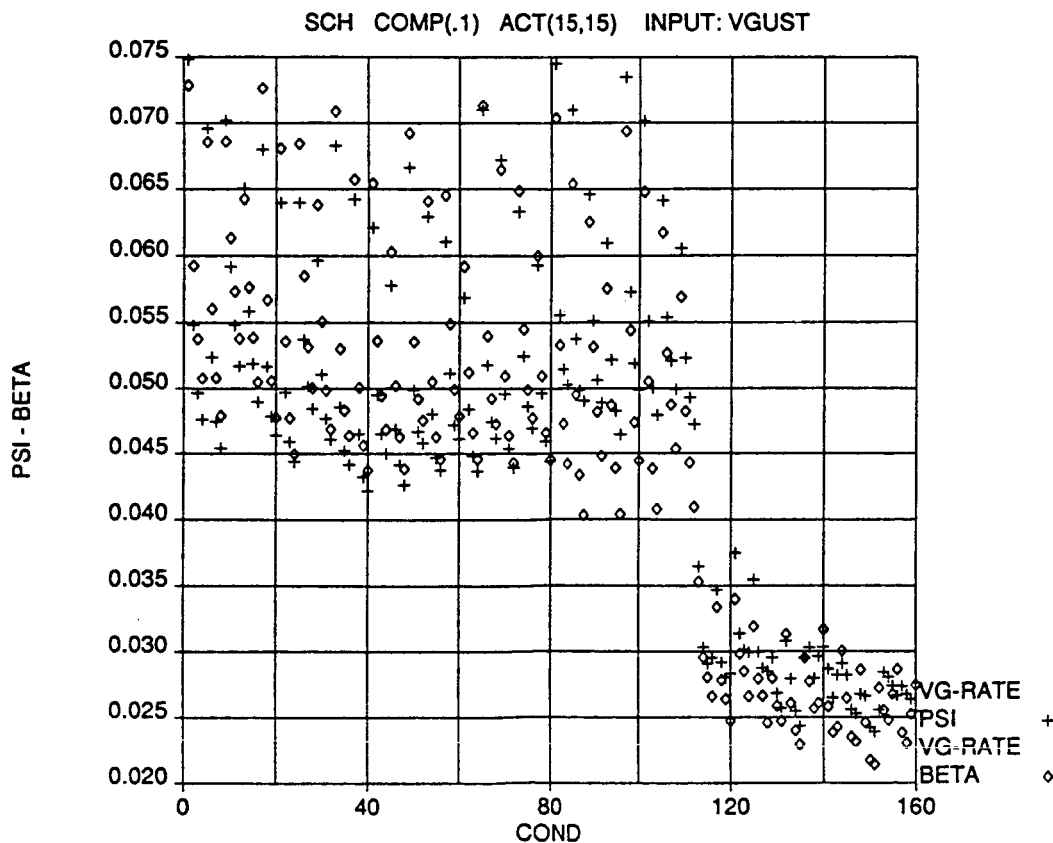
Plot 41. Closed Loop Adverse Command Frequency Response From ψ_{CMD} To β
(Typical of all conditions)



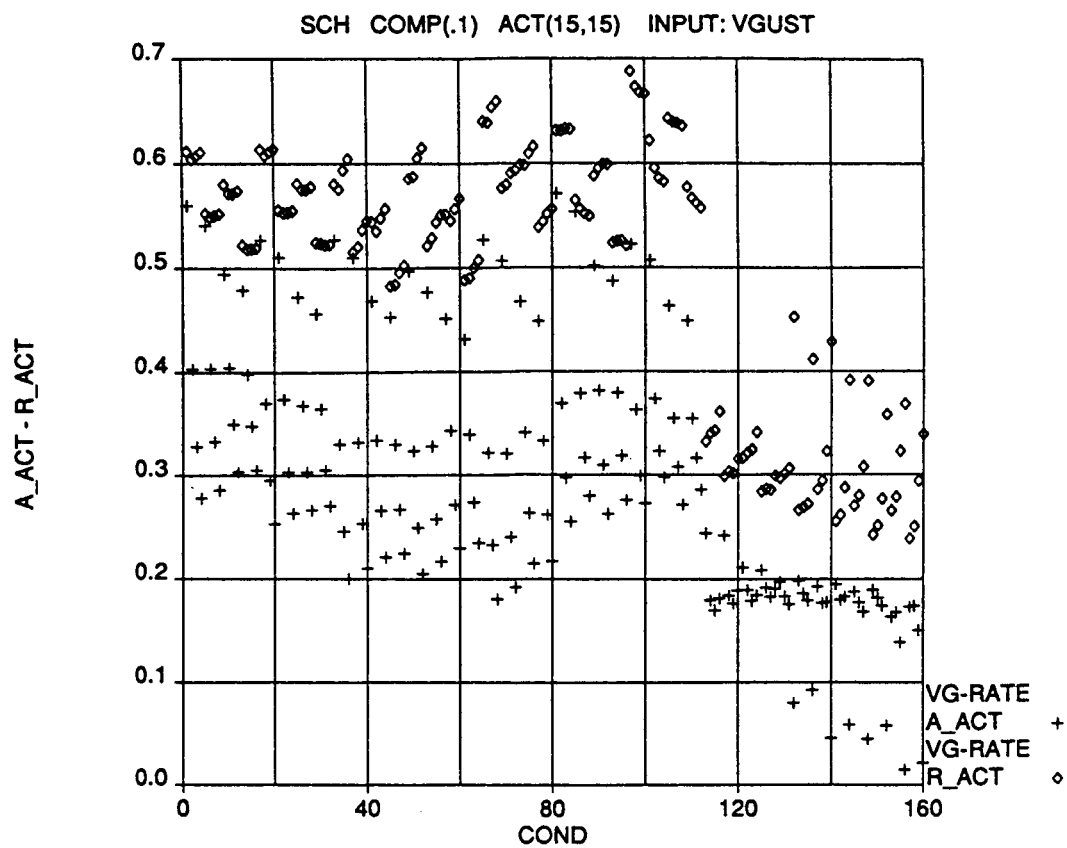
Plot 42. Position Covariance Responses of ψ_{CMD} To β to 1 ft/sec RMS
Dryden Turbulence at Each Flight Condition



Plot 43. Position Covariance Responses of Aileron and Rudder to 1 ft/sec RMS Dryden Turbulence at Each Flight Condition

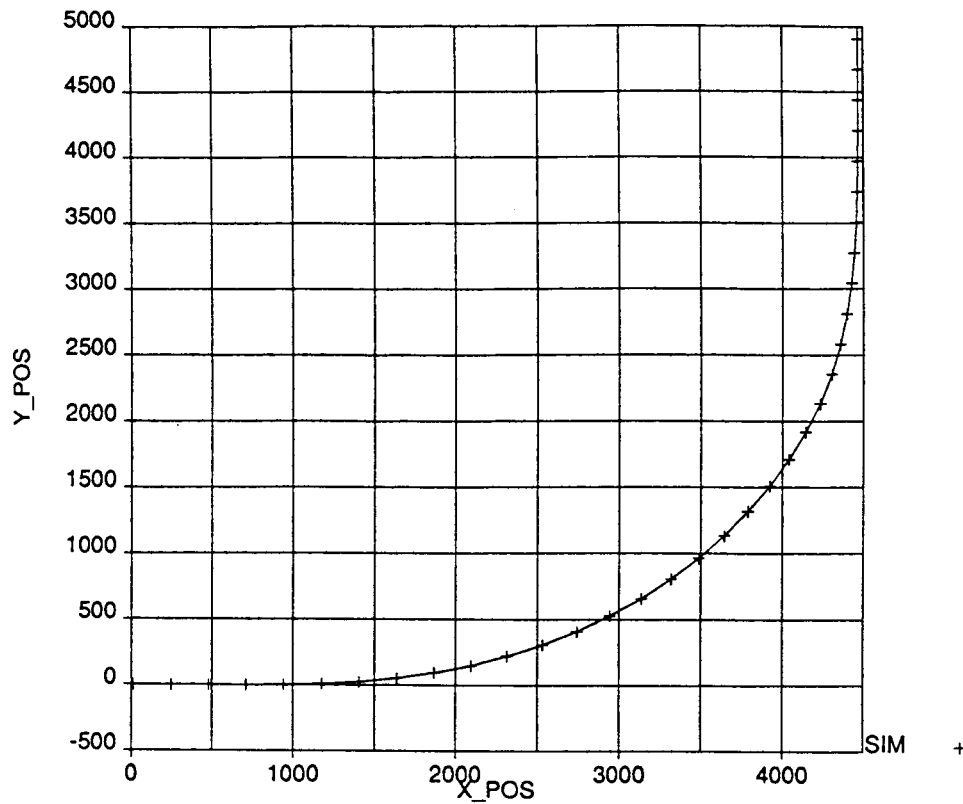


Plot 44. Rate Covariance Response of ψ_{CMD} To β to 1 ft/sec RMS Dryden Turbulence at Each Flight Condition

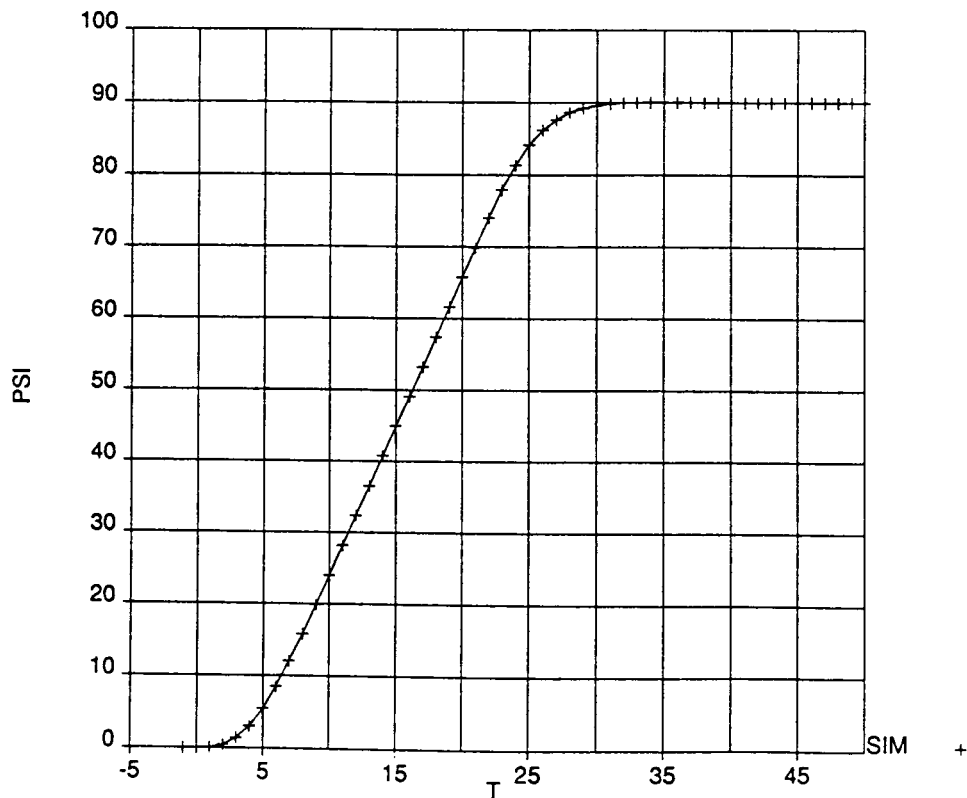


Plot 45. Rate Covariance R response of Aileron and Rudder to 1 ft/sec RMS Dryden Turbulence at Each Flight Condition

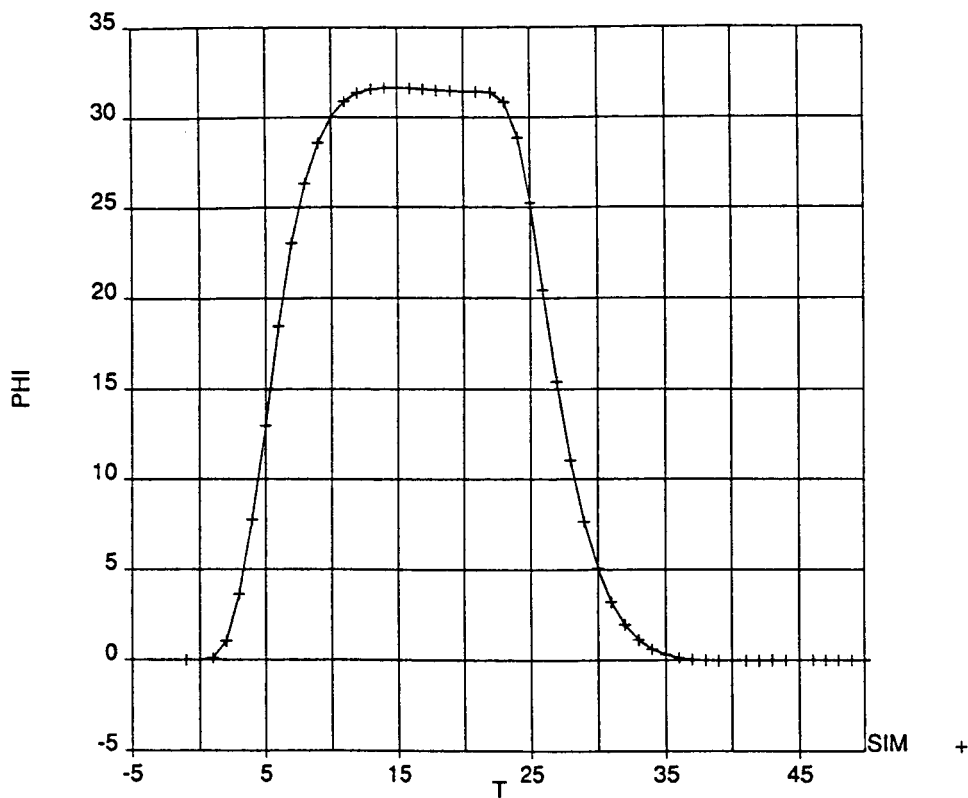
**TIME SIMULATION RESULTS FOR
HEADING CONTROLLER**



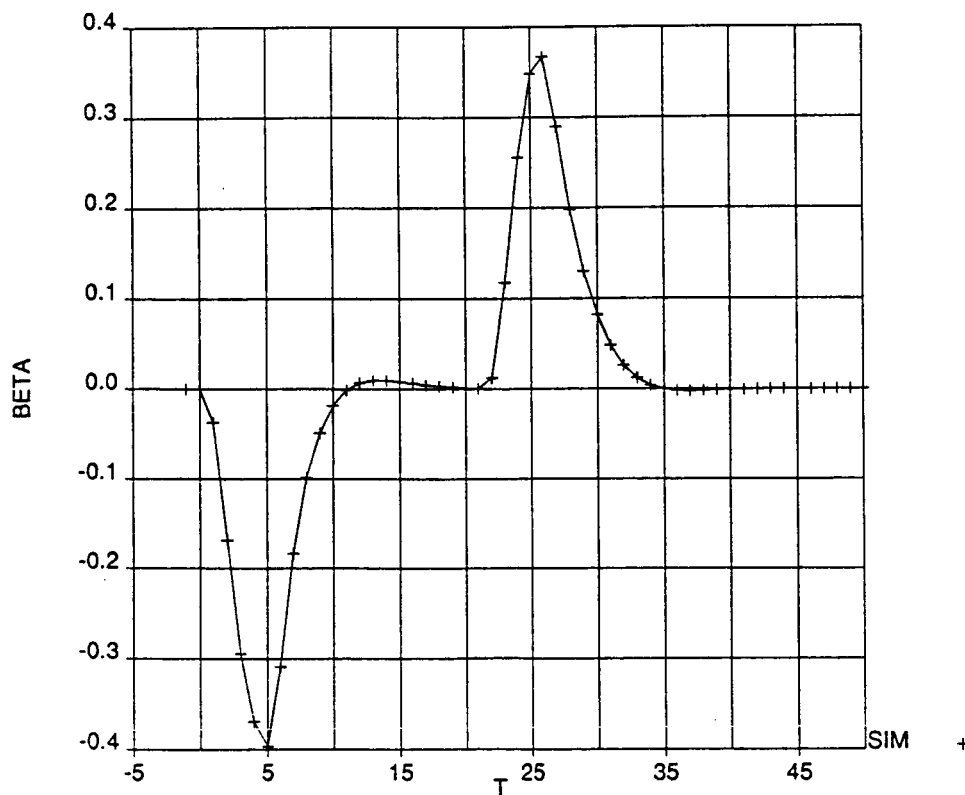
Plot 46. Ground Track Path Response to 90° Step in Heading Command
Low speed flight condition: flaps = 1, V_{CAS} = 138 knots



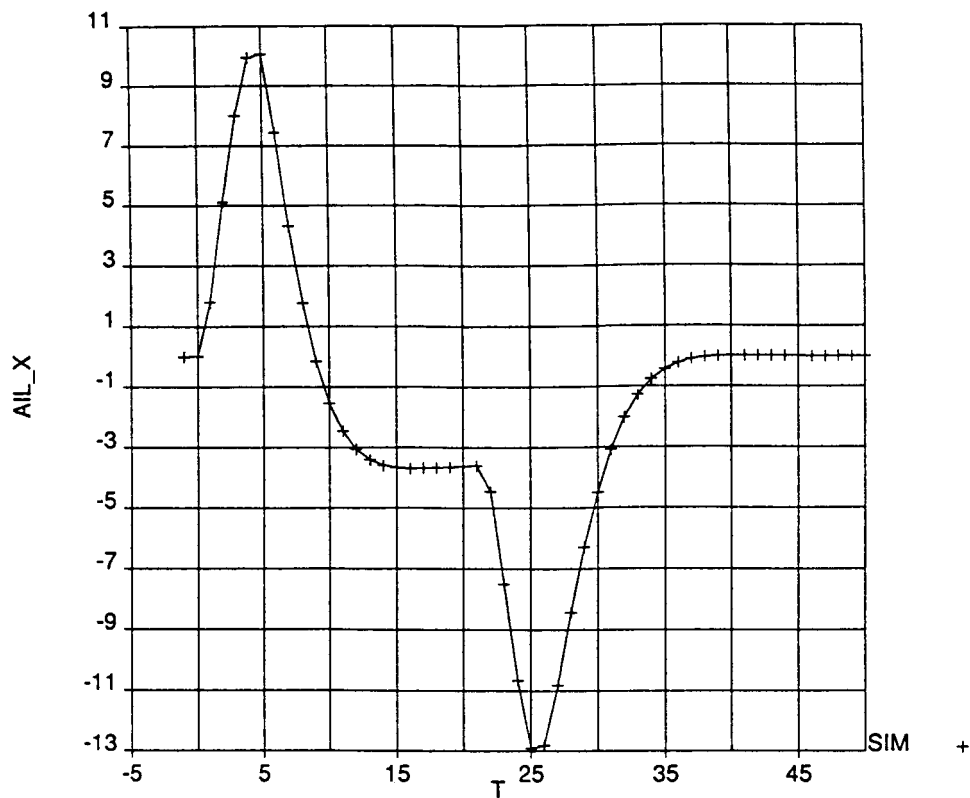
Plot 47. Heading Response to 90° Step in Heading Command
Low speed flight condition: flaps = 1, V_{CAS} = 138 knots



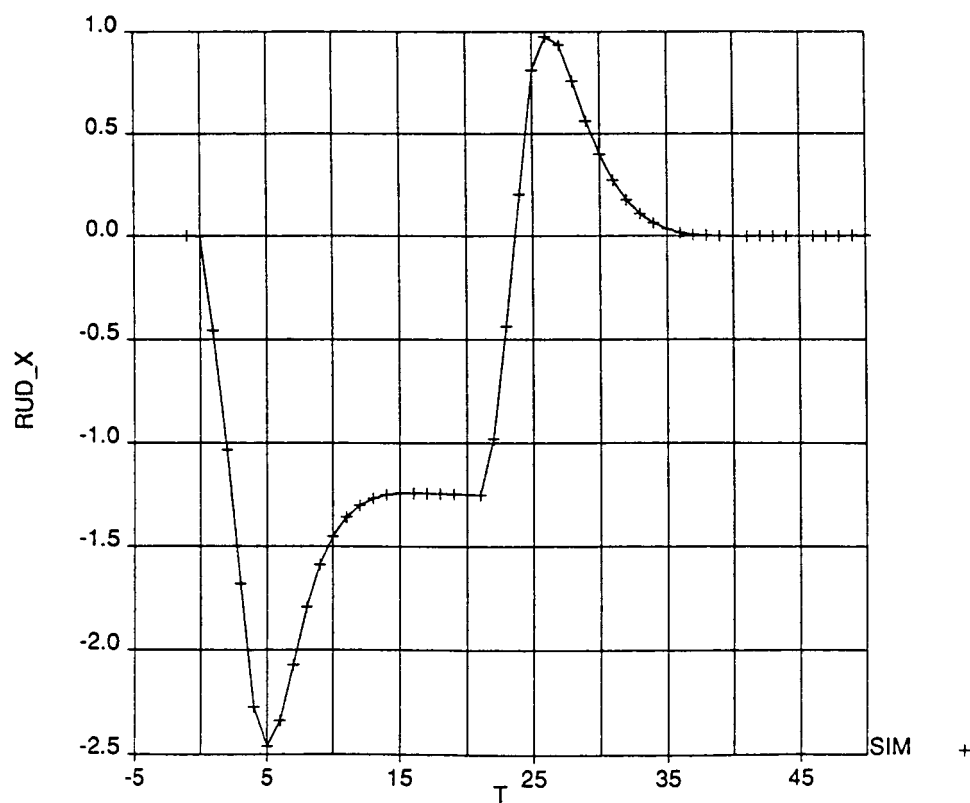
Plot 48. Bank Angle Response to 90° Step in Heading Command
 Low speed flight condition: flaps = 1, V_{CAS} = 138 knots



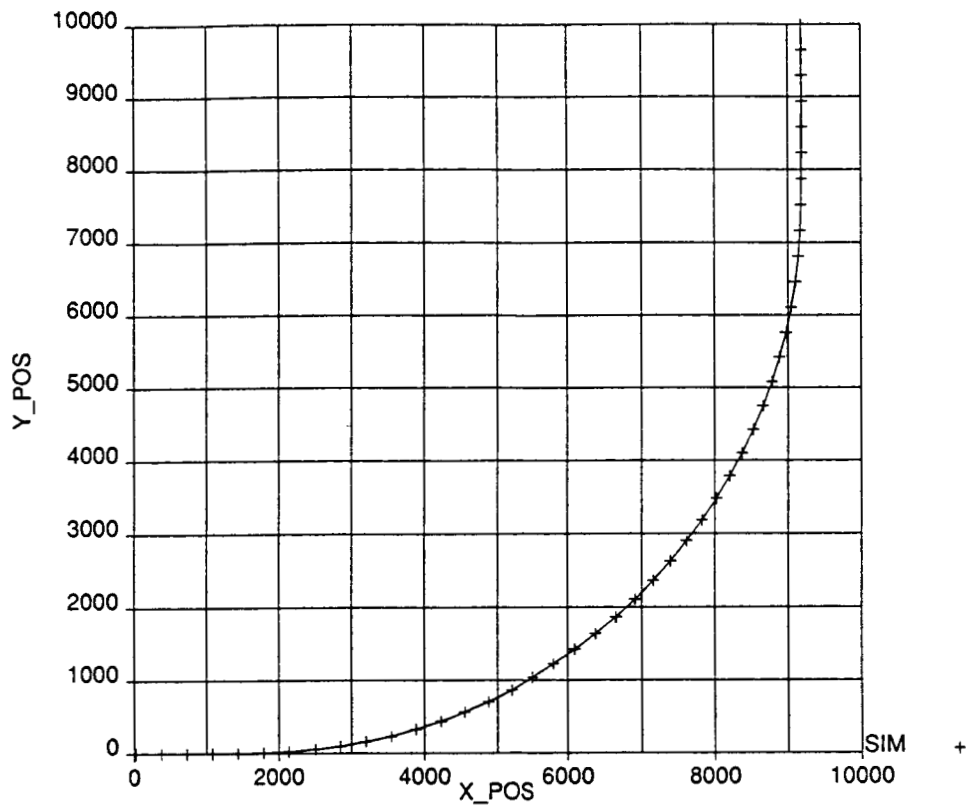
Plot 49. Sideslip Response to 90° Step in Heading Command
 Low speed flight condition: flaps = 1, V_{CAS} = 138 knots



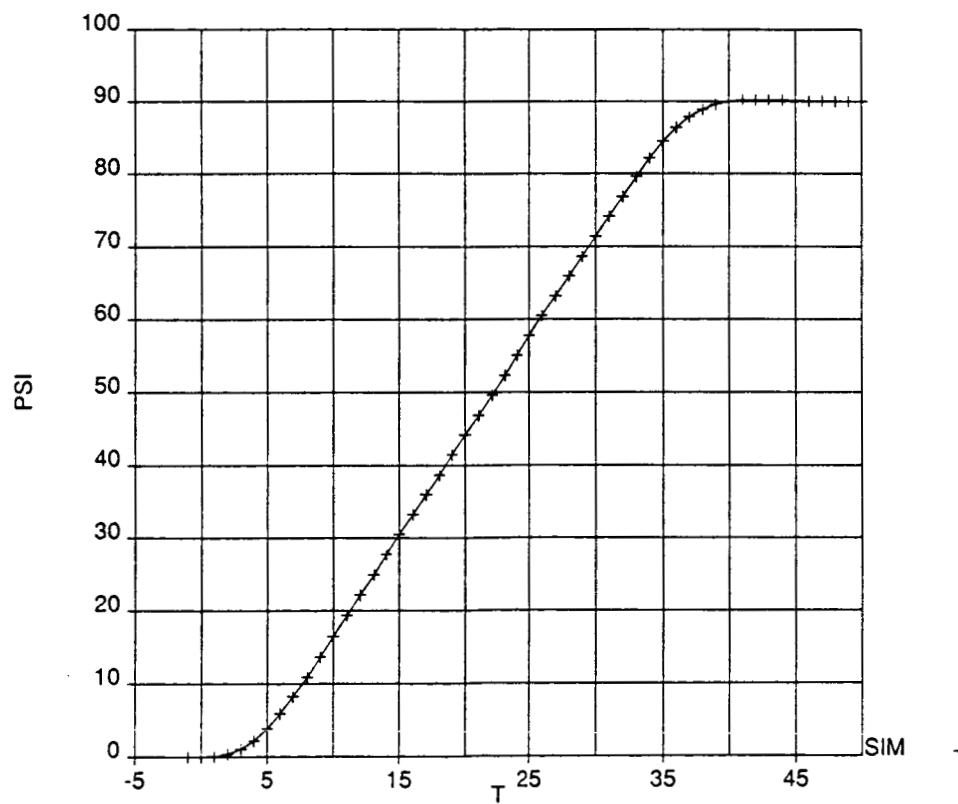
Plot 50. Aileron Response to 90° Step in Heading Command
 Low speed flight condition: flaps = 1, V_{CAS} = 138 knots



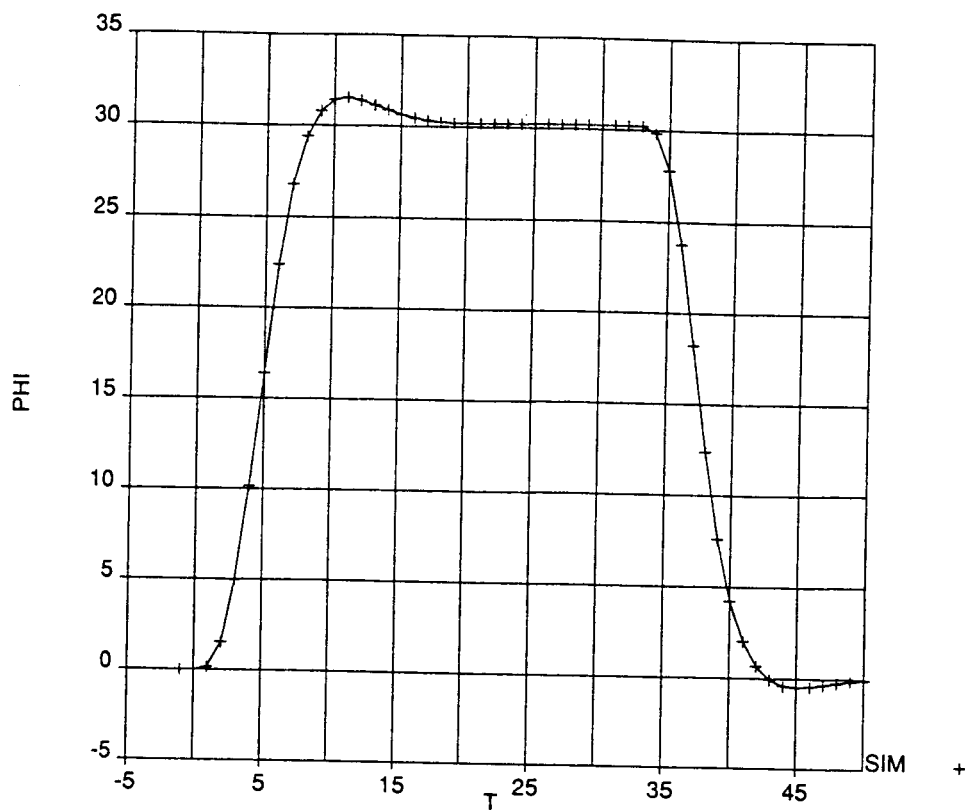
Plot 51. Rudder Response to 90° Step in Heading Command
 Low speed flight condition: flaps = 1, V_{CAS} = 138 knots



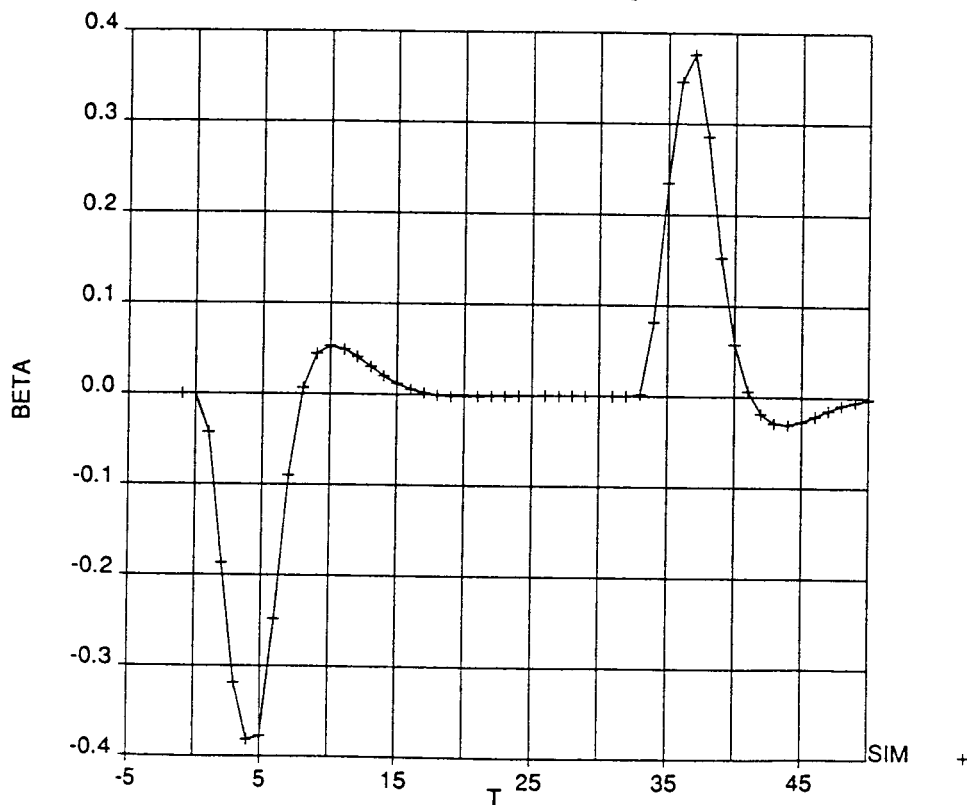
Plot 52. Ground Track Path Response to 90° Step in Heading Command
 High speed flight condition: flaps = 1, V_{CAS} = 210 knots



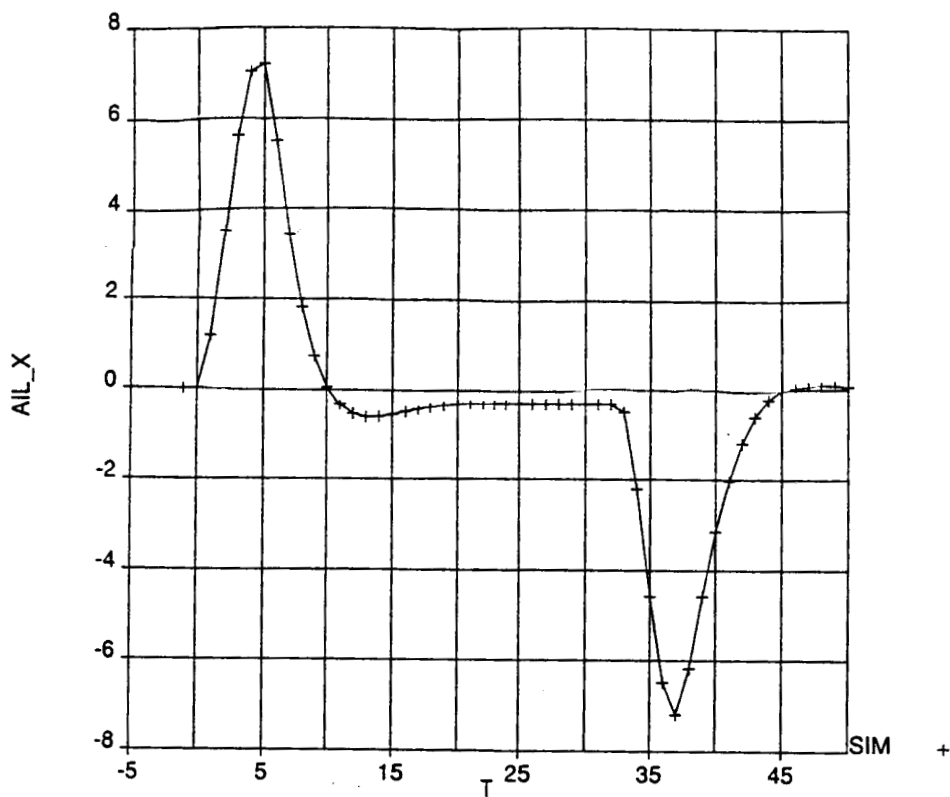
Plot 53. Heading Response to 90° Step in Heading Command
 High speed flight condition: flaps = 1, V_{CAS} = 210 knots



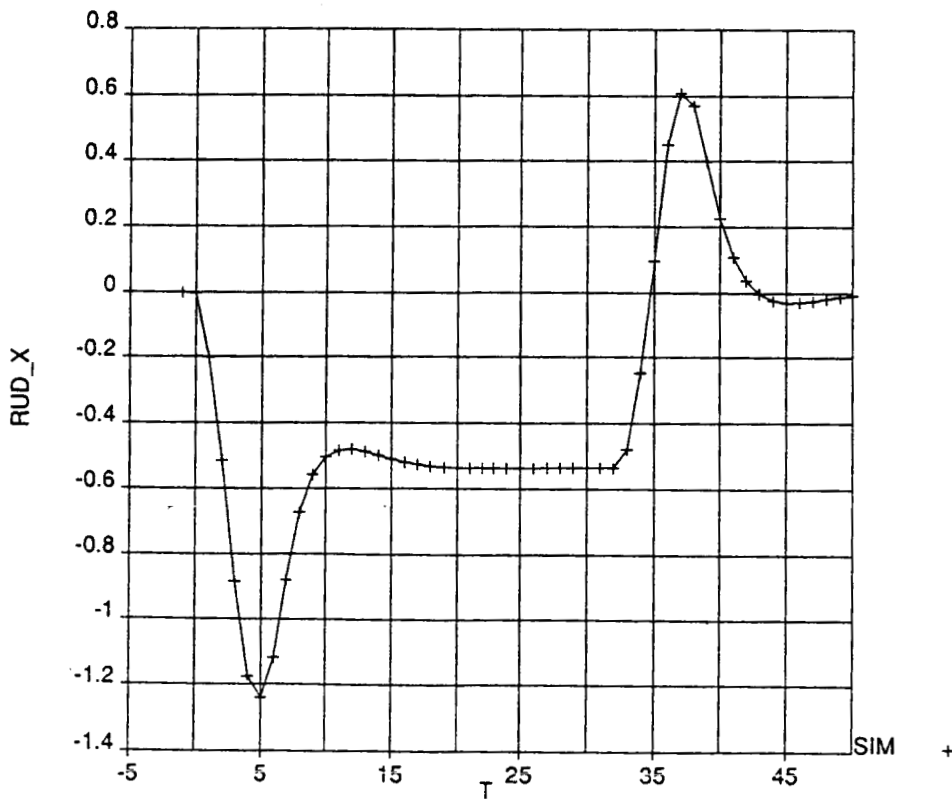
Plot 54. Bank angle response to 90° Step in Heading Command
High speed flight condition: flaps = 1, $V_{CAS} = 210$ knots



Plot 55. Sideslip Response to 90° Step in Heading Command
High speed flight condition: flaps = 1, $V_{CAS} = 210$ knots

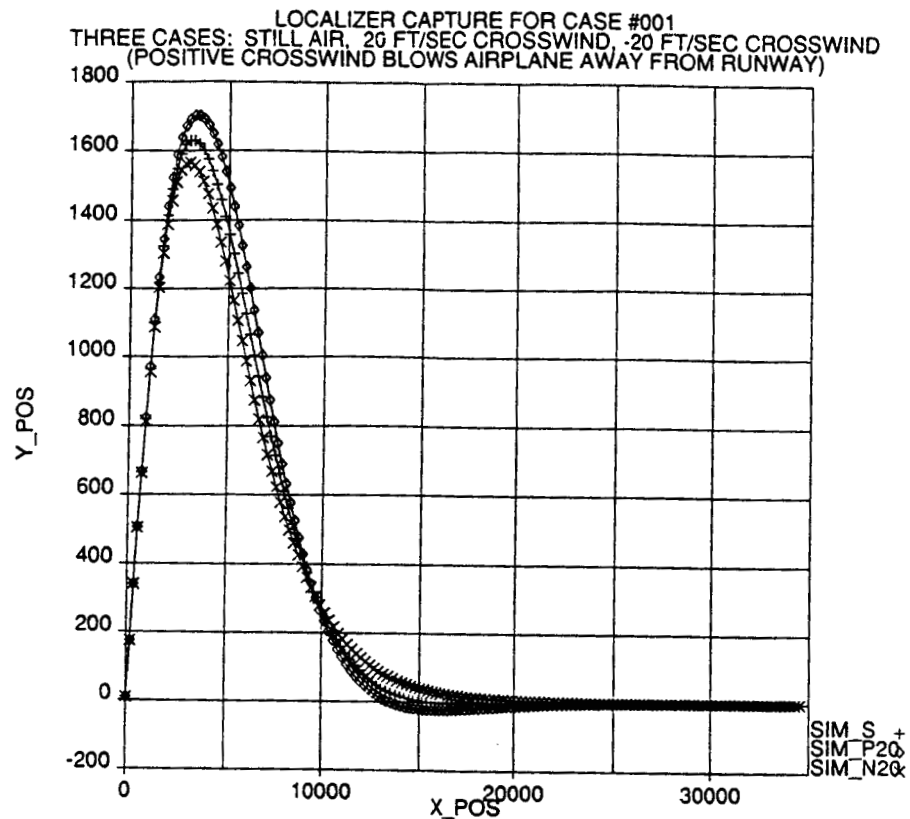


Plot 56. Aileron Response to 90° Step in Heading Command
 High speed flight condition: flaps = 1, V_{CAS} = 210 knots



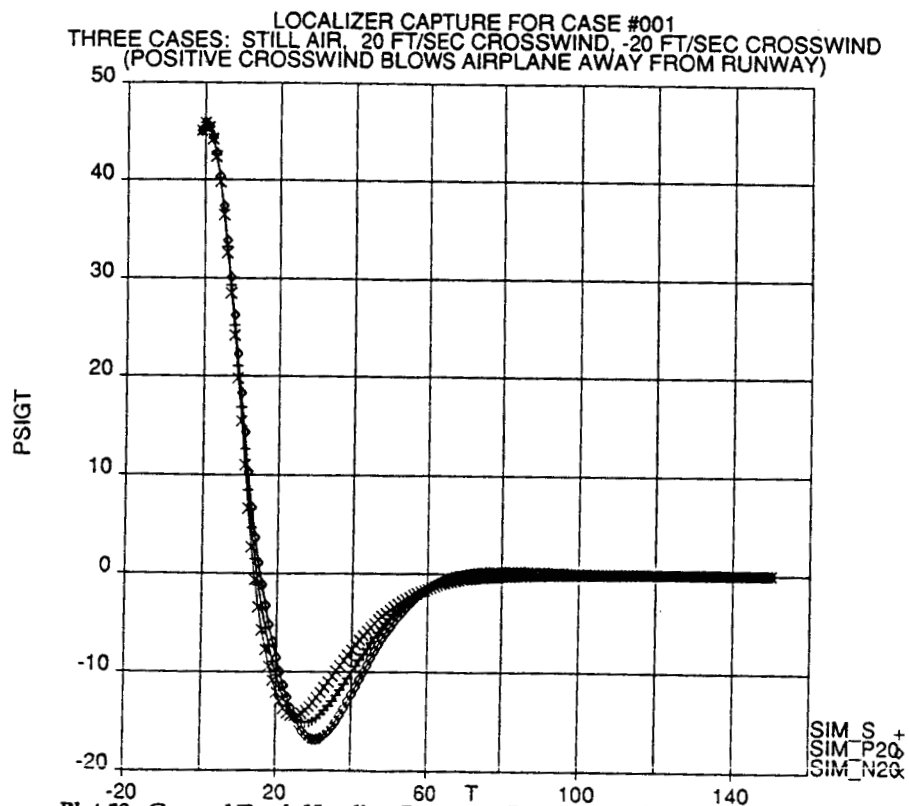
Plot 57. Rudder Response to 90° Step in Heading Command
 High speed flight condition: flaps = 1, V_{CAS} = 210 knots

**TIME SIMULATION RESULTS FOR
LOCALIZER CAPTURE AND TRACK CONTROLLER**



Plot 58. Ground Track Response During Localizer Capture and Track

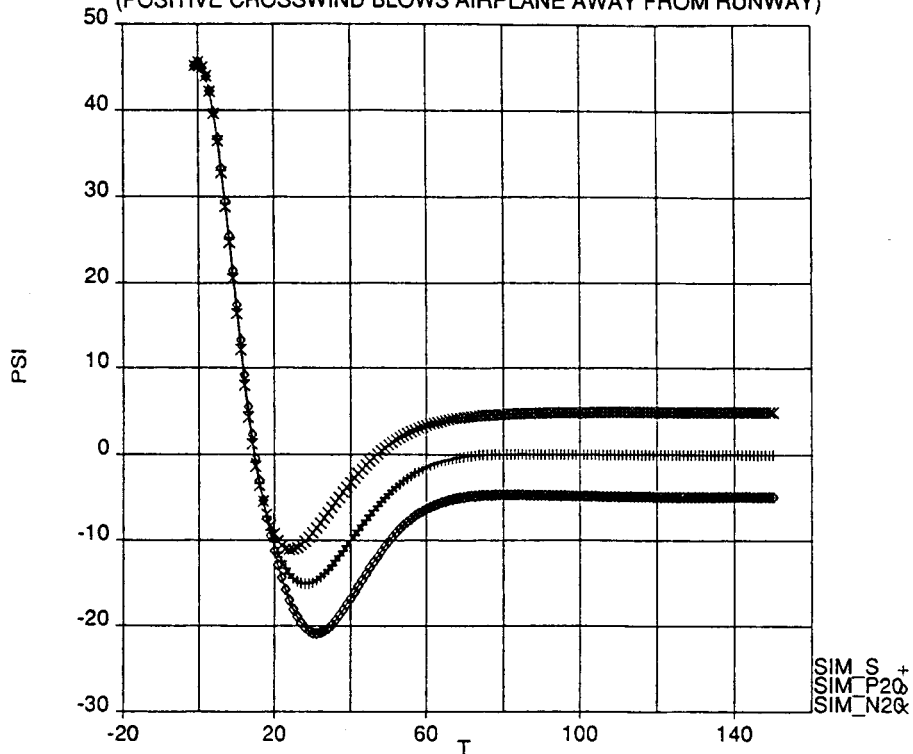
Initial condition: heading 45° from runway heading
Low speed flight condition: flaps = 1, VCAS = 138 knots



Plot 59. Ground Track Heading Response During Localizer Capture and Track

Initial condition: heading 45° from runway heading
Low speed flight condition: flaps = 1, VCAS = 138 knots

LOCALIZER CAPTURE FOR CASE #001
THREE CASES. STILL AIR, 20 FT/SEC CROSSWIND, -20 FT/SEC CROSSWIND
(POSITIVE CROSSWIND BLOWS AIRPLANE AWAY FROM RUNWAY)

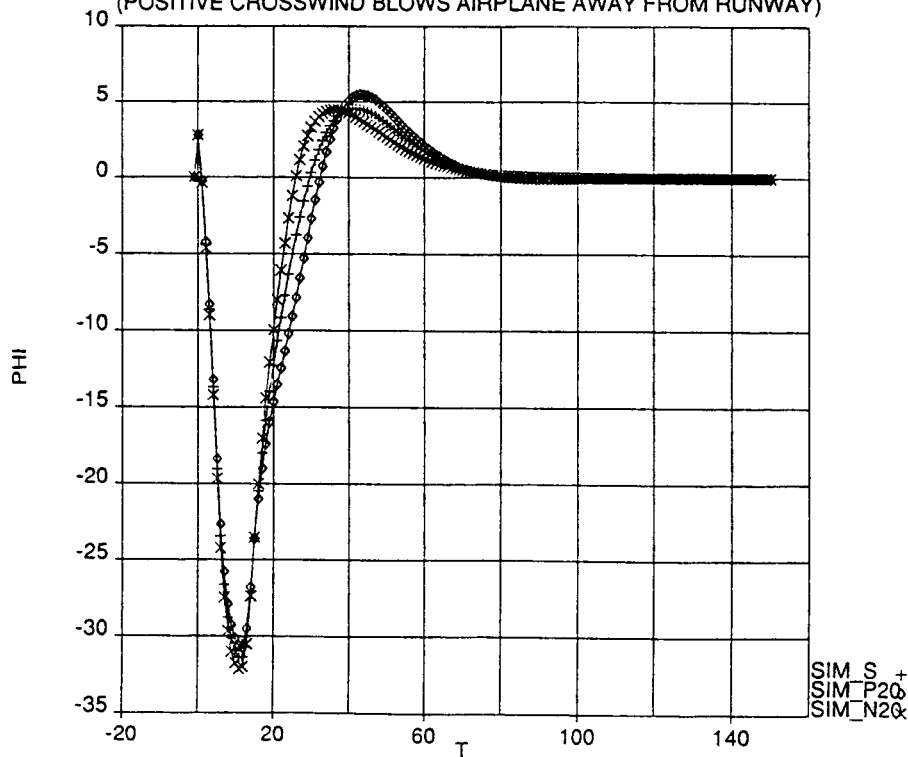


Plot 60. Body Axis Heading Response During Localizer Capture and Track

Initial condition: heading 45° from runway heading

Low speed flight condition: flaps = 1, VCAS = 138 knots

LOCALIZER CAPTURE FOR CASE #001
THREE CASES. STILL AIR, 20 FT/SEC CROSSWIND, -20 FT/SEC CROSSWIND
(POSITIVE CROSSWIND BLOWS AIRPLANE AWAY FROM RUNWAY)

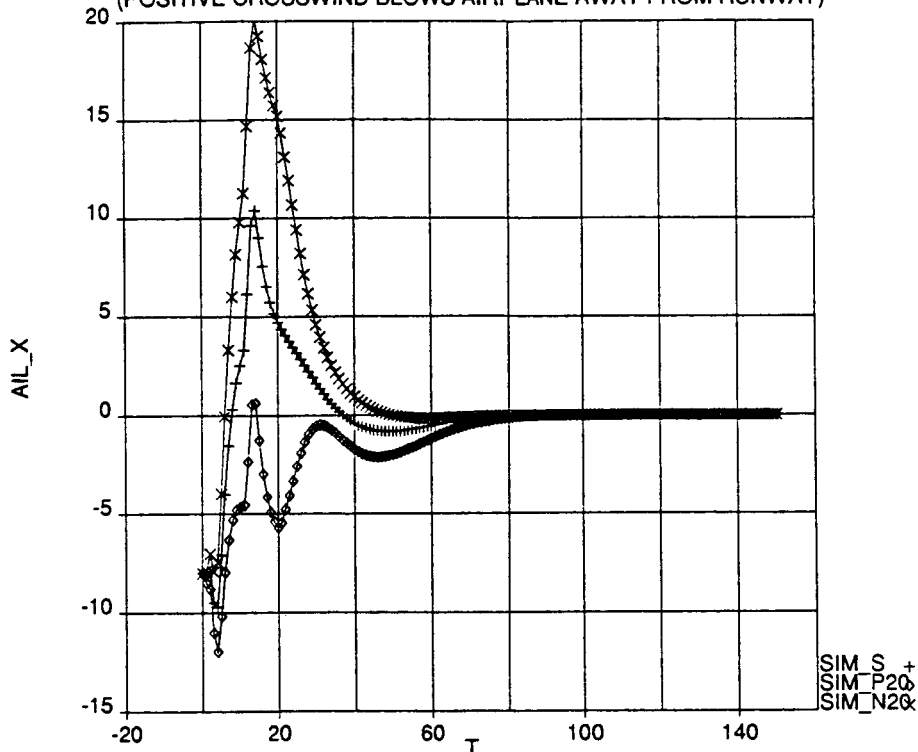


Plot 61. Bank Angle Response During Localizer Capture and Track

Initial condition: heading 45° from runway heading

Low speed flight condition: flaps = 1, VCAS = 138 knots

LOCALIZER CAPTURE FOR CASE #001
 THREE CASES: STILL AIR, 20 FT/SEC CROSSWIND, -20 FT/SEC CROSSWIND
 (POSITIVE CROSSWIND BLOWS AIRPLANE AWAY FROM RUNWAY)

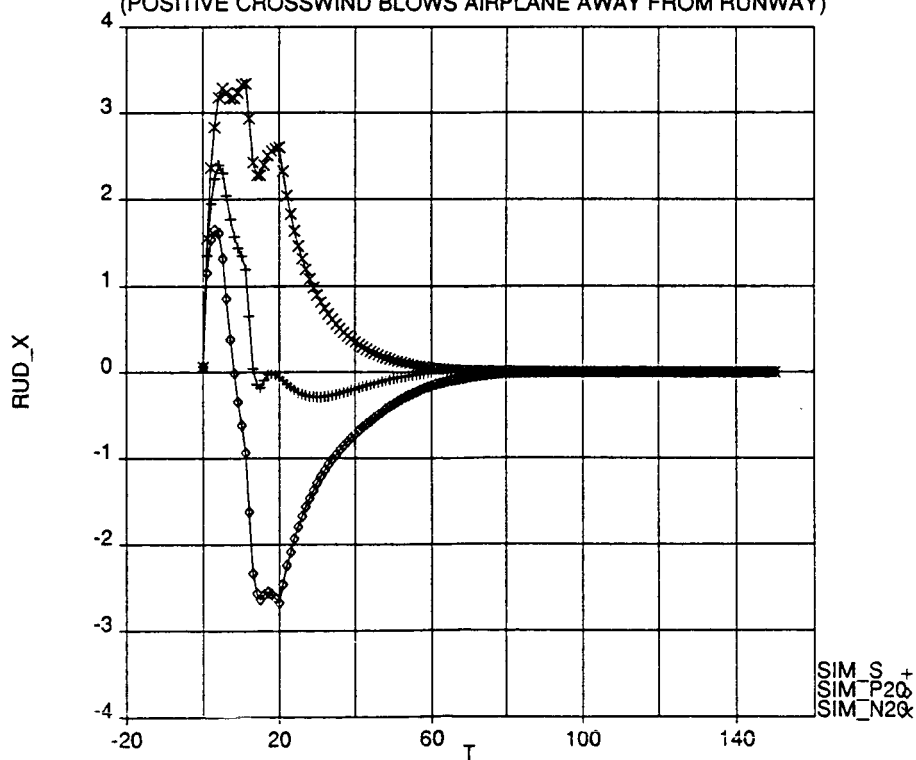


Plot 62. Aileron Response During Localizer Capture and Track

Initial condition: heading 45° from runway heading

Low speed flight condition: flaps = 1, VCAS = 138 knots

LOCALIZER CAPTURE FOR CASE #001
 THREE CASES: STILL AIR, 20 FT/SEC CROSSWIND, -20 FT/SEC CROSSWIND
 (POSITIVE CROSSWIND BLOWS AIRPLANE AWAY FROM RUNWAY)

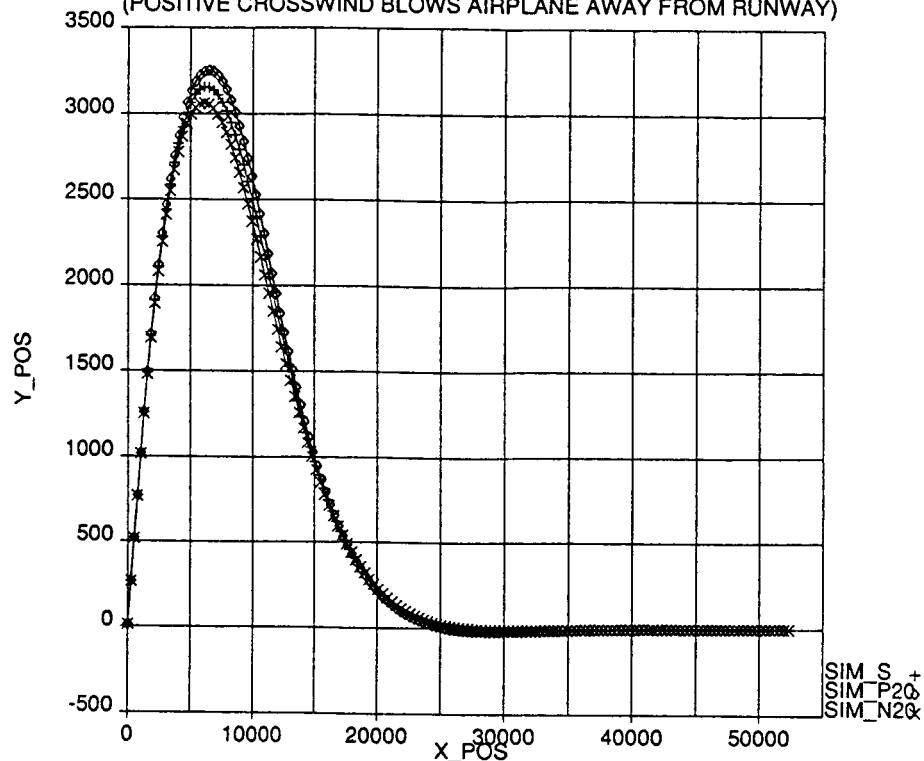


Plot 63. Rudder Response During Localizer Capture and Track

Initial condition: heading 45° from runway heading

Low speed flight condition: flaps = 1, VCAS = 138 knots

LOCALIZER CAPTURE FOR CASE #004
 THREE CASES: STILL AIR, 20 FT/SEC CROSSWIND, -20 FT/SEC CROSSWIND
 (POSITIVE CROSSWIND BLOWS AIRPLANE AWAY FROM RUNWAY)

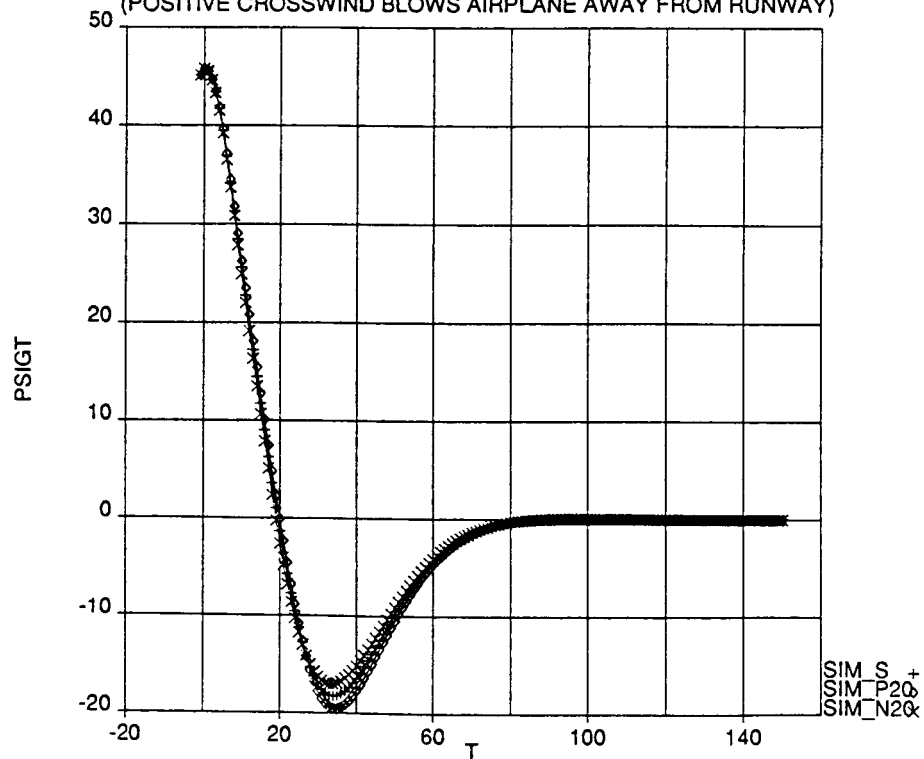


Plot 64. Ground Track Response During Localizer Capture and Track

Initial condition: heading 45° from runway heading

High speed flight condition: flaps = 1, $V_{CAS} = 210$ knots

LOCALIZER CAPTURE FOR CASE #004
 THREE CASES: STILL AIR, 20 FT/SEC CROSSWIND, -20 FT/SEC CROSSWIND
 (POSITIVE CROSSWIND BLOWS AIRPLANE AWAY FROM RUNWAY)

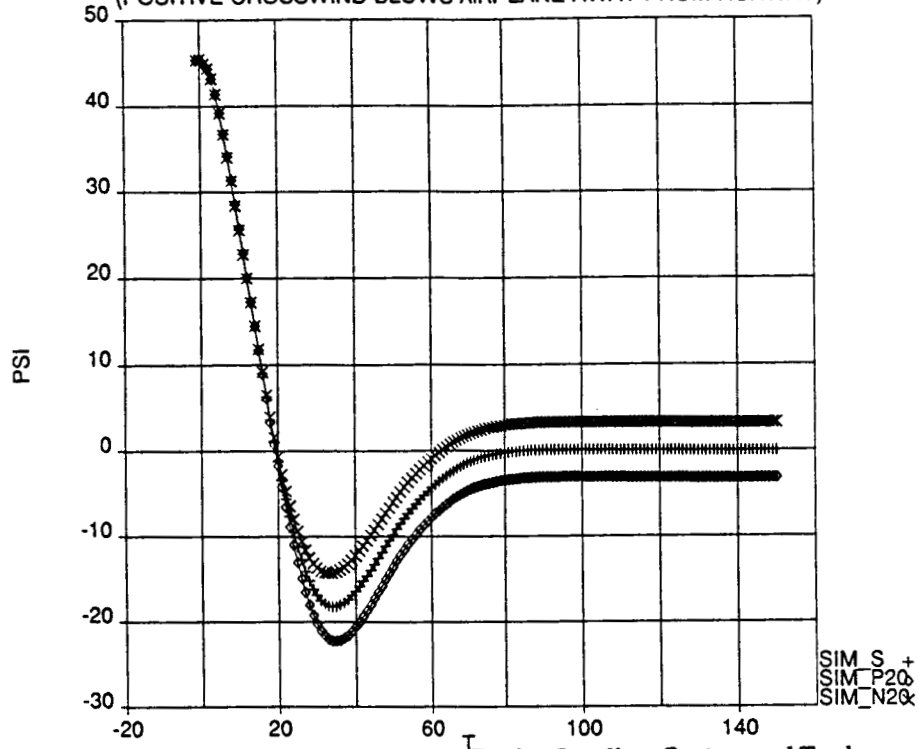


Plot 65. Ground Track Heading Response During Localizer Capture and Track

Initial condition: heading 45° from runway heading

High speed flight condition: flaps = 1, $V_{CAS} = 210$ knots

LOCALIZER CAPTURE FOR CASE #004
 THREE CASES: STILL AIR, 20 FT/SEC CROSSWIND, -20 FT/SEC CROSSWIND
 (POSITIVE CROSSWIND BLOWS AIRPLANE AWAY FROM RUNWAY)

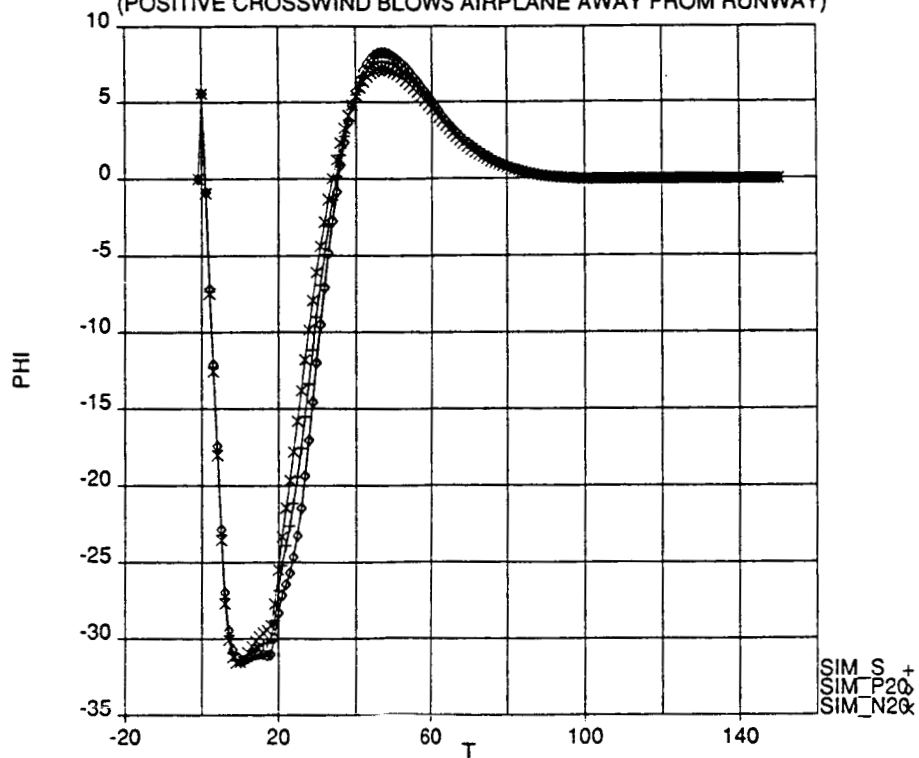


Plot 66. Body Axis Heading Response During Localizer Capture and Track

Initial condition: heading 45° from runway heading

High speed flight condition: flaps = 1, $V_{CAS} = 210$ knots

LOCALIZER CAPTURE FOR CASE #004
 THREE CASES: STILL AIR, 20 FT/SEC CROSSWIND, -20 FT/SEC CROSSWIND
 (POSITIVE CROSSWIND BLOWS AIRPLANE AWAY FROM RUNWAY)

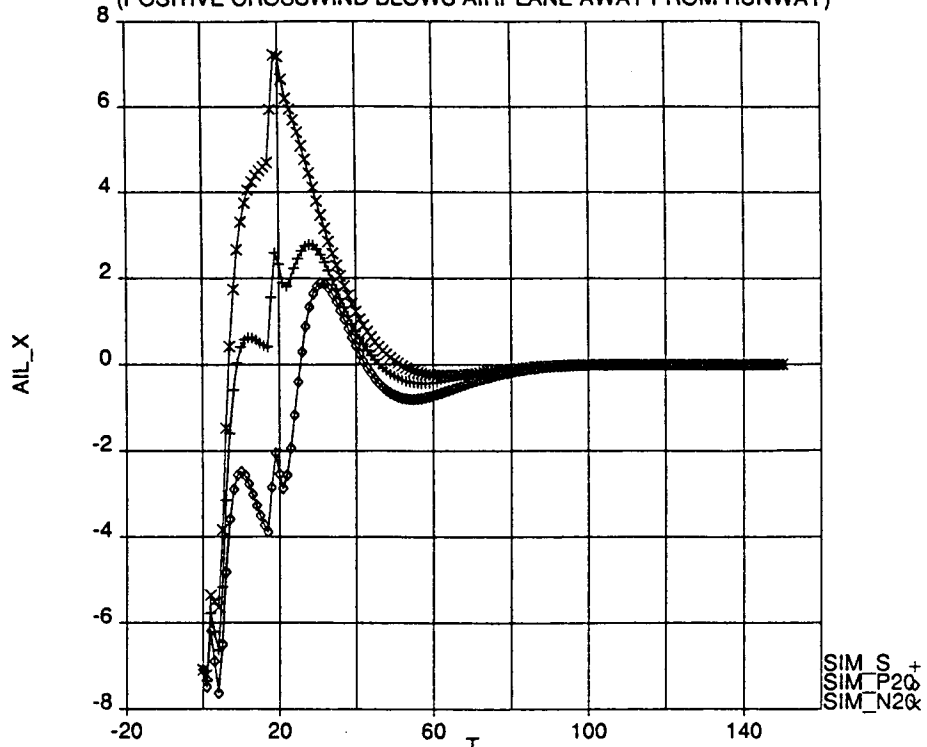


Plot 67. Bank Angle Response During Localizer Capture and Track

Initial condition: heading 45° from runway heading

High speed flight condition: flaps = 1, $V_{CAS} = 210$ knots

LOCALIZER CAPTURE FOR CASE #004
 THREE CASES: STILL AIR, 20 FT/SEC CROSSWIND, -20 FT/SEC CROSSWIND
 (POSITIVE CROSSWIND BLOWS AIRPLANE AWAY FROM RUNWAY)

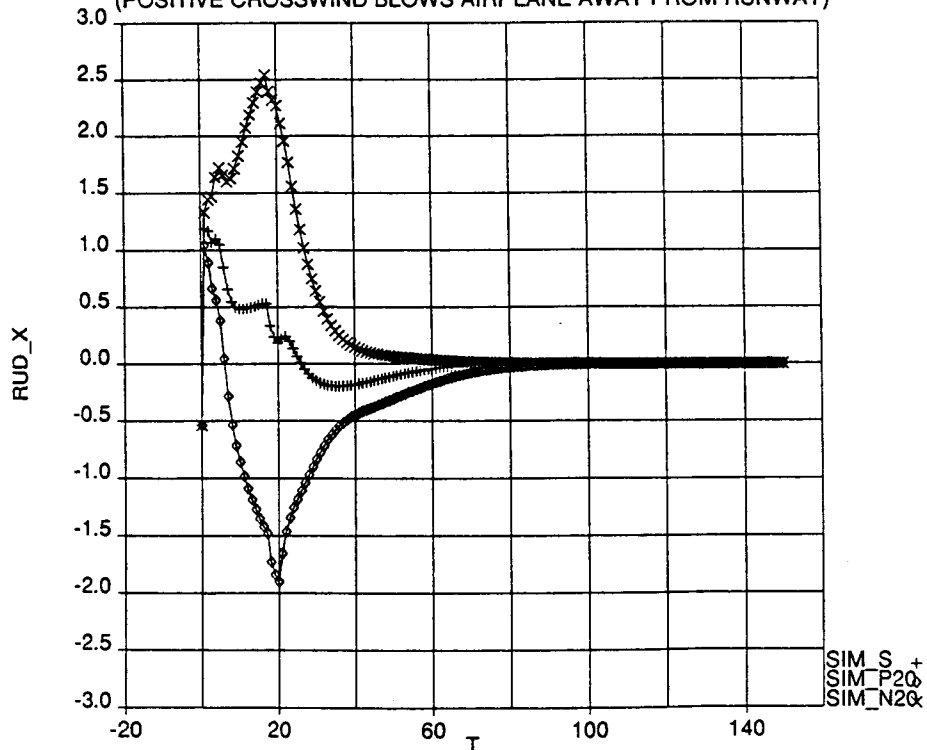


Plot 68. Aileron Response During Localizer Capture and Track

Initial condition: heading 45° from runway heading

High speed flight condition: flaps = 1, $V_{CAS} = 210$ knots

LOCALIZER CAPTURE FOR CASE #004
 THREE CASES: STILL AIR, 20 FT/SEC CROSSWIND, -20 FT/SEC CROSSWIND
 (POSITIVE CROSSWIND BLOWS AIRPLANE AWAY FROM RUNWAY)

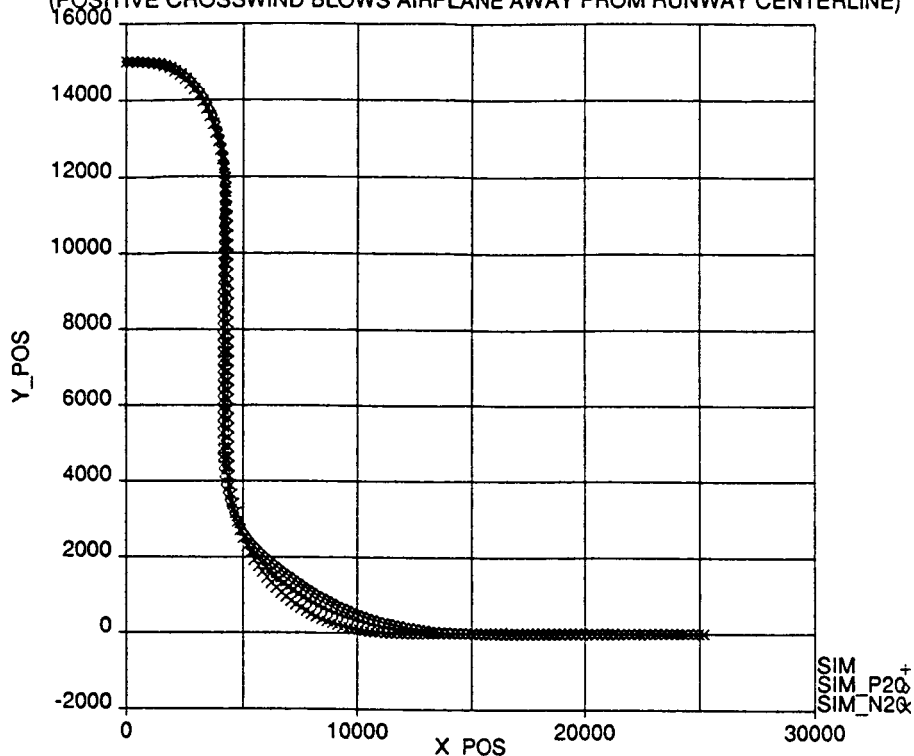


Plot 69. Rudder Response During Localizer Capture and Track

Initial condition: heading 45° from runway heading

High speed flight condition: flaps = 1, $V_{CAS} = 210$ knots

LOCALIZER CAPTURE FOR CASE #001
 THREE CASES: STILL AIR, 20 FT/SEC CROSSWIND, -20 FT/SEC CROSSWIND
 (POSITIVE CROSSWIND BLOWS AIRPLANE AWAY FROM RUNWAY CENTERLINE)

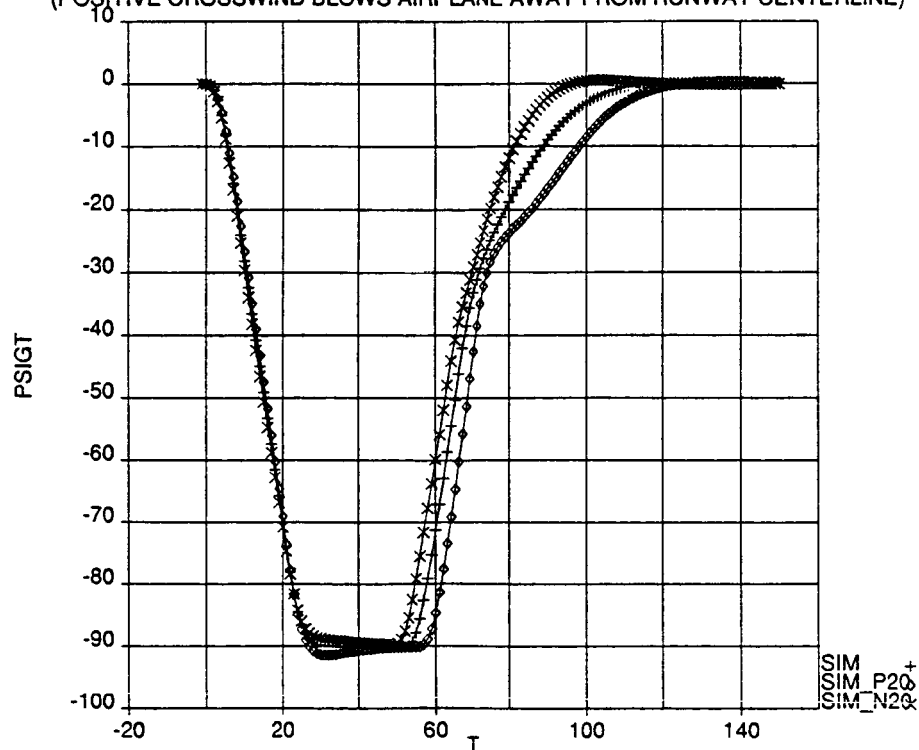


Plot 70. Ground Track Response During Localizer Capture and Track

Initial condition: 15000 ft offset from runway

Low speed flight condition: flaps = 1, $V_{CAS} = 138$ knots

LOCALIZER CAPTURE FOR CASE #001
 THREE CASES: STILL AIR, 20 FT/SEC CROSSWIND, -20 FT/SEC CROSSWIND
 (POSITIVE CROSSWIND BLOWS AIRPLANE AWAY FROM RUNWAY CENTERLINE)

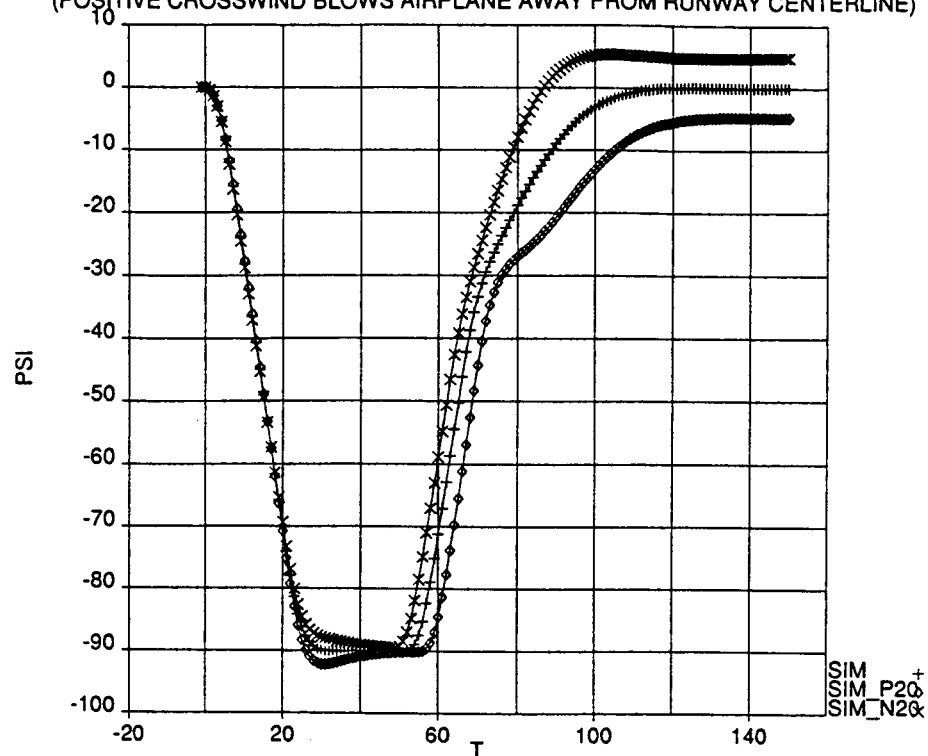


Plot 71. Ground Track Heading Response During Localizer Capture and Track

Initial condition: 15000 ft offset from runway

Low speed flight condition: flaps = 1, $V_{CAS} = 138$ knots

LOCALIZER CAPTURE FOR CASE #001
 THREE CASES: STILL AIR, 20 FT/SEC CROSSWIND, -20 FT/SEC CROSSWIND
 (POSITIVE CROSSWIND BLOWS AIRPLANE AWAY FROM RUNWAY CENTERLINE)

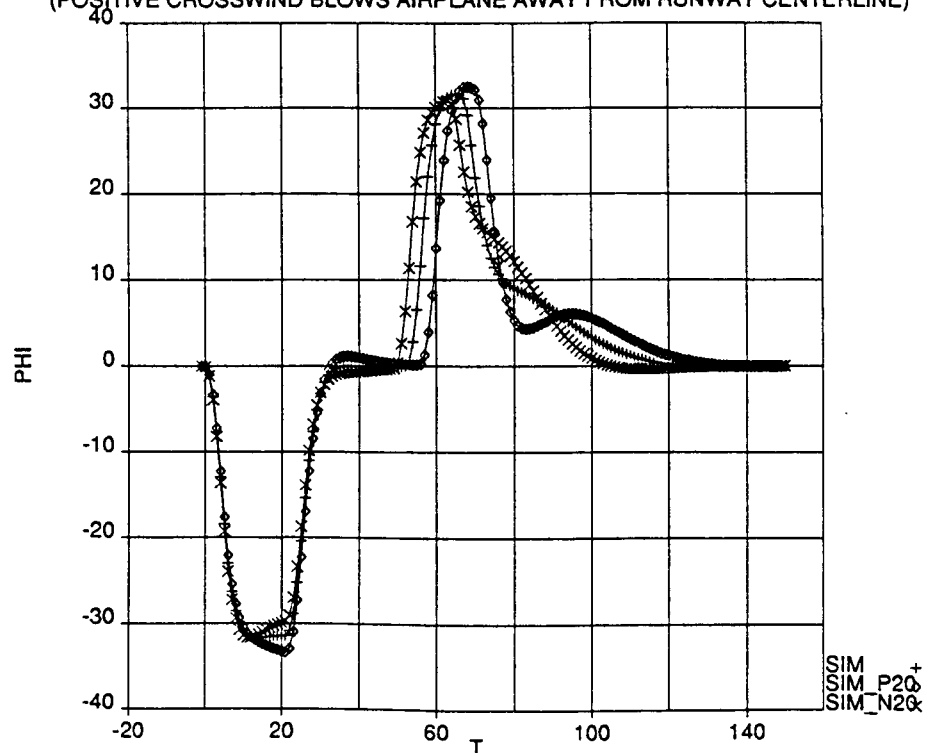


Plot 72. Body Axis Heading Response During Localizer Capture and Track

Initial condition: 15000 ft offset from runway

Low speed flight condition: flaps = 1, $V_{CAS} = 138$ knots

LOCALIZER CAPTURE FOR CASE #001
 THREE CASES: STILL AIR, 20 FT/SEC CROSSWIND, -20 FT/SEC CROSSWIND
 (POSITIVE CROSSWIND BLOWS AIRPLANE AWAY FROM RUNWAY CENTERLINE)

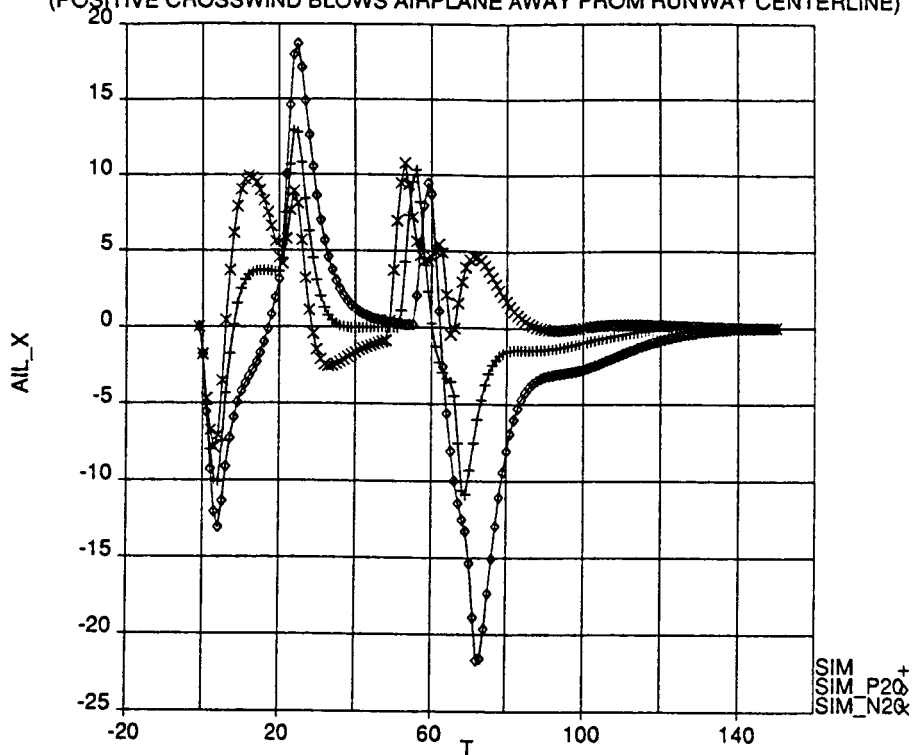


Plot 73. Bank Angle Response During Localizer Capture and Track

Initial condition: 15000 ft offset from runway

Low speed flight condition: flaps = 1, $V_{CAS} = 138$ knots

LOCALIZER CAPTURE FOR CASE #001
 THREE CASES: STILL AIR, 20 FT/SEC CROSSWIND, -20 FT/SEC CROSSWIND
 (POSITIVE CROSSWIND BLOWS AIRPLANE AWAY FROM RUNWAY CENTERLINE)

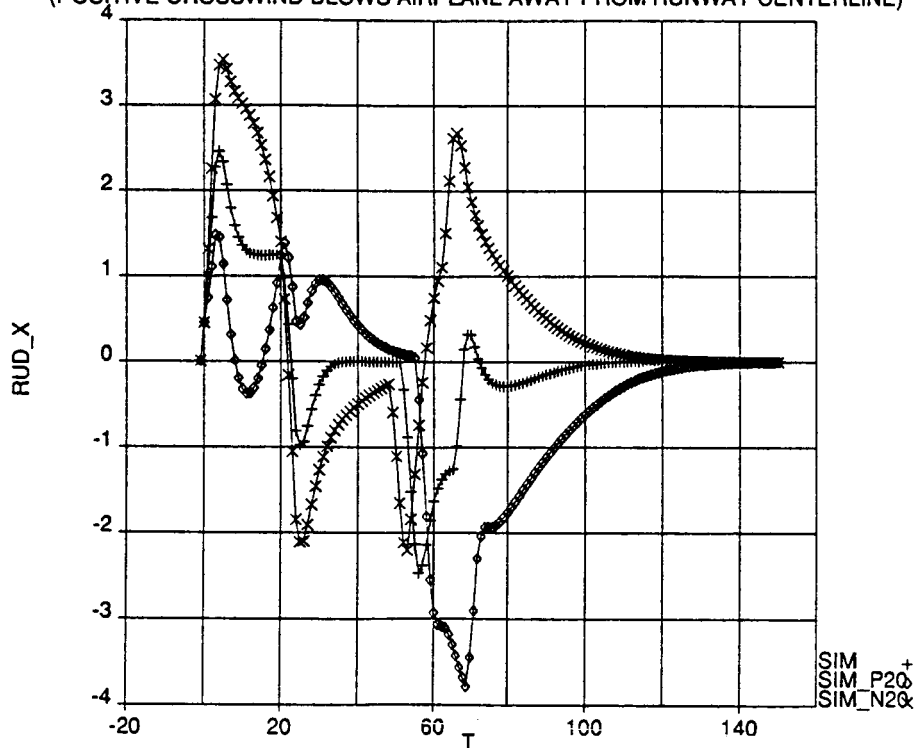


Plot 74. Aileron Response During Localizer Capture and Track

Initial condition: 15000 ft offset from runway

Low speed flight condition: flaps = 1, $V_{CAS} = 138$ knots

LOCALIZER CAPTURE FOR CASE #001
 THREE CASES: STILL AIR, 20 FT/SEC CROSSWIND, -20 FT/SEC CROSSWIND
 (POSITIVE CROSSWIND BLOWS AIRPLANE AWAY FROM RUNWAY CENTERLINE)

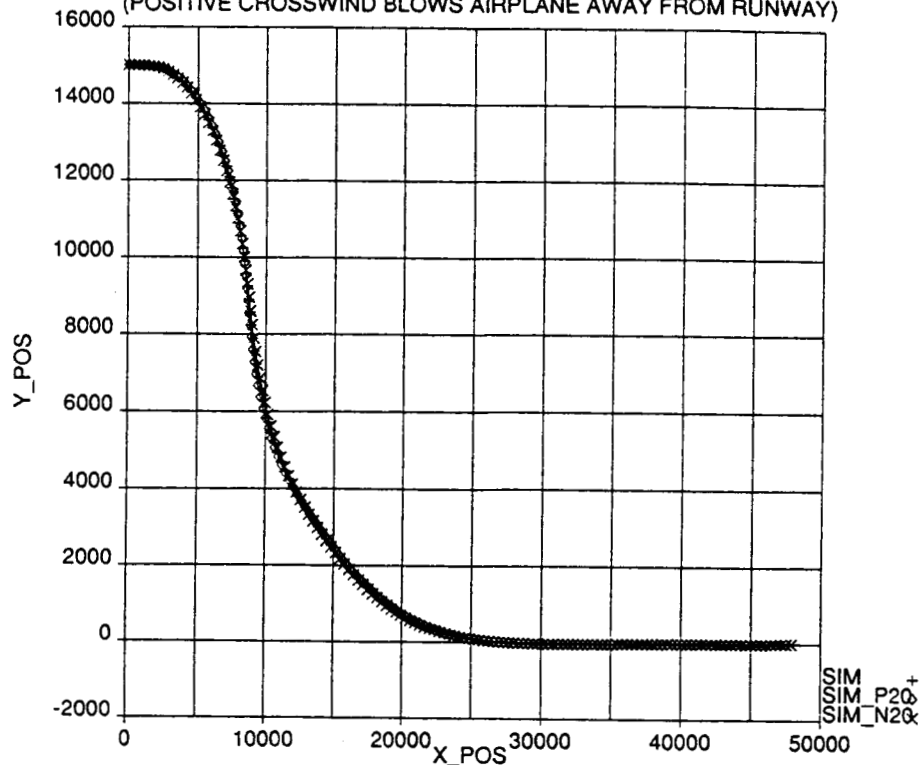


Plot 75. Rudder Response During Localizer Capture and Track

Initial condition: 15000 ft offset from runway

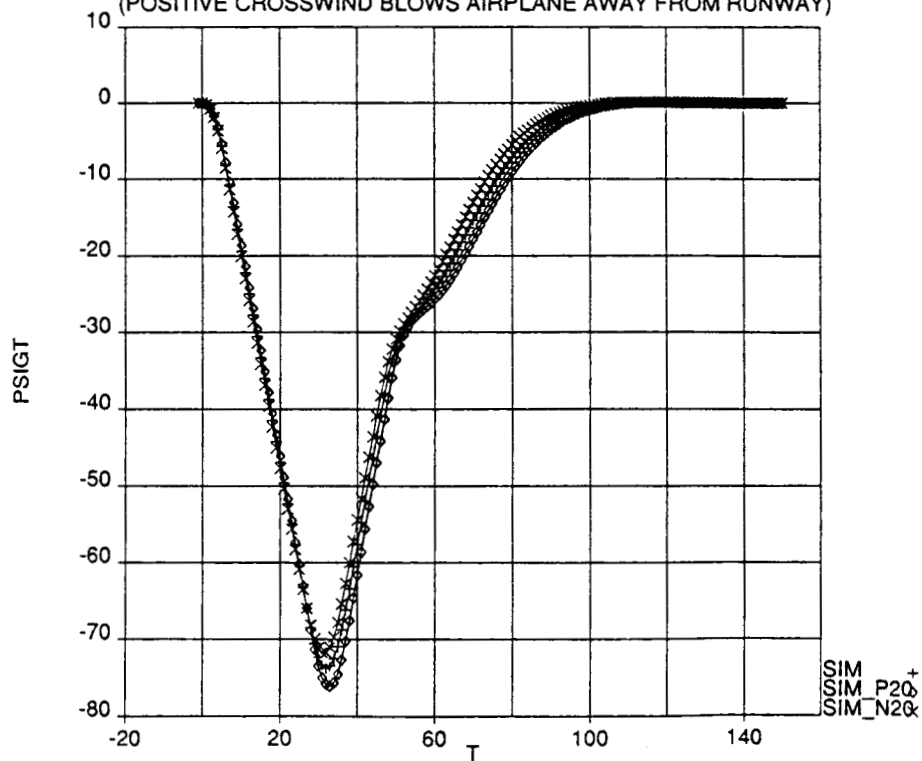
Low speed flight condition: flaps = 1, $V_{CAS} = 138$ knots

LOCALIZER CAPTURE FOR CASE #004
 THREE CASES: STILL AIR, 20 FT/SEC CROSSWIND, -20 FT/SEC CROSSWIND
 (POSITIVE CROSSWIND BLOWS AIRPLANE AWAY FROM RUNWAY)



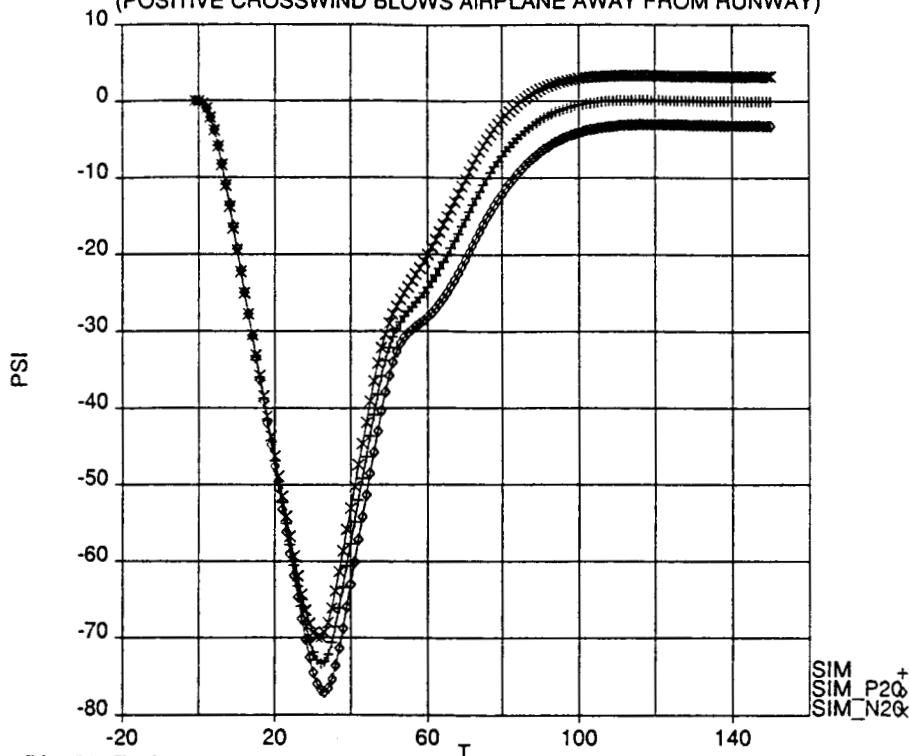
Plot 76. Ground Track Response During Localizer Capture and Track
 Initial condition: 15000 ft offset from runway
 High speed flight condition: flaps = 1, $V_{CAS} = 210$ knots

LOCALIZER CAPTURE FOR CASE #004
 THREE CASES: STILL AIR, 20 FT/SEC CROSSWIND, -20 FT/SEC CROSSWIND
 (POSITIVE CROSSWIND BLOWS AIRPLANE AWAY FROM RUNWAY)



Plot 77. Ground Track Heading Response During Localizer Capture and Track
 Initial condition: 15000 ft offset from runway
 High speed flight condition: flaps = 1, $V_{CAS} = 210$ knots

LOCALIZER CAPTURE FOR CASE #004
 THREE CASES: STILL AIR, 20 FT/SEC CROSSWIND, -20 FT/SEC CROSSWIND
 (POSITIVE CROSSWIND BLOWS AIRPLANE AWAY FROM RUNWAY)

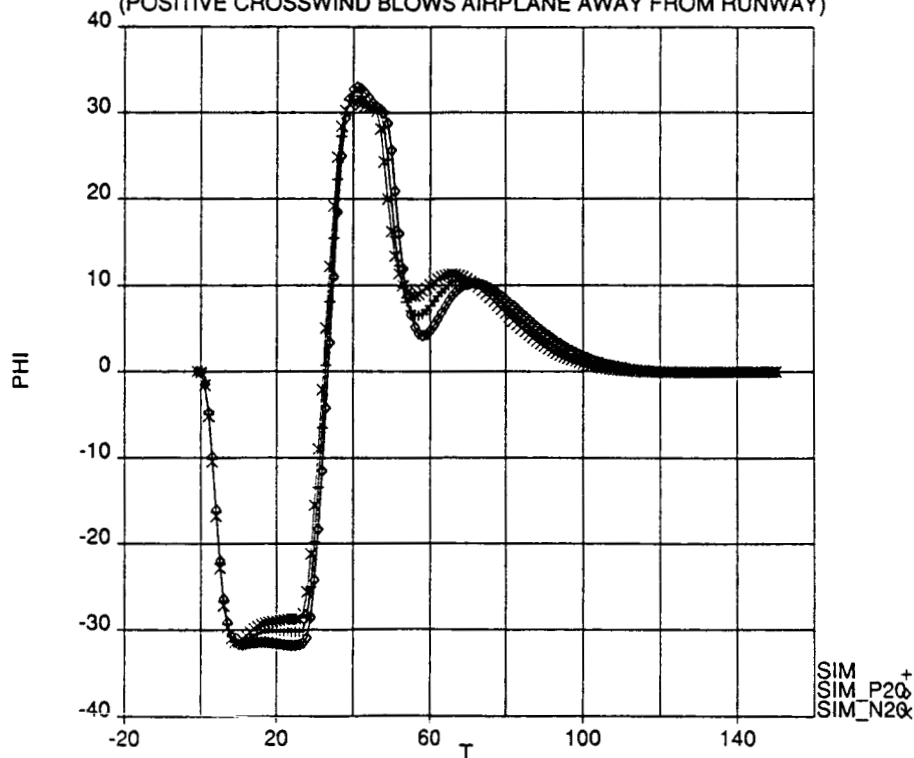


Plot 78. Body Axis Heading Response During Localizer Capture and Track

Initial condition: 15000 ft offset from runway

High speed flight condition: flaps = 1, $V_{CAS} = 210$ knots

LOCALIZER CAPTURE FOR CASE #004
 THREE CASES: STILL AIR, 20 FT/SEC CROSSWIND, -20 FT/SEC CROSSWIND
 (POSITIVE CROSSWIND BLOWS AIRPLANE AWAY FROM RUNWAY)

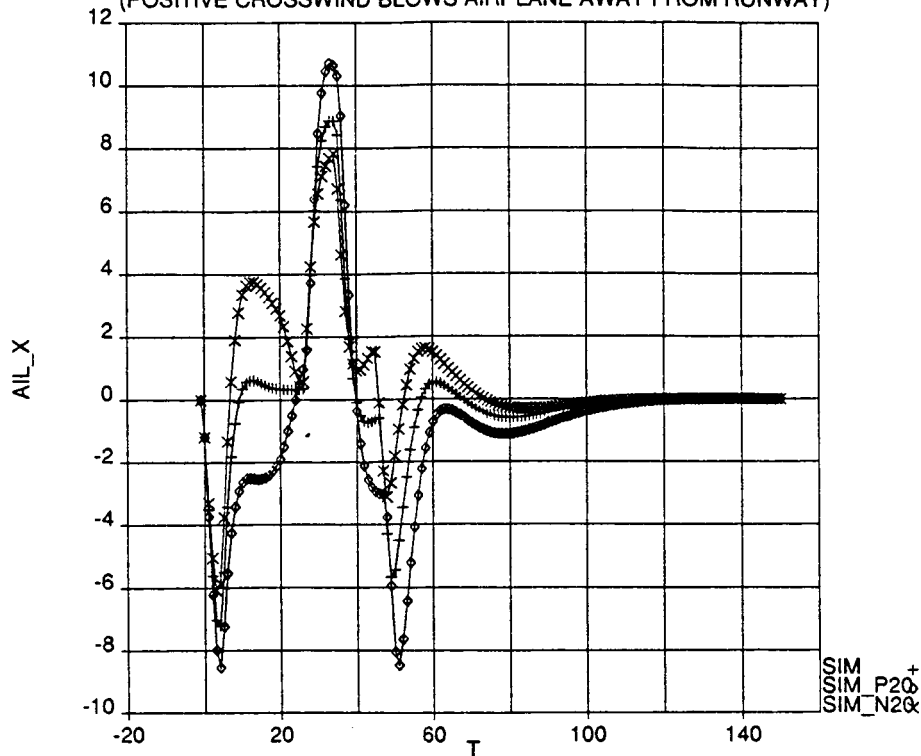


Plot 79. Bank Angle Response During Localizer Capture and Track

Initial condition: 15000 ft offset from runway

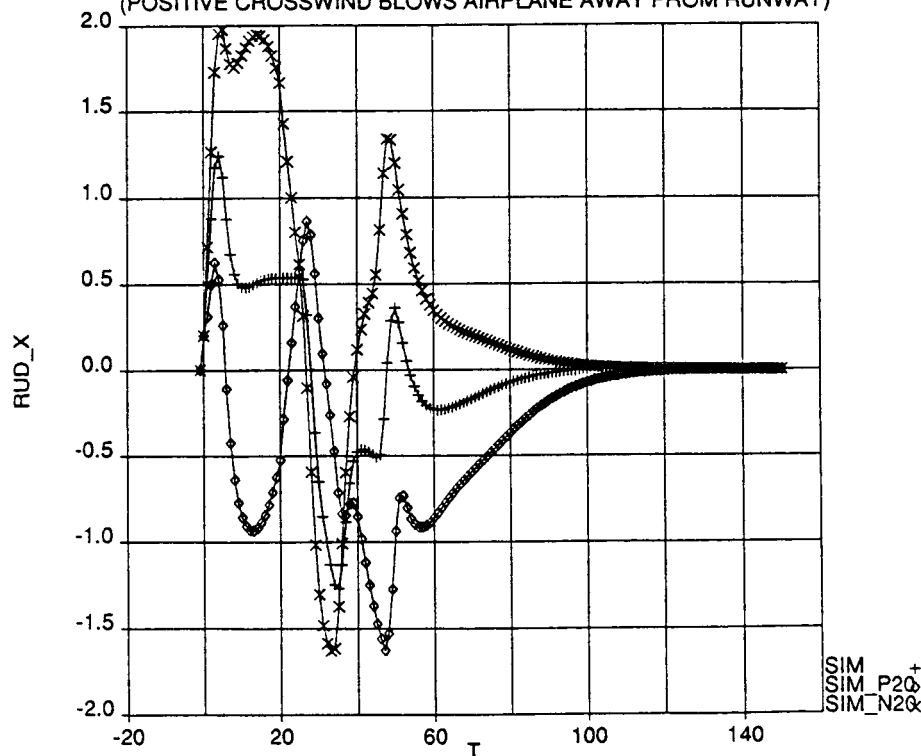
High speed flight condition: flaps = 1, $V_{CAS} = 210$ knots

LOCALIZER CAPTURE FOR CASE #004
THREE CASES: STILL AIR, 20 FT/SEC CROSSWIND, -20 FT/SEC CROSSWIND
(POSITIVE CROSSWIND BLOWS AIRPLANE AWAY FROM RUNWAY)



Plot 80. Aileron Response During Localizer Capture and Track
Initial condition: 15000 ft offset from runway
High speed flight condition: flaps = 1, $V_{CAS} = 210$ knots

LOCALIZER CAPTURE FOR CASE #004
THREE CASES: STILL AIR, 20 FT/SEC CROSSWIND, -20 FT/SEC CROSSWIND
(POSITIVE CROSSWIND BLOWS AIRPLANE AWAY FROM RUNWAY)



Plot 81. Rudder Response During Localizer Capture and Track
Initial condition: 15000 ft offset from runway
High speed flight condition: flaps = 1, $V_{CAS} = 210$ knots

SIMULATION PROGRAM


```

      PROGRAM SIM
C
C This program performs a simulation of the lateral axis of a 737-200.
C Two modes of operation are available:
C   1) Heading / Sideslip control
C   2) Localizer capture and track / Sideslip control
C Note that mode 1 is used as the inner loop for mode 2.
C
C A linear point simulation plant model is used along with a linear controller
C whose gains are scheduled as functions of the trim flight condition.
C
C
      CHARACTER LINE*80
      REAL A(4,4), B(4,3), MACH, G(2,6), X(6), U_C(2), U_X(3),
+        XA_DOT(4), XB_DOT(4)
C
C I/O files:
C Unit 5: Linear plant model and trim flight condition data
C Unit 6: Time simulation output data
C
      OPEN (UNIT=5, FILE='OL/LAT004.MDL', STATUS='OLD')
      OPEN (UNIT=6, FILE='SIM.GGP', STATUS='UNKNOWN')
C
C Read in plant model and flight condition data for gain scheduling
C
100  READ (5,8010) LINE
      IF (LINE(1:1) .NE. 'A') GO TO 100
      DO 110 I = 1,4
          READ (5,*) (A(I,J), J=1,4)
110  CONTINUE
C
200  READ (5,8010) LINE
      IF (LINE(1:1) .NE. 'B') GO TO 200
      DO 210 I = 1,4
          READ (5,*) (B(I,J), J=1,2)
210  CONTINUE
C
300  READ (5,8010) LINE
      IF (LINE(6:8) .NE. 'DFM') GO TO 300
      READ (LINE(14:23),8020) FLAP
C
400  READ (5,8010) LINE
      IF (LINE(6:9) .NE. 'MACH') GO TO 400
      READ (LINE(14:23),8020) MACH
C
500  READ (5,8010) LINE
      IF (LINE(6:7) .NE. 'VP') GO TO 500
      READ (LINE(14:23),8020) VTAS
C
600  READ (5,8010) LINE
      IF (LINE(6:9) .NE. 'VCAS') GO TO 600
      READ (LINE(14:23),8020) VCAS
C
C
C Build lateral gust input
C
      DO 700 I = 1,4
          B(I,3) = - 57.3 * A(I,1) / VTAS
700  CONTINUE
C
C
C Aileron feedback gains: scheduled as functions of trim flight condition
C G(1,1) = Aileron sideslip gain
C G(1,2) = Aileron roll rate gain
C G(1,3) = Aileron bank angle gain
C G(1,4) = Aileron yaw rate gain
C G(1,5) = Aileron integral sideslip error gain
C G(1,6) = Aileron heading error gain
C
      G(1,1) = -4.2
C
      IF (VCAS .LT. 125.) THEN

```

```

      G(1,2) = -.80
    ELSE IF (VCAS .LT. 200.) THEN
      G(1,2) = -.80 + (VCAS - 125.) * .42 / 75.
    ELSE IF (VCAS .LT. 360.) THEN
      G(1,2) = -.38 + (VCAS - 200.) * .20 / 160.
    ELSE
      G(1,2) = -.18
    ENDIF
C
    IF (MACH .LT. 0.15) THEN
      G(1,3) = -1.4
    ELSE IF (MACH .LT. 0.31) THEN
      G(1,3) = -1.4 + (MACH - 0.15) * 0.8 / 0.16
    ELSE IF (MACH .LT. 0.9) THEN
      G(1,3) = -0.6 + (MACH - 0.31) * 0.3 / 0.59
    ELSE
      G(1,3) = -0.3
    ENDIF
C
    IF (MACH .LT. 0.1) THEN
      G(1,4) = -1.9
    ELSE IF (MACH .LT. 0.36) THEN
      G(1,4) = -1.9 + (MACH - 0.1) * 1.25 / 0.26
    ELSE IF (MACH .LT. 0.9) THEN
      G(1,4) = -0.65 + (MACH - 0.36) * 0.275 / 0.54
    ELSE
      G(1,4) = -0.375
    ENDIF
C
    G(1,5) = 0.0
C
    G(1,6) = -4.1
C
C Rudder feedback gains: scheduled as functions of trim flight condition
C G(2,1) = Rudder sideslip gain
C G(2,2) = Rudder roll rate gain
C G(2,3) = Rudder bank angle gain
C G(2,4) = Rudder yaw rate gain
C G(2,5) = Rudder integral sideslip error gain
C G(2,6) = Rudder heading error gain
C
    G(2,1) = -4.1 - FLAP * 1.5 / 40.
C
    G(2,2) = .1625 * VCAS / 100. - .5625
    IF (G(2,2) .LT. -0.4) G(2,2) = -0.4
    IF (G(2,2) .GT. -0.075) G(2,2) = -0.075
C
    G(2,3) = G(2,2)
C
    IF (VCAS .LT. 100.) THEN
      G(2,4) = 5.0
    ELSE IF (VCAS .LT. 200.) THEN
      G(2,4) = 5.0 - (VCAS - 100.) * 1.6 / 100.
    ELSE IF (VCAS .LT. 360.) THEN
      G(2,4) = 3.4 - (VCAS - 200.) * .65 / 160.
    ELSE
      G(2,4) = 2.75
    ENDIF
C
    G(2,5) = -5.5
C
    G(2,6) = 2.2
C
C Initail conditions for simulation
C
C Actuators
C
    RUD_C = 0.
    RUD_X = 0.
    AIL_C = 0.

```

```

      AIL_X      = 0.
C
C States
C
      BETA      = 0.
      P         = 0.
      PHI       = 0.
      R         = 0.
      PSI       = 0.
      Y_POS     = 15000.
      X_POS     = 0.
C
C Beta filter and integrator
C
      BETA_F    = 0.
      BETA_I    = 0.
C
C Commands
C
      PSI_C     = 0.
      PSI_X     = 0.
      BETA_C    = 0.
      BETA_X    = 0.
C
C Limits
C
      PHI_MAX   = 30.
      R_MAX     = 32.2 * PHI_MAX / VTAS
      P_MAX     = 7.
      RD_MAX    = 32.2 * P_MAX / VTAS
      Y_THRSH   = 57.3 * (VTAS + 75.) * (VTAS + 75.) /
+               (32.2 * PHI_MAX)
C
C Simulation controls
C
      ILOCAL    = 1
      T_INIT    = -1.
      T_FINAL   = 150.
      DT        = 0.05
      NPRINT    = 20
      IPRINT    = 0
C
C
C WRITE(6,9100)
C
C Simulation loop
C
      DO 5000 T = T_INIT, T_FINAL, DT
C
C Set disturbance levels
C
      X_WIND    = 0.
      Y_WIND    = T
      IF (Y_WIND .LT. 0.) Y_WIND = 0.
      IF (Y_WIND .GT. 20.) Y_WIND = 20.
C
C Translate earth fixed wind into body coordinate lateral gust
C
      V_GUST    = - X_WIND * SIN(PSI/57.3) + Y_WIND * COS(PSI/57.3)
C
C Set heading command:
C ILOCAL = 0 gives heading controller
C ILOCAL = 1 gives localizer controller
C
      IF (ILOCAL .EQ. 0) THEN
C
      IF (T .GE. 0.) PSI_C = 90.
C
      ELSE
C

```

```

      YABS = ABS(Y_POS)
      YSIGN = 1.
      IF (YABS .GT. 1.) YSIGN = YABS / Y_POS
      PSI_ABS = ABS(PSI)

C
C   Check to see if cross track is greater than threshold value
C   If greater, command turn toward runway
C   If less,
C       a) command heading 30 degrees from runway if heading toward runway
C       b) command heading 5 degrees from runway if heading away from runway
C       c) monitor for switching to localizer controller when:
C           i) localizer controller turn rate greater than
C               heading controller turn rate
C           ii) heading is less than 35 degrees
C           iii) heading is in direction of the runway centerline
C
      IF (YABS .GT. Y_THRSH) THEN
        PSI_C = PSI_C + 10. * (-YSIGN*90. - PSI_C) * DT
        LATCH = 0
      ELSE
        PSI_DOTA = 10. * (-YSIGN*30. - PSI_C)
        IF (PSI*YSIGN.GT.0.) PSI_DOTA = 10. * (-YSIGN*5. - PSI_C)
        C_DOT = 0.04 * Y_POS + VTAS * SIN(PSIGT/57.3)
        PSI_DOTL = (-0.1 * 57.3 / VTAS) * C_DOT
        IF ( ((ABS(PSI_DOTL) .GT. ABS(PSI_DOTA)) .AND.
+         (ABS(PSI_X) .LT. 35.) .AND. (PSI_X*YSIGN .LT. 0.))
+         .OR. (LATCH .EQ. 1) ) THEN
          PSI_C = PSI_C + PSI_DOTL * DT
          LATCH = 1
        ELSE
          PSI_C = PSI_C + PSI_DOTA * DT
        ENDIF
      ENDIF

C
      ENDIF

C   Apply roll rate and roll angle limits to heading command
C
      PSI_R_MAX = PSI_RATE + RD_MAX * DT
      PSI_R_MIN = PSI_RATE - RD_MAX * DT
      PSI_RATE = 0.4 * (PSI_C - PSI_X)
      IF (PSI_RATE .GT. PSI_R_MAX) PSI_RATE = PSI_R_MAX
      IF (PSI_RATE .LT. PSI_R_MIN) PSI_RATE = PSI_R_MIN
      IF (PSI_RATE .GT. R_MAX) PSI_RATE = R_MAX
      IF (PSI_RATE .LT. -R_MAX) PSI_RATE = -R_MAX
      PSI_X = PSI_X + PSI_RATE * DT

C
C   Compute sideslip command filter output
C
      BETA_X = BETA_X + 0.5 * (BETA_C - BETA_X) * DT

C
C   Form heading and sideslip errors and integrate sideslip error
C
      PSI_ERR = PSIGT - PSI_X
      BETA_ERR = BETA_F - BETA_X
      BETA_I = BETA_I + BETA_ERR * DT

C
C   Compute aileron and rudder commands using feedback signals and gains
C
      X(1) = BETA_F
      X(2) = P
      X(3) = PHI
      X(4) = R
      X(5) = BETA_I
      X(6) = PSI_ERR

C
      CALL PRODUCT (G, 2, 6, X, U_C)

C
      AIL_X = AIL_X + 15. * (U_C(1) - AIL_X) * DT
      RUD_X = RUD_X + 15. * (U_C(2) - RUD_X) * DT

C
C   Compute plant model response to control inputs and wind disturbance

```

```

C      X(1) = BETA
      U_X(1) = AIL_X
      U_X(2) = RUD_X
      U_X(3) = V_GUST

C      CALL PRODUCT (A, 4, 4, X, XA_DOT)
      CALL PRODUCT (B, 4, 3, U_X, XB_DOT)

C      BETA = BETA + (XA_DOT(1) + XB_DOT(1)) * DT
      P = P + (XA_DOT(2) + XB_DOT(2)) * DT
      PHI = PHI + (XA_DOT(3) + XB_DOT(3)) * DT
      R = R + (XA_DOT(4) + XB_DOT(4)) * DT
      PSI = PSI + R * DT
      B_AIR = BETA - (57.3 / VTAS) * V_GUST
      PSI_AIR = PSI + B_AIR
      X_VEL = VTAS * COS(PSI_AIR/57.3) + X_WIND
      Y_VEL = VTAS * SIN(PSI_AIR/57.3) + Y_WIND
      X_POS = X_POS + X_VEL * DT
      Y_POS = Y_POS + Y_VEL * DT
      PSIGT = 57.3 * ATAN2(Y_VEL, X_VEL)

C      Complementary filter for sideslip estimate using initalial sideslip rate and
C      air data sideslip - break frequency at 0.1 radians
C      B_DOT_I = XA_DOT(1) + XB_DOT(1)
      BETA_F = BETA_F + (B_DOT_I + 0.1*(B_AIR - BETA_F)) * DT

C      Write data to output file for post processing
C      IF ((IPRINT .EQ. 0) .OR. (IPRINT .GE. NPRINT)) THEN
      WRITE (6,9200) T, BETA, P, PHI, R,
+      PSI, PSIGT, X_POS, Y_POS, Y_THRSH,
+      PSI_C, PSI_X, BETA_C, BETA_X, BETA_F,
+      B_AIR, B_DOT_I, V_GUST, X_WIND, Y_WIND,
+      AIL_X, RUD_X, BETA_I, ILOCAL, LATCH
      IPRINT = 1
      ELSE
      IPRINT = IPRINT + 1
      ENDIF

C      5000 CONTINUE
C      End of simulation loop
C      WRITE(6,9300)

C      8010 FORMAT(A80)
C      8020 FORMAT(G10.5)
C      9100 FORMAT('$ LOCALIZER CAPTURE FOR CASE #004',/,
C      + '$ NO CROSSWIND (STILL AIR)',/,
C      + '$ ',/,
C      + '$ 20 FT/SEC CROSSWIND (RAMPED IN DURING FIRST 20 SECONDS)',/,
C      + '$ (POSITIVE CROSSWIND BLOWS AIRPLANE AWAY FROM RUNWAY)',/,
C      + 'SIM',/,
C      + ' T BETA P PHI R MORE',/,
C      + ' PSI PSIGT X_POS Y_POS Y_THRSH MORE',/,
C      + ' PSI_C PSI_X BETA_C BETA_X BETA_F MORE',/,
C      + ' B_AIR B_DOT_I V_GUST X_WIND Y_WIND MORE',/,
C      + ' AIL_X RUD_X BETA_I ILOCAL LATCH')

C      9200 FORMAT(1X,5G15.5,/,
C      + 2X,5G15.5,/,
C      + 2X,5G15.5,/,
C      + 2X,5G15.5,/,
C      + 2X,3G15.5,2I15)

```

```

9300  FORMAT('*EOF')
C
      END
C
C
C  Subroutine to form product of matrix and vector
C
      SUBROUTINE PRODUCT(A, NROW, NCOL, X, Y)
C
      REAL  A(NROW, NCOL),  X(NCOL), Y(NROW)
C
C
      DO 200 I = 1,NROW
          Y(I) = 0.
          DO 100 J = 1,NCOL
              Y(I) = Y(I) + A(I,J) * X(J)
100      CONTINUE
200      CONTINUE
C
C
      END

```

REFERENCES

1. I. Horowitz, "Synthesis of Feedback Systems", AP Inc., 1963.
2. "Proposed MIL Standard and Handbook - Flying Qualities of Piloted Airplanes", MIL-F-8785C, 5 November 1980.
3. C. Thompson, E. E. Coleman, and J. B. Blight, "Integral LQG Controller Design for a Fighter Aircraft", AIAA paper 87-2452CP, Guidance & Control Conference, 1987.
4. A. A. Lambregts, "Integrated System Design for Flight and Propulsion Control Using Total Energy Principles", AIAA-83-2561, Guidance & Control Conference, 1983.
5. K. R. Bruce, J. R. Kelly, and L. M. Pearson Jr., "NASA B737 Flight Test Results of the Total Energy Control System", AIAA-86-2143CP, Guidance & Control Conference, 1986.
6. I. Kaminer and P. O'Shaughnessy, "4D-TECS Integration for NASA TCV Airplane", AIAA-88-4067CP, Guidance & Control Conference, 1988.
7. A. A. Lambregts and R. Hansen, "Development of Two Autoland Flare Control Laws that Reduce Touchdown Dispersion for NASA Terminal Configured Vehicle Program's B737 Airplane", D6-37006, The Boeing Company, 1978.
8. P. Salo, "Delta Coordinate Controller Implementation to Avoid 'Fictitious gain' Problem Arising from Gain Scheduling", Boeing Intercompany Controls Symposium, Seattle, April 1987.

Report Documentation Page

1. Report No. NASA CR-4268		2. Government Accession No.		3. Recipient's Catalog No.	
4. Title and Subtitle Design of Integrated Pitch Axis for Autopilot/ Autothrottle and Integrated Lateral Axis for Autopilot/ Yaw Damper for NASA TSRV Airplane Using Integral LQG Methodology				5. Report Date January 1990	
				6. Performing Organization Code	
7. Author(s) Isaac Kaminer, Russell A. Benson, Edward E. Coleman, and Yaghoob S. Ebrahimi				8. Performing Organization Report No.	
				10. Work Unit No. 505-66-41-04	
9. Performing Organization Name and Address Boeing Commercial Airplane Company P. O. Box 3707, M/S 7W-78 Seattle, WA 98124-2207				11. Contract or Grant No. NAS1-18027	
				13. Type of Report and Period Covered Contractor Report	
12. Sponsoring Agency Name and Address National Aeronautics and Space Administration Langley Research Center Hampton, VA 23665-5225				14. Sponsoring Agency Code	
15. Supplementary Notes Langley Technical Monitor: Richard M. Hueschen Langley Contracting Officer's Technical Representative: Cary R. Spitzer Final Report - Task 6					
16. Abstract Two designs are presented in this document: 1) an integrated longitudinal autopilot/autothrottle design and 2) an integrated lateral autopilot/yaw damper/sideslip controller design. It is shown herein that a systematic top-down approach to a complex design problem combined with proper application of modern control synthesis techniques yields a satisfactory solution in a reasonable period of time.					
17. Key Words (Suggested by Author(s)) Autopilot Autothrottle Integral LQG Integrated Control			18. Distribution Statement Unclassified - Unlimited Subject Category 08		
19. Security Classif. (of this report) Unclassified		20. Security Classif. (of this page) Unclassified		21. No. of pages 148	
				22. Price A07	